UNITED NATIONS EDUCATIONAL, SCIENTIFIC AND CULTURAL ORGANIZATION
INTERNATIONAL ATOMIC ENERGY AGENCY
INTERNATIONAL CENTRE FOR THEORETICAL PHYSICS

SMR: 960/10

WORKSHOP ON NONLINEAR CONTROL AND CONTROL OF CHAOS

(17 - 28 June 1996)

"Controlling Chaos in Biological Systems: From Rat Brains to Human Hearts"

presented by:

William Ditto
Georgia Institute of Technology
Applied Chaos Laboratory
School of Physics
Atlanta, GA 30332-0430
U.S.A.

0.19 M, 0.1 M, and 0 M. The filter was then incubated for 60 minutes in buffer A supplemented with 5 percent dehydrated Carnation milk and 0.05 percent NP-40 and for another 60 minutes in the same buffer containing 1 percent rather than 5 percent dehydrated Carnation milk. The binding reaction was carried out by adding ^{32}P-labeled fusion protein to the buffer (10^6 cpm/ml) and incubating for 12 hours. For labeling fusion protein, the bacterial cells were collected by centrifugation and lysed by repeated freeze and thawing in buffer (20 mM Hepes-KOH, pH 7.5, 50 mM NaCl, 2 mM EDTA, and 0.2 percent deoxycholate). In most cases the fusion proteins represented at least 10 percent of the total bacterial protein. Protein preparations obtained after centrifugation at 12,000*g* for 20 minutes or further purification steps were incubated at 37°C for 90 minutes in a solution of 20 mM Hepes-KOH, pH 7.5, 100 mM NaCl, 12 mM $MgCl_2$, 1 mM dithiothreitol (DTT), 100 μCi of [γ-^{32}P]ATP, and 25 U of heart muscle kinase catalytic subunit (Sigma). The solution containing the phosphoproteins was then dialyzed against a buffer (10 mM Hepes-KOH, pH 7.5, 60 mM KCl, 1 mM EDTA, 1 mM DTT) to remove the unincorporated radioactivity. The specific activity of the ^{32}P-labeled protein was estimated to be 2.5 to 5.0 × 10^4 cpm/pmol of the polypeptide.

14. W. K. Miskimins *et al.*, *Proc. Natl. Acad. Sci. U.S.A.* **82**, 6741 (1985); D. R. Rawlins, G. Milman, S. D. Hayward, G. S. Hayward, *Cell* **42**, 859 (1985); J. E. Ferrell and G. S. Martin, *J. Biol. Chem.* **264**, 20723 (1989); B. R. Copeland, R. J. Richter, C. E. Furlong, *ibid.* **257**, 15065 (1982); M. A. Blanar and W. J. Rutter, *Science* **256**, 1014 (1992); W. S. Lee, C. C. Kao, G. O. Bryant, X. Liu, A. J. Berk, *Cell* **67**, 365 (1991).
15. K. Klaiber *et al.*, *Neuron* **5**, 221 (1990).
16. M. Li, Y. N. Jan, L. Y. Jan, unpublished data.
17. K. G. Chandy, *Nature* **352**, 26 (1991).
18. T. Hoshi, W. N. Zagotta, R. W. Aldrich, *Science* **250**, 533 (1990); W. N. Zagotta, T. Hoshi, R. W. Aldrich, *ibid.* **250**, 568 (1990); J. P. Ruppersberg *et al.*, *Nature* **352**, 711 (1991).
19. F. Bezanilla and C. M. Armstrong, *J. Gen. Physiol.* **70**, 567 (1977).
20. The recording was done in 88 mM NaCl, 2.4 mM $NaHCO_3$, 1 mM KCl, 0.82 mM $MgSO_4$, 0.41 mM $CaCl_2$, 0.33 mM $Ca(NO_3)_2$, 10 mM Hepes, pH 7.5 (the MBSH solution), 18° ± 1°C. Digital substraction of leak currents was done by using scaled average currents evoked by ten 20-mV hyperpolarizing pulses from the holding potential of −100 mV.
21. E. Y. Isacoff, Y. N. Jan, L. Y. Jan, *Nature* **353**, 86 (1991).
22. A. M. J. VanDongen, G. C. Frech, J. A. Drewe, R. H. Joho, A. M. Brown, *Neuron* **5**, 433 (1990).
23. G. A. Lopez, Y. N. Jan, L. Y. Jan, *ibid.* **7**, 327 (1991); E. R. Liman, P. Hess, F. Weaver, G. Koren, *Nature* **353**, 752 (1991); D. M. Papazian, L. C. Timpe, Y. N. Jan, L. Y. Jan, *ibid.* **349**, 305 (1991).
24. R. MacKinnon and G. Yellen, *Science* **250**, 276 (1990); H. A. Hartmann *et al.*, *ibid.* **251**, 942 (1991); G. Yellen, M. E. Jurman, T. Abramson, R. MacKinnon, *ibid.*, p. 939; A. J. Yool and T. L. Schwarz, *Nature* **349**, 700 (1991); L. Heginbotham and R. MacKinnon, *Neuron* **8**, 483 (1992); M. P. Kavanaugh *et al.*, *ibid.*, p. 493; G. E. Kirsch *et al.*, *ibid.*, p. 499.
25. N. Unwin, *Neuron* **3**, 665 (1989).
26. E. Cooper, S. Couturier, M. Ballivet, *Nature* **350**, 235 (1991).
27. Y. Gu *et al.*, *Neuron* **6**, 879 (1991); X. M. Yu and Z. W. Hall, *Nature* **352**, 64 (1991); S. Verrall and Z. W. Hall, *Cell* **68**, 23 (1992).
28. For immunoblots protein was fractionated by SDS-PAGE and transferred onto a nitrocellulose filter. The filter was incubated in a blocking solution [10 mM tris, pH 8, 150 mM NaCl, 1 percent Tween 20, 2 percent bovine serum albumin (BSA), 3 percent normal goat serum] for 30 minutes at room temperature. Binding to primary antibodies was effected by adding the rabbit antiserum to the blocking solution and incubating for 30 minutes at room temperature. The excess unbound antibodies were removed with TST solution (blocking solution without BSA and normal goat serum). The binding to secondary antibodies [horseradish peroxidase (HRP)–conjugated goat antibodies to rabbit immunoglobulin G (Amersham)] was performed in TST solution with a dilution of 1:10,000. The specific antibody binding was visualized by chemiluminescence (ECL system, Amersham).
29. The bacteria cell pellet was resuspended in buffer of 50 mM Hepes-KOH, pH 7.5, 100 mM KCl, 2 mM EDTA, 1 mM DTT, and 0.5 percent deoxycholate. The cell lysate was prepared by sonicating the cell suspension at medium scale twice for 30 seconds. Nucleic acid in the lysate was precipitated by polyamine and cleared by 20 minutes of centrifugation at 10,000*g*. This starting material was then fractionated on a Fast Protein Liquid Chromatography (FPLC) Mono Q (Pharmacia LKB) column with a 50 mM to 500 mM linear gradient of KCl. The activity was monitored by immunoblot (*28*) and the activity pool was then fractionated on FPLC phenol Sepharose with a 2 M to 100 mM linear gradient of $(NH_4)_2SO_4$ or directly purified through affinity column containing antibodies to the FLAG peptide tag (IBI), which recognize the peptide sequence DYKD (Fig. 1A). The activity was then concentrated by hydroxylapitite chromatography. This material was then analyzed on a FPLC Superose 6 column with a buffer containing 25 mM Hepes-KOH, pH 7.5, 0.5 M KCl, 2 mM EDTA, 2 mM DTT, and 5 percent (w/v) glycerol. The fraction collector was activated to collect 500 μl per fraction after the first 5-ml elution. The activity was followed by membrane binding analysis with ^{32}P-labeled NShB and quantified by spectrometry.
30. J. A. Drewe *et al.*, *J. Neurosci.* **12**, 538 (1992).
31. We thank C. Miller for the recombinant baculovirus for Shaker expression, D. McKinnon for the BK1 clone, R. Joho and A. Brown for the DRK1 clone, R. Aldrich for the pShB(Δ6-46) construct, M. Blanar for the pAR(ΔRI)59/60 vector, L. Qin for advice on tissue culture and immunoassays, E. Isacoff, Y. Kubo, G. Lopez, and P. Slesinger for advice on electrophysiological recording, M. Doherty for oligonucleotide synthesis, L. Ackerman for photography, B. Bannerman for typing the manuscript, and G. Feger, E. Giniger, E. Isacoff, A. Jarman, Y. Kubo, M. Sheng, V. Siegel, P. Slesinger, and M-L. Tsaur for comments on the manuscript. Supported by a Helen Hay Whitney Foundation fellowship (M.L.), the Muscular Dystrophy Association (M.L.), and the Howard Hughes Medical Institute (Y.N.J. and L.Y.J.).

11 May 1992; accepted 9 July 1992

Controlling Cardiac Chaos

Alan Garfinkel, Mark L. Spano, William L. Ditto, James N. Weiss

The extreme sensitivity to initial conditions that chaotic systems display makes them unstable and unpredictable. Yet that same sensitivity also makes them highly susceptible to control, provided that the developing chaos can be analyzed in real time and that analysis is then used to make small control interventions. This strategy has been used here to stabilize cardiac arrhythmias induced by the drug ouabain in rabbit ventricle. By administering electrical stimuli to the heart at irregular times determined by chaos theory, the arrhythmia was converted to periodic beating.

The realization that many apparently random phenomena are actually examples of deterministic chaos offers a better way to understand complex systems. Phenomena that have been shown to be chaotic include the transition to turbulence in fluids (*1*), many mechanical vibrations (*2*), irregular oscillations in chemical reactions (*3*), the rise and fall of epidemics (*4*), and the irregular dripping of a faucet (*5*). Several studies have argued that certain cardiac arrhythmias are instances of chaos (*6, 7*). This is important because the identification of a phenomenon as chaotic may make new therapeutic strategies possible.

Until recently the main strategy for dealing with a system displaying chaos was to develop a model of the system sufficiently detailed to identify the key parameters and then to change those parameters enough to take the system out of the chaotic regime. However this strategy is limited to systems for which a theoretical model is known and that do not display irreversible parametric changes (often the very changes causing the chaos) such as aging.

Recently a strategy has emerged that does not attempt to take the system out of the chaotic regime but uses the chaos to control the system. The key to this approach lies in the fact that chaotic motion includes an infinite number of unstable periodic motions (*8*). A chaotic system never remains long in any of these unstable motions but continually switches from one periodic motion to another, thereby giving the appearance of randomness. Ott, Grebogi, and Yorke (OGY) (*9*) postulated that it should be possible to stabilize a system around one of these periodic motions by using the defining feature of chaos, the extreme sensitivity of chaotic systems to perturbations of their initial conditions.

The OGY theory was first applied experimentally to controlling the chaotic vibrations of a magnetoelastic ribbon (*10*) and subsequently to a diode resonator circuit

A. Garfinkel is in the Department of Physiological Science, University of California, Los Angeles, CA 90024–1527. M. L. Spano is at the Naval Surface Warfare Center, Silver Spring, MD 20903. W. L. Ditto is in the Department of Physics, The College of Wooster, Wooster, OH 44691. J. N. Weiss is in the Department of Medicine (Cardiology), University of California, Los Angeles, CA 90024.

11) and to the chaotic output of lasers (12). We have found that it is possible to control a chaotic cardiac arrhythmia using the same basic properties of chaotic systems that were exploited by OGY but that are here employed in a new method of chaos control suitable for use in systems where no systemwide parameters can be readily manipulated as required by the OGY method.

Experimental arrhythmia model. Our cardiac preparation consisted of an isolated well-perfused portion of the interventricular septum from a rabbit heart, arterially perfused through the septal branch of the left coronary artery with a physiologic oxygenated Kreb's solution at 37°C (13). The heart was stimulated by passing a 3-ms constant-voltage pulse, typically 10 to 30 V, at twice the threshold between platinum electrodes embedded in the preparation, by means of a Grass SD9 stimulator triggered by computer. Electrical activity was monitored by recording monophasic action potentials with Ag-AgCl wires on the surface of the heart. Monophasic action potentials and a stimulus marker tracing were recorded on a modified videocassette recorder (Model 420, A. R. Vetter, Inc.) and one of the monophasic action potential traces was simultaneously digitized at 2 kHz by a 12-bit A-D converter board (National Instruments model AT-MIO-16). The digitized trace was processed in real time by a computer to detect the activation time of each beat from the maximum of the first derivative of the voltage signal.

Arrhythmias were induced by adding 2 to 5 μM ouabain with or without 2 to 10 μM epinephrine to the arterial perfusate. The mechanism of ouabain-epinephrine–induced arrhythmias is probably a combination of triggered activity and nontriggered automaticity caused by progressive intracellular Ca^{2+} overload from Na^{+} pump inhibition and increased Ca^{2+} current (14, 15). We reasoned that this arrhythmia might progress to chaos because in cardiac myocytes intracellular Ca^{2+} is regulated by several interactively coupled processes whose delicate balance is disrupted by ouabain. The resultant oscillations in intracellular Ca^{2+} cause spontaneous beating by activating arrhythmogenic inward currents from electrogenic Na^{+}-Ca^{2+} exchange and Ca^{2+}-activated nonselective cation channels (14). Typically the ouabain-epinephrine combination induced spontaneous beating, initially at a constant interbeat interval and then progressing to bigeminy and higher order periodicity before developing a highly irregular aperiodic pattern of spontaneous beating in ~85 percent of the preparations. The duration of the aperiodic phase was variable, lasting up to several minutes before spontaneous electrical activity irreversibly ceased, probably correspond-

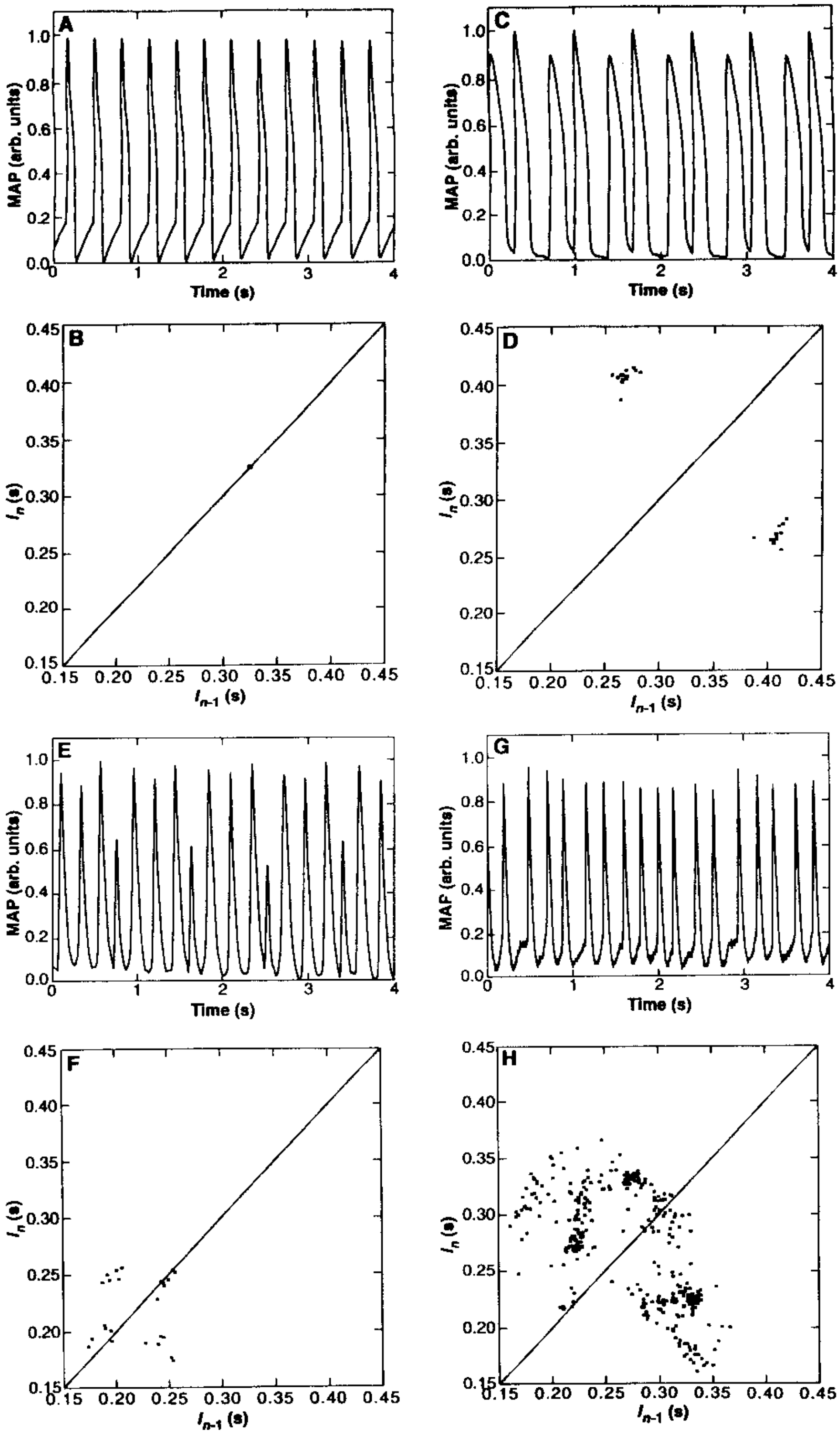

Fig. 1. Recordings of monophasic action potentials (MAPs) (**A**, **C**, **E**, and **G**) and their respective Poincaré maps of interbeat intervals (**B**, **D**, **F**, and **H**) at various stages during arrhythmias induced by ouabain-epinephrine in typical rabbit septa. Typically the arrhythmia was initially characterized by spontaneous periodic beating at a constant interbeat interval (A and B), then developed bigeminal or period 2 patterns (C and D) or higher order periodicities such as a period 4 pattern (E and F), and lastly a completely aperiodic pattern (G and H). Note that in the Poincaré map of the final stage the points form an extended structure that is not point-like or a set of points (that is, not periodic) and is not space-filling (that is, not random). This is a sign of chaos.

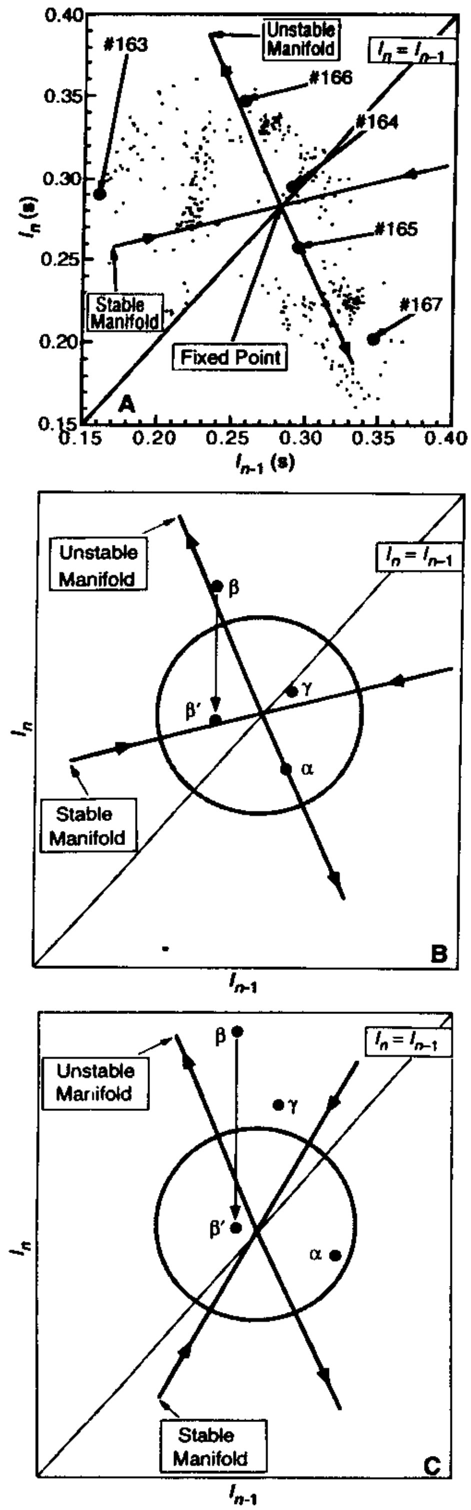

Fig. 2. (**A**) The Poincaré map of the aperiodic phase of a ouabain-epinephrine–induced arrhythmia in a typical heart preparation illustrating the structure of the chaotic attractor. (**B**) Blowup of the Poincaré map in the region of the unstable fixed point illustrating schematically the idealized chaos control method. (**C**) A schematic of the actual implementation achieved with chaos control. Note that the stable manifold has shifted, a common variation among data runs. The circles in (B) and (C) enclose the region about the fixed point in which chaos control is enabled.

ing to progressive severe membrane depolarization from Na^+ pump inhibition. The spontaneous activity induced by ouabain-epinephrine in this preparation showed a number of features symptomatic of chaos. Most important, in progressing from spontaneous beating at a fixed interbeat interval to highly aperiodic behavior, the arrhythmia passed through a series of transient stages that involved higher order periodicities. These features are illustrated in Fig. 1, in which the nth interbeat interval (I_n) has been plotted against the previous interval (I_{n-1}) at various stages during ouabain-epinephrine–induced arrhythmias. Such a Poincaré map (5) allows us to view the dynamics of the system as a sequence of pairs of points (I_{n-1}, I_n), thus converting the dynamics of our system to a map. This map has several special features. The first is that a periodic motion appears as a finite set of points in such a plot (Fig. 1, A to C). When the arrhythmia progressed to the aperiodic stage, truly random aperiodicity would have demonstrated no structure in the Poincaré map. Chaotic aperiodicity however is represented by an extended structure that is not a single point (or finite set of points) and yet is not space-filling. Figure 1D illustrates that the aperiodic phase of the ouabain-epinephrine–induced arrhythmia fell into the latter category, supporting a chaotic rather than a random process. In 11 preparations the Poincaré maps consistently showed patterns similar to Fig. 1D, and these patterns are consistent with chaotic aperiodicity. Figure 1, A to D, as shown are from different preparations. However virtually all preparations exhibited at least one period doubling before the arrhythmia became chaotic (although it is not clear whether the transitions to chaos in our preparations are the result of a period doubling route to chaos).

Method of chaos control. The control of chaos begins with the realization that, where the attractor crosses the line of identity ($I_n = I_{n-1}$), it must contain an unstable periodic motion of period 1. (If it were stable, the attractor would be only a single point lying on the diagonal of Fig. 1). Such a crossing point is called an unstable fixed point and represents constant interbeat intervals (with period 1). These unstable fixed points have associated directions along which the trajectory approaches and diverges from the fixed point. These directions are called the stable and unstable manifolds, respectively. A typical sequence of interbeat intervals during aperiodic beating induced by ouabain-epinephrine in a rabbit septum is indicated in Fig. 2A (points 163 through 167). From point 163 to 164 the state of the system (or state point) moves toward the unstable fixed point. Thus point 163 must lie close to the stable manifold (direction). Points 164 through 167 diverge from the unstable fixed point and hence reveal an unstable manifold (direction). In the chaotic region unstable fixed points on the attractor possess at least one unstable and one stable manifold (*16*). Thus the local geometry around a fixed point in a Poincaré map plot is that of a saddle. In this case the saddle is a flip saddle; that is, while the distances of successive state points from the fixed point increase in an exponential fashion along the unstable manifold (one of the signs of chaos) the state points alternate on opposite sides of the stable manifold (*17*). The flip saddle appears as a short interbeat interval followed by a long interval and vice versa.

Our method of chaos control, which we call proportional perturbation feedback (PPF), consists of delivering a perturbation (near the desired fixed point) that forces the system state point onto the stable manifold of the desired fixed point. Consequently the system will naturally move toward the unstable fixed point rather than away from it. Contrast this with the OGY method, which moves the stable manifold to the current system state point rather than vice versa. Both methods use a linear approximation of the dynamics in the neighborhood of the desired fixed point. OGY then varies a systemwide parameter to move the stable manifold to the system state point; our method perturbs the system state point to move it toward the stable manifold. Thus the magnitude of our perturbation is the same as predicted by the OGY equations, but the sign is opposite. We developed the PPF method when it became obvious that our cardiac preparation possessed no systemwide parameter that could be changed sufficiently quickly to implement classical OGY control.

The procedure begins by determining the location of the unstable fixed point ξ_F, as well as its local stable and unstable contravariant eigenvectors, $\mathbf{f}_s$ and $\mathbf{f}_u$ respectively. If ξ_n is the current position of the system on the Poincaré map and p is the predicted timing of the next natural beat, the required advance in timing δp is proportional to the projection of the distance $\xi_n - \xi_F$ onto the unstable manifold (the unstable contravariant eigenvector):

$$\delta p = C(\xi_n - \xi_F)\cdot\mathbf{f}_u \qquad (1)$$

where:

$$C = \frac{\lambda_u}{\lambda_u - 1}\,\frac{1}{\mathbf{g}\cdot\mathbf{f}_u} \qquad (2)$$

The constant of proportionality C depends on the unstable eigenvalue λ_u. This eigenvalue determines the rate of the exponential divergence of the system from the fixed point along the unstable manifold and is

Control of Spatiotemporal Chaos

Several groups have studied the control of spatiotemporal chaos. Although a good definition of *spatial* chaos does not exist, these groups have examined spatially coupled systems which are chaotic in isolation.

(Sepulchre, Babloyantz: 1993) extended the OGY technique to stabilize the chaotic oscillations of a 9x9 network of coupled oscillators in a numerical experiment. At nonzero coupling the dimensionality of the network was determined not to be low, suggesting a very large number of unstable degrees of freedom. Several unstable periodic motions of the network were found and subsequently stabilized by small periodic microkicks to *every* oscillator. (As in the PPF technique, the perturbations were applied to the variables, not to the parameters.)

Is distributed control necessary to control a network of oscillators? Is a subnetwork of controlling nodes sufficient? Three numerical experiments suggest that global control of certain convectively unstable media may be achieved locally. (Gang, Kaifen: 1993) successfully employed negative feedback to control an *anisotropic* one-dimensional open system described by a partial differential equation. One technique was to inject a monochromatic wave (feedback in k-space). A second technique was to pin the system at one place in space (feedback in x-space). In each case, the local control propagate throughout the entire system. Similarly, (Auerbach: 1994) succeeded in controlling a chain of *asymmetrically* coupled quadratic maps. Controllers were distributed periodically in space, each perturbing a local parameter based on local measurements. The local control was convected downstream: Finally, (Aranson, Levine, Tsimring: 1994) proposed a technique for controlling certain *isotropic* convectively unstable media. These media include unstable defects which can break up and nucleate more defects. (Certain models of cardiac tissue are examples.) Control was obtained by stabilizing one such defect which then swept all chaotic fluctuations away. Thus, to date, local control begets global control only in special media.

Chaos Workshop
Recommended Texts

Popular
Gleick, *Chaos: The Making of a New Science*
Stewart, *Does God Play Dice? The Mathematics of Chaos*
Peterson, *Newton's Clock: Chaos in the Solar System*

Intro
Baker & Gollub, *Chaotic Dynamics: An Introduction*
Moon, *Chaotic and Fractal Dynamics*
Percival & Richards, *Introduction to Dynamics*

Advanced
Ott, *Chaos in Dynamical Systems*
Tabor, *Chaos and Integrability in Nonlinear Dynamics*
Cvitanovic, *Universality in Chaos*

References for Catalogue Section

I. Aranson, H. Levine, L. Tsimring,
Phys. Rev. Lett. **72**, 2561 (1994).

D. Auerbach,
Phys. Rev. Lett. 72, (1994).

D. Auerbach, C. Grebogi, E. Ott, J. A. Yorke,
Phys. Rev. Lett. **69**, (1992).

A. Azevedo, S. M. Rezende,
Phys. Rev. Lett. **66**, 1342 (1991).

B. Blazejczyk, T. Kapitaniak, J. Wojewoda, J. Brindley,
Appl. Mech. Rev. **46** (7), 385 (1993).

Y. Braiman, I. Goldhirsch,
Phys. Rev. Lett. **66**, 2545 (1991).

T. L. Carroll, I. Triandaf, I. Schwartz, L. Pecora,
Phys. Rev. A **46**, 6189 (1992).

G. Chen, X. Dong,
Int. J. Bif. & Chaos **3**, 1363 (1993).

Y. H. Chen, H. H. Bau,
Phys. Rev. Lett. **69**, 3128 (1993).

W. L. Ditto, L. M. Pecora,
Sci. Am. **269** (2), 78 (1993).

W. L. Ditto, M. L. Spano, J. F. Lindner,
(to appear in *Physica D*, 1995).

W. L. Ditto, S. N. Rauseo, M. L. Spano,
Phys. Rev. Lett. **65**, 3211 (1990a).

W. L. Ditto, M. L. Spano, H. T. Savage, S. N. Rauseo, J. Heagy, E. Ott,
Phys. Rev. Lett. **65**, 533 (1990b).

G. Duffing,
Erzwungene Schwingungen bei Veränderlicher Eigenfrequenz,
(F. Vieweg u. Sohn, Braunschweig, 1918).

L. Fronzoni, M. Giocondo, M. Pettini,
Phys. Rev. A **43**, 6483 (1991).

M. Gad-el-Hak,
Appl. Mech. Rev. **42** (10), 261 (1989).

M. Gad-el-Hak,
AIAA Journ. **32**(9), 1753 (1993).

References for Catalogue Section

B. Peng, V. Petrov, K. Showalter,
J. Phys. Chem. **95**, 4957 (1991).

V. Petrov, V. Gaspar, J. Masere, K. Showalter,
Nature **361**, 240 (1993).

K. Pyragas,
Phys. Lett. A **170**, 421 (1992).

K. Pyragas,
Phys. Lett. A **181**, 203 (1993).

K. Pyragas, A. Tamaševičius,
Phys. Lett. A **180**, 99 (1993).

Z. Qu, G. Hu, B. Ma,
Phys. Lett. A **178**, 265 (1993).

S. Rajasekar, M. Lakshmanan,
Physica D **67**, 282 (1993).

C. Reyl, L. Flepp, R. Badii, E. Brun,
Phys. Rev. E **47**, 267 (1993).

R. W. Rollins, P. Parmananda, P. Sherard,
Phys. Rev. E **47**, 780 (1993).

F. J. Romeiras, C. Grebogi, E. Ott, W. P. Dayawansa,
Physica D **58**, 165 (1992).

R. Roy, T. W. Murphy, T. D. Maier, Z. Gills, E. R. Hunt,
Phys. Rev. Lett. **68**, (1992).

S. J. Schiff, K. Jerger, D. H. Duong, T. Chang, M. L. Spano, W. L. Ditto,
Nature **370** 615 (1994).

J. A. Sepulchre, A. Babloyantz,
Phys. Rev. E **48**, 945 (1993).

R. Shermer,
Phys. Rev. A **46**, 7614 (1992).

T. Shinbrot, W. Ditto, C. Grebogi, E. Ott, M. Spano, J. A. Yorke,
Phys. Rev. Lett. **68**, 2863 (1992).

T. A. Shinbrot, C. Grebogi, E. Ott, J. A. Yorke,
Nature **363**, 411 (1993).

T. Shinbrot, E. Ott, C. Grebogi, J. A. Yorke,
Phys. Rev. Lett. **65**, 3215 (1990).

References for Catalogue Section

H. Gang, H. Kaifen,
Phys. Rev. Lett. **71**, 3794 (1993).

A. Garfinkel, M. L. Spano, W. L. Ditto, J. N. Weiss,
Science **257**, 1230 (1992).

Z. Gills, C. Iwata, R. Roy, I. B. Schwartz, I. Triandaf,
Phys. Rev. Lett. **69**, 3169 (1992).

B. A. Huberman, L. Lumer,
IEEE Trans. Circuits. Syst. **37**, 547 (1990).

E. R. Hunt,
Phys. Rev. Lett. **67**, 153 (1991).

V. In, W. L. Ditto, M. L. Spano,
Phys. Rev. E **51**, R1 (1995).

E. A. Jackson, A. Hübler,
Physica D **44**, 407 (1990).

G. A. Johnson, M. Löcher, E. R. Hunt,
Phys. Rev. E **51**, R1625 (1995).

L. R. Keefe,
Phys. Fluids A **5**, 931 (1993).

E. J. Kostelich, C. Grebogi, E. Ott, J. A. Yorke,
Phys. Rev. E **47**, 305 (1993).

Lüscher, A. Hübler,
Helv. Phys. Acta **62**, 544 (1989).

R. Lima, M. Pettini,
Phys. Rev. A **41**, 726 (1990).

G. Nitsche, U. Dressler,
Physica D **58**, 153 (1992).

K. Ogata,
Control Engineering,
(Prentice Hall, Englewood Cliffs, NJ, 1990).

E. Ott, C. Grebogi, J. A. Yorke,
Phys. Rev. Lett. **64**, 1196 (1990).

P. Parmananda, P. Sherard, R. W. Rollins, H. D. Dewald,
Phys. Rev. E **47**, 3003 (1993).

L. M. Pecora, T. L. Carroll,
Phys. Rev. Lett. **64**, 821 (1990).

References for Catalogue Section

J. Singer, Y.-Z. Wang, H. H. Bau,
Phys. Rev. Lett. **66**, 1123 (1991).

S. Sinha, R. Ramaswamy, J. S. Rao,
Physica D **43**, 118 (1990).

M. L. Spano, E. Ott,
(to appear in *Physics Today*, May 1995).

J. Starret, R. Tagg,
Phys. Rev. Lett. **74**, 1974 (1995).

F. Takens,
in *Dynamical Systems and Turbulence*,
D. Rand, L.-S. Young, Editors,
(Springer, Berlin, 1981).

J. M. T. Thompson, H. B. Stewart,
Nonlinear Dynamics and Chaos,
(John Wiley & Sons, Chichester, 1986).

Reprinted from

PHYSICA D

Physica D 86 (1995) 198–211

Techniques for the control of chaos

William L. Ditto[a], Mark L. Spano[b], John F. Lindner[c]

[a]Applied Chaos Laboratory, Georgia Institute of Technology, Atlanta, GA 30332, USA
[b]Naval Surface Warfare Center, 10901 New Hampshire Ave., Silver Spring, MD 20903, USA
[c]Department of Physics, The College of Wooster, Wooster, OH 44691, USA

N·H

ELSEVIER

Physica A, Physica B, Physica C and Physica D are published by Elsevier Science B.V., Amsterdam

Subscription data

Physica A (ISSN 0378-4371). For 1995, volumes 212–222 are scheduled for publication. Physica A is published semimonthly.
Physica B (ISSN 0921-4526). For 1995, volumes 203–214 are scheduled for publication. Physica B is published monthly.
Physica C (ISSN 0921-4534). For 1995, volumes 237–255 are scheduled for publication. Physica C is published two to three times per month.
Physica D (ISSN 0167-2789). For 1995, volumes 79–88 are scheduled for publication. Physica D is published semimonthly.
Subscription prices are available upon request from the publisher.
A combined subscription to Physica A, Physica B, Physica C and Physica D is available at a reduced rate.

Subscriptions are accepted on a prepaid basis only and are entered on a calendar year basis. Issues are sent by surface mail except to the following countries where air delivery via SAL is ensured: Argentina, Australia, Brazil, Canada, China, Hong Kong, India, Israel, Japan, Malaysia, Mexico, New Zealand, Pakistan, Singapore, South Africa, South Korea, Taiwan, Thailand, USA. For all other countries airmail rates are available upon request.
Please address all your requests regarding orders and subscription queries to: Elsevier Science B.V., Journal Department, P.O. Box 211, 1000 AE Amsterdam, The Netherlands. Telephone: +31-20-485 3642, Telefax: +31-20-485 3598. Claims for issues not received should be made within six months of our publication (mailing) date.

US mailing notice – Physica D (ISSN 0167-2789) is published semimonthly by Elsevier Science B.V., Molenwerf 1, P.O. Box 211, 1000 AE Amsterdam, The Netherlands. The annual subscription price in the USA is US$ 2321 (valid in North, Central and South America only), including air speed delivery. Second class postage paid at Jamaica, NY 11431.
USA Postmasters: Send address changes to Physica D, Publications Expediting, Inc., 200 Meacham Avenue, Elmont, NY 11003. Airfreight and mailing in the USA by Publication Expediting.

Printed in the Netherlands

ELSEVIER

Physica D 86 (1995) 198-211

PHYSICA D

Techniques for the control of chaos

William L. Ditto[a], Mark L. Spano[b], John F. Lindner[c]

[a] Applied Chaos Laboratory, Georgia Institute of Technology, Atlanta, GA 30332, USA
[b] Naval Surface Warfare Center, 10901 New Hampshire Ave., Silver Spring, MD 20903, USA
[c] Department of Physics, The College of Wooster, Wooster, OH 44691, USA

Abstract

The concepts of chaos and its control are reviewed. Both are discussed from an experimental as well as a theoretical viewpoint. Examples are then given of the control of chaos in a diverse set of experimental systems. Current and future applications are discussed.

1. Introduction

Chaos - A rough, unordered mass of things.

Ovid, "Metamorphoses"

Shakespeare once asked, "What's in a name?" The answer is nothing and everything. Nothing because "A rose by any other name would smell as sweet." And yet, without a name Shakespeare would not have been able to write about that rose or to distinguish it from other flowers that smell less pleasant. So also with chaos. The dynamical phenomenon we call chaos has always existed, but until its naming we had no way of distinguishing it from other aspects of nature such as randomness or order. And lacking any way to treat it as a separate entity, we would not even be able to conceive of manipulating it or controlling it. Thus the naming of chaos by James Yorke [1] in 1975 was an essential first step towards identifying it and learning to control it.

From this identification came the recognition that chaos is pervasive in our world. Chaos was first suspected in the weather patterns [2] that govern our lives. It is easy to make simple electronic circuits that are chaotic [3]. Mechanical systems on such wildly different scales as laboratory pendula [4] and orbiting planets [5] have been shown to exhibit chaos. Laser emissions [6] can fluctuate chaotically. The human heart shows evidence [7] of beating to chaotic rhythms. Chemical reactions [8,9] oscillate in chaotic fashion. Of these diverse systems, we have learned to control all of those that are on the smaller scale. Systems on a more universal scale such as the weather and the planets remain beyond our control.

In what follows we will discuss the concept of chaos, from both a theoretical and a laboratory viewpoint, always with an eye towards methods

SSDI 0167-2789(95)00101-8

of controlling and exploiting it. Afterwards we will look at the application of these methods to the systems mentioned above.

2. The concept of chaos

A violent order is disorder; and
A great disorder is an order. These
Two things are one.

Wallace Stevens, "Connoisseur of Chaos"

Before its discovery and naming, chaos was inevitably confused with randomness and indeterminacy. Because many systems *appeared* random, they were actually thought to *be* random. This was true despite the fact that many of these systems seemed to fall into periods of almost periodic behavior before returning to more "random" motion. Indeed this observation leads to one of the definitions of chaos: the superposition of a very large number of unstable periodic motions. A chaotic system may dwell for a brief time on a motion that is very nearly periodic and then may change to another motion that is periodic with a period that is perhaps five times that of the original motion and so on. This constant evolution from one (unstable) periodic motion to another produces a long-term impression of randomness, while showing short-term glimpses of order. These glimpses are not misleading, since chaos is deterministic and not random in nature.

A second definition of chaos is this: the sensitivity of a system to small changes in its initial conditions. This is the "butterfly effect" of legend. The story goes as follows: the small breeze created by a butterfly's wings in China may eventually mean the difference between a sunny day and a torrential rainstorm in California. If you visualize the motion of a chaotic system in phase space, you soon see that all these unstable periodic motions have corresponding trajectories in phase space. And since there are a very large number of these unstable motions in a bounded space, the trajectories corresponding to each unstable periodic motion must be packed quite closely together. Thus only a very small perturbation may push the system from one unstable periodic motion to any of a large number of others.

This last is both the hope and the despair of those who have to deal with chaotic systems. It is the despair because it effectively renders long term prediction of these systems impossible. For instance, in a computer simulation a small perturbation may be introduced by numerical round-off, while, in the real world, systems are invariably perturbed by noise. Thus, if a system is chaotic, these small perturbations quickly (indeed, exponentially) grow until they completely change the behavior of the system.

Paradoxically, the cause of the despair is also the reason to hope. Because if a system is so sensitive to small changes, could not small changes be used to control it? This realization led Ott, Grebogi and Yorke [10] (OGY) to propose an ingenious and versatile method for the control of chaos, the details of which are given in the following section.

3. The idea of control

At which the universal host up sent
A shout that tore hell's concave, and beyond
Frighted the reign of Chaos and old Night.

John Milton, "Paradise Lost"

The starting point for the control of chaos is the phase space of the system. Dynamical systems trace smooth trajectories in phase space as they proceed forward in time. For periodic systems these trajectories are curves that are traced repeatedly every period of the system. For example, the phase space of a driven simple pendulum consists of one dimension for its position and one dimension for its momentum. The trajectory of the pendulum in this space is simply a circle which is traced over and over, as

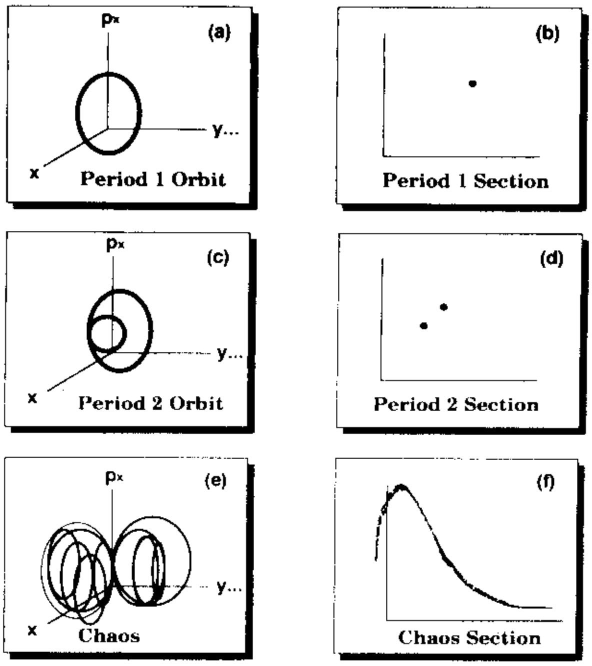

Fig. 1. Phase space trajectories (a), (c), (e) and their corresponding Poincaré sections (b), (d), (f) for period 1, period 2 and chaotic orbits.

in Fig. 1a. This trajectory contains all the information that is needed to predict the future dynamics of the system. In fact it contains too much information. A more useful representation can be obtained by cutting through this phase space with a plane which intersects the circle in two places. The infinite number of points on the circle trajectory has been reduced to merely two. If we further confine ourselves to *directed* piercings of the plane, we are left with only a single point (Fig. 1b). Such a *Poincaré section* reduces our information to a manageable level.

If our experiment were more complex, perhaps a driven pendulum with two masses placed at different points on a flexible string or the simple pendulum driven well beyond its linear regime, more complex motions might occur. One such might be a motion in which the trajectory traced a double loop in its phase space (Fig. 1c). A Poincaré section through this trajectory would show two points (Fig. 1d). This pendulum could, of course, still execute a simple, single loop trajectory given the right initial conditions and parameters. This single loop defines the *period one* trajectory of the system. The double loop trajectory takes twice as long and is accordingly dubbed *period two*. The usefulness of the Poincaré section is now apparent: the number of points in the section immediately reveals the underlying periodicity of the system. Generally, any periodic system of period n will have a section which consists of a finite set of n distinct points which reflect the fundamental periodicity of the system.

By way of contrast, a truly random system will behave in such a way that the trajectories in phase space wander over the entire volume of space available to the system. Its corresponding section will be filled uniformly and densely.

Chaos falls between these two extremes. If chaos were merely a superposition of a number of periodic motions, one might expect to see a finite number of points indicating several periodic motions characteristic of the chaotic section. However, since chaos is better thought of as the superposition of an *infinite* number of periodic motions, the number of points in the section is also infinite. In general, these points form an extended geometric structure, called the system's *chaotic attractor*, which is not a finite set of points (i.e., does not represent periodic motion) and which also does not fill space (i.e., is not random), as shown in Fig. 1f. (Generally a chaotic attractor is a fractal object.) Knowledge of this attractor and of its response to a small perturbations of the system are the only ingredients that are necessary for the control of chaos.

In order to control chaos according to the OGY scheme, it is only necessary to identify an unstable periodic point in the attractor, to characterize the shape of the attractor locally around that point and to determine the response of the attractor at that point to an external stimulus. Let's look at each of these three steps in detail.

The identification of unstable periodic motions is fairly straightforward process of looking for close returns in the Poincaré section. (Of course it is easier to find points with low order periodicity (small n), but chaos control has been successfully implemented to select periodic motions of order up to about 90!) This is one of the strengths of the OGY method of control: the ability to control on any period motion from the infinity of motions present in the system. This capability would allow an engineering to design highly flexible systems employing chaos control.

Characterizing the shape of the attractor is also easy. Once we have determined which unstable fixed point we wish to control about, we observe the motion of the point representing the current state of the system (*system state point*) on the attractor. In low dimensional chaotic systems, this point will occasionally approach the vicinity of our chosen unstable fixed point and then move away again. It turns out that, in the neighborhood of the unstable fixed point, the approach is consistently along the same direction (called the *stable direction*) and the departure along another direction (called the *unstable direction*), as indicated in Fig. 2. These two directions, one of which is stable (incoming) and the other of which is unstable (departing), form a saddle around the unstable fixed point. These *eigenvectors*, along with the speed with which the system state point approaches or departs the vicinity of the unstable fixed point (*stable* or *unstable eigenvalues* respectively), are all that is necessary to characterize the shape of the attractor locally around our chosen point.

The final criterion, determining the response of the attractor to an external stimulus, is perhaps the most difficult of the three to learn. Here we must introduce a change into the system by varying one of the system parameters. The difficulty lies in first identifying the system parameters and then locating one that may be quickly changed. (More on this will be discussed in the experimental section below.) Once such an identification has been made, the position of the unstable fixed point is measured for several values of the parameter just slightly different from the nominal value (Fig. 3). These measurements tell us the change of the attractor position with respect to a change in the system parameter and complete the knowledge of the system

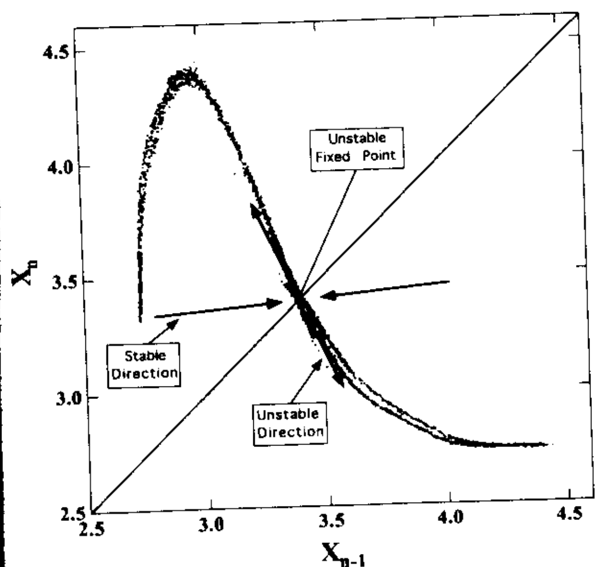

Fig. 2. The geometry around an unstable fixed point on a chaotic attractor. The shape is that of a saddle.

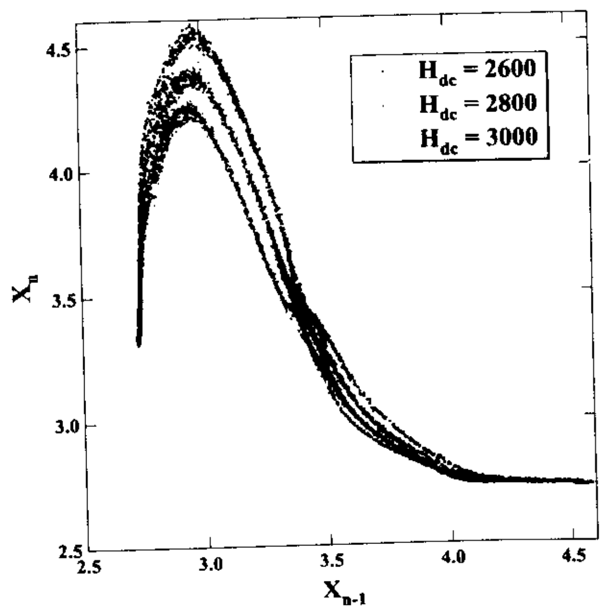

Fig. 3. Determining the response of a chaotic attractor to a change in a system parameter, H_{dc}. The change in the unstable fixed point position with a change in the parameter yields the vector quantity g.

needed for control. We now have all the information needed to control chaos.

4. The fundamental equations for the control of chaos

The fundamental error of their matrimonial union; that of having based a permanent contract on a temporary feeling.

Thomas Hardy, "Jude the Obscure"

4.1. Perturbing a fixed point

Consider a two dimensional space

$$\boldsymbol{x} = \begin{bmatrix} x_1 \\ x_2 \end{bmatrix} \quad \text{or} \quad \boldsymbol{x}^{\mathrm{T}} = [x_1 \quad x_2] \,. \tag{1}$$

In this space there is a map that depends on a parameter p,

$$\boldsymbol{x}_{n+1} = f(\boldsymbol{x}_n, p) \,. \tag{2}$$

This map has a fixed point whose location also depends on the parameter p:

$$\boldsymbol{x}_{\mathrm{F}} = f(\boldsymbol{x}_{\mathrm{F}}, p) \,. \tag{3}$$

Change the parameter every iteration and the fixed point changes:

$$\boldsymbol{x}_{\mathrm{F}}(p_n) = f(\boldsymbol{x}_{\mathrm{F}}(p_n), p_n) \,. \tag{4}$$

This is shown graphically in Fig. 4a. The perturbed, or shifted, fixed point can be estimated with the aid of the following *shift vector* $\boldsymbol{s}$:

$$\boldsymbol{x}_{\mathrm{F}}(p_{n+1}) \sim \boldsymbol{x}_{\mathrm{F}}(p_n) + (p_{n+1} - p_n)\boldsymbol{s} \,, \tag{5}$$

$$\boldsymbol{s} \equiv \frac{\mathrm{d}}{\mathrm{d}p} \boldsymbol{x}_{\mathrm{F}}(p)|_{p = p_n} \sim \frac{\boldsymbol{x}_{\mathrm{F}}(p_{n+1}) - \boldsymbol{x}_{\mathrm{F}}(p_n)}{p_{n+1} - p_n} \,. \tag{6}$$

4.2. Linearize about a fixed point

Represent the map in the vicinity of the fixed point by a two dimensional square matrix.

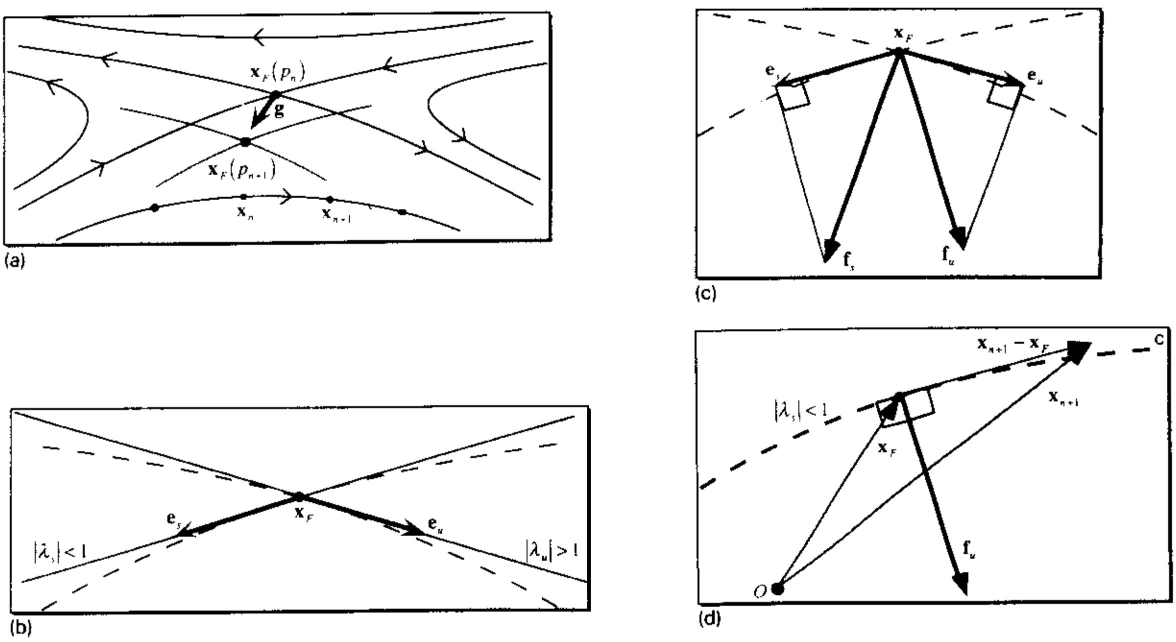

Fig. 4. (a) Movement of unstable fixed point due to parameter change. (b) The eigenvectors around the unstable fixed point which may be nonorthogonal, $\boldsymbol{e}_u^{\mathrm{T}}\boldsymbol{e}_s \neq 0$. The eigenvalues satisfy $|\lambda_s| < 1 < |\lambda_u|$. (c) New "perpendicular" basis vectors $\{\boldsymbol{f}_u, \boldsymbol{f}_s\}$ in terms of old "parallel" basis vectors $\{\boldsymbol{e}_u, \boldsymbol{e}_s\}$ found by demanding $\boldsymbol{f}_s^{\mathrm{T}}\boldsymbol{e}_s = 1 = \boldsymbol{f}_u^{\mathrm{T}}\boldsymbol{e}_u$ and $\boldsymbol{f}_u^{\mathrm{T}}\boldsymbol{e}_s = 0 = \boldsymbol{f}_s^{\mathrm{T}}\boldsymbol{e}_u$. (d) Graphical representation of an iterate of the map near the unstable fixed point. Control is achieved by changing a system parameter such that the projection of $\boldsymbol{x}_{\mathrm{F}} - \boldsymbol{x}_{n+1}$ onto $\boldsymbol{f}_u$ is zero as shown. In words this is simply the requirement that there be no relative motion between the fixed point $\boldsymbol{x}_{\mathrm{F}}$ and the mapped point $\boldsymbol{x}_{n+1}$ perpendicular to the stable direction.

$$(x_{n+1} - x_F) \sim M(x_n - x_F)\,, \tag{7}$$

$$x_{n+1} \sim x_F + M(x_n - x_F)\,. \tag{8}$$

The matrix M is characterized by its eigenvectors and eigenvalues:

$$Me_u = \lambda_u e_u\,, \tag{9a}$$

$$Me_s = \lambda_s e_s\,, \tag{9b}$$

where the subscripts u and s correspond to the unstable and stable directions respectively. The eigenvectors are normalized, $e_u^T e_u = 1$ and $e_s^T e_s = 1$, but may be nonorthogonal, $e_u^T e_s \neq 0$ as shown in Fig. 4b. The eigenvalues satisfy $|\lambda_s| < 1 < |\lambda_u|$.

4.3. Manipulate block matrices to solve for M

$$[Me_u \quad Me_s] = [\lambda_u e_u \quad \lambda_s e_s]\,, \tag{10}$$

$$M[e_u \quad e_s] = [e_u \quad e_s]\begin{bmatrix}\lambda_u & 0\\ 0 & \lambda_s\end{bmatrix}, \tag{11}$$

$$M = [e_u \quad e_s]\begin{bmatrix}\lambda_u & 0\\ 0 & \lambda_s\end{bmatrix}[e_u \quad e_s]^{-1}\,. \tag{12}$$

4.4. Introduce new basis vectors at the fixed point

Define new "perpendicular" basis vectors $\{f_u, f_s\}$ in terms of old "parallel" basis vectors $\{e_u, e_s\}$ by demanding $f_s^T e_s = 1 = f_u^T e_u$ and $f_u^T e_s = 0 = f_s^T e_u$ as shown in Fig. 4c. These basis vectors are simply related:

$$[f_u \quad f_s]^T[e_u \quad e_s] = \begin{bmatrix}f_u^T\\ f_s^T\end{bmatrix}[e_u \quad e_s]$$
$$= \begin{bmatrix}f_u^T & f_u^T e_s\\ f_s^T e_u & f_s^T e_s\end{bmatrix} = \begin{bmatrix}1 & 0\\ 0 & 1\end{bmatrix} = \mathbf{1}\,, \tag{13}$$

$$\begin{bmatrix}f_u^T\\ f_s^T\end{bmatrix} = [e_u \quad e_s]^{-1}\,. \tag{14}$$

This matrix equation may be solved to explicitly relate components.

$$\begin{bmatrix}f_{u1} & f_{u2}\\ f_{s1} & f_{s2}\end{bmatrix} = \begin{bmatrix}e_{u1} & e_{s1}\\ e_{u2} & e_{s2}\end{bmatrix}$$
$$= \frac{1}{e_{u1}e_{s2} - e_{s1}e_{u2}}\begin{bmatrix}e_{s2} & -e_{s1}\\ -e_{u2} & e_{u1}\end{bmatrix}, \tag{15}$$

$$f_{u1} = \frac{e_{s2}}{e_{u1}e_{s2} - e_{s1}e_{u2}} \quad \text{and} \quad f_{u2} = \frac{-e_{s1}}{e_{u1}e_{s2} - e_{s1}e_{u2}}\,, \tag{16a}$$

$$f_{s1} = \frac{-e_{u2}}{e_{u1}e_{s2} - e_{s1}e_{u2}} \quad \text{and} \quad f_{s2} = \frac{e_{u1}}{e_{u1}e_{s2} - e_{s1}e_{u2}}\,. \tag{16b}$$

M may be expressed in terms of the parallel and perpendicular basis vectors,

$$M = [e_u \quad e_s]\begin{bmatrix}\lambda_u & 0\\ 0 & \lambda_s\end{bmatrix}\begin{bmatrix}f_u^T\\ f_s^T\end{bmatrix}$$
$$= [e_u \quad e_s]\begin{bmatrix}\lambda_u f_u^T\\ \lambda_s f_s^T\end{bmatrix} = \lambda_u e_u f_u^T + \lambda_s e_s f_s^T\,. \tag{17}$$

This implies the following useful result:

$$f_u^T M = f_u^T(\lambda_u e_u f_u^T + \lambda_s e_s f_s^T)$$
$$= \lambda_u f_u^T e_u f_u^T + \lambda_s f_u^T e_s f_s^T$$
$$= \lambda_u 1 f_u^T + \lambda_s 0 f_s^T = \lambda_u f_u^T\,. \tag{18}$$

Thus f_u^T is a left eigenvector of M with the same eigenvalues as e_u.

4.5. Determine value of control parameter

To achieve control we demand that the next iterate fall near the stable direction. This yields the following condition (as illustrated as Fig. 4d):

$$f_u^T(x_{n+1} - x_F(p_n)) = 0\,. \tag{19}$$

That is the vector displacement from the fixed point to the next iterate has no component along f_u^T.

4.6. OGY formula

For concreteness, imagine shifting the fixed point just before applying the mapping. That is, consider the following sequence:

$$\boldsymbol{s}: \boldsymbol{x}_F(p_n) \to \boldsymbol{x}_F(p_{n+1}) \,, \tag{20}$$

$$\boldsymbol{M}: \boldsymbol{x}_n \to \boldsymbol{x}_{n+1} \,. \tag{21}$$

Expand the shift and the map:

$$(\boldsymbol{x}_{n+1} - \boldsymbol{x}_F(p_{n+1})) \sim \boldsymbol{M}(\boldsymbol{x}_n - \boldsymbol{x}_F(p_{n+1})) \,. \tag{22}$$

Using Eq. (5) we find

$$\begin{aligned}(\boldsymbol{x}_{n+1} &- \boldsymbol{x}_F(p_n) - (p_{n+1} - p_n)\boldsymbol{s} \\ &\sim \boldsymbol{M}(\boldsymbol{x}_n - \boldsymbol{x}_F(p_n) - (p_{n+1} - p_n)\boldsymbol{s}) \,.\end{aligned} \tag{23}$$

Project this result on $\boldsymbol{f}_u^T$:

$$\begin{aligned}&\boldsymbol{f}_u^T(\boldsymbol{x}_{n+1} - \boldsymbol{x}_F(p_n) - (p_{n+1} - p_n)\boldsymbol{s}) \\ &\quad \sim \lambda_u \boldsymbol{f}_u^T(\boldsymbol{x}_n - \boldsymbol{x}_F(p_n) - (p_{n+1} - p_n)\boldsymbol{s}) \,.\end{aligned} \tag{24}$$

Using Eq. (19) and defining $\delta p_n \equiv p_{n+1} - p_n$ and $\delta \boldsymbol{x}_n \equiv \boldsymbol{x}_n - \boldsymbol{x}_F(p_n)$:

$$\boldsymbol{0} - \delta p_n \boldsymbol{f}_u^T \boldsymbol{s} \sim \lambda_u \boldsymbol{f}_u^T \delta \boldsymbol{x}_n - \delta p_n \lambda_u \boldsymbol{f}_u^T \boldsymbol{s} \,, \tag{25}$$

$$\delta p_n(\lambda_u - 1) \boldsymbol{f}_u^T \boldsymbol{s} \sim \lambda_u \boldsymbol{f}_u^T \delta \boldsymbol{x}_n \,, \tag{26}$$

$$\delta p_n \sim \frac{\lambda_u}{\lambda_u - 1} \frac{\boldsymbol{f}_u^T \delta \boldsymbol{x}_n}{\boldsymbol{f}_u^T \boldsymbol{s}} \,, \tag{27}$$

this is the formula of Ott, Grebogi, and Yorke [10].

4.7. Alternate formula

Alternately, imagine shifting and mapping simultaneously.

$$(\boldsymbol{x}_{n+1} - \boldsymbol{x}_F(p_{n+1})) \sim \boldsymbol{M}'(\boldsymbol{x}_n - \boldsymbol{x}_F(p_n)) \qquad (28))$$

(compare Eqs. (28) and (22).) As before, expand the shift and map, project onto $\boldsymbol{f}_u^T$, and simplify:

$$\begin{aligned}(\boldsymbol{x}_{n+1} &- \boldsymbol{x}_F(p_n) - (p_{n+1} - p_n)\boldsymbol{s}) \\ &\sim \boldsymbol{M}'(\boldsymbol{x}_n - \boldsymbol{x}_F(p_n)) \,,\end{aligned} \tag{29}$$

$$\begin{aligned}&\boldsymbol{f}_u^T(\boldsymbol{x}_{n+1} - \boldsymbol{x}_F(p_n) - (p_{n+1} - p_n)\boldsymbol{s}) \\ &\quad \sim \lambda_u' \boldsymbol{f}_u'^T(\boldsymbol{x}_n - \boldsymbol{x}_F(p_n)) \,,\end{aligned} \tag{30}$$

$$\boldsymbol{0} - \delta p_n \boldsymbol{f}_u'^T \boldsymbol{s} \sim \lambda_u' \boldsymbol{f}_u'^T \delta \boldsymbol{x}_n \,, \tag{31}$$

$$\delta p_n \sim -\lambda_u' \frac{\boldsymbol{f}_u'^T \delta \boldsymbol{x}_n}{\boldsymbol{f}_u'^T \boldsymbol{s}} \,. \tag{32}$$

This is the alternate, slightly simpler formula of Dressler and Nitsche [13].

4.8. Summary and discussion

The control formulas can be summarized by the following:

$$\delta p_n = C \boldsymbol{f}_u^T \delta \boldsymbol{x}_n \,, \tag{33}$$

δp_n is the amount one needs to change the system parameter from its nominal value in order to control the system. The perturbation δp_n is updated once every period of the system. It is proportional to the distance of the system state point, $\boldsymbol{x}_n$, from the fixed point, $\boldsymbol{x}_F$, projected onto the perpendicular unstable direction, $\boldsymbol{f}_u$. The constant C is itself calculable from the shift of the attractor position with respect to a change in the system parameter, $\boldsymbol{s}$, projected onto the perpendicular unstable direction $\boldsymbol{f}_u$ and from the value of the unstable eigenvalue, λ_u. All of these are known from our earlier measurements.

A simplified example may serve to clarify the matter. Fig. 5a shows an unstable fixed point with its stable and unstable directions. The system state point, $\boldsymbol{x}_n$, is shown approaching the fixed point near the stable *manifold*. If left to itself, the natural motion of the system would be to approach the unstable fixed point along the

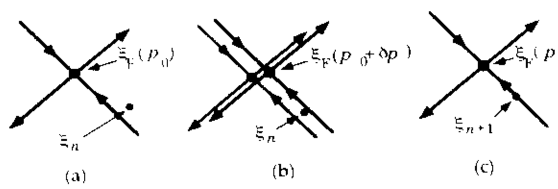

Fig. 5. An outline of the OGY control method: (a) the system state point approaches the unstable fixed point. It will naturally tend to move in along the stable direction and out along the unstable direction; (b) the saddle point (unstable fixed point) is positioned so that the system state point tends to move back toward the original unstable fixed point; (c) the system state point reaches the original unstable fixed point and the perturbation is turned off. In real-world systems with noise, the control would have to applied continuously to balance the state point onto the stable direction and hence onto the unstable fixed point.

stable direction and then move away from the fixed point along the unstable manifold (towards the upper right). However, if we introduce the OGY perturbation into the system, we move the unstable fixed point and its accompanying manifolds to the other side of the system state point (Fig. 5b). The new motion of the system state point will still be along the stable manifold with motion away from the *new* fixed point along the unstable manifold (towards the lower left). However this is motion towards the old unstable fixed point. Thus the OGY scheme has controlled the system exactly onto the original stable manifold and thus into the unstable fixed point (Fig. 5c). In a perfect world, it would remain there forever. However if there is even the slightest error in the calculation of C it will only move close to the fixed point. Or in the presence of noise it will be perturbed from the fixed point after it has reached it. Both of these problems are easily handled by repeating the OGY control once each period of the system.

This act of moving the saddle point to control the motion of the system state point is similar to balancing a baseball on a saddle. Small movements of the saddle keep the ball at the point of unstable equilibrium; it is not necessary to change the shape or nature of the saddle itself.

Many methods of "control" have been proposed. Those related to the OGY method [9,11] use perturbations that are typically small (a few percent of the magnitude of the accessible system parameter). Thus it is easy to design systems that implement this control. This is in sharp contrast to the model-based methods [12] which seek to fundamentally change the nature of the chaotic system under study by introducing "perturbations" to the adjustable parameter that are comparable to its size. Such methods are more properly named the "removal of chaos" rather than "control" because they fundamentally change the nature of the system under study. The gentle nudges prescribed by OGY control leave the fundamental dynamics of the system essentially unchanged. The fixed point and its manifolds are only shifted slightly by the perturbation and, between perturbations, the motion of the system remains chaotic, moving on an attractor that differs little from the original. It is only in the long term, when *averaged* over many periods and over motion on several slightly different attractors, that the motion is non-chaotic. In this sense the OGY method is truly a *control* of chaos and hence it is able to select any of the periodic orbits that are embedded in the chaotic motion.

5. Experimental realities

In all chaos there is a cosmos,
in all disorder a secret order.

Carl Jung

An experimental physicist's first reaction to the OGY scheme might well be one of horror; in any real-world system the number of degrees of freedom (positions plus momenta) may be quite large, possibly even infinite and the OGY scheme requires the measurement of all of them! Two facts conspire to make the OGY method not only possible but also simple to implement.

The first is that many physical systems, while technically infinite dimensional, actually only express a small number of these dimensions. Thus even though the magnetomechanical ribbon (discussed below) is a distributed mass system and therefore technically infinite dimensional, its motion is quite low dimensional and its attractor is well represented in a three dimensional phase space and hence a two dimensional Poincaré section. Thus only two experimental variables need to be measured to correctly characterize its chaotic attractor.

The second fact of importance to the experimentalist is that the Poincaré section may be replaced in the OGY scheme by a *delay coordinate embedding*. This embedding relies on the intuition that the information obtained by measuring all the system variables (positions and momenta) at one given time may also be obtained by measuring only one system variable at several subsequent times. The system state vector (the set of all the positions and momenta, $x_n = (x^1(t_n),\ x^2(t_n), \ldots, p^1(t_n),\ p^2(t_n), \ldots))$, is replaced by a delay coordinate vector, $(x^i(t_n),\ x^i(t_n - \Delta t), x^i(t_n - 2\,\Delta t), x^i(t_n - 3\,\Delta t), \ldots)$, where the superscript i indicates one particular experimental measurable and where Δt is some appropriately chosen delay, (For the section, if the system is periodically driven, Δt is usually chosen to be the period of the driving force. In non-driven systems the appropriate delay is usually related to some fundamental time scale inherent in the system.) In fact it may be shown that the attractor as represented in the phase space and the attractor reconstructed from the delay coordinate embedding have the same topological properties, thereby allowing one to be substituted for the other with (relative) impunity [13].

With these two simplifications in hand, control of low dimensional chaotic systems becomes straightforward. In fact it turns out that the OGY method is also extremely robust. By this we mean that, as long as the perturbation δp is sufficient to move the saddle point to the opposite side of the system state point as shown in Fig. 5b, it does not matter if the saddle is moved well past the state point or just barely past it. The corollary to this is that the control scheme is quite resistant to external noise and to errors arising from imprecision in the measurement of the position and shape of the attractor.

We note in passing that Eq. (33) give rise to two variant methods of control. In the first method, one completely measures all the items mentioned above, calculates the constant C, and then proceeds to control the system. The alternative arises from the fact that, although many values (λ_u, f_u and g) are needed to characterize the attractor, they are all folded into the single constant C. Thus, if a period of adjustment can be tolerated, one might simply guess a value of C and then adjust it empirically until control is achieved. This latter method, requiring knowledge only of the location of the desired fixed point and an educated guess at C makes this quite suitable for incorporation into automatic control systems.

6. Implementations of control

Not chaos-like together crushed and bruised
But, as the world, harmoniously confused.

Alexander Pope, "Windsor Forest"

6.1. Mechanics

The first experimental control of chaos was achieved in a magnetoelastic ribbon experiment [4]. This system is sketched in Fig. 6. The ribbon, an amorphous magnetic material about 100 mm long by 3 mm wide by 0.025 mm thick, is extremely nonlinear in its response to a magnetic field. In zero field it is stiff enough to support its own weight in an upright position. When a small magnetic field is applied, its stiffness decreases by an order of magnitude and the ribbon buckles under its own weight. At still larger fields, the material again becomes stiff and resumes an upright position. If a magnetic field, $\boldsymbol{H}_{dc}$, is applied to start the ribbon in the soft regime and to that is added an ac magnetic field, $\boldsymbol{H}_{ac}$, that alternately takes the ribbon from soft to stiff and back again at some frequency, f, the ribbon will oscillate about its equilibrium point. At high enough values of $\boldsymbol{H}_{ac}$ and f, the ribbon's motion will become chaotic.

The positions of the ribbon is measured once

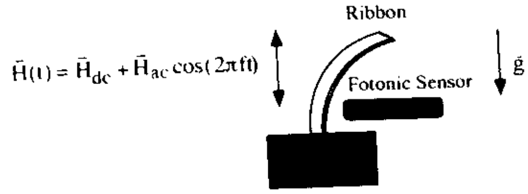

Fig. 6. Schematic of the magnetoelastic ribbon experiment.

each period, $T = 1/f \approx 1$ Hz, of the driving field by means of a beam of light directed at a small spot on the ribbon. The intensity of the reflected light varies as $1/r^2$, yielding highly accurate and noise-free measurements of the ribbon position. These are sent to the computer controlling the experiment, which also control the strengths of the magnetic fields. In theory, either of the three system parameters, H_{dc}, H_{ac} or f, could be used to control the chaos. We choose to use H_{dc}. The gray data in Fig. 7a show the position of the ribbon as a function of time when the ribbon is moving chaotically. When the computer initiates the period 1 control, the position of the ribbon (measured once each period T; i.e., stroboscopically) is shown in black in Fig. 7a. The corresponding attractor (plotted as a delay coordinate embedding and with the same color coding) is shown in Fig. 7b.

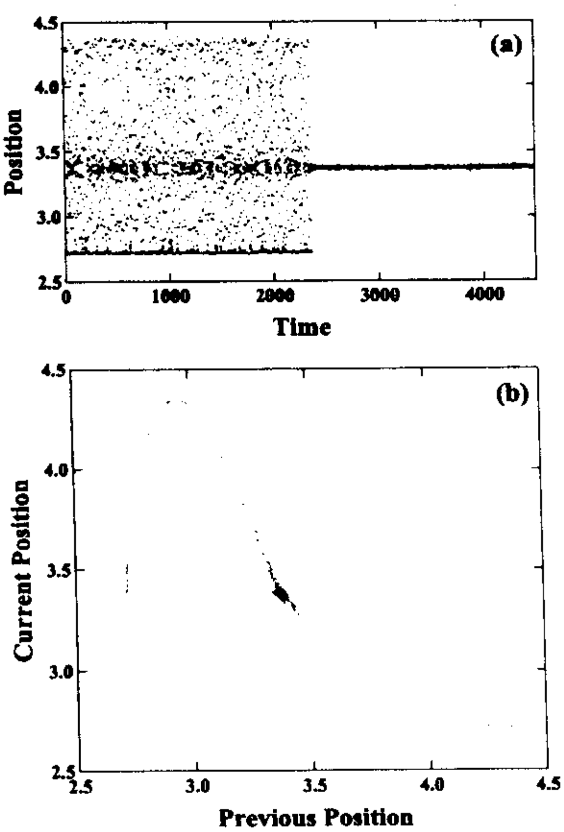

Fig. 7. (a) Ribbon position as a function of time for chaotic motion (grey) followed by controlled motion (black); (b) The same data presented as a delay coordinate embedding.

As mentioned above the OGY method may select any of a number of periods from the chaotic signal. Fig. 8 shows the same system switching from chaos to period 4 to period 1 to period 2 to period 1 and finally back to period 4. There are interludes of chaos between each section of control because the computer must wait for the ribbon's position to approach the vicinity of the new unstable fixed point. This time can actually be decreased by a new technique called targeting [14,15], in which the sensitivity of the chaotic system to small perturbations plus a *global* (but still empirical) knowledge of the chaotic attractor are employed to direct the system rapidly to any desired point on the attractor.

The question arises as to whether one might control about a point that does not lie on the chaotic attractor. It turns out that the difficulty in such a case lies not in the control itself, but in getting the system to the vicinity of the desired point. For if the point in question is not on the attractor, it will never be visited. However, once control is established at a "normal" unstable fixed point, it is often possible to adjust some system parameter (in this case the temperature) so that the attractor smoothly changes to one that does not include the point in question. Yet it has been shown experimentally that the control will be maintained about this point. The reason is that, although the point is no longer part of the attractor, the local geometry about the point has not changed appreciably and thus the algorithm still calculates the proper control perturbations. This is an important result for understanding the robustness of the method even under large changes to the system itself.

6.2. *Electronics*

In an experiment [3] of great potential importance for our electronics-based world, Earle Hunt of Ohio University also used the empirical

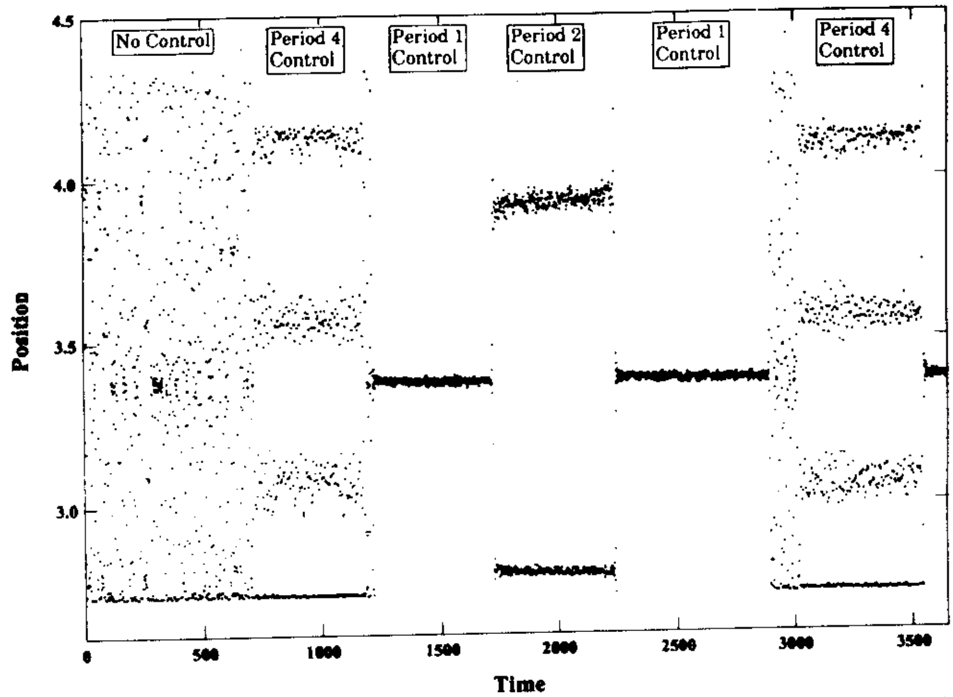

Fig. 8. The ability of the OGY method to select out various periodic motions from those comprising the chaotic motion. (Note that the fact that the motions presented here are all a power of two is purely coincidental; the control could have as easily been performed about the period 3 or period 5 motion instead.)

version of the OGY scheme to control the chaotic oscillations of a diode resonator. The significance of his experiment lies in the extension of the applicability of the method to high frequencies (53 kHz) and in his ability to control high periods (his current record is period 87!).

6.3. Lasers

In conjunction with Hunt, Rajarshi Roy et al. [6] of Georgia Tech controlled the chaotic oscillations of a chaotic multimode laser. This laser would autonomously become chaotic at pumping levels exceeding a certain threshold. The system is somewhat higher dimensional than the previous systems, making the control more difficult to obtain. Additionally the system is not periodically driven, making it necessary to choose a "natural periodicity characteristic of the system" as the time scale for analyzing their data and applying the control signals. A third intricacy is that the natural frequency mentioned above is on the order of hundreds of kilohertz. They developed a method related to the OGY method to control of the system up to period 9. Thus the laser could be operated stably at power levels exceeding by as much as a factor of 15 those which might be attained without chaos control.

6.4. Biology

The authors have recently extended the techniques of chaos control to the field of biology [7]. In this experiment a section of a rabbit's heart was induced to beat chaotically by the injection of the drug ouabain. The measurable quantity here is the interval between heartbeats, which is about 0.8 sec in the healthy tissue. The effect of the drug is to accelerate the heartbeat and to cause the interbeat intervals to vary chaotically. The chaotic attractor for this situation is shown in Fig. 9a.

There are several factors that distinguish this experiment from the earlier successes at chaos control. The first is that the data for the delay coordinate embedding are no longer equally spaced in time, but are rather intervals between events. The second factor is that there are no adjustable system parameters that may be modified quickly enough to implement the unmodified OGY control scheme. The authors accordingly developed a method whereby the perturbation is applied directly to the system variables, rather than to some system parameter. This method uses the same local linearization around the unstable fixed point as used by OGY, but instead of moving the saddle point to the system state point, this method moves the system state point back to the saddle by giving the state point small nudges equal in magnitude but opposite in sign to those yielded by eqs. 1 and 2. To calculate these nudges it was necessary to use the observed chaotic attractor to predict the time of the next heartbeat. Then an electrical stimulus was used to induce a heartbeat before the predicted natural beat could occur, thereby shortening the next interbeat interval. The amount of time to advance the next beat was calculated so as to place the system state point (Fig. 9b) directly onto the stable direction of the attractor. Thus the succeeding beat would tend to naturally move toward the desired unstable fixed point rather than away from it.

The results are shown in Fig. 10. It was not possible in these early experiments to achieve a good period 1 (i.e., "normal") heartbeat. But it was possible to control the chaos consistently into a period 3 beat, which, while not optimal, is better for pumping blood than chaotic beating.

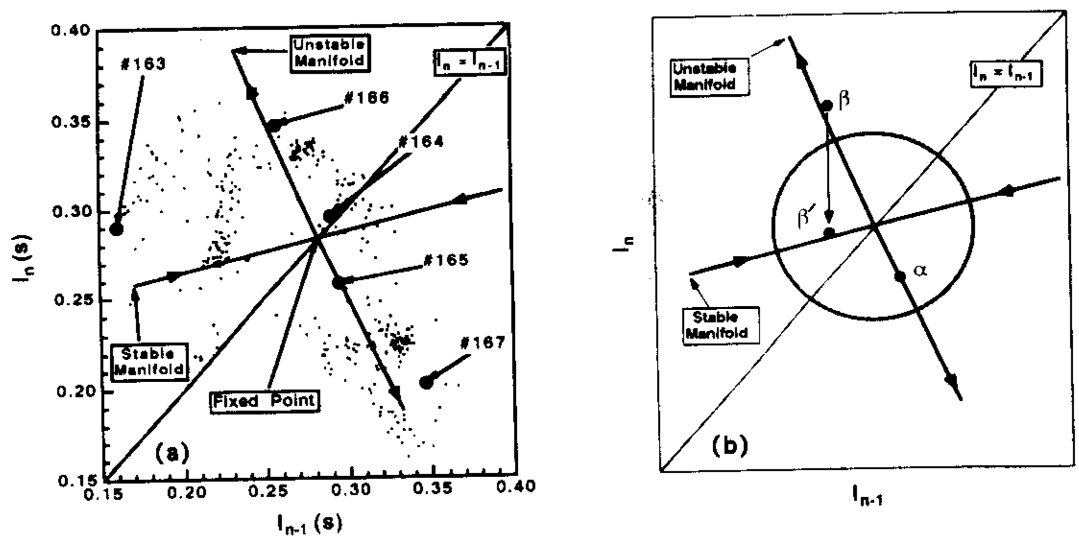

Fig. 9. Current interbeat interval, I_n, versus previous interbeat interval, I_{n-1}, for the rabbit heart experiment. (a) Starting with point 163, the system approaches the unstable fixed point along the stable direction and then leaves it along the unstable directions. (The unstable eigenvalue is negative, thereby causing subsequent points to alternate above and below the unstable fixed point. However the *distance* from the fixed point increases in an experimental fashion, as is typical of chaotic motion.) (b) An idealized drawing of the control. The point α should be identified with point 165 in (a). The next point would naturally tend to be β (point 166). However a stimulus is applied to the heart causing it to beat early and thereby shortening the next interbeat interval to β' on the stable manifold. Thus the next interval will tend to move along the stable manifold toward the fixed point.

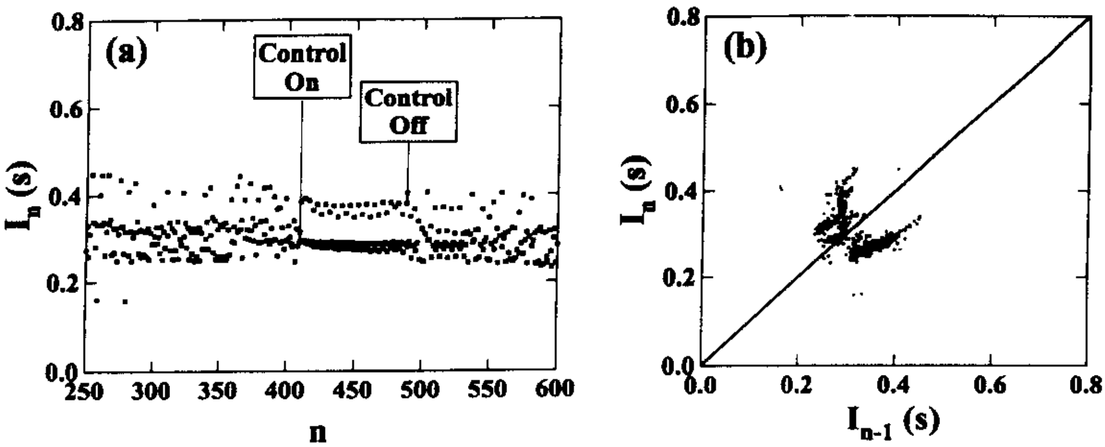

Fig. 10. (a) Interbeat intervals as a function of time for the rabbit heart experiment. (b) Delay coordinate embedding for the same data. The pre-control data is grey, while the controlled data is shown in black.

As for the relevance to human heart arrhythmias, there is evidence that atrial and ventricular fibrillation may be examples of chaos. Thus future work may be able to present strategies for dealing with these serious and widespread arrhythmias.

6.5. Chemistry

The best known oscillatory chemical reaction, the Belousov–Zhabotinsky reaction, may exhibit either periodic or chaotic signatures, depending on the flow rates of the reactants into the tank. These rates comprise the system parameters to be used for control. The variable that is measured is the voltage of a bromide electrode inserted into the tank. Using the OGY method, Petrov et al. [8] at West Virginia University were able to stabilize both period 1 and 2 oscillations in their reactor.

Rollins et al. [9] at Ohio University have also applied chaos control to a chemical system. They developed a recursive method (based on the Dressler and Nitsche modification of the OGY method) that makes available a wider choice of accessible system parameter for use in controlling the chaos.

7. Future of control

Chaos often breeds life, when order breeds habit.

Henry B. Adams, "The Education of Henry Adams"

7.1. Theory

Two fundamental questions dominate future chaos control theories. The first is the problem of controlling higher dimensional chaos in physical systems. A start has been made in this direction in a recent paper by Auerbach, Grebogi, Ott and Yorke [16] on controlling chaos in systems of arbitrarily high dimensions. The method can be "implemented directly from time series data, irrespective of the overall dimension of the phase space." Although applied in numerical studies, this method has yet to be tested experimentally.

The second question has yet to be addressed: the problem of control in a spatiotemporal system. Many fluid dynamical and biological systems may be modeled as a multi-dimensional array of oscillators connected to each in some complex fashion. Such systems exhibit both spatial as well as temporal chaos. The study of such systems, while of obvious importance for real-world applications, is as yet in its infancy.

7.2. Experiment

The importance of chaos control in electronic circuits was mentioned above and should be stressed once again. In a world dominated by electronics, the ability not only to remove chaos where it is not wanted, but also to make more flexible circuitry by exploring chaos and its control could have a tremendous impact on our lives. The control of chemical reactions is no less important, since an increase of only a few percent in the efficiency of a commercial chemical reaction could conceivably save millions of dollars. The 15-fold increase in the power at which a laser can be operated stably promises new applications for these modern tools. And the ability to control one of the great diseases of modern times could be a boon beyond reckoning. The challenge for experimentalists now lies not only in achieving control of higher dimensional and spatiotemporal chaos, but also in guiding the achievements of the past three years out of the laboratory and into our lives.

References

[1] J. Gleick, Chaos (Viking, New York, 1987) p. 65; see also T.-Y. Li and J.A. Yorke, Amer. Math. Monthly 82 (1975) 985.
[2] E.N. Lorenz, J. Atmos. Sci. 20 (1963) 130.
[3] E.R. Hunt, Phys. Rev. Lett. 67 (1991) 53.
[4] W.L. Ditto, S.N. Rauseo and M.L. Spano, Phys. Rev. Lett. 65 (1990) 3211.
[5] G.J. Sussman and J. Wisdom, Science 241 (1988) 433.
[6] R. Roy, T.W. Murphy, Jr., T.D. Maier and Z. Gills, Phys. Rev. Lett. 68 (1992) 1259.
[7] A. Garfinkel, M.L Spano, W.L. Ditto and J.N. Weiss, Science 257 (1992) 1230.
[8] V. Petrov, V. Gaspar, J. Masere and K. Showalter, Nature 361 (1993) 240.
[9] R.W. Rollins, P. Parmananda and P. Sherard, Phys. Rev. E 47 (1993) R780.
[10] E. Ott, C. Grebogi and J.A. Yorke, Phys. Rev. Lett. 64 (1990) 1196.
[11] B. Peng, V. Petrov and K. Showalter, J. Chem. Phys. 95 (1991) 4957.
[12] A. Hubler, Helv. Phys. Acta 62 (1989) 291.
[13] U. Dressler and G. Nitsche, Phys. Rev. Lett. 68 (1992) 1.
[14] T. Shinbrot, E. Ott, C. Grebogi and J.A. Yorke, Phys. Rev. Lett. 65 (1990) 3215; Phys. Rev. A 45 (1992) 4165.
[15] T. Shinbrot, W. Ditto, C. Grebogi, E. Ott, M. Spano and J.A. Yorke, Phys. Rev. Lett. 68 (1992) 2863.
[16] D. Auerbach, C. Grebogi, E. Ott and J.A. Yorke, Phys. Rev. Lett. 69 (1992) 3479.

Note to authors

Physica is published in four sections:

Physica A (*Statistical and theoretical physics*) contains papers in all fields of statistical physics as well as on general theoretical physics subjects. The emphasis of the journal is on fostering the interaction between experimental, theoretical and computational research in statistical physics. The field of statistical physics is meant to comprise any phenomena where the relationship between microscopic properties and macroscopic behaviour plays a role.

Physica B (*Condensed matter*) contains papers and review articles in the realm of physics of condensed matter. Both experimental and theoretical contributions are invited, although theoretical papers should preferably be related to experimental results.

Physica C (*Superconductivity*) serves as a rapid channel for publications on superconductivity and related subjects. This includes theoretical papers on the fundamental issues raised by high-T_c superconductivity, reports on measurements of a wide variety of physical properties of high-T_c superconductors, on new materials and new preparation techniques, on thin-film and device-oriented work and on theoretical results pertinent to such experiments. New results in the traditional areas of superconductivity as well as on novel phenomena (e.g., heavy-fermion superconductivity) will also be included.

Physica D (*Nonlinear phenomena*) contains papers and review articles reporting experiments, techniques and ideas which, although they may be derived and explained in the context of a particular field, advance the understanding of nonlinear phenomena in general. Contributions of this type in the recent literature have dealt with: wave motion in physical, chemical and biological systems; chaotic motion in models relevant to turbulence; quantum and statistical mechanics governed by nonlinear field equations; instability, bifurcation, pattern formation and cooperative phenomena.

Instructions to authors for Physica D

Submission. Manuscripts should be sent in *triplicate* to one of the editors or coordinating editors with preference given to those whose interests appear to be close to the subject of the paper (addresses given on the inside front cover page).

Submission of a paper will be taken to imply that it represents original work not previously published, that it is not being considered elsewhere for publication, and that if accepted for publication it will not be published elsewhere in the same form, in any language without the consent of the publisher.

The master copy and original drawings will be returned to the authors in case their paper is not accepted for publication.

Proposals for review articles (approximately 500–1000 words) should be sent to any one of the editors. The editors will evaluate each proposal on the basis of 1) subject matter and 2) presentation and readability.

Manuscripts should be written in English and typed with double spacing, wide margins and on one side of the page only.

The *title* should be concise and specific. The name of the institute where the research was carried out should be stated with each author's name.

An *abstract* of not more than 150 words should be provided in English, summarizing the new information and the author's conclusions.

Keywords (five or less) should be provided for the subject index, and, if possible, the appropriate PACS classification codes.

References in the text should be numbered (e.g., "Jones and Smith [1] have reported that . . .") in ascending order, and listed on a separate sheet stating the author, journal, volume and the year of publication (in brackets) and the number of the first page.

Example: [1] S. Jones and P. Smith, Phys. Rev. 190 (1964) 2016.

Formulae should be clearly written. Special attention should be paid to characters that can be easily misread, such as i (lower case), I (cap.), l (el), 1 (one), ′ (prime); o (lower case), O (cap.), 0 (zero), ° (degree); u, v (vee), ν (Greek nu), V (cap.); ×, x, X; z, Z; p, P, ρ (Greek rho); etc.

Drawings and any *lettering* should be done in India ink, or by means of a high-quality printing device. The figures should be numbered and the captions listed on a separate sheet.

Colour plates: Illustrations can be printed in colour when they are judged by the Editor to be essential to the presentation. The Publisher and the author will each bear part of the extra costs involved. Further information concerning colour illustrations and the cost to the author is available from the Publisher.

Proofs. Proofs will usually be printed on low-quality paper. Proofs will be sent to the author 4–6 weeks after acceptance. Please note that the proofs have been proofread by the Publisher and only a cursory check by the author is needed; we are unable to accept changes in, or additions to, the edited manuscript at this stage. In order to guarantee the fastest possible production times, the proofs must be returned within 48 hours after receipt, preferably by fax. If no reply is received from the author, the Publisher assumes that there are no further corrections to be made and will proceed with publication of the article.

Electronic submission. The Publisher welcomes the submission of your manuscript as an electronic file. If you have not yet already done so, please send the electronic file of your accepted manuscript directly to the Publisher at the address below. In this case please inform the Publisher immediately that an electronic manuscript is on its way. Please note that no deviations from the version accepted by the Editor of the Journal are permissible without the prior and explicit approval by the Editor. Such changes should be clearly indicated on an accompanying print-out of the file.

LaTeX papers. If the electronic file is suitable for processing by the publisher, the article will be published without rekeying the full text. The article should be encoded in LaTeX, preferably using the Elsevier document style 'elsart' or alternatively the standard document style 'article' or the document style 'revtex'.

The Elsevier LaTeX package (including detailed instructions to authors) can be obtained using anonymous FTP from the Comprehensive TeX Archive Network (CTAN):

Host name	*CTAN directory*
ftp.dante.de	/pub/tex/macros/latex209/contrib/elsevier
ftp.tex.ac.uk	/pub/archive/macros/latex209/contrib/elsevier
ftp.shsu.edu	/tex-archive/macros/latex209/contrib/elsevier

The files, as well as instructions in the form of a booklet, can also be obtained from Elsevier.

No changes from the version accepted by the editor of the journal are permissible, without the prior and explicit approval by the editor.

The publisher reserves the right to decide whether to process a manuscript from authors' files or not. Articles coded in a simple manner with few user-defined macros are most likely to be handled this way. In case the file is used, *no* proofs will be sent to the author, unless explicitly requested.

If sent via electronic mail, files should be accompanied by a clear identification of the article (name of journal, editor's reference number) in the "subject field" of your electronic-mail message. Authors should include an ASCII table (available from the publisher) in their files, to enable any transmission errors to be detected. For diskettes, allowed formats are 3.5" or 5.25" MS-DOS, or 3.5" Macintosh.

Addresses. Mail: Elsevier Science Publishers, Desk Editorial Department Physica D, P.O. Box 103, 1000 AC Amsterdam, The Netherlands. Electronic mail: v.ijfs@elsevier.nl, for the attention of Ms. V. IJfs.

Refereeing. All papers are subjected to refereeing, and in case a paper cannot be accepted in the form it was submitted, the submitting author will be informed about the referee's comments.

Acceptance. Acceptance forms will be sent by the editor. There is *no* page charge. Upon acceptance of an article by the journal, the author(s) will be asked to transfer copyright of the article to the publisher. This transfer will ensure the widest possible dissemination of information.

Offprints. 50 offprints of each article will be supplied to the first author free of charge (in case of an article with colour illustrations this amounts to 200 offprints free of charge). An order form for offprints will be provided and should be returned to the publishers.

Reprinted from

PHYSICS LETTERS A

Physics Letters A 206 (1995) 54–60

Disorder-enhanced synchronization

Y. Braiman [a], W.L. Ditto [a], K. Wiesenfeld [a], M.L. Spano [b]

[a] *School of Physics, Georgia Institute of Technology, Atlanta, GA 30332, USA*

[b] *Naval Surface Warfare Center, 10901 New Hampshire Ave., Silver Spring, MD 20903, USA*

Received 11 April 1995; revised manuscript received 18 May 1995; accepted for publication 11 June 1995
Communicated by A.R. Bishop

ELSEVIER

PHYSICS LETTERS A

Aims and scope
Physics Letters A ensures the rapid publication of short communications in all fields of Physics, excluding Nuclear Physics and Particle Physics.

Abstracted/indexed in:
Chemical Abstracts; Current Contents: Physical, Chemical and Earth Sciences; Engineered Materials Abstracts; INSPEC; Metals Abstracts; Physics Briefs

Subscription information 1995
PHYSICS LETTERS A (ISSN 0375-9601) and PHYSICS LETTERS B (ISSN 0370-2693) will each be published weekly. For 1995 13 volumes, volumes 198–210 (78 issues altogether) of Physics Letters A have been announced. For 1995 24 volumes, volumes 341–364 (96 issues altogether) of Physics Letters B have been announced. The subscription prices for these volumes are available upon request from the Publisher. PHYSICS REPORTS (ISSN 0370-1573) will be published approximately weekly. For 1995 12 volumes, volumes 252–263 (72 issues altogether) of Physics Reports have been announced. The subscription price for these volumes is available upon request from the Publisher.
A combined subscription to the 1995 issues of Physics Letters A, Physics Letters B and Physics Reports is available at a reduced rate.
Subscriptions are accepted on a prepaid basis only and are entered on a calendar year basis. Issues are sent by SAL (Surface Air Lifted) mail wherever this service is available. Airmail rates are available upon request. Please address all enquiries regarding orders and subscriptions to:

Elsevier Science B.V.
Order Fulfillment Department
P.O. Box 211, 1000 AE Amsterdam
The Netherlands
Tel. + 31 20 4853642, Fax: +31 20 4853598

Claims for issues not received should be made within six months of our publication (mailing) date.

US mailing notice – Physics Letters A (ISSN 0375-9601) is published weekly by Elsevier Science B.V., P.O. Box 211, 1000 AE Amsterdam, The Netherlands. Annual subscription price in the USA is US$ 2634.00 (valid in North, Central and South America only), including air speed delivery. Second class postage paid at Jamaica, NY 11431.
USA POSTMASTERS: Send address changes to Physics Letters A, Publications Expediting, Inc., 200 Meacham Avenue, Elmont, NY 11003. AIRFREIGHT AND MAILING in the USA by Publications Expediting, Inc., 200 Meacham Avenue, Elmont, NY 11003.

The paper used in this publication meets the requirements of ANSI/NISO Z39.48-1992 (Permanence of Paper).

Printed in The Netherlands

North-Holland, an imprint of Elsevier Science

2 October 1995

PHYSICS LETTERS A

ELSEVIER

Physics Letters A 206 (1995) 54–60

Disorder-enhanced synchronization

Y. Braiman [a], W.L. Ditto [a], K. Wiesenfeld [a], M.L. Spano [b]

[a] *School of Physics, Georgia Institute of Technology, Atlanta, GA 30332, USA*
[b] *Naval Surface Warfare Center, 10901 New Hampshire Ave., Silver Spring, MD 20903, USA*

Received 11 April 1995; revised manuscript received 18 May 1995; accepted for publication 11 June 1995
Communicated by A.R. Bishop

Abstract

We find that an increase in the disorder of an array of Josephson junctions can lead to significant improvement in the synchronization of the array. Both this effect and the opposite, more expected behavior are seen over a broad parameter range.

Synchronizing a population of non-identical oscillators is a problem that arises in a variety of contexts in physics and biology [1,2]. The question is, given a set of coupled nonlinear oscillators with a distribution of natural frequencies, to what degree will the oscillators exhibit frequency and phase locking? Here we present a simple example, where we find the unexpected result that *disorder can significantly increase the synchronization of a coupled array*.

The problem of mutual synchronization is of particular relevance in the study of Josephson junction arrays [3], where (in one application) the goal is to generate high power, high frequency voltage oscillations with a narrow linewidth. A single Josephson junction can convert a dc bias current into voltage oscillations as fast as a terahertz [4], an extraordinarily high frequency for an electronic device; however, the power output is rather small (typically about 10 nW). To generate higher powers, one can employ an array of junctions, with the hope that the individual elements will execute synchronized (in-phase) oscillations. Both series and parallel one-dimensional arrays have been studied in this regard, as have two-dimensional arrays. While the in-phase state is the most desirable, in principle it exists only when the elements are identical. It is natural to assume that the more nearly identical the elements, the better will be the observed synchronization.

The problem with this assumption is that even if the junctions are physically identical, the in-phase state may be dynamically unstable and the system must evolve to a different, symmetry-broken state. Depending on parameter values the attracting state may have very poor synchronization, as in the example shown in Fig. 1a. In such a situation, the introduction of disorder can significantly improve the synchronization of the system. Fig. 1b shows an example of what happens when the identical elements are replaced by a set of elements with a spread of $\pm 3.5\%$ in the natural frequency, keeping unchanged the value of the average critical current. In this paper we investigate the conditions under which

0375-9601/95/$09.50
SSDI 0375-9601(95)00570-6

disorder-enhanced synchronization will occur, and describe the underlying mechanism which leads to this effect.

Consider first the case of a parallel array of identical current-biased Josephson junctions coupled via inductors. The governing dynamical equations in dimensionless form are

$$\ddot{\phi}_j + \gamma\dot{\phi}_j + \sin\phi_j = I + \kappa(\phi_{j+1} - 2\phi_j + \phi_{j-1}), \tag{1}$$

where $j = 1, 2, \ldots, N$, and we used free end boundary conditions $\phi_0 = \phi_1$ and $\phi_{N+1} = \phi_N$. Here, ϕ_j is the phase difference in the macroscopic wave function across the jth junction, $\gamma = (\Omega RC)^{-1}$, $\kappa = (\Omega^2 LC)^{-1}$, $\Omega^2 = 4\pi e I_c/hC$, R is the junction resistance, C is the junction capacitance, L is the coupling inductance, e is the electronic charge, h is Planck's constant, and I is the bias current. Current is measured in units of the critical current I_c, time is in units of Ω^{-1}. In these units the voltage across the jth junction is $\dot{\phi}j$ in units of $h\Omega/4\pi e$.

Physically, κ plays the role of a coupling constant. Of course, in the uncoupled limit $\kappa = 0$, the initial conditions completely determine the relative phases of the voltage oscillations, and there is no possibility that the dynamics will drive the system into the synchronized state. On the other hand, with $\kappa \neq 0$, Eq. (1) admits the so-called in-phase state, defined by $\phi_j(t) = \phi_{\text{in}}(t)$ for all j. However, for a broad range of parameter values, the in-phase state is unstable, and the array evolves to some stable symmetry-broken solution. We can determine the local stability of the in-phase state by setting $\phi_j = \phi_{\text{in}} + \eta_j$, where the η_j are small, and linearizing Eq. (1) (a stability analysis for the continuum limit of this problem may be found in Ref. [5])

$$\ddot{\eta}_j + \gamma\dot{\eta}_j + \eta_j\cos\phi_{\text{in}} = \kappa(\eta_{j+1} - 2\eta_j + \eta_{j-1}), \tag{2}$$

with $\eta_0 = \eta_1$ and $\eta_{N+1} = \eta_N$. These equations can be decoupled via the following transformation,

$$\eta_j = \sum_{k=0}^{N-1} h_k \cos\left[\left(\pi k\left(j - \tfrac{1}{2}\right)/N\right)\right],$$

so that

$$\ddot{h}_k + \gamma\dot{h}_k + \{\cos\phi_{\text{in}}(t) + 2\kappa[1 - \cos(\pi k/N)]\}h_k = 0. \tag{3}$$

Local stability of the in-phase state requires that all h_k decay asymptotically in time. If we write $\cos\phi_{\text{in}}(t) = c_0 + c(t)$, where c_0 is the time average part of $\cos\phi_0$, and introduce $h_k = \exp(-\frac{1}{2}\gamma t)\psi_k$, Eq. (3) becomes

$$\ddot{\psi}_k + \left\{-\tfrac{1}{4}\gamma^2 + c_0 + 2\kappa[1 - \cos(\pi k/N)]\right\}\psi_k + c(t)\psi_k = 0. \tag{4}$$

Eq. (4) is known as Harper's model [6]. This equation has been widely studied in relation to electron motion in a magnetic field [7], the dynamics of an electron in one-dimensional random and quasiperiodic systems [8] and the Anderson model [9]. For values of bias current I just above unity, $c(t)$ is a narrow-peaked function, so the overlap integral of $c(t)$ with ψ_k is negligibly small. In this approximation the eigenfrequencies are given by $\omega_k^2 = -\frac{1}{4}\gamma^2 + c_0 + 2\kappa[1 - \cos(\pi k/N)]$. The condition for stability of the in-phase state is that Re $\omega_k < \frac{1}{2}\gamma$ for all k. Since $\kappa > 0$, the condition for stability reduces to Re $\omega_1 < \frac{1}{2}\gamma$. We have tested the validity of the above approximation numerically for $N = 5, 7, 9$ and bias curents $1.01 \leq I \leq 1.05$ (these values make the effective nonlinearity large). The numerical and analytical values of the critical values of κ agree to within a 10% error over this range of bias current. For high values of the bias current (so the effective nonlinearity is small) we can make a different approximation. Namely, $\phi_0(t)$ overturns at a nearly constant rate ω, so $c(t)$ can be approximated as $\cos(\omega t)$. (Note that ω is equal to the time-averaged voltage in these dimensionless units.) Eq. (4) then takes the form of the Mathieu equation. The behavior of ψ_k depends on the ratio between $-\frac{1}{4}\gamma^2 + c_0 + 2\kappa[1 - \cos(\pi k/N)]$ (the constant coefficient) and unity (the coefficient of the time-dependent term). We have found numerically that there is a broad parameter range where all of the ψ_k are bounded, which is sufficient to ensure that h_k goes to zero, which in turn means that the in-phase solution is stable. Similarly, there is a broad parameter range over which the in-phase state is unstable.

We now turn to the effect of disorder, i.e. the situation where the elements are no longer identical.

While there are a number of ways to introduce disorder into the system, we choose to modify Eq. (1) to read

$$\ddot{\phi}_j + \gamma\dot{\phi}_j + I_j \sin \phi_j = I + \kappa(\phi_{j+1} - 2\phi_j + \phi_{j-1}). \tag{5}$$

That is, we introduce [1] a spread in the critical currents $I_j = 1 + \epsilon\xi_j$, where ξ_j is a random number uniformly distributed between -0.5 and $+0.5$. The effect of critical-current variations on the coherence of Josephson junction arrays was studied in Ref. [10]. In our numerical simulations we used a 4th order Runge–Kutta algorithm, with initial conditions for the $\dot{\phi}_j$ randomly distributed between 0 and 2π and for the ϕ_j randomly distributed between 0 and 1. We define a temporal measure of the synchronization, σ, as the standard deviation from the average signal,

$$\sigma(\epsilon) = \lim_{T\to\infty} \frac{1}{T}\int_0^T \frac{\sqrt{\Sigma_{j=1}^N\left(\dot{\phi}_j - \langle\dot{\phi}\rangle\right)^2}}{\langle\dot{\phi}\rangle}\, dt, \tag{6}$$

where $\langle\dot{\phi}\rangle = N^{-1}\Sigma_{j=1}^N\dot{\phi}_j(t)$. We consider $\dot{\phi}$ because it is a natural physical variable for this system, i.e. the voltage. For an in-phase state, $\sigma = 0$; in general an increase in synchronization results in a decrease of σ. In Fig. 2 we show $\sigma(\epsilon)$ for three different realizations of the disorder. The other parameters are the same as in Figs. 1. In each of the three cases the initial conditions were identical, thus the only parameter which is varied here is the amount of disorder ϵ. In one case (the middle curve) $\sigma(\epsilon)$ decreases smoothly with ϵ, in another (the lowest curve), $\sigma(\epsilon)$ remains constant at first and then decreases abruptly at $\epsilon = 0.06$ so that the dynamics is best synchronized for a finite level of disorder; for the other realization (the upper curve) the synchronization is slowly degraded as the level of disorder is increased. These three cases are representative of all the cases we observed in our simulations; all three types can be considered typical. For example, for an array of 21 junctions and a fixed set of parameters (exclusive of the disorder), in roughly half of the runs a low level of disorder resulted in a significant improvement in synchronization; in the other cases the disorder either had little effect or degraded the output. For sufficiently large levels of disorder the synchronization always diminishes. To make certain that the improvement in $\sigma(\epsilon)$ is not simply due to a change in the *average* critical current, we also tested the behavior of an identical array subject to small variation of the critical currents I_{cr} (we used only 2% variations in the average critical current in numerical simulations of the disordered array). The inset in Fig. 2 shows $\sigma(\epsilon)$ (the upper curve) and the average voltage V_{av} (the lower curve) of the identical array as a function of I_{cr}. To obtain this curve we started with the initial conditions corresponding to the asymmetric orbit of the identical array and then smoothly varied the critical currents of all the elements in array. One clearly observes that (a) for the identical array $\sigma(\epsilon)$ is not as sensitive to changes in critical current as compared to the effect of disorder for the disordered array and (b) an increase in average voltage (oscillation frequency) does not automatically imply an increase in synchronization.

To better quantify the effect, we measured the probability $P(\epsilon)$ that for a given level of disorder ϵ, σ is less than its nominal value for the case of identical junctions. The results for an array with $N = 21$ are shown in Fig. 3: the resulting curve passes through a broad maximum at around $\epsilon \approx 0.1$. For each value of ϵ we used 200 different realizations of critical currents and initial conditions. We used only such realizations of the critical currents which obey $I_{av} = 1 + |N^{-1}\Sigma_{j=1}^N\ (I_j - 1)| \leqslant 0.02$, thus allowing 2% spread in the average critical currents. The initial conditions were chosen at random with the phases uniformly distributed between 0 and 2π, and the phase derivatives uniformly distributed in between 0 and 1. We can interpret Fig. 3 as showing that there is an optimum level of disorder leading to maximum "performance". Stated in this way, the effect is reminiscent of the phenomenon of stochastic resonance [11].

We now turn to the dynamical mechanism responsible for this disorder-enhanced synchronization. Extensive numerical simulations for a reasonably large array ($N = 21$) over the parameter range used in

[1] Strictly speaking we should also introduce different γ values for different elements, but we expect the basic phenomenology to be the same.

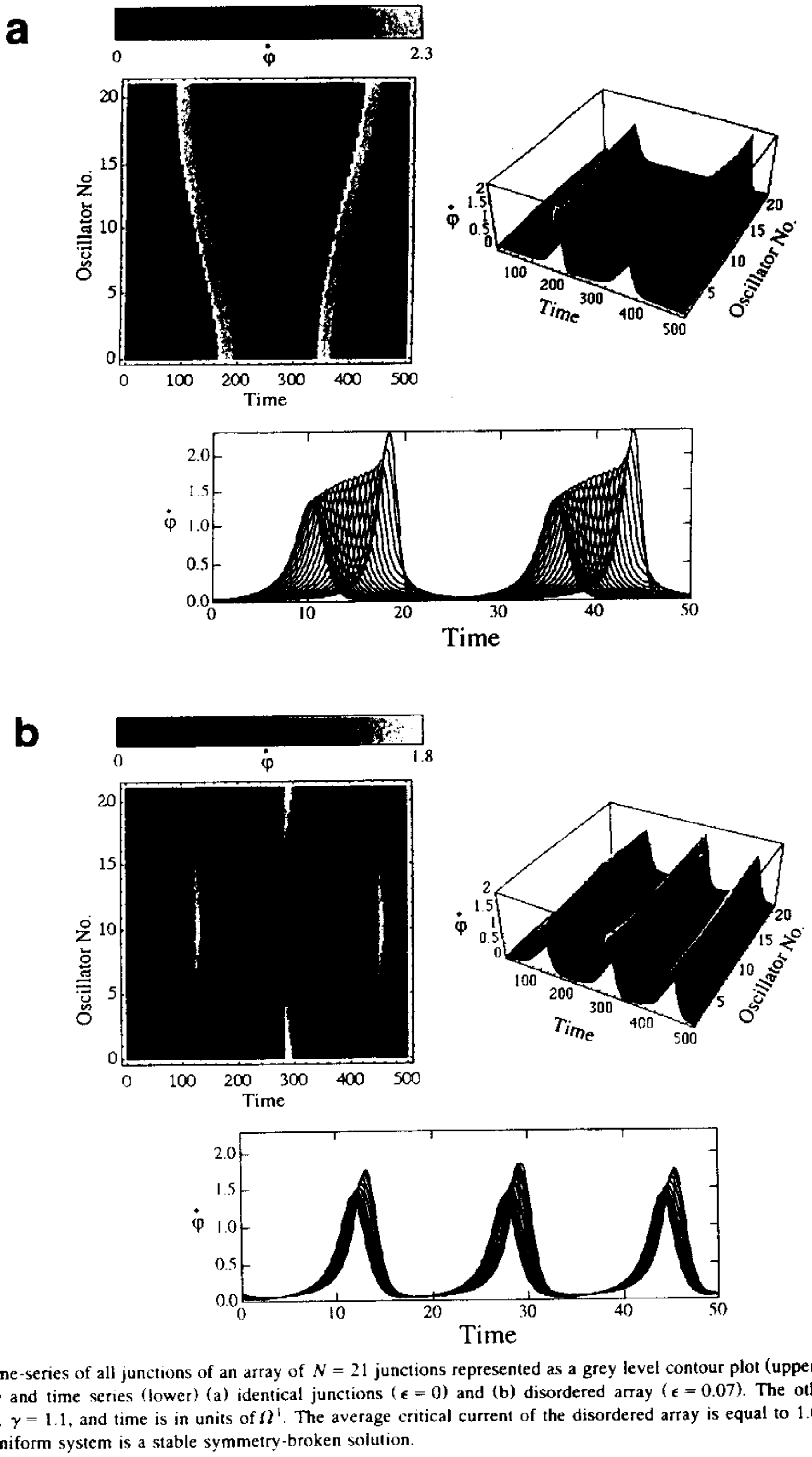

Fig. 1. Voltage time-series of all junctions of an array of $N = 21$ junctions represented as a grey level contour plot (upper left), 3-D contour plot (upper right) and time series (lower) (a) identical junctions ($\epsilon = 0$) and (b) disordered array ($\epsilon = 0.07$). The other parameters are $\kappa = 3.0$, $I = 1.02$, $\gamma = 1.1$, and time is in units of Ω^{1}. The average critical current of the disordered array is equal to $1.0 \pm 1 \times 10^{-4}$. The solution for the uniform system is a stable symmetry-broken solution.

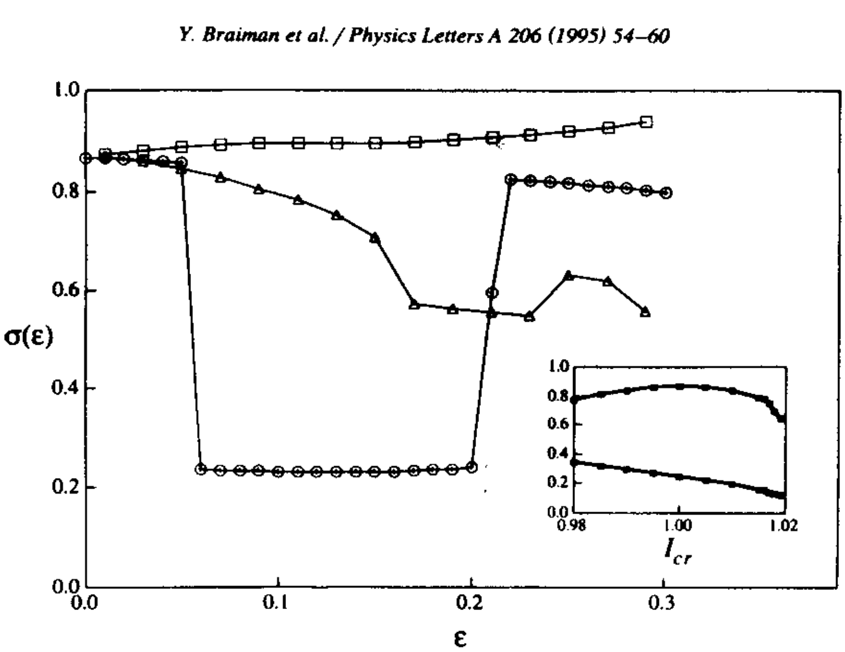

Fig. 2. Temporal measure of synchronization σ as a function of disorder ϵ for three different realizations of critical currents. The lowest curve (circles) shows a sharp increase in synchronization (decreasing σ); the middle curve (triangles) shows a smooth increase in synchronization, while the upper curve (squares) shows a modest decrease in synchronization. The other parameters are $N = 21$, $\kappa = 3.0$, $I = 1.02$, $\gamma = 1.1$. The inset shows the behavior of $\sigma(\epsilon)$ (the upper curve) and V_{av} (the lower curve) as a function of I_{cr} for the identical array.

Figs. 1–3 have led us to the following scenario. Recall that we begin with a disorder-free system ($\epsilon = 0$) in a parameter regime where the in-phase state is unstable; on the other hand, the array has (at least) two distinct (stable) coexisting attractors. The different stable orbits have different degrees of synchronization σ. We observe disorder-enhanced synchronization when the poorly synchronized attractor has a large basin of attraction while the highly synchronized attractor has a small basin. This comes about in one of two ways as we now describe. Let us call the poorly synchronized orbit A and the better synchronized orbit B. Owing to the relative sizes of their basins of attraction, for most initial conditions the array settles onto orbit A. Introducing a small spread in critical currents does not significantly alter the geometry of the orbits (i.e. it may change the detailed dynamics of each element, but does not affect the synchronization properties of the array as a whole). On the other hand, the disorder does change the basins of attraction of A and B. It may also lead to the creation of new merged attractors: the geometry of these orbits is effectively the union of A and B, so we will refer to these orbits as AB. In Fig. 4 we show the phase behavior of the first junction together with the time series of all 21 elements of the array. Fig. 4a shows an example of the orbit A (poorly synchronized), Fig. 4b shows the orbit B, and Fig. 4c shows the orbit AB which appears after A and B have merged. Depending on the realization

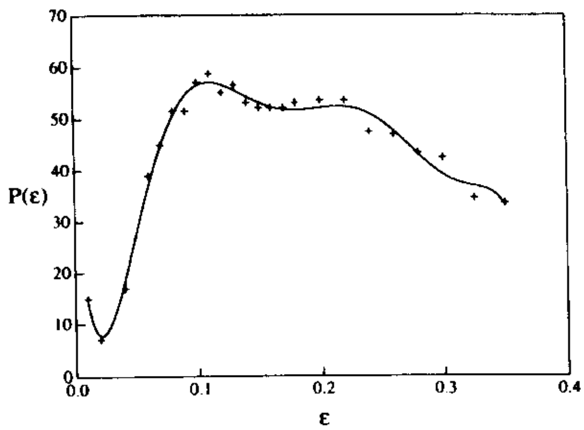

Fig. 3. Percentage P of realizations showing improved synchronization as a function of disorder ϵ. The curve shown is for guiding the eye. The other parameters are as in Fig. 2.

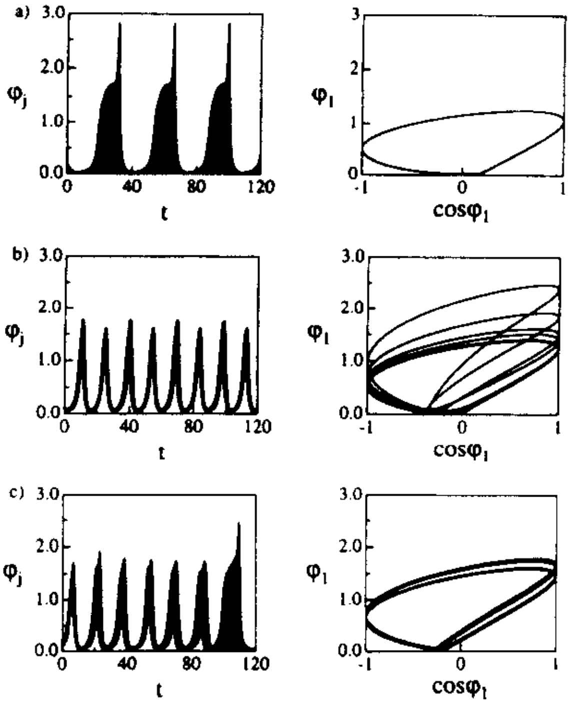

Fig. 4. Time series $\dot{\phi}_j$ of all elements (left) and phase space plot ($\dot{\phi}_1$ versus $\cos\phi_1$) of the first junction (right) demonstrating three orbit types: (a) orbit A (poorly synchronized), (b) orbit B (highly synchronized), and (c) orbit AB (merged orbit). The parameter values for (a), (b), and (c) are the same (see Fig. 2) except for the realization of critical currents and initial conditions. The amount of disorder is $\epsilon = 0.15$.

of critical currents, the disorder may either increase the basin size of B or create the orbit AB, in either case increasing the probability that the orbit is attracted to a state with improved synchronization.

These two cases (shown in Figs. 4a and 4b) correspond to two different signatures (upper and lower respectively) shown in Fig. 2. Recall that Fig. 2 was generated by varying ϵ while leaving the initial condition fixed such that it lies in the basin of A when $\epsilon = 0$. The lowest curve in Fig. 2 shows a sudden transition when the initial condition crosses the basin boundary from A to B. The middle curve shows a more gradual decrease in σ as the system goes from A to the merged orbit AB. Looking again at Fig. 4c, one sees the roughly intermittent character of AB as it "switches" between the two original behaviors.

The effect of increased synchronization with disorder also can be also achieved by choosing a regular variation in critical currents along the array. To demonstrate this we ran simulations where we changed the critical currents of just two junctions, $I_j = 1 - \epsilon$ and $I_i = 1 + \epsilon$, thereby keeping the average critical current equal to unity. Interestingly, we found that decreasing the critical current of the middle junction (while increasing the critical currents of an edge junction) caused the synchronization to increase; for the opposite realization we observed no significant change in synchronization. We also performed simulations in which we changed the critical current of just one junction, keeping the critical currents of all the other junctions unaltered. When the critical current of the disordered junction j was less than unity ($I_j < 1$), the synchronization was increased; the greatest effect was when this was the middle junction. In contrast, for $I_j > 1$ no significant change in synchronization was observed.

In summary, we have shown that disorder may lead to an increase in the temporal synchronization of a 1-D array of nonlinear coupled oscillators. We have observed this effect in a particular oscillator array; however, the mechanism responsible for disorder-enhanced synchronization is general enough that we suspect it will be observed in other systems, and may well be common.

We thank Professor T. Uzer for helpful discussions. This work was supported by the Office of Naval Research, through contracts N00014-91-J-1257 (Y.B. and K.W.), and the ONR Young Investigators Program (W.D.). M.L.S. acknowledges support from the Naval Surface Warfare Center's Independent Research Program and from the Physics Division of the Office of Naval Research.

References

[1] Y. Kuramoto, Chemical oscillations, waves, and turbulence (Springer, Berlin, 1984).

[2] S. Strogatz, in: Biomathematics, Vol. 100 (Springer, Berlin, 1993).

[3] A.K. Jain, K.K. Likharev, J.E. Lukens and J.E. Sauvageau, Phys. Rep. 109 (1984) 309.

[4] R.P. Robertazzi and R.A. Buhrman, IEEE Trans. Mag. 25 (1989) 1384.

[5] S. Pagano, M.P. Soerensen, R.D. Parmentier, P.L. Christiansen, O. Skovgaard, J. Mygind, N.F. Pedersen and M.R. Samuelsen, Phys. Rev. B 33 (1986) 174.
[6] P.G. Harper, Proc. R. Phys. Soc. A 68 (1955) 874.
[7] D.R. Hofstadter, Phys. Rev. B 14 (1976) 2239.
[8] D.J. Thouless, Phys. Rep. 13 (1974) 93;
B. Souillard, Phys. Rep. 103 (1984) 41.
[9] P.W. Andersen, Phys. Rev. 109 (1958) 1492.
[10] M. Octavio, C.B. Whan and C.J. Lobb, Appl. Phys. Lett. 60 (1992) 766.
[11] F. Moss, A. Bulsara and M. Schlesinger, eds., Proc. NATO Advanced Research Workshop on Stochastic resonance in physics and biology, special issue, J. Stat. Phys. 70 (1993) 1–514.

PHYSICS LETTERS A

Instructions to Authors (short version)

(A more detailed version of these instructions is published in the preliminary pages to each volume.)

Submission of papers

Contributions in triplicate should be sent to the editor whose expertise covers the research reported and with whom the author can communicate efficiently. Editorial Board, addresses and primary interests are given on page 2 of the cover. In case of doubt, contributions can be submitted directly to the Publisher at the address below. However, it should be realized that such papers will have to be forwarded to one of the Editors, which will result in some delay.

Original material. By submitting a paper for publication in Physics Letters A the authors imply that the material has not been published previously nor has been submitted for publication elsewhere and that the authors have obtained the necessary authority for publication.

Refereeing. All contributions will be refereed. The Editors reserve the right to edit contributions, whenever necessary, and to refuse papers which in their opinion do not satisfy conditions as to standard or contents. Linguistic corrections not affecting the meaning will be carried out by the Publisher.

Types of contributions

The *length* of the papers is not formally limited, but expedient and compact formulation, appropriate to a letters journal, is expected. The Editor may require the removal of figures, lengthy introductions, derivations, descriptions of apparatus or speculations if these are not essential for the efficient and clear communication of important new results. An *abstract* of less than 50 words is required.

Manuscript preparation

All manuscripts should be written in good English. The paper copies of the text should be prepared with double line spacing and wide margins, on numbered sheets. See notes opposite on electronic versions of manuscripts.

Structure. Please adhere to the following order of presentation: Article title, Author(s), Affiliation(s), Abstract, PACS codes and keywords, Main text, Acknowledgements, Appendices, References, Figure captions, Tables.

Corresponding author. The name, complete postal address, telephone and fax numbers and the e-mail address of the corresponding author should be given on the first page of the manuscript.

PACS codes/keywords. Please supply one or more relevant PACS-1995 classification codes and 2–5 keywords of your own choice for indexing purposes.

References. References to other work should be consecutively numbered in the text using square brackets and listed by number in the Reference list. Please refer to the more detailed instructions for examples.

Illustrations

Illustrations should also be submitted in triplicate: one master set and two sets of copies. The *line drawings* in the master set should be original laser printer or plotter output or drawn in black india ink, with careful lettering, large enough (3–5 mm) to remain legible after reduction for printing. The *photographs* should be originals, with somewhat more contrast than is required in the printed version. They should be unmounted unless part of a composite figure. Any scale markers should be inserted on the photograph, not drawn below it.

Colour plates. Figures may be published in colour, if this is judged essential by the Editor. The Publisher and the author will each bear part of the extra costs involved. Further information is available from the Publisher.

After acceptance

Notification. You will be notified by the Editor of the journal of the acceptance of your article and invited to send an electronic version of the accepted text to the Publisher.

Copyright transfer. You will be asked to transfer the copyright of the article to the Publisher. This transfer will ensure the widest possible dissemination of information.

No proofs. In order to speed up publication, all proofreading will be done by the Publisher and proofs are *not* sent to the author(s).

Electronic manuscripts

The Publisher welcomes the receipt of an electronic version of your accepted manuscript (preferably encoded in LaTeX). If you have not already supplied the final, revised version of your article (on diskette) to the Journal Editor, you are requested herewith to send a file with the text of the accepted manuscript directly to the Publisher by e-mail or on diskette (allowed formats 3.5" or 5.25" MS-DOS, or 3.5" Macintosh) at the address given below. Please note that no deviations from the version accepted by the Editor of the journal are permissible without the prior and explicit approval by the Editor. Such changes should be clearly indicated on an accompanying printout of the file.

Author benefits

No page charges. Publishing in Physics Letters A is free.

Free offprints. The corresponding author will receive 50 offprints free of charge. An offprint order form will be supplied by the Publisher for ordering any additional paid offprints.

Discount. Contributors to Elsevier Science journals are entitled to a 30% discount on all Elsevier Science books.

Contents Alert. Physics Letters A is included in Elsevier's pre-publication service Contents Alert and CoDaS.

Further information (after acceptance)

Elsevier Science B.V., Physics Letters A
Desk Editorial Department
P.O. Box 103, 1000 AC Amsterdam
The Netherlands
Tel.: +31 20 4852638
Fax: + 31 20 4852319
E-mail: NHPDESKED@ELSEVIER.NL

Printed in The Netherlands

North-Holland, an imprint of Elsevier Science

Experimental Maintenance of Chaos

Visarath In,[1] Susan E. Mahan,[1] William L. Ditto,[1] and Mark L. Spano[2,1]

[1]*Applied Chaos Laboratory, School of Physics, Georgia Institute of Technology, Atlanta, Georgia 30332*

[2]*Naval Surface Warfare Center, Carderock Division, Silver Spring, Maryland 20903*

(Received 25 January 1995)

We present a method for the anticontrol or maintenance of chaos designed for easy application to physical and biological systems. The method is based on the return map of the experimental data and requires only small, very infrequently applied time-dependent perturbations of a single system parameter and does not require any model equations for or *a priori* knowledge of the system dynamics. The method is shown to be able to reliably sustain chaos in a magnetomechanical ribbon experiment.

PACS numbers: 05.45.+b, 75.80.+q

Since Ott, Grebogi, and Yorke (OGY) [1] published their paper on the theory of the control of chaos, a major thrust of the work in experimental chaos has been to convert the chaos found in various physical systems into periodic motion. Since the experimental control of chaos was first demonstrated [2] in a mechanical system (a magnetoelastic ribbon), the control of chaos has been implemented in lasers [3], electronic circuits[4], chemical reactions [5], and biological systems [6,7]. Although chaos control may be very advantageous in many systems [8], it has been suggested that pathological destruction of chaotic behavior (possibly due to some underlying disease) may be implicated in heart failure [9] and some types of brain seizures [7]. Thus some systems may require chaos and/or complexity in order to function properly. Another situation in which the maintenance of chaos might be useful is the mixing of fluids [10]. Experimental work by Schiff *et al.* [7] demonstrated an *ad hoc* method for increasing the complexity (decreasing the periodicity) of an *in vitro* hippocampal rat brain slice preparation. Recent theoretical and computational work by Yang *et al.* [11] indicates that intermittent chaotic systems can be made to exhibit continuous chaotic behavior (no intermittent periodic episodes).

The main contribution of this Letter is a general theoretical method for the maintenance of chaos, which is then implemented experimentally in a magnetomechanical system demonstrating intermittency [12]. This intermittency appears as chaos interspersed with long periodic episodes. This method is readily applicable to experiment and relies only on experimentally measured quantities for its implementation.

As opposed to the *ad hoc* method for increasing the complexity implemented by Schiff *et al.* [7] (which they term anticontrol), the method of chaos anticontrol proposed by Yang *et al.* [11] is based on the observation that a map-based system in a regime of transient chaos, such as that near a transition periodicity into chaos, has special regions in its phase space that they term "loss regions." If the system enters such a region it immediately ceases its chaotic motion. Yang *et al.* [11] identify these regions along with n preiterates of each loss region. If the system enters a preiterate, they apply a small perturbation to an accessible system parameter in order to interrupt the progression of the system toward a loss region. The perturbation places the system in a region of phase space that is neither a loss region nor a preiterate of one. This requires explicit knowledge of the map of the system and is accordingly difficult to accomplish. Thus the lack of generality of the Schiff method and the difficulty of experimental implementation of the Yang method are the motivation for the present work.

We propose a general anticontrol method that is more readily applicable to experiment and that relies only on experimentally measured quantities for its implementation. To start we make only the following assumptions about the system: (1) the dynamics of the system can be represented as an n-dimensional nonlinear map (e.g., by a surface of section or a return map) such that points or iterates on such a map are given by $\vec{\xi}_n = \vec{f}(\vec{\xi}_{n-1}, p)$, where p is some accessible system parameter; (2) there is at least one specific region of the map (termed a loss region) that lies on the attractor into which the iterates will fall when making the transition from chaos to periodicity; and (3) the structure of the map does not change significantly with small changes $\delta p \equiv p - p_0$ in the control parameter p about some initial value p_0.

On the return map derived from a system, the locations of loss regions are determined by observing immediate preiterates of undesired points which correspond to periodic orbits. Clusters of these preiterates are identified as the loss regions. The extent of each loss region is determined by the distribution of points in that region (Fig. 1). The time evolution of each region may be traced back through m preiterates, as desired.

Next, in a fashion similar to the OGY chaos control method [1], we change p slightly, observing the resulting change in each loss region's location, and estimate the local shift of the attractor $\vec{g}$ for each loss region with respect to a change in p as follows:

$$\vec{g} = \frac{\partial \vec{f}(\vec{\xi}_n, p)}{\partial p} \approx \frac{\Delta \vec{f}(\vec{\xi}_n, p)}{\Delta p}.$$

 0031-9007/95/74(22)/4420(4)$06.00

FIG. 1. Return map constructed from experimental data showing the loss region and its preiterates (circles). Region (R_L) denotes the loss region, region (R_{L-1}) denotes the first preiterate of the loss region going back in time, and region (R_p) denotes the period 1 orbits clustering on the diagonal of the map. The other four circles denote the (R_{L-m}) preiterate regions. Any orbit that falls into any one of the R_{L-m} regions will proceed directly into the R_{L-1} region and then proceed onto the loss region followed by the unwanted periodic orbit.

As an approximation we take $\vec{g}$ to be the same for all loss regions on the attractor for sufficiently small parameter changes δp (otherwise calculation of $\vec{g}$ for each loss region is required). This is not strictly necessary in order to implement the method but is simply a convenience that is approximately true for many systems (including our magnetoelastic ribbon) and for small δp's.

Anticontrol can be applied once the system has entered the mth preiterate of the loss region. Since the map is constructed as a return map (or delay coordinate embedding) with ξ_n vs ξ_{n-1}, the y coordinate of the nth point becomes the x coordinate of the $(n+1)$st point. Since we know the x coordinate of the next point and the *size* of the region that this $(n+1)$st point would normally fall into, we calculate a minimum distance that we must move the attractor so that this next point falls outside of that region. This distance d is translated into the appropriate parameter change δp by $\delta p_n = d_{n+1}/|\vec{g}|$, where the direction of the motion is along $\vec{g}$.

If each of the m preiterates of the loss region is circumscribed by a circle of radius r_m (the worst case), we have $\delta p_n = 2r_m/|\vec{g}|$ where it is understood that the $(n+1)$st point falls into the mth preiterate region. This is the maximum perturbation needed to achieve anticontrol and guarantees that the next point will fall outside the mth preiterate region by moving the point one full diameter of the circle surrounding the loss region. We can improve upon this worst case. With a return map, we know the x coordinate of the next point. Because we have the choice of whether to apply the perturbation in either the positive or the negative $\vec{g}$ direction, we can select the sign of the perturbation to move the next point to the left if this x coordinate is in the left half of the preiterate region and vice versa. Thus the minimum distance to move is reduced to r_m and, consequently, $\delta p_n = r_m/|\vec{g}|$, a significant reduction in the strength of the perturbation.

Additionally, if the shape of the preiterate region of interest is approximately linear (linelike) and its slope is perpendicular to $\vec{g}$, then d is at most r_m and may approach the thickness of this linear segment ($\delta p_n \ll r_m|\vec{g}|$). Thus, while not necessary to achieve anticontrol, a detailed knowledge of the *shape* of the loss region and its preiterates can further reduce the size of the perturbation required to achieve anticontrol.

The experimental system [13] consists of a gravitationally buckled magnetoelastic ribbon driven parametrically by a sinusoidally varying magnetic field. The ribbon is clamped at its lower end and its position is measured at a point a short distance above the clamp. The Young modulus of the ribbon can be varied by more than a factor of 10 by application of an external magnetic field. We apply an ac magnetic field of amplitude H_{ac} and frequency f added to a dc field of amplitude H_{dc}, such that $H_{applied}(t) = H_{dc} + H_{ac}\sin(2\pi ft)$. We choose $f = 0.95$ Hz, $H_{ac} = 0.961$ Oe, and $H_{dc} = -1.221$ Oe in order to put the system in a state of intermittent chaos. We construct a return map by measuring the position ξ_n of a point on the ribbon once every driving period and by then plotting the current position ξ_n vs ξ_{n-1}.

On the return map, we identify the loss region and its preiterates (circles in Fig. 1). The loss region (R_L) is denoted by the circle just to the left of the diagonal. Its first preiterate (R_{L-1}) lies to the right of the diagonal. The other circles denote earlier preiterates (R_{L-m}). Points that enter any of these regions will eventually go to the region R_{L-1}. Once there they will proceed into the loss region R_L on the next iterate. Then the system becomes periodic. This appears as a cluster of points (R_p) on the diagonal of the map. The points that enter the preiterate regions mediate the intermittent transition from chaos to periodicity [12]. During anticontrol we apply a perturbation when an orbit enters the region R_{L-1} so that the next orbit will fall out of R_L.

The extent of the mth preiterate region is determined by observing the set of points that after m iterations fall into the loss region, as well as neighboring points that do not fall into the loss region after m iterations. The boundary of the loss region lies between these points. The $\vec{g}$ vector is determined by changing p_0 by ± 0.0068 Oe. As illustrated in Fig. 1, the two loss regions are very close to the cluster denoting the periodic orbit. Rarely during anticontrol the orbit is kicked into the period 1 region. This requires us on the succeeding iteration to implement anticontrol for the periodic region as well in

(a)

(b)

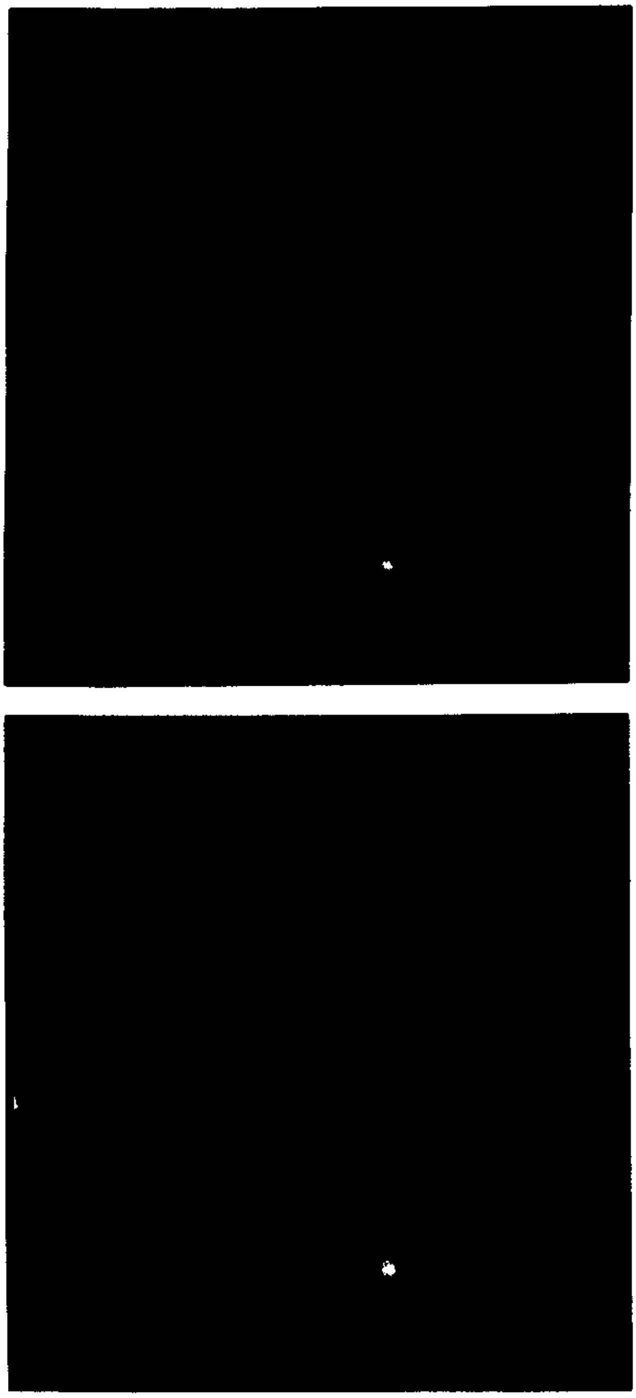

FIG. 4. 3D histograms of (a) the unperturbed and (b) the anticontrolled data distributed over the attractor (return map) of Fig. 1. The scale of (a) is enhanced by a factor of 10 in order to make visible the chaotic transients present in the data. The period 1 peak (which lies on the diagonal line) is so strong that it would be off the scale even had the vertical scale not been enhanced by this factor of 10.

unstable periodic motions that comprise the chaos itself. Hence it is not removed. To reiterate, we interrupt only the sequence of preiterates that lead to entrapment in a periodic motion. It is because we take this approach, rather than the approach of completely excluding the system for the region of phase space around the unstable periodic motion, that we are able to maintain the chaos with only rare interventions (~0.12% of the time).

In summary, we have presented a general method for the anticontrol of chaotic systems which is straightforward to implement and need be rarely applied to keep a system chaotic. This method has been demonstrated to work in a magnetomechanical experiment with no failures.

Mark L. Spano is supported by the NSWC Independent Research Program and the Office of Naval Research (Division of Physics & Chemistry). W. L. Ditto is supported by the ONR Young Investigator Program.

[1] E. Ott, C. Grebogi, and J. A. Yorke, Phys. Rev. Lett. **64**, 1196 (1990).

[2] W. L. Ditto, S. N. Rauseo, and M. L. Spano, Phys. Rev. Lett. **65**, 3211 (1990).

[3] R. Roy, T. W. Murphy, T. D. Maier, Z. Gills, and E. R. Hunt, Phys. Rev. Lett. **68**, 1259 (1992).

[4] E. R. Hunt, Phys. Rev. Lett. **67**, 1953 (1991).

[5] V. Petrov, V. Gaspar, J. Masere, and K. Showalter, Nature (London) **361**, 240 (1993).

[6] A. Garfinkel, M. L. Spano, W. L. Ditto, and J. N. Weiss, Science **257**, 1230 (1992).

[7] S. J. Schiff, K. Jerger, D. H. Duong, T. Chang, M. L. Spano, and W. L. Ditto, Nature (London) **370**, 615 (1994).

[8] For a nice review, see T. A. Shinbrot, C. Grebogi, E. Ott, and J. A. Yorke, Nature (London) **363**, 411 (1993). Also of interest is W. L. Ditto and L. M. Pecora, Sci. Am. **269**, No. 2, 78 (1993).

[9] For instance, some studies of heart rate variability suggest that losing complexity in the heart rate will increase the mortality rate of cardiac patients. See, for example, M. A. Woo, W. G. Stevenson, D. K. Moser, R. M. Harper, and R. Trelease, Am. Heart J. **123**, 704 (1992); A. L. Goldberger, Ann. Biomed. Eng. **18**, 195 (1990).

[10] J. M. Ottino, Sci. Am. **260**, No. 1, 40 (1989); J. M. Ottino, F. J. Muzzio, M. Tjahjadi, J. G. Franjione, S. C. Jana, and H. A. Kusch, Science **257**, 754 (1992); J. M. Ottino, Guy Metcalfe, and S. C. Jana, in *Proceedings of the 2nd Experimental Chaos Conference* (World Scientific, Singapore, 1995), pp. 3–20.

[11] W. Yang, M. Ding, A. Mandell, and E. Ott, Phys. Rev. E **51**, 102 (1995).

[12] The statistics associated with the dwell times the system spends in periodic motion are consistent with type III intermittency. For a discussion of intermittency types, see P. Berge, Y. Pomeau, and C. Vidal, *Order Within Chaos* (John Wiley & Sons and Hermann, Paris, 1984).

[13] W. L. Ditto, S. Rauseo, R. Cawley, C. Grebogi, G. H. Hsu, E. Kostelich, E. Ott, H. T. Savage, R. Segnan, M. L. Spano, and J. A. Yorke, Phys. Rev. Lett. **63**, 923 (1989).

Books

Books is an editorial service for readers' information. To order any book listed or any U.S. book in print, please remit retail price, plus $2.00 postage and handling charge for each book, to **Science News Books**, 1719 N Street, NW, Washington, DC 20036. All books sent postpaid. Domestic orders only. Please allow 4-6 weeks for delivery.

Cold Fusion: The Making of a Scientific Controversy — F. David Peat. Guides the general reader through the cold fusion debate, starting with the March 1989 announcement of controlled nuclear fusion in a laboratory setting and proceeding through the denouncements of that claim to some ongoing experiments that continue to yield unexplained results. Peat, the author of *Superstrings and the Search for the Theory of Everything*, explains the process of cold fusion and its possible implications for meeting future energy needs. Originally published in hardcover in 1989. Contemporary, 1990, 188 p., illus., paperback, $8.95.

Creatures, Corals, and Colors — David L. Bull and Ann Scarborough-Bull. A celebration of the seafloor's colorful pageantry, from the chilly kelp forests off the southern California coast to the psychedelic coral gardens of the Caribbean. The text, spectacularly illustrated with more than 150 color photographs, explores the natural history of unique underwater habitats, introducing the general reader to the creatures of the deep and examining their mysterious coexistence. Audubon Pk Pr, 1990, 132 p., color illus., hardcover, $35.95.

The Discovery of the Bismarck — Robert D. Ballard. It took two years and a painstaking sonar survey of 100 square miles of seafloor before Ballard and his crew located the *Bismarck*, Hitler's greatest battleship. This gripping account of the *Bismarck's* maiden journey, her sinking, Ballard's search, her discovery and her exploration is generously illustrated with historical and underwater photographs as well as artists' renderings. Warner Bks, 1990, 231 p., color/b&w illus., hardcover, $35.00.

The First Weeks of Life — Miriam Stoppard. This comprehensive guide begins by familiarizing mothers with their newborn's appearance and behavior and continues through care and feeding in the hospital and at home. Chapters are extensively illustrated with photographs and diagrams, providing fundamental information such as how to clean and change newborns and how to warm bottles or remove a nursing baby from the breast. Includes a chapter on women's postpartum changes, both physical and emotional. Originally published in Great Britain in 1989. Ballantine, 1990, 160 p., color/b&w illus., hardcover, $17.95.

Lonely Hearts of the Cosmos: The Story of the Scientific Quest for the Secret of the Universe — Dennis Overbye. A history of cosmology — the scientific effort to determine the origin and fate of the universe — and an introduction to cosmologists who have probed phenomena ranging from black holes to an expanding universe. Writing for the general reader, Overbye conveys the inspiration, excitement and frustration of this cosmic quest. HarperCollins, 1990, 438 p., hardcover, $25.00.

Overcoming Bladder Disorders: Compassionate, Authoritative Medical and Self-Help Solutions for Incontinence, Cystitis, Interstitial Cystitis, Prostate Problems and Bladder Cancer — Rebecca Chalker and Kristene E. Whitmore. A guide to the diagnosis, treatment and prevention of the most common bladder problems. Includes an index of diagnostic tests and a glossary of drug treatments. Har-Row, 1990, 338 p., illus., hardcover, $19.95.

The Second Fifty Years: Promoting Health and Preventing Disability — Robert L. Berg and Joseph S. Cassells, Eds. This report, compiled by the Institute of Medicine, examines 13 health threats to the elderly and offers policy and research recommendations to improve the quality of life and health care for the aging U.S. population. Extensively referenced chapters address, among other threats, poor nutrition, osteoporosis, depression, physical inactivity and sensory loss. Natl Acad Pr, 1990, 332 p., charts, hardcover, $29.95.

What Light Through Yonder Window Breaks? More Experiments in Atmospheric Physics — Craig F. Bohren. In this sequel to *Clouds in a Glass of Beer*, Bohren continues to explore the world of atmospheric physics, explaining such everyday phenomena as highway mirages and winter frost on the *inside* of windows. Written for science enthusiasts interested in the physics of everyday life, the book reflects both the curiosity and the skepticism with which scientists approach the world. Wiley, 1991, 190 p., illus., paperback, $12.95.

Sorting out fact from fiction and myth from reality in schizophrenia is no easy task. In *Schizophrenia Genesis*, one of the world's leading experts presents an absorbing account of what is actually known about the subject.

Irving I. Gottesman draws on the latest genetic and environmental research, and on recent findings from neurobiology, to investigate the origins of schizophrenia. He argues that the disorder can be understood only by considering both the genetic evidence and the familial and societal pressures associated with schizophrenia's onset and course. Included are discussions of the diagnostic controversies that have swirled around schizophrenia, genetic counseling and social policies affecting all those touched by the disorder. *—from the publisher*

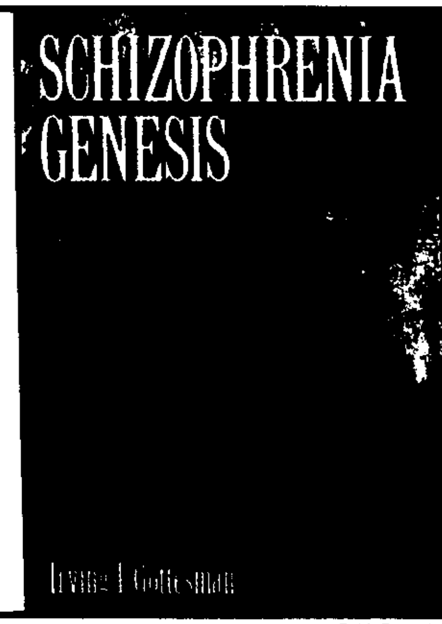

"For anyone who has ever had an interest in understanding schizophrenia [this book] is the definitive source book. It is a clearly written book that is, nevertheless, so packed with information about all aspects of schizophrenia, including first-person accounts by patients and their families, that readers will find themselves going back again and again to absorb the full fare that is offered."

—L. Erlenmeyer-Kimling
Columbia University

W. H. Freeman, 1990, 296 pages, 6" x 9", paperback, $14.95

SchizGenesis

Science News Books
1719 N Street, NW, Washington, DC 20036

Please send me ______ copy(ies) of *Schizophrenia Genesis*. I include a check payable to Science News Books for $14.95 plus $2.00 postage and handling (total $16.95) for each copy. Domestic orders only.

Name ______________________

Address ______________________

City ______________________

State ______________ Zip ______________

Daytime Phone (______) ______________________
(used only for problems with order)

RB1363

SCIENCE NEWS®

The Weekly Newsmagazine of Science

A Science Service Publication
Volume 139, No. 4, January 26, 1991

SCIENCE NEWS (ISSN 0036-8423) is published weekly on Saturday, except the last week in December, for $34.50 for 1 year or $58.00 for 2 years (foreign postage $6.00 additional per year) by Science Service, Inc., 1719 N Street, N.W., Washington, D.C. 20036. Second-class postage paid at Washington, D.C., and additional mailing office. POSTMASTER: Send address changes to SCIENCE NEWS, 231 West Center Street, Marion, OH 43305. Change of address: Four to six weeks' notice is required — old and new addresses, including zip codes, must be provided.

Editorial and Business Offices:
1719 N St., N.W., Washington, D.C. 20036
(202-785-2255)

Subscription Department:
231 West Center St., Marion, OH 43305
For new subscriptions only, call 1-800-247-2160.

This Week

Research Notes

Articles

Cover: Navy researchers have succeeded in controlling the chaotic wavering of a metallic ribbon by judiciously adjusting the magnetic field driving the ribbon's motion. The image on the left shows how slight changes in the magnetic field can shift the position of the computer-generated "chaotic attractor" corresponding to the ribbon's motion; each color represents the effect of a slightly different magnetic field. Such control, focused on a single point in the attractor, enables the researchers to keep the ribbon's motion from changing erratically. The inset demonstrates the possibility of maintaining control even in the face of ambient "noise" and measurement errors. (Images: Naval Surface Warfare Center)

Departments

Letters

Reef richness and risks

In "Bleached Reefs" (SN: 12/8/90, p.364), I was erroneously cited as saying that coral reefs may support more species than all other marine ecosystems combined. What I said was that they may have more species than any other *individual* marine ecosystem.

This is an important difference, because I agree with marine species-diversity authority Howard Sanders in feeling that the two most species-rich marine ecosystems are coral reefs and the deep-water community living at the base of the continental slope. In both ecosystems, the great majority of species have yet to be scientifically described, so it is premature to say which has the largest number. But coral reefs certainly have the highest biomass and productivity *per unit area*. In addition, they are under the greatest threat. Deep-sea communities should be the last to be affected by global change.

The risk at which coral reefs are now placed by the record seawater temperatures of 1990 and preceding years may become irreversible within a few years unless prompt steps are taken to protect them by halting global warming, treating sewage, reforesting watersheds, halting unsustainable harvesting of corals, reef organisms or sand, and developing mariculture as an alternative to overfishing. Otherwise, tropical marine countries will soon face large economic costs from depletion of their fisheries, reduced nourishment of beach sand for tourism, loss of shoreline protection from hurricanes, and destruction of the capacity to adapt to rising sea levels.

Thomas J. Goreau
President
Global Coral Reef Alliance
Chappaqua, N.Y.

Data differentiation

While MANSCAN images did successfully differentiate among people using varying degrees of short-term memory in a "memory" experiment at EEG Systems Laboratory, these data were not used to predict eventual accuracy of response, as suggested in "Shadows of Thoughts Revealed" (SN: 11/10/90, p.297). Predictability of performance accuracy was studied in an earlier experiment focusing on visuomotor responses.

Judy Illes
Research Neuropsychologist
EEG Systems Laboratory
San Francisco, Calif.

On labels and learning

In his reply to my letter on the origin of seemingly paradoxical behaviors such as altruism (SN: 9/15/90, p.163; 12/8/90, p.362), Tom Cole objected, in effect, that I was sneaking religion in through the back door and that it had no place in a scientific discussion.

It's curious that Mr. Cole could assert so confidently that my views were "obviously based on a fundamentalist interpretation of the Bible," considering that my letter mentioned neither Christianity nor the Bible — and neither did the particular ideas of C.S. Lewis that I paraphrased. Also, Mr. Cole's character-

Letters continued on p.58

Quasar Clumps Dim Cosmological Theory

A research satellite launched last June has allowed astronomers to peer deeper into space with X-ray eyes than ever before. And the distant vistas they've glimpsed show evidence of what appear to be giant clusters of quasars eight to 12 billion light-years from Earth – more than halfway to the edge of the observable universe. These clusters suggest the universe began getting lumpy earlier – and on a larger scale – than previous sky maps had indicated, researchers reported last week.

Combined with other recent observations of large-scale clumping (SN: 1/12/91, p.22), cosmologists say the perplexing new finding, if confirmed, may force them to abandon a standard theory – known as the cold-dark-matter model – of how the universe evolved. "This may be the start of the death knell for the cold-dark-matter theory," says physicist Paul Steinhardt, at the University of Pennsylvania in Philadelphia.

Scientists proposed the theory as a way of reconciling two snapshots of the universe – one representing the distant past and another of the present. Several measurements indicate that the ubiquitous background microwave radiation, believed a remnant from the Big Bang, has the same intensity everywhere in space. This suggests the universe began as an incredibly smooth and uniform soup of matter and energy (SN: 1/20/90, p.36). The conundrum is how it evolved into its current lumpy collection of stars and galaxies.

Because the *observed* mass in the cosmos is too small to gravitationally bind large objects, cosmologists at first suspected that the universe contains a large quantity of invisible, ordinary dark matter to supply the needed gravitational glue.

But the garden-variety dark matter – composed of protons, neutrons or other familiar building blocks – interacts strongly with light. During the early history of the universe, this interaction would have suppressed gravity's tug and prevented tiny lumps or fluctuations in the density of primordial matter from growing fast enough to account for the present large-scale structures.

To solve the problem, theorists turned to the concept of *cold* dark matter, which postulates a type of hidden material that interacts weakly with light and has more time to expand the size of primordial lumps. But the simplest form of this model – in which all hidden matter is cold – still cannot explain the picture of the universe emerging from recent observations, Steinhardt and others say.

Next month, the U.S.-European Roentgen Satellite (ROSAT) will complete its first sky survey. Up to this point, it has resolved X-ray sources in greater detail and detected sources about 2.5 times fainter than other X-ray-probing satellites.

One of ROSAT's detectors imaged very dense, fuzzy patches of low-energy X-rays from dimmer sources about 8 to 12 billion light-years from Earth, Guenther Hasinger of the Max Planck Institute for Extraterrestrial Physics in Garching, Germany, reported last week at a meeting of the American Astronomical Society in Philadelphia. Based on this intensity, the rough shape of the fuzzy images and their proximity to individual quasars, he speculates that the X-ray emissions originate from clusters of quasars with a diameter of 15 to 75 million light-years.

Hasinger adds that further ROSAT observations with the same detector, expected to resume this August, may confirm the validity of the quasar-cluster interpretation. Stephen S. Holt of the NASA Goddard Space Flight Center in Greenbelt, Md., notes that ROSAT offers a prime tool to discern quasars, since many radiate 100 times more intensely in X-ray than in visible light. – *R. Cowen*

Heavenly bodies make their UV film debut

When the space shuttle Columbia landed last month after a nine-day research mission called Astro, one anxious scientist still didn't know if his shuttle-borne experiment had worked. Theodore P. Stecher of NASA's Goddard Space Flight Center in Greenbelt, Md., had to retrieve and develop 900 frames of ultraviolet-sensitive film from the payload before he could assess the success of the Ultraviolet Imaging Telescope, the mission's sole picture-taking instrument.

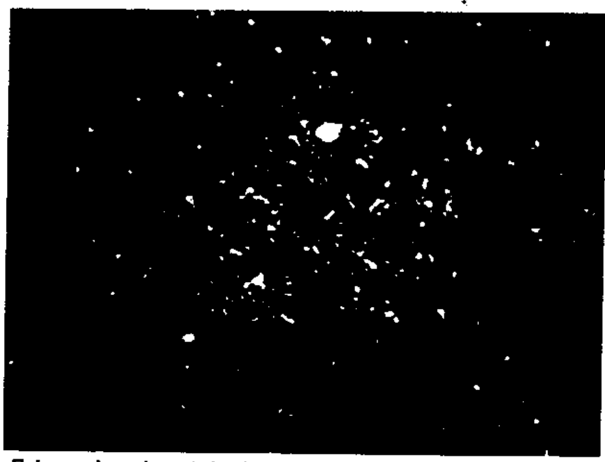

NASA Goddard

False-color ultraviolet image of the globular cluster Omega Centauri. The brightest areas denote regions of highest light intensity; the darkest areas denote the lowest intensity.

Last week, at the American Astronomical Society meeting in Philadelphia, Stecher announced that the telescope had performed well indeed, and he presented several images to prove it.

The central region of the globular cluster Omega Centauri (pictured here) occupies a region of the Milky Way some 17,000 light-years from Earth and houses nearly a million stars. Until now, none of those stars had been photographed in the ultraviolet. Optical pictures of the cluster, taken by ground-based telescopes, detect mainly red giant stars and yellow main-sequence stars, whereas the ultraviolet image primarily spotlights hotter, less common stars that evolved from red giants by ejecting their outer atmosphere.

Stecher points out that the ultraviolet photograph, in contrast to optical images, does not show a strong concentration of stars at the very center of the cluster. Whether the apparent dark areas or "holes" in the core represent light-obscuring dust clouds, stars too dim to detect or an actual gap in the cluster remains unclear, says Goddard astronomer Susan G. Neff.

Neff notes another curious feature: an unusually large variation in stellar light intensity, indicated by the presence of several different hues in the false-color image. She says that Omega Centauri may have collided at some earlier time with another cluster to create the mix of ultraviolet intensities and the lower-than-expected core density apparent in the globular cluster today.

The Ultraviolet Imaging Telescope also captured on film the spiral galaxy M81, about 12 million light-years from Earth. Bright spots in the galaxy's curving arms reveal areas where starbirth concentrates. Some of these bright regions form a ring – barely visible in optical images of M81 – about 19,500 light-years from the galactic center. Neff suggests that gravitational pull from another galaxy that passed nearby, perhaps the irregular galaxy M82, could have helped form the ring-shaped feature. – *R. Cowen*

Ultrasound reveals sickle-cell stroke risk

A new ultrasound method may help identify children and teenagers with sickle cell anemia who run a high risk of stroke, alerting physicians in time to begin preventive treatment.

Sickle cell anemia is a genetic disorder in which the normally round, puffy red blood cells contain defective oxygen-carrying molecules and sometimes become rigid and crescent-shaped. The disease causes frequent painful episodes when the distorted red blood cells block blood flow through tiny capillaries.

But an even greater threat lurks for sickle-celled children and teens if the arteries carrying blood to the brain become narrowed with a buildup of scar tissue. Researchers don't know what triggers the deposits, but they do know that these youngsters risk suffering a stroke – which can cause potentially lethal brain damage – when their abnormal red cells pile up in the already narrowed arteries, reducing the blood flow to the brain.

Physicians caring for sickle cell patients have had no way to tell which individuals possessed this added vulnerability until after signs of blood-flow restriction appeared. By that time, irreversible brain damage may already have occurred. Strokes can cause mental retardation, paralysis, coma and even death.

Scientists at the Medical College of Georgia in Augusta have now developed an ultrasound method, called transcranial Doppler, that uses sound waves to gauge the speed of blood flow to the brain. Neurologist Robert J. Adams and his colleagues reasoned that blood would travel at a higher velocity in narrowed arteries than in healthy ones, providing an early warning of impending stroke.

Their preliminary findings suggest the technique holds promise as a screening tool, Adams reported last week at the American Heart Association's annual science writers forum in Savannah, Ga. His team studied 250 children and teens with sickle cell anemia, using transcranial Dopper imaging to identify 40 individuals with higher-than-normal blood velocities (more than 160 centimeters per second). Six patients in that high-risk group suffered strokes within months of the ultrasound test, while only one stroke occurred among the 210 children with normal blood velocities, Adams says, suggesting that blood velocity can indeed foreshadow vessel occlusion.

The team then focused on seven of the youngsters who showed no discernible symptoms of stroke but whose ultrasound tests had indicated abnormally high blood velocities. Adams says such children may experience slight reductions in blood flow to the brain, which could lead to subtle brain damage that goes undetected during clinical examination. Using a magnetic resonance imaging device to visualize damaged tissue, the researchers discovered abnormal brain areas in three of the seven, whereas a group of 17 other youngsters who had normal ultrasound test values showed no brain injuries in the same type of images. Only further research will tell whether the three with brain abnormalities had suffered a "silent stroke," Adams says.

"This test may predict [sickle cell] patients at risk for stroke," says neurologist Steven G. Pavlakis at the Cornell University Medical College in New York City. If additional evidence confirms its predictive power, physicians might reduce these children's stroke threat by giving them blood transfusions every three to four weeks, he adds. Such transfusions would help prevent stroke by substituting normal blood cells for the sickling cells, Pavlakis says.

It's unclear whether the ultrasound method can uncover stroke jeopardy in a wider population, says John R. Marler at the National Institute of Neurological Disorders and Stroke in Bethesda, Md. Adams says he believes the technique holds promise for detecting stroke risk in the general population, but agrees that additional studies must establish its range of usefulness. – *K.A. Fackelmann*

Climate test: Hum heard 'round the world

From remote Heard Island far off the Antarctic coast, scientists next week will send sound waves throughout the world's oceans as part of an experiment to determine whether greenhouse gases are indeed warming the planet.

A simple physical fact underlies their technique: Sound travels faster through warm water than through cold water. By measuring changes in the speed of sound over a decade, scientists hope to obtain a clear answer about global warming.

Investigators will test the feasibility of this idea into early February. A dozen listening stations scattered around the globe will monitor the Heard Island transmissions in an attempt to measure the time it takes for the sound to cross the seas. If the experiment proves successful, scientists plan to begin routinely measuring sound speed in the ocean within the next few years. Walter H. Munk of the Scripps Institution of Oceanography in La Jolla, Calif., organized the Heard Island experiment.

This is the first attempt to establish a monitoring program over such vast distances, says Ted Birdsall of the University of Michigan in Ann Arbor, a principal investigator in the experiment. Researchers have used similar techniques to measure the speed of sound along a 4,000-kilometer stretch between Hawaii and North America, but next week's experiment will seek to more than quadruple that length. Sites on the east and west coasts of North America lie about 18,000 km – nearly halfway around the world – from Heard Island.

The experimenters will make their signal heard in such far-off places by exploiting a natural sound channel in the oceans. The channel exists in the region where sound travels the slowest – a layer sandwiched between the warm surface waters and the extremely dense layer below. When acoustic waves traveling through the sound channel begin to stray into the "faster" adjacent layers, refraction sends them back into the channel. In a 1960 experiment, sound waves from a single explosion off western Australia traveled through the sound channel and were clearly recorded at Bermuda.

In the Heard Island experiment, a transmitter lowered from a ship to a depth of 200 meters will create a low-frequency hum of about 57 hertz. The signal will be extremely faint by the time it reaches listening stations, so investigators will use complex processing techniques to isolate it from other noises.

Because marine mammals can hear sounds of that frequency, the experiment also involves biologists, who will observe the behavior of whales around the ship.

Computer climate models estimate that greenhouse gases should cause the world's oceans to warm by about 0.005°C per year at a depth of 1,000 meters. Direct measurements of ocean temperatures would not reveal such a small rise within a few years, but a program monitoring the speed of sound could detect clear signs of a greenhouse warming over five to 10 years, says project coordinator Robert Spindel of the University of Washington in Seattle. Over 10 years, the estimated warming would cut a few seconds off the signal's 3.5-hour trip from Heard Island to the Pacific coast of North America, he says.

In the past few years, climate experts have vigorously debated the meaning of a global warming trend apparent in records of continental and sea-surface temperatures. Because the planet's surface climate can fluctuate naturally, most scientists say they cannot tell whether the buildup of greenhouse pollutants in the atmosphere has indeed caused the observed warming trend.

The deep ocean, with its naturally stable climate, provides a means of sidestepping those problems, says Albert J. Semtner Jr. of the Naval Postgraduate School in Monterey, Calif., an oceanographer involved in the Heard Island experiment. "We think this is a clean way, an experimentally simple and clear way, to look for global warming," he says.

– *R. Monastersky*

Beverages intoxicated by lead in crystal

Lead crystal, containing 24 to 32 percent lead oxide, is revered for its brilliance and clarity. But preliminary experiments by two New York City researchers now indicate that extremely high levels of lead, a toxic heavy metal, can migrate from crystal decanters into the beverages they hold. The team's findings suggest that "long-term storage *of anything* in lead crystal is really to be avoided," says Joseph H. Graziano, who led the study.

Graziano, a toxicologist at Columbia University's College of Physicians and Surgeons, recalls that when internist Conrad Blum first questioned him about lead migration from glass, he thought Blum was "crazy." But Blum's home tests, showing the apparent leaching of lead from crystal into wine, piqued his curiosity. The two Columbia researchers describe their subsequent investigation in the Jan. 19 LANCET.

Blum supplied three lead-crystal decanters from home. He and Graziano cleansed each decanter and poured in port. Two days later, they began periodic samplings of the wine. "When we analyzed the first sample, I couldn't believe it," Graziano says. Lead showed a steady increase, from an initial level of 89 micrograms of lead per liter to between 2,160 and 5,330 µg/l four months later.

White wine doubled its lead concentrations within an hour of being poured into one lead-crystal glass, and tripled within four hours, they found.

Alcoholic beverages in 14 lead-crystal decanters brought in by colleagues showed similar spikes. Two brandies stored in lead crystal for more than five years accumulated 19,900 to 21,500 µg/l lead, the researchers found. (EPA's lead standard for drinking water is 50 µg/l, and there have been discussions of lowering it to 20 µg/l.)

Because a single glass of the contaminated brandy "contains as much lead as you would ordinarily become exposed to in a month from all other sources" – including air, water, diet and dust – Graziano contends that consuming such drinks would be "stupid."

And in a letter submitted Jan. 8 to the JOURNAL OF PEDIATRICS, Graziano, Blum and Columbia colleague Vesna Slavkovic report that apple juice and infant formula leach lead from crystal as effectively as alcohol does. In juice samples that sat in lead-crystal baby bottles for four hours, lead levels spiked from an initial 1 µg/l to 166 µg/l. Warm formula attained comparable levels in 15 minutes and reached 280 µg/l in four hours. Because infants are more sensitive to lead's effects than adults, the authors suggest "that the sale of these [crystal baby bottles] be forbidden," and have sent the new data to the FDA.

According to a statement issued last week by the Lead Industries Association (LIA), the alcohol study suggests "there is negligible risk" from beverages placed in lead-crystal barware "for short periods of time, such as during a meal." LIA and another industry group, the International Lead Zinc Research Organization, plan a study of the risks posed by long-term storage of alcohol in lead-crystal decanters. FDA is already conducting a similar investigation. *– J. Raloff*

C_{60}: Definitely a beauty, maybe a beast

Since last August, physics graduate student Lowell D. Lamb and his coworkers at the University of Arizona in Tucson have donned gloves and masks when working with chemistry's latest darling, a soccerball-shaped molecule known as buckminsterfullerene. That's when Henry K. Hall Jr., a chemist at the university, alerted them to health hazards that may lurk in the 60-carbon beauty.

No one has reported ill effects from buckminsterfullerene, but Hall and others urge researchers to proceed with caution. If biologists were to happen upon a new animal species with teeth and claws, they would take precautions even though the animal might turn out to be a pussycat. The same should hold for scientists probing new chemical species, Hall warns.

By some estimates, hundreds of researchers now spend at least part of their time studying C_{60}, its molecular cousins such as C_{70} and C_{84}, and the solid materials, called fullerites, into which these cage-like molecules assemble (SN: 12/8/90, p.357). The fullerites join diamond and graphite as the third material form of carbon atoms.

But the same structural symmetries and physical oddities that render these celebrity chemicals so intriguing may represent the molecular equivalent of teeth and claws, researchers are finding.

Robert Whetten of the University of California, Los Angeles, and his coworkers have been outspoken about such possibilities. In the Jan. 9 JOURNAL OF PHYSICAL CHEMISTRY, they report that C_{60}, in the presence of light, efficiently transforms oxygen molecules into a so-called singlet state, an especially reactive form that can sabotage biochemical harmonies underlying the health of cells and tissues. The researchers do not yet know if C_{60} actually can initiate these processes under physiological conditions, Whetten notes. Besides pegging buckminsterfullerene as a potential health threat, the findings show how the molecule's electrons harness and shunt light-energy as C_{60} interacts with nearby molecules.

"The degree to which C_{60} is present in the environment becomes a very important question," the UCLA researchers state in their paper. That the synthesis of C_{60} yields fine powders only heightens their concern. "We feel it is important to warn researchers to take precautions against skin contact and breathing of the dusts, at least until the physiological properties of the material have been better characterized," warn Whetten, Francois N. Diederich and Christopher S. Foote of UCLA, and Fred Wudl of the University of California, Santa Barbara, in a letter in the Dec. 17, 1990 CHEMICAL & ENGINEERING NEWS. *– I. Amato*

Asthma culprit cloned

It starts with some wheezing, a hoarse, dry cough and a growing sensation of pressure that leaves victims panicked and gasping for breath. War in the Middle East notwithstanding, this is not a poison gas attack. These symptoms represent common occurrences for the more than 8 million Americans with asthma.

Despite decades of work, scientists have yet to design the perfect asthma drug – one that specifically targets the potent biochemical mediators of this immune overreaction. But new research led by a Japanese physiological chemist may speed the development of such a drug.

Takao Shimizu at the University of Tokyo, with colleagues there and at the Protein Engineering Research Institute in Osaka, has cloned the cell-surface receptor for a blood compound called platelet-activating factor (PAF) – one of the body's most potent alarm chemicals and the one responsible for much of the biochemical mayhem underlying asthma attacks and other inflammatory reactions.

When released from blood cells in response to an allergic reaction or toxic exposure, PAF triggers circulating platelets to release substances that promote bronchial spasms and leakage of fluid into the lungs. The newfound ability to mass-produce PAF receptors should help medicinal chemists design drugs that can calm the oversensitive receptors, the researchers assert in the Jan. 24 NATURE.

"It's very good work, an important development," says Donald J. Hanahan, a PAF biochemist at the University of Texas Health Sciences Center in San Antonio. He notes that PAF is made of fat rather than protein, and says the new work seems to mark the first cloning of a receptor for a fat-mediated cellular signal. As such, Hanahan says, the new research may also help explain how prostaglandins and leukotrienes – extremely potent, fat-based mediators of pain and inflammation – perform their biological duties. □

Fiftieth search honors student scientists

One young researcher cultivated metal-enriched seaweed in his garage to make methane; another found a correlation between the number of calories her classmates consumed and their stress levels before taking school tests. A fledgling computer scientist who loves baseball modeled the effects of spin and air drag on the ball's trajectory. These student scientists are among the 40 finalists in the 50th annual Science Talent Search, a nationwide competition designed to identify, encourage and honor budding talent in science, mathematics and engineering.

Selected from among 1,573 high school seniors who entered the competition, the finalists completed projects in a diverse range of fields, including mathematics, behavioral science, chemistry, nutrition and physics. Some went to research laboratories, stayed by their computers, visited children's play groups or ventured to the seashore to conduct their scientific inquiries. One finalist studied the importance of friendships in the well-being of nursing-home patients, another examined number theory, and a third used sunblocking agents to help develop a tough, weatherproof varnish.

The students, 17 females and 23 males, will gather in Washington, D.C., on Feb. 28 for a five-day, all-expenses-paid visit, where they will compete for a total of $205,000 in science scholarships. Through a series of interviews, a board of judges will select 10 top winners to receive four-year scholarships, which range from $10,000 to $40,000. Each of the remaining 30 will receive a $1,000 scholarship. All finalists will have the opportunity to talk with scientists in the area.

The talent search is sponsored by Westinghouse Electric Corp. and administered by Science Service, Inc.

This year's finalists, aged 15 to 18, will display their research projects to the public on March 2 and 3 at the Washington Hilton Hotel in Washington, D.C.

The 40 winners are:

ALABAMA: Mehul Vipul Mankad, St. Paul's Episcopal School, Mobile; Weily Soong, Vestavia Hills H.S., Vestavia Hills.

CALIFORNIA: Wei-Jen Jerry Shan, John W. North H.S., Riverside; Rageshree Ramachandran, Rio Americano H.S., Sacramento; Tessa Lorrell Walters, San Gabriel H.S., San Gabriel.

COLORADO: Mark Allen Larson, Horizon Sr. H.S., Brighton.

CONNECTICUT: Don H. Kim, Greenwich H.S., Greenwich.

DISTRICT OF COLUMBIA: Joel Ellis Moore, St. Albans School.

FLORIDA: Clifford Lee Wang, Vero Beach H.S., Vero Beach.

ILLINOIS: Joseph Izak Seeger, Evanston Township H.S., Evanston; Irwin Lee, Naperville North H.S., Naperville.

IOWA: Nupur Ghoshal, Ames H.S., Ames.

MICHIGAN: Lori Ann Stec, Detroit Country Day School, Birmingham.

NEBRASKA: Kimberly Ann Chapman, Marian H.S., Omaha.

NEW JERSEY: Denis Alexandrovich Lazarev, Elmwood Park Memorial Jr.-Sr. H.S., Elmwood Park; Dean Ramsey Chung, Mountain Lakes H.S., Mountain Lakes; Stanley Lu, Bridgewater-Raritan H.S. West, Raritan.

NEW MEXICO: Cameron Rea Haight, Santa Fe H.S., Santa Fe.

NEW YORK: Cheryl Lynn Pederson, Byram Hills H.S., Armonk; Jim Way Cheung, Bronx H.S. of Science, New York City; Ciamac Moallemi, Benjamin N. Cardozo H.S., New York City; Ani Jean-Mee Fleisig, Nuri Mehmet Kodaman, Townsend Harris H.S., New York City; William Ching, Riverdale Country School, New York City; Tara Sophia Bahna-James, La Guardia H.S. of Music and the Arts, New York City; Petal Pearl Haynes, Yves Jude Jeanty, Linda Tae-Ryung Kang, Sunmee Louise Kim, Debby Ann Lin, Tien-An Yang, Stuyvesant H.S., New York City; Michael John Lopez, Ward Melville H.S., Setauket.

NORTH CAROLINA: Ashley Melia Reiter, North Carolina School of Science and Mathematics, Durham.

OHIO: Jeremy Randall Riddell, The Miami Valley School, Dayton.

PENNSYLVANIA: Susan Elaine Criss, Fox Chapel Area H.S., Pittsburgh.

TEXAS: Wade William Butin, Klein H.S., Spring.

VIRGINIA: Judson Lawrence Berkey, Venkataramana Kuntimaddi Sadananda, Daniel Moshe Skovronsky, Thomas Jefferson H.S. for Science and Technology, Alexandria; Tatiana Tamara Schnur, Robinson Secondary School, Fairfax.

Antibody treatment joins AIDS battle

Antibody injections can help stave off severe bacterial diseases in some children infected with the AIDS virus (HIV), a new study shows.

Because children's immune systems have yet to reach full potency, HIV — which weakens immunity — leaves them especially vulnerable to bacterial infections such as pneumonia and meningitis. Noting that physicians already prescribe classes of antibodies known as immunoglobulins for other immune deficiencies, researchers reasoned that the same treatment might help HIV-infected children fight these life-threatening secondary infections.

Although the immunoglobulin injections did not improve children's chances of surviving through the entire 2½-year study, they did reduce the number of hospital stays among the children with less severe HIV infections, reports study director Anne D. Willoughby of the National Institute of Child Health and Human Development. She and her colleagues announced the results at a press conference last week.

The study involved 372 children, 2 months to 12 years of age, at 28 medical centers across the United States. All showed immunologic or clinical symptoms of HIV infection when the study began, and some met diagnostic criteria for AIDS. About half received monthly intravenous injections of purified immunoglobulins (400 milligrams per kilogram of body weight) obtained from healthy adult donors.

To gauge the severity of HIV infection, investigators measured blood levels of white cells called CD4 lymphocytes, which decline as the infection progresses. Among children whose CD4 counts exceeded 200 at the study's beginning, 68 percent of the immunoglobulin-treated group escaped serious bacterial infections for two straight years, compared with 48 percent of the placebo group, Willoughby says. The injections did not appear to help children with CD4 counts below 200.

During the study, many children began taking the antiviral drug AZT to combat HIV or antibiotics to treat bacterial infections, but Willoughby says this did not interfere with the interpretation of the results.

Scientists have no indication that the treatment can boost immunity in HIV-infected adults. Children may benefit from the injections because their immune systems lack reserves of antibody-producing cells. A child's immune system "needs to go to school in a sense," explains William T. Shearer, a pediatric immunologist at the Texas Children's Hospital in Houston.

In a separate study of children with symptomatic HIV infection, researchers led by Philip A. Pizzo of the National Cancer Institute focused on ddI, an experimental drug that targets the virus. They report in the Jan. 17 New England Journal of Medicine that ddI appears safe and shows "promising" anti-HIV activity in children. They note, however, that its stability in the stomach varied greatly from one child to the next, making dosage requirements tricky to determine. Physicians will need to monitor patients' blood levels of ddI and adjust dosage accordingly, the researchers conclude. — *W. Gibbons*

A Melancholy Breach

Science and clinical tradition clash amid new insights into depression

By BRUCE BOWER

In the past decade, psychiatrists, psychologists and others dealing with depressed patients have experienced an odd mix of optimism and unease.

Their optimism stems from a growing confidence in various combinations of talk therapies and drug treatments to allay mild to extreme forms of depression. Their unease emanates from a harsh exchange between two clinical camps over how best to subdue the sometimes life-threatening symptoms of "major" or severe depression.

An increasingly powerful, research-oriented camp trumpets scientific data supporting a marriage of antidepressant drugs with short-term psychotherapy aimed at altering depression-inducing thoughts and behaviors. A second group of mental health workers, with a perspective grounded in Freudian psychoanalysis, eschews the pursuit of scientific data. Instead, they rely on decades of clinical experience with long-term "psychodynamic psychotherapy" focused on unconscious conflicts and emotions. These therapists grant medication a supporting role at best.

A lawsuit launched in 1982 epitomized this rift. A former patient at a prestigious mental hospital in Rockville, Md., sued the hospital for negligence because it had failed to treat his severe depression with antidepressant drugs. Hospital clinicians had offered the man only intensive, four-times-a-week psychodynamic psychotherapy. The case, known as *Osheroff v. Chestnut Lodge*, achieved considerable notoriety in the mental health community before an out-of-court settlement in 1987, for an undisclosed amount of money, staved off a jury trial.

Friction between biologically and psychodynamically oriented therapists shows no signs of dissipating in the 1990s, especially as insurance dollars for mental health care dwindle. Another ongoing and related dispute – involving both mental health workers and organizations of mental patients and their families – concerns whether major depression and other serious mental disorders primarily represent diseases or stem in critical ways from social and emotional factors.

As these issues continue to generate heated debate, two new investigations shine some precious light on depression's causes and treatments.

Women suffer from all forms of depression at twice the rate of men largely because of cultural and social factors rather than biological predisposition, concludes the National Task Force on Women and Depression in its final report, released last December. The 20-member task force, commissioned by the American Psychological Association (APA), spent three years reviewing research and synthesizing the findings.

Some investigators maintain that the depression gender gap reflects women's greater ease in talking about emotional distress and contacting mental health workers. The APA report, however, accepts the gap as genuine and characterizes it as a product of several risk factors – predominantly social and cultural ones – that promote depression among women. Those factors, according to the report, include physical and sexual abuse, unhappy marriages, poverty and a culturally sanctioned tendency for women to dwell on feelings of depression rather than act to overcome them. Researchers often neglect social factors that influence depression among women, says report coauthor Bonnie R. Strickland, a psychologist at the University of Massachusetts in Amherst.

In addition, hormonal changes related to reproductive events, including menstruation, pregnancy, childbirth and infertility, may further influence women's depression, according to the report. In the case of major depression, the task force grants culture and upbringing equal power with female physiology.

Bouts of major depression last for at least two weeks. Some people suffer only one or a few such episodes, while others spend years dipping in and out of a dark well of melancholy. Typical symptoms include a loss of interest and pleasure in virtually all activities, feelings of helplessness and hopelessness, sleep and appetite disturbances, loss of energy, and thoughts of suicide. An estimated 15 percent of severely depressed people kill themselves, and many more attempt suicide. A recent survey by the National Institute of Mental Health indicates that recurring, severe depression afflicts about 2.5 million men and women in the United States.

According to the task force report, scientific studies show that two forms of short-term psychotherapy – usually lasting a few months – provide help to women suffering from mild to severe depression. Interpersonal therapy examines how conflicts with others and disturbed relationships contribute to depression. Cognitive-behavioral therapy attempts to correct the distorted thinking, attitudes and behaviors that characterize depression.

Many clinicians treat severely depressed people with long-term psychodynamic psychotherapy, but the task force asserts that virtually no scientific studies have charted the effectiveness of this approach, leaving its supporters to take guidance from clinical reports and experience.

Antidepressant medication proves "at least partially effective" for women with major depression, according to the report, particularly when physicians carefully monitor individual doses of these powerful drugs.

However, the task force charges that much antidepressant research suffers from a "gender-related blind spot." Comparisons of men's and women's responses to the drugs rarely appear, and few studies examine the effects of tailoring women's antidepressant doses to the menstrual cycle – a strategy that may improve medication effectiveness, according to the report's authors.

Regardless of gender, continued high daily doses of imipramine – a commonly used antidepressant – quell most recurrences of major depression with remarkably few side effects, according to a new study reported in the December 1990 ARCHIVES OF GENERAL PSYCHIATRY.

Short-term psychotherapy, combined with generous doses of imipramine or chemically related antidepressants, pulls many individuals out of the depths of depression, says study coauthor David J. Kupfer, a psychiatrist at the University of Pittsburgh School of Medicine. When depression lifts after a few weeks or months, treatment with the same amount of medication for at least three years usually keeps mood on an even keel, he contends.

Most clinicians currently reduce the prescribed antidepressant dose or stop drug treatment altogether once an individual under their care sheds the cloak of depression.

"We can now tell people, 'The dose of antidepressant that gets you well keeps you well,'" says psychologist Ellen Frank, also of the Pittsburgh School of Medicine, who directed the investigation.

Frank and her colleagues studied 230 people who had experienced recurring periods of major depression for an average of 12.5 years. All participants entered the study during an episode of depression. For the first 17 weeks, they received a relatively high daily dose of imipramine — about 200 milligrams — and sessions of interpersonal therapy every week or two. This approach eased depression for 98 women and 30 men. The rest of the participants left the study, mainly due to a lack of response to the treatments or intolerable side effects from imipramine.

The remaining volunteers received one of five maintenance treatments for the next three years. Twenty-eight participants stayed on the same daily imipramine doses that helped spur their recovery; 23 received daily placebo capsules; 26 attended monthly interpersonal therapy sessions; 26 got interpersonal therapy and placebos; and 25 got therapy and the full daily dose of imipramine.

Of the 53 participants who stayed on imipramine, 41 remained free of depression for the entire three years. The combination of interpersonal therapy and imipramine showed no clear advantage over imipramine alone, probably because the drug's effects proved so successful that psychotherapy added little over the long haul, Kupfer says.

Only one-fifth of the placebo-only group avoided depressive episodes during the maintenance period. Volunteers who went without imipramine but received monthly interpersonal therapy fared better, with about half remaining well for the entire three years. Interpersonal therapy may thus offer a "window of wellness" to many women who wish to discontinue antidepressants during pregnancy, Frank notes.

No statistically significant difference emerged between the responses of men and women in the maintenance study.

Imipramine and chemically related antidepressants can cause a number of side effects, including dry mouth, blurred vision, weight gain, drowsiness, lowered blood pressure, constipation and impotence. But of the 22 volunteers who dropped out of drug treatment during the maintenance period, only four cited medication side effects as the reason, Kupfer observes.

He notes that general practitioners — who see the bulk of severely depressed patients — often refrain from prescribing antidepressants out of fear that individuals in the throes of melancholy will take intentional overdoses. Yet no suicides, and only one attempted suicide, occurred among participants in the Pittsburgh study, Kupfer says.

With careful blood monitoring of high-dose antidepressants, presumably including the new and widely touted fluoxetine (Prozac), "the danger of suicides and overdoses isn't what primary-care physicians have been led to believe," Kupfer maintains.

Despite the growing evidence of antidepressants' benefits and the absence of scientific data to back psychodynamic therapy as an effective treatment for major depression, psychodynamic proponents and their critics continue to skirmish in the aftermath of the *Osheroff* case. Two psychiatrists at the center of the debate squared off in the April 1990 AMERICAN JOURNAL OF PSYCHIATRY.

APA/Thorina Rose

Psychiatric patients have a right to treatments with a scientific stamp of approval, which psychodynamic therapy lacks, contends Gerald L. Klerman of Cornell University Medical College in New York City. Klerman, a codeveloper of interpersonal therapy, believes substantial evidence exists for treating severe depression with a combination of antidepressant drugs and short-term therapy.

"The issue is not psychotherapy versus biological therapy, but rather opinion versus evidence," he maintains.

Alan A. Stone of Harvard University in Cambridge responds that psychodynamic psychotherapy promotes gains in self-knowledge and emotional awareness not captured by stringent scientific studies. Many mental health workers still rely on the psychodynamic approach to treat mild to major depression because the therapy passes clinical, if not scientific, muster, he says.

Most scientific studies of treatments for mental disorders remain preliminary and should not "dictate to clinicians the clinical standards of care," he adds.

Some clinicians say the *Osheroff* settlement has already cast a pall over patient care. "It seems that if we so much as inquire whether a depression might be related to the stresses or losses of life before blasting it with a chemical, we are virtually guilty of malpractice," writes psychiatrist Matthew P. Dumont in the October 1990 AMERICAN JOURNAL OF ORTHOPSYCHIATRY.

Dumont, medical director of the Chelsea (Mass.) Community Counseling Center, charges that psychiatry "should openly declare its identity as an arm of the drug industry." Pharmaceutical money now underwrites most of psychiatry's academic research, professional journals and scientific conferences, he argues. What's more, psychiatrists and other physicians each receive thousands of dollars' worth of logo-inscribed reprints, coffee mugs, pens, calendars and other gifts annually from drug company representatives, creating a clear conflict of interest when it comes time to write prescriptions, Dumont says.

His argument echoes testimony at a Dec. 11 hearing convened by the Senate Labor and Human Resources Committee. Some participants, including a former public relations official for a pharmaceutical firm, claimed that drug companies devise expensive giveaways to bribe physicians into prescribing their products. Representatives of the pharmaceutical industry and the American Medical Association denied the charge, pleading the importance of quick communication between drug companies and physicians concerning the rapid advances in drug treatment.

Many psychiatric leaders defend their profession's ties to major drug companies as a boon to research on mental disorders such as major depression.

Meanwhile, back at the front lines of depression treatment, optimism and unease hang tough. □

A FOREST OF KINGS

THE UNTOLD STORY of THE ANCIENT MAYA

LINDA SCHELE
AND
DAVID FREIDEL

Morrow, 1990, 542 pages,
7½" x 10", hardcover, $29.95

The recent interpretation of Maya hieroglyphs has given us the first written history of the New World as it existed before the European invasion. *A Forest of Kings* is the story of Maya kingship, from the beginning of its institution and the first great pyramid builders two thousand years ago to the decline of Maya civilization and its destruction by the Spanish. Here the great historic rulers of Precolumbian civilization come to life again with the rediscovery of their language. At its height, Maya civilization flourished under great kings like Shield-Jaguar, who ruled for more than sixty years, expanding his kingdom and building some of the most impressive works of architecture in the ancient world. Long placed on a mist-shrouded pedestal as austere, peaceful stargazers, the Maya elites are now known to have been the rulers of populous, aggressive city-states.

Kingship was the primary political and religious institution of the ancient Maya and unified the Maya view of art, politics, war and religion. The Maya were at once highly civilized, skilled in architecture and astronomy, and, to us, violent and barbaric, engaging in ritual bloodletting and many wars.

The true artistry of the Maya glyphs and artifacts is evident in the 24-page color section. In addition, Maya history is brought clearly to life through the more than 250 illustrations, maps and charts that are found throughout the text.

— from the publisher

ForestKings

Science News Books
1719 N Street, NW, Washington, DC 20036
Please send ______ copy(ies) of **A Forest of Kings.** *I include a check payable to Science News Books for $29.95 plus $2.00 postage and handling (total $31.95) for each copy. Domestic orders only.*
Name ______________________
Address ______________________
City ________ *State* ________ *Zip* ________
Daytime Phone (____)________ (used only for problems with order) RB1366

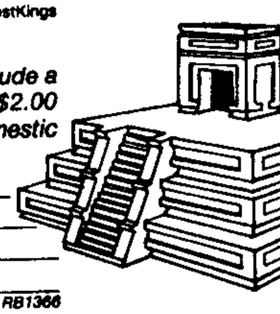

Letters continued from p.51

ization of Lewis makes me wonder how much he really knows about him. Lewis was an eminent professor of English literature at both Oxford and Cambridge, a noted philosopher and a successful author of fiction and nonfiction. He was highly respected for the lucid, rigorous logic of his analytical thought. Although well known as an orthodox Christian apologist, he was *not* a fundamentalist, a creationist or a "young-Earther," as Mr. Cole seems to be using those terms.

Mr. Cole's letter raises a deeper issue, however. It is ironic that someone defending the intellectual virtue of science should display the very same knee-jerk rejection of unfamiliar ideas, and pejorative labeling of those who propose them, that religious fundamentalists are so often accused of. No scientist, even an amateur one, should be so quick to conclude that he has "nothing to learn in the way of science" from anyone, much less from so distinguished a scholar as C.S. Lewis.

Peter H. Shaw
Irving, Texas

When Senator McCarthy wanted to blacklist someone he opposed, the label "communist" was used to silence that person. Apparently, "fundamentalist" is the label now in vogue for that purpose.

Censorship, especially in the Letters section, does not serve the advancement of knowledge. Thank you for allowing your readers the opportunity to hear Mr. Shaw for ourselves and to decide on the validity of his thesis.

John N. Bowman
Macon, Ga.

Astronomy

Ron Cowen reports from Philadelphia at a meeting of the American Astronomical Society

Supernova yields cosmic yardstick

Observations of remnants of supernova 1987A by camera and spectrograph have furnished new clues to the life of a star whose catastrophic explosion – as a supernova – astronomers witnessed four years ago. The observations may also lead to an even greater cosmic payoff – a more accurate determination of the distance between Earth and the Large Magellanic Cloud, the galaxy containing the burned-out star.

Astronomers say their new estimate of the distance to that galaxy represents a first step toward developing a better yardstick for the age and size of the universe, says Nino Panagia of the Space Telescope Science Institute in Baltimore. Attaining such a yardstick, he believes, might also lead to an eventual recalibration with unprecedented accuracy of the Hubble constant – the change in the expansion velocity of the universe with distance.

Panagia and his colleagues, including scientists from Harvard University and the Space Telescope European Coordinating Facility in Garching, Germany, based their work on observations by the International Ultraviolet Explorer (IUE) satellite and Hubble Space Telescope.

NASA/European Space Agency

Instruments aboard these craft examined nitrogen-rich gas ejected from 1987A thousands of years before this heavenly body exploded as a supernova. Most of this wispy gas envelope eventually collapsed into a ring. But that ring went undetected until the supernova explosion heated it, causing the gas to radiate ultraviolet light. Finding this ring, Panagia notes, ends a debate about the geometry of the ejected gas.

A Hubble image of 1987A (see photo), taken in August and released last week, shows the supernova core surrounded by a ring of glowing gas tilted 47° from an imaginary plane cutting through the Earth and the stellar core.

Once they glimpsed the ring, Panagia and his co-workers set about precisely calculating its distance from Earth. From Hubble data, they determined that the ring has an angular diameter of 1.66 arcseconds – comparable to the separation of two auto headlights viewed from 100 miles away. The astronomers then measured the diameter of the ring, a second factor needed to calculate its distance from Earth.

In analyzing spectroscopic IUE data, they found that light from the edge of the ring closest to Earth reached the satellite 80 days after the first detection of the supernova explosion. Ultraviolet emissions from the ring's farthest edge did not arrive until 340 days later. This time difference allowed the researchers to calculate the ring's diameter of 1.37 light years. Using straightforward geometry, they then determined that the supernova lies 169,000 light years from Earth. Previous estimates ranged from 143,000 to 179,000 light years.

At the Cerro Tololo Inter-American Observatory in La Serena, Chile, other astronomers used a high-resolution spectrograph to deduce the speed at which 1987A's gas ring is moving out from the supernova's core. Based on this velocity and the location of a still-wispy shell of gas about 12 light years from the ring, Arlin P.S. Crotts of Columbia University in New York City and Stephen B. Heathcote of Cerro Tololo conclude that 1987A began ejecting its gas cloud at least 400,000 years before it went supernova. They also estimate that the star ended the ejection and evolved from a red supergiant to a blue supergiant some 20,000 years before it exploded.

Biomedicine

Kathy A. Fackelmann reports from Savannah, Ga., at the American Heart Association's 18th science writers forum

Proteins guide early heart development

During the first few months of development, a human embryo's single-chambered heart must somehow transform itself into the four-chambered heart that, if all goes well, will serve as a powerful pump throughout life. If embryonic heart development goes awry, a life-threatening defect – such as a hole in the heart – can result.

In a quest that may someday lead to treatments for infants with heart defects, scientists are homing in on a set of proteins that may guide this *in utero* development.

The embryo's single-cavity heart contains a layer of jelly-like material sandwiched between an outer layer of muscle tissue and an inner tissue layer known as the endocardium. Between the fourth and eighth weeks of gestation, certain cells lining the endocardium, called endothelial cells, break away and migrate through the cardiac jelly, eventually forming tissue pads that divide the heart into four chambers.

But what triggers the cellular journey? Roger R. Markwald, a biologist at the Medical College of Wisconsin in Milwaukee, and his colleagues suggested in 1989 that so-called adherons – packets of proteins carrying a glue-like substance – adhere to embryonic endothelial cells and somehow cause them to begin their migration. The team reported experiments demonstrating that chick-embryo endothelial cells placed atop a gel layer in a petri dish broke away from their neighbors and started to travel into the gel when exposed to adherons isolated from the cardiac jelly of embryonic chick hearts.

The researchers have now begun to characterize the mysterious adherons. Their unpublished results suggest that cardiac adherons contain at least five key proteins, Markwald told SCIENCE NEWS. The team now hopes to identify each of these proteins and find out how they guide the crucial transformation to a four-chamber heart. Ultimately, says Markwald, such knowledge might enable researchers to develop drugs that spur self-repair in a newborn's defective heart.

Brain neurons blamed for dizzy spells

In a bygone era, fainting or dizzy spells signified a response to great passion or trauma. Modern science has since taken the romance out of these episodes, ascribing many of them to the mundane activity of standing up too quickly.

When a person stands up, a complex system called the baroreflex kicks into action: Nerve endings in key blood vessels detect the resulting drop in pressure and send a message to brain neurons, which respond by boosting blood pressure. Scientists know that the baroreflex often begins to fail with age, leading to dizziness, fainting spells and even stroke. But the exact nature of this failure has remained elusive.

George Hajduczok, a physiologist at the University of Iowa in Iowa City, now reports evidence suggesting that the blame lies with malfunctioning neurons. He and his colleagues studied 11 elderly purebred beagles and five young beagles. They increased blood pressure within the dogs' carotid arteries, which contain pressure-sensing nerve endings. Young dogs quickly sensed that change and lowered the activity of the sympathetic nervous system – which boosts blood pressure – by 70 percent, whereas elderly beagles damped such activity by only 20 percent, the researchers found.

A separate experiment showed that elderly dogs can lower sympathetic nervous system activity as much as young dogs, but only for a few seconds – a finding that suggests the problem lies with the brain neurons rather than the nerve endings.

Such studies may help explain why some elderly people experience dangerous swings in blood pressure. A faulty baroreflex, says Hajduczok, can cause fainting when pressure dips too low, or a stroke when pressure soars too high.

RIBBON OF CHAOS

Researchers develop a lab technique for snatching order out of chaos

By IVARS PETERSON

Initially standing upright like a stiff stalk of grass, a paper-thin metal ribbon begins to bend over. It bows low, then straightens. It bends again, this time making just a quick nod. Then it does a string of low bows, a few brief nods and another low bow, sometimes throwing in a wiggle or two. Wavering unpredictably, the ribbon's motion follows no apparent pattern.

Now a researcher adjusts the magnetic field in which the ribbon dances. In a few seconds, the ribbon's chaotic motion settles into a repeating pattern: first a deep bow, then a nod, then another deep bow, a nod and so on. Instead of abruptly and arbitrarily shifting from one type of motion to another, the ribbon endlessly repeats the same combination of moves.

This laboratory demonstration marks an unprecedented feat. For the first time, researchers have controlled the chaotic behavior of a real-world physical system simply by making small adjustments to one of the parameters governing the system's behavior. Physicists William L. Ditto, Steven N. Rauseo and Mark L. Spano of the Naval Surface Warfare Center in Silver Spring, Md., describe their achievement in the Dec. 24, 1990 PHYSICAL REVIEW LETTERS.

The first indication that such control might be attained surfaced in the March 12, 1990 PHYSICAL REVIEW LETTERS. In a theoretical paper, Edward Ott, Celso Grebogi and James A. Yorke of the University of Maryland in College Park introduced the notion that – just as small disturbances can radically alter a chaotic system's behavior – tiny adjustments can also stabilize its behavior.

The success of this strategy for controlling chaos hinges on the fact that the apparent randomness of a chaotic system is really only skin deep. Beneath this chaotic unpredictability hides an intricate but highly ordered structure – a complicated web of interwoven patterns of regular, or periodic, motion.

Normally, a chaotic system continually shifts from one pattern to another, creating an appearance of randomness. In controlling chaos, the idea is to lock the system into one particular type of repeating motion.

In their paper, Ott and his co-workers described their success in demonstrating the control of chaos in a numerical experiment on a computer. The Navy team has now matched this success in the laboratory.

"Far from being a numerical curiosity that requires experimentally unattainable precision, we believe this method can be widely implemented in a variety of systems, including chemical, biological, optical, electronic, and mechanical systems," Ditto, Rauseo and Spano write in their paper.

Their experimental equipment looks rudimentary. The key component – resembling a piece of stiff tinsel – consists of a metal strip 65 millimeters long, 3 millimeters wide and 25 micrometers thick, planted in a clamp that keeps it upright. Three pairs of electromagnetic coils the size of bicycle rims generate the magnetic fields surrounding the clamped ribbon.

But the metal ribbon, made from a specially prepared iron alloy, has a remarkable property: It changes its stiffness in accordance with the strength of an external magnetic field.

At first, the ribbon stands erect. Increasing the magnetic field along the ribbon's length causes the strip to soften, and the ribbon begins to droop under its own weight. Once the magnetic field reaches a certain value – only a few times larger than Earth's modest magnetic field – the ribbon abruptly begins to stiffen again, causing it to straighten.

Using a slowly oscillating magnetic field, the researchers can force the ribbon to droop and straighten in sync with the field. "It's like turning a dial and making the ribbon stiffer or softer, then letting gravity do the rest," Spano says.

However, increasing the forcing field's frequency or strength pushes the ribbon into a chaotic regime in which its motion becomes unpredictable. "It clearly exhibits the hallmark of a chaotic system – that is, getting continuously thrown from one periodic motion to another," Rauseo says.

He and his co-workers can construct a kind of map of this irregular motion by monitoring the ribbon's displacement at the end of each cycle of the oscillating magnetic field. If the ribbon repeats the same motion at regular intervals, then its position will be the same at the end of each cycle. The entire map then consists of a single point.

However, if its motion is irregular, then the ribbon's position will vary each time, and the map will show an array of scattered points, which happen to fall into a particular pattern (see cover). Such an array is known as a chaotic attractor. As the ribbon moves, a computer builds up an image, point by point, of the system's attractor.

To control the ribbon's motion, the researchers display the attractor on a computer screen and select a point that corresponds to a particular type of periodic motion. Then they wait until the ribbon's motion, as represented by successive dots on the computer screen, shows up near the point they've selected on the attractor. That close encounter triggers a simple computer program that calculates how much and in which direction to adjust the underlying, steady magnetic field to keep the ribbon trapped in the desired periodic motion.

Corralling the ribbon's motion is akin to balancing a ball on a saddle, Spano says. The ball won't roll off the saddle's raised front or back, but continual adjustments – in the case of the ribbon, a steady train of small magnetic nudges – are needed to kick it back into position as it begins rolling off at the sides.

By making slight adjustments approximately every second to the steady, vertical magnetic field acting on the ribbon, the researchers can maintain the ribbon's regular motion for as long as they want. As soon as they relinquish control, the ribbon resumes its chaotic dance. They can then reestablish control, bringing the ribbon back to the same periodic motion it had before, or, just as easily, putting it into a different type of regular motion.

"We don't avoid the chaos; we stay in the chaotic region," Ditto says. "We take advantage of the system's sensitive dependence on initial conditions."

The trick is to exploit the fact that a chaotic system already encompasses an infinite number of unstable, periodic motions, or orbits. That makes it possible to zero in on one particular type of motion, or periodic orbit, or to switch rapidly from one type of motion to another.

The theory developed by Ott, Grebogi and Yorke suggests that scientists could use this technique for controlling many different chaotic systems. "The method is very general and should be capable of yielding greatly improved performance in a wide variety of situations," they assert in their March report.

Surprisingly, researchers don't even need to know the mathematical equations describing the dynamical behavior of a particular system in order to make the control technique work. It's sufficient to observe the system long enough to map its chaotic attractor and to determine by experiment a few crucial quantities necessary for establishing control.

"You don't need to have a deep theoretical understanding of what's going on," Rauseo says.

"All you need to know is, in effect, the shape of the saddle, and that you can get from observations of the system," Spano adds. "You don't need an equation."

To simplify matters further, researchers need bother with only one control parameter. The Navy team, for example, could control the magnetic ribbon's motion by making small adjustments to the oscillating magnetic field's frequency or strength, to the steady magnetic field's strength, or even to the ambient temperature. They chose the parameter they could adjust most easily: the steady magnetic field.

"We kind of expected this might be a very difficult thing to do," Ditto says. "It was actually remarkably easy for us to implement."

Random disturbances persist, springing from an array of environmental factors such as temperature fluctuations and errors in the measurements necessary for characterizing the system's attractor and saddle. But so long as this "noise" remains small, a controlled system, kept in line by a constant stream of nudges, stays under control. "You can achieve control even in the face of noise and imperfect measurements," Grebogi says.

In the past, most scientists and engineers considered a chaotic system's extreme sensitivity to initial conditions as something to be avoided. To ensure that, say, a chemical reaction or a bridge would function reliably and predictably, they tried to design systems that shunned chaos. Both the Navy and Maryland groups now argue that chaos may offer a great advantage, allowing system designers greater flexibility and making possible systems that adapt more quickly to changing needs.

To confine the chaotic oscillations of a magnetoelastic ribbon (bottom) to a single type of repeating motion, as depicted on the system's chaotic attractor (right), researchers make small adjustments to the steady magnetic field acting vertically on the ribbon.

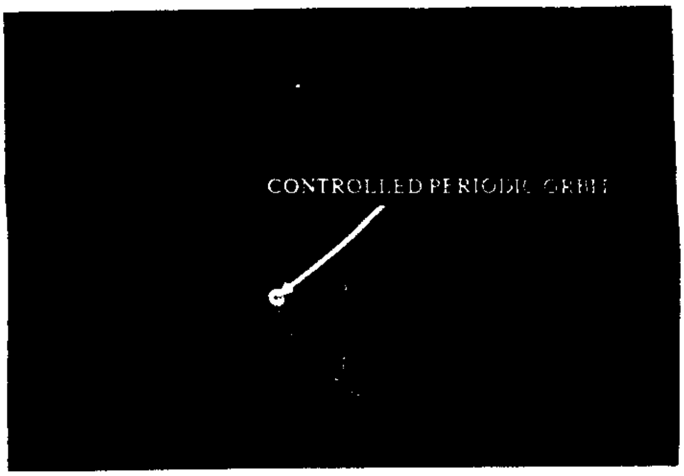

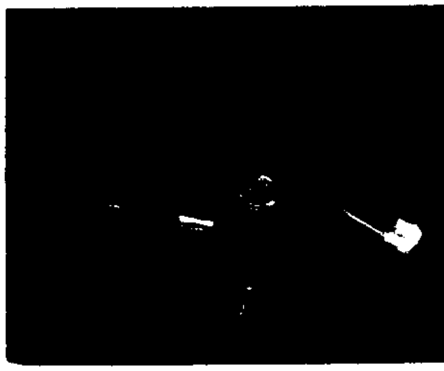

Photos: Naval Surface Warfare Center

"This characteristic is often regarded as an annoyance, yet it provides us with an extremely useful capability without a counterpart in nonchaotic systems," contend Troy Shinbrot, Ott, Grebogi and Yorke in a new paper in which they outline a shortcut for achieving control of a chaotic system. That paper accompanies the Navy report in the Dec. 24 PHYSICAL REVIEW LETTERS.

"In particular, the future state of a chaotic system can be substantially altered by a tiny perturbation," the Maryland researchers write. "If we can accurately sense the state of the system and intelligently perturb it, this presents us with the possibility of rapidly directing the system to a desired state."

It's like using a feather instead of a sledgehammer to achieve a certain result, Spano says.

The Navy team considers its magnetic ribbon not only a fascinating vehicle for vividly demonstrating the intricacies of chaotic dynamics but also a candidate for a "smart" material – one that automatically responds to changes in its environment by changing its properties to achieve a desired result (SN: 3/10/90, p.152). "We would like to exploit the chaotic behavior of the ribbon instead of avoiding it," says Ditto. "We want to make a device that can adapt to the real world. That's where we're headed."

The Navy is interested in using smart materials, such as magnetoelastic ribbons, for designing quieter submarines, controlling vibrations, detecting motion, and improving tracking and pointing devices.

As a potential peaceful application, Grebogi envisions a hypothetical set of chemicals that, when mixed in different concentrations, reacts to produce dyes of different colors. Chemical engineers might design a factory for producing various dyes by building separate chemical reactors, one for each color. But by introducing and controlling chaos, they could get away with building a single reactor. If they adjusted the ingredient concentrations so that the system's products would shift chaotically from one color to another, then a simple control scheme involving tiny adjustments in the concentration of one ingredient would suffice to stabilize the reaction so that it produced only one color. The same control system would also allow them to shift dye production rapidly from one color to another.

"Thus, when designing a system intended for multiple uses, purposely building chaotic dynamics into the system may allow for the desired flexibility," Ott, Grebogi and Yorke suggest.

A conventional heart pacemaker, for example, supplies a steady beat, whereas a person's heart varies its pace depending on his or her exertions. A pacemaker patterned on a chaotic phenomenon might make such rapid adjustments to the heartbeat when needed, Ditto says.

Indeed, the recent success in controlling chaos raises the issue of how common this control mechanism may be in biological systems. For example, controlled chaos may play a role in the human ability to quickly produce strings of different speech sounds.

"Such multipurpose flexibility is essential to higher life forms, and we, therefore, speculate that chaos may be a necessary ingredient in their regulation by the brain," Ott, Grebogi and Yorke say.

"We think biological systems use chaos, and the richness in chaotic behavior, to change [their] behavior on the fly," Ditto says. "We've provided some of the first evidence that this type of mechanism is possible." □

Are you someone who'd use a RAM chip as fertilizer? Do you think that the best way to boot up a computer is with a steel toe? Then *The Devouring Fungus* is the book for you. *Anyone* who's ever had *anything* to do with computers — from the sophisticated hacker to the confused office worker to the unsuspecting parent who finally relented to the kids' demand for a PC — will find something here to chuckle about.

—from the publisher

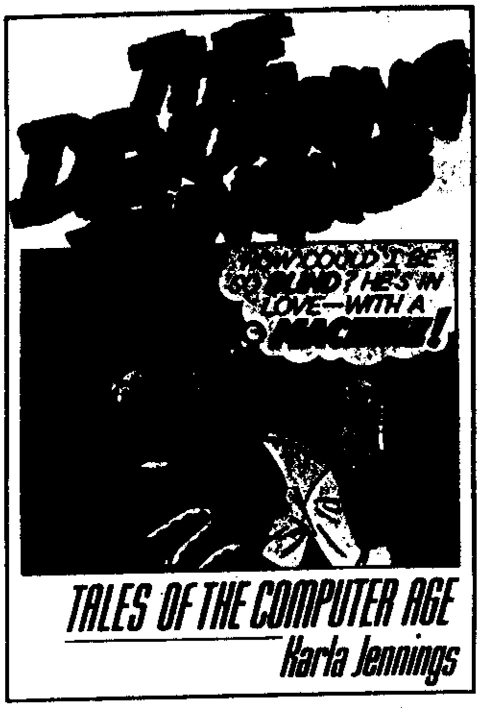

W. W. Norton, 1990, 237 pages, 5½" x 8¼" paperback, $10.95

Science News Books DevourFungus
1719 N Street, NW, Washington, DC 20036

Please send me ______ copy(ies) of **The Devouring Fungus.** I include a check payable to Science News Books for $10.95 plus $2.00 postage and handling (total $12.95) for each copy. Domestic orders only.

Name ______________________
Address ______________________
City ______________________
State ______________ Zip ______________
Daytime Phone (______) ______________
(used only for problems with order) RB1365

"Karla Jennings . . . has not only gathered together more computer lore in one spot than ever before, she presents it with the same gentle good humor that is found in all hackers. The book is right on; why didn't I write it?"

—Robert X. Cringely, field editor, InfoWorld

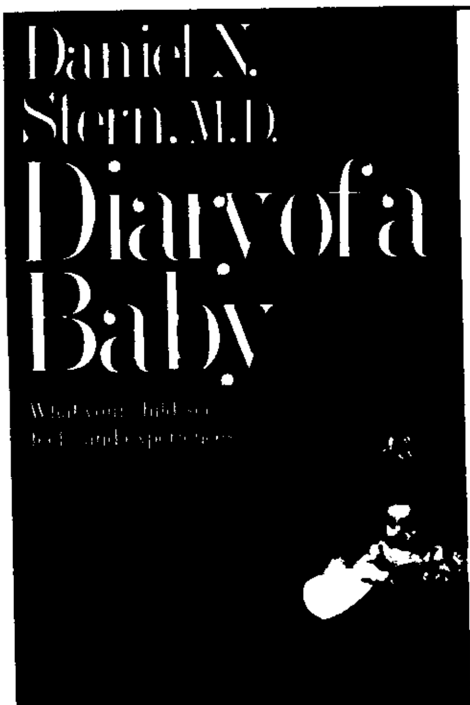

Harper Collins, 1990, 165 pages, 6" x 9½", hardcover, $18.95

Every new parent desperately wants to know what goes on in the mind of a baby. Now a noted authority on infant psychology brings us closer than ever before to penetrating a young child's consciousness. In alternating sections of evocative prose representing the baby's own voice, and explanatory text, Stern draws on the latest research findings to recreate the baby's world. By structuring the book as one child's "diary" from six weeks to four years, Stern personalizes the rich theoretical information the book provides.

What does an infant actually see when he or she looks at a shaft of light? What makes a baby focus on his mother's face or avert his eyes? How does an infant come to see herself as separate from the world around her? How does a baby's experience of an event differ from our own? To answer such questions, Diary of a Baby *takes us through the small moments and simple exchanges in a baby's life that result in lifelong patterns of development.*

Each chapter focuses on an ordinary event in a baby's life — eating, going on an outing among strangers, momentarily getting lost. The author first describes what's happening on the surface, then retells the story from the baby's vantage point, and finally explains how we know what we know about this facet of infant behavior.

This unique work — a scientific tour de force and a moving portrait of inner experience — brings us closer to the infant and invites a powerful communion between parent and child.

—from the publisher

Science News Books DiaryBaby
1719 N Street, NW
Washington, DC 20036

Please send me ______ copy(ies) of *Diary of a Baby.* I include a check payable to Science News Books for $18.95 plus $2.00 postage and handling (total $20.95) for each copy. Domestic orders only.

Name ______________________
Address ______________________
City ______________________
State ______________ Zip ______________
Daytime Phone (______) ______________
(used only for problems with order) RB1364

Environment

Ironing away a greenhouse wrinkle

An unusual strategy for slowing global greenhouse warming – fertilizing the Antarctic Ocean with iron – has received mixed reviews from scientists exploring its feasibility. While one group suggests that fertilization won't do the trick, others say their initial research indicates it might appreciably slow carbon dioxide buildup in the atmosphere, although they caution that scientists must still address many basic questions about the strategy, including its potential to alter the ocean ecosystem.

Oceanographers at the Moss Landing (Calif.) Marine Laboratories suggested last year that the Antarctic Ocean's unusually low concentrations of single-celled plants called phytoplankton result from an iron deficiency that keeps these organisms from making full use of the rich supplies of available nutrients. If so, the team theorized, fertilizing the waters with iron could enhance phytoplankton photosynthesis – an effect that would pull large amounts of carbon dioxide from the atmosphere, helping to counteract the buildup of this greenhouse gas.

Now a thumbs-down response comes from Tsung-Hung Peng of the Oak Ridge (Tenn.) National Laboratory and Wallace S. Broecker of Columbia University's Lamont-Doherty Geological Observatory in Palisades, N.Y. Using a computer model of the world's oceans, these researchers found that currents bring water to the region too slowly for the fertilization scheme to make a significant difference. If their model is correct, a century's worth of iron fertilization would reduce the global concentration of atmospheric carbon dioxide to a level only 5 to 15 percent below what it would be without fertilization, they say. "Even if iron fertilization worked perfectly, it would not significantly reduce the atmospheric CO_2 content," they assert in the Jan. 17 NATURE.

Jorge L. Sarmiento, a mathematical modeler at Princeton (N.J.) University, argues that a 15 percent reduction would represent a significant effect, dramatically slowing the rise in carbon dioxide. What's more, he told SCIENCE NEWS, his computer simulations indicate that fertilization would lower carbon dioxide levels by about double the amount calculated by Peng and Broecker.

Nonetheless, he says, "it's very unlikely that iron fertilization will have practical applications." For one thing, oceanographers don't know whether an iron deficiency really limits the Antarctic phytoplankton population; indeed, that theory runs counter to traditional thinking about the region's ecology. And even if the strategy could lower carbon dioxide levels, its cost might be prohibitive; once begun, the treatments would have to continue forever. Moreover, scientists express concern that fertilization could disrupt aquatic ecosystems – a threat that hasn't escaped environmentalists, who vehemently oppose the strategy. Environmentalists and other critics also worry that the fertilization prospect might derail crucial attempts to control the world's use of fossil fuels, the source of most carbon dioxide pollution.

"This is not to be viewed as a fix-it or cure-all to the CO_2 problem," says Oskar R. Zaborsky, director of the National Research Council's board on biology. Even if fertilization worked, he says, it could not replace other actions such as energy conservation.

He says scientists are proceeding with caution on the iron question: "No one is suggesting initiating a treatment process at this time." Researchers are planning ship-board and laboratory experiments and are even discussing a small-scale field study in which they would fertilize about 400 square kilometers of the Antarctic Ocean. Ecologists and biologists say an experiment of this size would not harm the aquatic system, Zaborsky adds.

Space Sciences

Why three planets radio the sun

When the solar wind, a continuous outpouring of electrically charged particles from the sun, collides at supersonic speed with the magnetic field of a planet, it creates a shock wave on the sunward side. This in turn triggers the emission of radio waves that radiate back toward the sun. The widths of the arc-shaped shock waves responsible for the radio signals from the solar system's inner three planets – Mercury, Venus and Earth – vary widely. The signals themselves, however, are quite similar, according to a new analysis of spacecraft data more than 10 years old.

Earth and Mercury owe their shock waves to magnetic fields generated by the dynamo at each planet's spinning core, says Chris T. Russell of the University of California, Los Angeles. He and two graduate students coauthored the analysis, which appears in the December GEOPHYSICAL RESEARCH LETTERS. The width of Earth's shock wave is about 10 times the planet's diameter. Owing to Mercury's roughly 50 percent smaller size and weaker magnetic field, its shock wave is only 5 percent as big as Earth's.

Venus, nearly Earth's twin in size, derives its weak magnetic field from a far different mechanism: the collision of the solar wind and that planet's upper atmosphere. The resulting shock wave is only about 10 percent as wide as Earth's.

Sunward-radiating radio waves spawned by these vastly different-sized shock waves share a number of common properties, the space physicists found. For instance, all radiate at extremely low frequencies – about 1 to 3 cycles per second. They also leave the shock wave around each planet at approximately the same range of angles. And the amplitudes or strengths of the radio signals – which naturally decrease with distance – appear comparable when measured at about the same distance from their source.

The new analysis also appears to have answered a long-standing question about which type of solar wind particles trigger the radio waves: negatively charged electrons or positively charged particles such as protons (ionized hydrogen atoms).

Previous studies, including one by Russell himself, had suggested that the solar wind ions took a "left-handed" spiral around the planetary magnetic field lines that captured them – a sign that the ions were positively charged. But in the new report, Russell's team concludes that the spiraling only *appeared* left-handed owing to the spacecrafts' motion relative to the solar wind. By analyzing the spiral's direction with respect to the flowing solar wind, they have now determined that it's actually right-handed, Russell says. This indicates the radio waves are really spawned by electrons, his team now reports.

An asteroid's offspring

Three classes of meteorites, all made of basalt but differing in other mineralogical details, may come from three asteroids that originally formed a single large asteroid. The three meteorite types – the eucrites, howardites and diogenites – came from an asteroid big enough for its surface rock to melt, possibly from the heat of radioactive elements inside it, concludes a team headed by Dale P. Cruikshank of NASA's Ames Research Center in Mountain View, Calif., in the January ICARUS.

The team suggests that a "parent" asteroid shattered in a collision with another such chunk, forming three smaller asteroids now known as 3551, 3908 and 4055, whose orbits carry them near Earth. Cruikshank's group found the similarity between the meteorite classes and the three asteroids by comparing laboratory studies of the meteorites with infrared spectral measurements and other observations of the asteroids, made with NASA's Infrared Telescope Facility on Mauna Kea, Hawaii.

ARTICLES

Controlling chaos in high dimensions: Theory and experiment

Mingzhou Ding and Weiming Yang
Program in Complex Systems and Brain Sciences, Center for Complex Systems and Department of Mathematics, Florida Atlantic University, Boca Raton, Florida 33431

Visarath In and William L. Ditto
Applied Chaos Laboratory, School of Physics, Georgia Institute of Technology, Atlanta, Georgia 30332

Mark L. Spano and Bruce Gluckman
Naval Surface Warfare Center, Carderock Division, Silver Spring, Maryland 20903
(Received 27 November 1995)

The main contribution of this work is the development of a high-dimensional chaos control method that is effective, robust against noise, and easy to implement in experiment. Assuming no knowledge of the model equations, the method achieves control by stabilizing a desired unstable periodic orbit with any number of unstable directions, using small time-dependent perturbations of a single system parameter. Specifically, our major results are as follows. First, we derive explicit control laws for time series produced by discrete maps. Second, we show how to apply this control law to continuous-time problems by introducing straightforward ways to extract from a continuous-time series a discrete time series that measures the dynamics of some Poincaré map of the original system. Third, we illustrate our approach with two examples of high-dimensional ordinary differential equations, one autonomous and the other periodically driven. Fourth, we present the result on our successful control of chaos in a high-dimensional experimental system, demonstrating the viability of the method in practical applications.

PACS number(s): 05.45.+b

I. INTRODUCTION

Chaotic phenomena arise ubiquitously in natural systems and in man-made devices [1]. Past work has focused mainly on the discovery and characterization of chaotic behavior occurring in situations where there is no goal-oriented intervention. Recently, ideas and techniques have been proposed to convert chaotic orbits to desired periodic ones by using temporally programmed small controls [2–9]. It is suggested that by doing so one improves the system's performance against some general classes of criteria [10]. This direction of research opens the possibility of utilizing the rich properties of chaos in practical applications and has thus attracted a great deal of interest. In the present paper we consider this chaos control paradigm in systems where the equations of motion are not known and the dynamical information is contained in a time series obtained from observing a single scalar function of the original phase space variables. Our main results are as follows.

(i) Assuming that the time series is produced by a discrete map we develop a high-dimensional chaos control method based on ideas proposed by So and Ott [7]. Here we use map-generated time series to ensure that the coefficients needed for the implementation of control are easy to estimate from experimental data. In addition, the expression of the control law involves only the knowledge about the unstable directions of the to-be-stabilized periodic orbit. This is an added practical benefit since such knowledge is often more reliably obtained from time series. It is also worth emphasizing that in this method one only needs to vary a single external parameter to control a system of arbitrary dimensionality with an arbitrary number of unstable directions.

(ii) We show that for a continuous-time system, as would be encountered in most experimental problems, simple methods can be used to extract from the continuous-time series a discrete-time series that probes the dynamics of some Poincaré map in the original phase space. Specifically, for an autonomous system, this is done by measuring the times between successive crossings of some predetermined threshold by the continuous-time series. We call these times interspike intervals. For a periodically driven system, either the interspike intervals or the more traditional stroboscopic samples can be used to form the discrete time series. In this fashion the explicit control law mentioned in (i) applies directly to continuous-time systems. Other advantages of basing the control method on discrete-time series generated by Poincaré maps are also discussed.

(iii) We illustrate our approach with two examples of ordinary differential equations, one an autonomous chemical reaction model of four variables and the other a pair of coupled Duffing oscillators with periodic forcing, a five dimensional system. In the second example, the periodic orbit to be stabilized has two unstable directions, and in the second example, we consider the control of a period-2 orbit.

(iv) We have applied the control method to a physical system of a magnetoelastic ribbon driven by a sinusoidally varying magnetic field. We have successfully achieved the control of high-dimensional chaos where other technique

1063-651X/96/53(5)/4334(11)/$10.00

have failed to do so. We have also demonstrated the robustness of the method by showing that it works effectively in the presence of rather substantial random noise.

The rest of this paper is organized as follows. In Sec. II we present the method of chaos control. Here we leave some of the detailed calculations to the Appendix. Section III shows how to extract a Poincaré-map-generated discrete-time series from a continuous-time system. We also discuss numerical results in this section. In Sec. IV we present the control results for the magnetoelastic ribbon experiment. We summarize the paper in Sec. V.

II. THE CONTROL METHOD

A. Delay coordinates

Consider a k-dimensional map

$$\mathbf{X}_{n+1}=\mathbf{F}(\mathbf{X}_n,p), \tag{1}$$

where $\mathbf{X}\in R^k$ and p is the chosen control parameter. Suppose that for $p=\bar{p}$ Eq. (1) exhibits a chaotic attractor. Let the scalar observation function be $x=h(\mathbf{X})$. Assuming no *a priori* knowledge of the equations of motion $\mathbf{F}$, we carry out the system analysis and control by using the time series

$$\{x_n\}=\{h(\mathbf{X}_n)\}, \tag{2}$$

where $n=1,2,3,\ldots$. (In Sec. III we shall describe ways to extract such discrete-time series for both autonomous and periodically driven *continuous-time* systems.) Employing delay coordinates [11], we reconstruct the high-dimensional dynamics from $\{x_n\}$ via

$$\mathbf{z}_n=\begin{pmatrix} z_n^{(1)} \\ z_n^{(2)} \\ \vdots \\ z_n^{(m)} \end{pmatrix}=\begin{pmatrix} x_{n-m+1} \\ x_{n-m+2} \\ \vdots \\ x_n \end{pmatrix}_{m\times 1},$$

where m is the dimension of the reconstructed phase space. Results in [11] state that, for large enough m, $\mathbf{z}_n$ is a global one-to-one representation of the variable $\mathbf{X}_n$ on the original attractor. Since the application of control in this work entails that we change the value of the parameter p according to a control law at every iteration of Eq. (1), the discrete map for $\mathbf{z}_n$ is

$$\mathbf{z}_{n+1}=\mathbf{G}(\mathbf{z}_n,p_{n-m+1},p_{n-m+2},\ldots,p_n), \tag{3}$$

where $\mathbf{G}$ generally depends on all the parameter variations effective during the time interval $n-m+1\leq t\leq n$ spanned by the delay vector $\mathbf{z}_n$ [6].

Below, by taking into account of the effect of the past parameter changes specified in Eq. (3), we derive the control laws that stipulates the choice of p_n to convert the natural chaotic dynamics of Eq. (1) to a periodic orbit selected from an infinitely many contained in the chaotic attractor. The parameter variations are assumed to be small around the nominal value $p=\bar{p}$ so that no new orbits are expected to be created in the process. Thus we seek to exploit unstable periodic orbits already existing in the chaotic attractor. This control approach is also flexible in that by simply changing to a different temporal programming of the parameter p one can switch the dynamics from one periodic behavior to another without major alterations to the system.

B. Stabilizing a fixed point

We begin by considering the stabilization of a saddle fixed point that may have more than one unstable direction. In this case, the control law to be derived admits an explicit expression. Moreover, the simple setting here allows us to better illustrate the main ideas involved.

An unstable fixed point $\bar{\mathbf{X}}$ in the original chaotic attractor when $p=\bar{p}$ satisfies

$$\bar{\mathbf{X}}(\bar{p})=\mathbf{F}(\bar{\mathbf{X}}(\bar{p}),\bar{p}). \tag{4}$$

Reflected in the delay coordinate space we have

$$\bar{\mathbf{z}}(\bar{p})=\mathbf{G}(\bar{\mathbf{z}}(\bar{p}),\bar{p},\bar{p},\ldots,\bar{p}), \tag{5}$$

where $\bar{\mathbf{z}}(\bar{p})=[\bar{x}(\bar{p}),\bar{x}(\bar{p}),\ldots,\bar{x}(\bar{p})]^T$, T denoting matrix transpose, and $\bar{x}(\bar{p})=h(\bar{\mathbf{X}}(\bar{p}))$. The location of this fixed point can be extracted from the time series. The procedure for finding it is simplified by knowing that it lies on the diagonal in the m-dimensional reconstructed phase space.

To describe the effect of control parameter variations on the linear dynamics near the fixed point, we introduce the $m\times m$ Jacobian matrix

$$\mathbf{A}_n=\mathbf{D}_{\mathbf{z}_n}\mathbf{G}(\mathbf{z}_n,p_{n-m+1},p_{n-m+2},\ldots,p_n) \tag{6}$$

and a set of m-dimensional column vectors [7]

$$\begin{aligned}\mathbf{B}_n^{(m)}&=D_{p_{n-m+1}}\mathbf{G}(\mathbf{z}_n,p_{n-m+1},p_{n-m+2},\ldots,p_n),\\ \mathbf{B}_n^{(m-1)}&=D_{p_{n-m+2}}\mathbf{G}(\mathbf{z}_n,p_{n-m+1},p_{n-m+2},\ldots,p_n),\\ &\ \ \vdots\\ \mathbf{B}_n^{(1)}&=D_{p_n}\mathbf{G}(\mathbf{z}_n,p_{n-m+1},p_{n-m+2},\ldots,p_n).\end{aligned} \tag{7}$$

Evaluating all the partial derivatives at $\bar{\mathbf{z}}(\bar{p})$ and $p_{n-m+1}=p_{n-m+2}=\cdots=p_n=\bar{p}$, we obtain near the fixed point

$$\mathbf{z}_{n+1}-\bar{\mathbf{z}}(\bar{p})=\mathbf{A}(\mathbf{z}_n-\bar{\mathbf{z}}(\bar{p}))+\mathbf{B}^{(m)}(p_{n-m+1}-\bar{p})+\mathbf{B}^{(m-1)}\times(p_{n-m+2}-\bar{p})+\cdots+\mathbf{B}^{(1)}(p_n-\bar{p}), \tag{8}$$

where we have dropped the reference to n in $\mathbf{A}$ and $\mathbf{B}$'s since they are now constant matrix and vectors. It should be noted that, due to the nature of the discrete-time series and delay coordinates used here, Eq. (3) in component form is

$$\begin{pmatrix} z_{n+1}^{(1)} \\ z_{n+1}^{(2)} \\ \vdots \\ z_{n+1}^{(m-1)} \\ z_{n+1}^{(m)} \end{pmatrix}=\begin{pmatrix} z_n^{(2)} \\ z_n^{(3)} \\ \vdots \\ z_n^{(m)} \\ g(\mathbf{z}_n,p_{n-m+1},p_{n-m+2},\ldots,p_n) \end{pmatrix}. \tag{9}$$

Thus most of the entries in the $\mathbf{A}$ matrix and the $\mathbf{B}$ vectors are zero. Specifically,

$$\mathbf{A}=\begin{pmatrix} 0 & 1 & 0 & \cdots & 0 \\ 0 & 0 & 1 & \cdots & 0 \\ \vdots & \vdots & \vdots & \vdots & \vdots \\ 0 & 0 & 0 & \cdots & 1 \\ a^{(m)} & a^{(m-1)} & a^{(m-2)} & \cdots & a^{(1)} \end{pmatrix}_{m\times m} \tag{10}$$

and

$$\mathbf{B}^{(i)}=\begin{pmatrix} 0 \\ 0 \\ \vdots \\ 0 \\ b^{(i)} \end{pmatrix}_{m\times 1}, \tag{11}$$

where $i=1,2,\ldots,m$. The use of Poincaré-map-generated time series reduces our task of obtaining the entire $\mathbf{A}$ and $\mathbf{B}^{(i)}$, to the estimation of only $a^{(1)},a^{(2)},\ldots,a^{(m)}$, $b^{(1)},b^{(2)},\ldots,b^{(m)}$ from the experimental data. We remark that, although it is possible to obtain the values of $a^{(i)}$'s and the $b^{(i)}$'s together at the same time, our experience indicates that the best strategy is to find the $a^{(i)}$'s first based on the unperturbed time series and then to apply the perturbation to calculate the $b^{(i)}$'s. The perturbation is applied in such a way that only one δp is not zero in the time interval spanned by $\mathbf{z}_n$. See Sec. IV for more discussions on the estimation of $a^{(i)}$'s and $b^{(i)}$'s.

Assume that $\mathbf{A}$ in Eq. (10) has u unstable directions and s stable directions $(s+u=m)$ with eigenvalues λ_i satisfying $|\lambda_1|>|\lambda_2|>\cdots>|\lambda_u|>1>|\lambda_{u+1}|>|\lambda_{u+2}|>\cdots>|\lambda_m|$. Let $\mathbf{e}_i$ denote the corresponding eigenvectors. Then a possible control approach is to choose suitable parameter variations according to Eq. (8) to push the trajectory $\mathbf{z}_{n+1}$ into the stable subspace spanned by the stable directions $\mathbf{e}_i$, $i=u+1,u+2,\ldots,m$. However, Dressler and Nistche [6] point out for the $m=2$ case that this strategy may sometimes leads to instabilities in the control parameters. When this happens, one generally needs larger and larger perturbations in p in order to bring the trajectory to stay inside the stable subspace. The control will eventually fail when either the required $\delta p=p-\bar{p}$ exceeds the predetermined maximum control $\delta p_{\max}$ or the value of δp becomes so large that the linear approximation in Eq. (8) is no longer valid. So and Ott proposes an idea to systematically remedy the situation [7]. (A similar approach can be found in [8].) It involves the introduction of a state-plus-parameters system, which includes the regular phase space variable $\mathbf{z}_n$ as well as all the previous variations of the parameter p according to Eq. (3).

The expanded phase space is $2m-1$ dimensional and the state vector $\mathbf{Y}_n$ assumes the form

$$\mathbf{Y}_n=\begin{pmatrix} \mathbf{z}_n \\ p_{n-m+1} \\ p_{n-m+2} \\ \vdots \\ p_{n-1} \end{pmatrix}_{(2m-1)\times 1}.$$

Based on Eq. (8), the linear dynamics around the fixed point

$$\bar{\mathbf{Y}}=\begin{pmatrix} \bar{\mathbf{z}}(\bar{p}) \\ \bar{p} \\ \bar{p} \\ \vdots \\ \bar{p} \end{pmatrix}$$

is [7]

$$\mathbf{Y}_{n+1}-\bar{\mathbf{Y}}=\tilde{\mathbf{A}}(\mathbf{Y}_n-\bar{\mathbf{Y}})+\tilde{\mathbf{B}}(p_n-\bar{p}), \tag{12}$$

where

$$\tilde{\mathbf{A}}=\begin{pmatrix} \mathbf{A} & \mathbf{B}^{(m)} & \mathbf{B}^{(m-1)} & \mathbf{B}^{(m-2)} & \cdots & \mathbf{B}^{(2)} \\ \mathbf{0} & 0 & 1 & 0 & \cdots & 0 \\ \mathbf{0} & 0 & 0 & 1 & \cdots & 0 \\ \vdots & \vdots & \vdots & \vdots & \vdots & \vdots \\ \mathbf{0} & 0 & 0 & 0 & \cdots & 1 \\ \mathbf{0} & 0 & 0 & 0 & \cdots & 0 \end{pmatrix}_{(2m-1)\times(2m-1)}, \tag{13}$$

with $\mathbf{0}$ an m-dimensional row vector of 0's and

$$\tilde{\mathbf{B}}=\begin{pmatrix} \mathbf{B}^{(1)} \\ 0 \\ \vdots \\ 0 \\ 1 \end{pmatrix}_{(2m-1)\times 1}. \tag{14}$$

We note that the eigenvalues of $\mathbf{A}$ are also the eigenvalues of $\tilde{\mathbf{A}}$ with the corresponding eigenvectors

$$\mathbf{k}_i=\begin{pmatrix} \mathbf{e}_i \\ 0 \\ \vdots \\ 0 \\ 0 \end{pmatrix},$$

$i=1,2,\ldots,m$. Clearly, the above m vectors are not enough to span the $(2m-1)$-dimensional expanded phase space. To do so one needs additional $m-1$ independent vectors. We argue that these vectors can be found in the null space of the matrix $\tilde{\mathbf{A}}^{m-1}$. Specifically, we show in the Appendix that the subspace of the vectors $\mathbf{k}$ satisfying $\tilde{\mathbf{A}}^{m-1}\mathbf{k}=\mathbf{0}$ is $(m-1)$ dimensional and more importantly any set of $m-1$ independent vectors denoted $\mathbf{k}_i$, $i=m+1,m+2,\ldots,2m-1$, from this space can be used together with $\mathbf{k}_i$, $i=u+1,u+2,\ldots,m$, to form the basis of the stable subspace $\mathbf{E}_s(\bar{\mathbf{Y}})$ of $\tilde{\mathbf{A}}$.

Suppose that at time n the system trajectory falls in the neighborhood of $\bar{\mathbf{Y}}$ called the control region. To stabilize the subsequent motion around this fixed point with u unstable directions, we attempt to apply u small parametric perturbations $\delta p_n,\delta p_{n+1},\ldots,\delta p_{n+(u-1)}$ in such a way that the deviation $\delta\mathbf{Y}_{n+u}=\mathbf{Y}_{n+u}-\bar{\mathbf{Y}}$ lies entirely [7] in the stable subspace $\mathbf{E}_s(\bar{\mathbf{Y}})$. After that we set the parameter to $\bar{p}$ and the orbit approaches the fixed point under the natural dynamics. Specifically, this control can be achieved as follows. Consider the transpose of $\tilde{\mathbf{A}}$ denoted $\tilde{\mathbf{A}}^T$. We know that both $\tilde{\mathbf{A}}$ and $\tilde{\mathbf{A}}^T$ have the same eigenvalue spectrum. Furthermore, as shown in the Appendix, the contravariant unstable eigenvectors $\mathbf{v}_i$ determined by

$$\tilde{\mathbf{A}}^T\mathbf{v}_i=\lambda_i\mathbf{v}_i \tag{15}$$

for $i=1,2,\ldots,u$ have the property that they are orthogonal to the stable subspace $\mathbf{E}_s(\bar{\mathbf{Y}})$ of $\tilde{\mathbf{A}}$. That is, the dot products $\mathbf{v}_i^T\mathbf{k}_j=0$ for $j=u+1,u+2,\ldots,m,m+1,m+2,\ldots,2m-1$. By choosing the values of $p_n,p_{n+1},\ldots,p_{n+(u-1)}$ such that

$$\begin{aligned}\mathbf{v}_1^T\delta\mathbf{Y}_{n+u}&=0,\\ \mathbf{v}_2^T\delta\mathbf{Y}_{n+u}&=0,\\ &\vdots\\ \mathbf{v}_u^T\delta\mathbf{Y}_{n+u}&=0,\end{aligned} \tag{16}$$

we place the deviation $\delta\mathbf{Y}_{n+u}$ in the stable subspace $\mathbf{E}_s(\bar{\mathbf{Y}})$. In the Appendix we find from the equations in (16) the control law governing the parameter perturbation p_n needed at time n to be

$$p_n=\bar{p}-\left(\sum_{k=1}^{u}\frac{(\lambda_k)^u}{(\mathbf{v}_k^T\bar{\mathbf{B}})\prod_{i=1,i\neq k}^{u}(\lambda_k-\lambda_i)}\mathbf{v}_k^T\right)\delta\mathbf{Y}_n. \tag{17}$$

Although the values of $p_{n+1},\ldots,p_{n+u-1}$ can also be solved together with p_n at time n, the presence of system noise makes it preferable to compute p_n using Eq. (17) at every iterate n.

The contravariant vectors $\mathbf{v}_k$ are also solved explicitly. From Eq. (15), by setting arbitrarily $v_k^{(m)}=1$, we obtain the following recursive relations to determine the other components $v_k^{(i)}$ of the vector $\mathbf{v}_k$:

$$\begin{aligned}v_k^{(1)}&=a^{(m)}/\lambda_k,\\ v_k^{(2)}&=(v_k^{(1)}+a^{(m-1)})/\lambda_k,\\ v_k^{(3)}&=(v_k^{(2)}+a^{(m-2)})/\lambda_k,\\ &\vdots\\ v_k^{(m-1)}&=(v_k^{(m-2)}+a^{(2)})/\lambda_k,\\ v_k^{(m)}&=1,\\ v_k^{(m+1)}&=b^{(m)}/\lambda_k,\\ v_k^{(m+2)}&=(v_k^{(m+1)}+b^{(m-1)})/\lambda_k,\\ v_k^{(m+3)}&=(v_k^{(m+2)}+b^{(m-2)})/\lambda_k,\\ &\vdots\\ v_k^{(2m-1)}&=(v_k^{(2m-2)}+b^{(2)})/\lambda_k.\end{aligned} \tag{18}$$

[Note that the conditions in Eq. (16) imply that the lengths of the vectors $\mathbf{v}_k$ do not play a role. Thus we can set $v_k^{(m)}=1$ for simplicity.] Solving these equations we get

$$\begin{aligned}v_k^{(i)}&=\sum_{j=1}^{i}a^{(m-j+1)}/(\lambda_k)^{i-j+1},\quad i=1,2,\ldots,m-1,\\ v_k^{(m)}&=1,\\ v_k^{(i)}&=\sum_{j=1}^{i-m}b^{(m-j+1)}/(\lambda_k)^{i-m-j+1},\\ &\qquad i=m+1,m+2,\ldots,2m-1.\end{aligned} \tag{19}$$

We emphasize that all the formulas in Eqs. (17) and (19) needed for implementing the control are expressed explicitly in terms of the variables $a^{(i)}$ and $b^{(i)}$, to be estimated from the experimental time series, and the unstable eigenvalues λ_i of $\mathbf{A}$ in Eq. (10).

For fixed points with one or two unstable directions, a situation likely to be encountered in practice, the control law in Eq. (17) reduces to

$$p_n=\bar{p}-\left(\frac{\lambda_1}{(\mathbf{v}_1^T\bar{\mathbf{B}})}\mathbf{v}_1^T\right)\delta\mathbf{Y}_n \tag{20}$$

for $u=1$ and to

$$p_n=\bar{p}-\left(\frac{(\lambda_1)^2}{(\mathbf{v}_1^T\bar{\mathbf{B}})(\lambda_1-\lambda_2)}\mathbf{v}_1^T+\frac{(\lambda_2)^2}{(\mathbf{v}_2^T\bar{\mathbf{B}})(\lambda_2-\lambda_1)}\mathbf{v}_2^T\right)\delta\mathbf{Y}_n \tag{21}$$

for $u=2$.

C. Stabilizing a period-N orbit

Let a period-N orbit in the original phase space when $p=\bar{p}$ be $\bar{\mathbf{X}}_n(\bar{p}),\bar{\mathbf{X}}_{n+1}(\bar{p}),\ldots,\bar{\mathbf{X}}_{n+N}(\bar{p})=\bar{\mathbf{X}}_n(\bar{p})$. The corresponding scalar time series $\{\bar{x}_n(\bar{p})\}$ is also periodic with a period of N. Suppose at time n the trajectory $\mathbf{z}_n$ in the m-dimensional reconstructed phase space comes near one of the periodic points denoted by $\mathbf{z}_n(\bar{p})$. The entire reconstructed periodic orbit is then $\mathbf{z}_n(\bar{p})$, $\mathbf{z}_{n-1}(\bar{p}), \ldots, \mathbf{z}_{n-N}(\bar{p})=\mathbf{z}_n(\bar{p})$. The Jacobian $\mathbf{A}_n$ in Eq. (6) and the $\mathbf{B}_n$ vectors in Eq. (7) evaluated along the orbit are now functions of n, satisfying the periodic conditions $\mathbf{A}_n=\mathbf{A}_{n-N}$ and $\mathbf{B}_n^{(i)}=\mathbf{B}_{n-N}^{(i)}$. Introducing the expanded state-plus-parameters phase space, we have, close to the periodic orbit, the linear iteration equation

$$\mathbf{Y}_{n+i}-\overline{\mathbf{Y}}_{n+i}=\bar{\mathbf{A}}_{n+i-1}(\mathbf{Y}_{n+i-1}-\overline{\mathbf{Y}}_{n+i-1})+\bar{\mathbf{B}}_{n+i-1}(p_{n+i-1}-\bar{p}), \tag{22}$$

where $i=1,2,3,\ldots$ and $\mathbf{Y}_{n+i}$, $\bar{\mathbf{A}}_{n+i}$, and $\bar{\mathbf{B}}_{n+i}$ are formed in the same way as their counterparts in Eq. (12). Assume that there are u unstable directions associated with the orbit. The control is accomplished by using u small perturbations $p_n, p_{n+1}, \ldots, p_{n+u-1}$ to place the deviation $\delta\mathbf{Y}_{n+u}=\mathbf{Y}_{n+u}-\overline{\mathbf{Y}}_{n+u}$ into the stable subspace $\mathbf{E}_s(\overline{\mathbf{Y}}_{n+u})$ of the matrix $\mathbf{J}_{n+u}=\bar{\mathbf{A}}_{n+u-1}\bar{\mathbf{A}}_{n+u-2}\cdots\bar{\mathbf{A}}_{n+u-N}$. Since the eigenvectors change from orbit point to orbit point the control law can no longer be expressed as explicitly as in the case of an $N=1$ fixed point. Below we give a brief description of the steps needed for arriving at the control law.

Let the unstable eigenvalues of the entire periodic orbit be $\lambda_1, \lambda_2, \ldots, \lambda_u$. The stable subspace at the orbit point $\overline{\mathbf{Y}}_{n+i}$ is determined by the matrix

$$\mathbf{J}_{n+i}=\bar{\mathbf{A}}_{n+i-1}\bar{\mathbf{A}}_{n+i-2}\cdots\bar{\mathbf{A}}_{n+i-N}. \tag{23}$$

As in the case of a fixed point there is no need to find this subspace explicitly for the formulation of the control law. Instead we consider the eigenvalue problem

$$\mathbf{J}_{n+i}^T\mathbf{v}_{n+i}^{(j)}=\lambda_j\mathbf{v}_{n+i}^{(j)}. \tag{24}$$

Multiplying Eq. (24) on both sides from the left by $\bar{\mathbf{A}}_{n+i-N-1}=\bar{\mathbf{A}}_{n+i-1}$ we get

$$\mathbf{J}_{n+i-1}^T\bar{\mathbf{A}}_{n+i-1}\mathbf{v}_{n+i}^{(j)}=\lambda_j\bar{\mathbf{A}}_{n+i-1}\mathbf{v}_{n+i}^{(j)}.$$

That is, the vector $\mathbf{v}_{n+i-1}^{(j)}$ is parallel to the vector $\bar{\mathbf{A}}_{n+i-1}^T\mathbf{v}_{n+i}^{(j)}$, namely,

$$\bar{\mathbf{A}}_{n+i-1}^T\mathbf{v}_{n+i}^{(j)}=c_{n+i-1}^{(j)}\mathbf{v}_{n+i-1}^{(j)}. \tag{25}$$

This definition implies the periodic condition $c_n^{(j)}=c_{n+N}^{(j)}$.

Iterating Eq. (22) u times yields

$$\begin{aligned}\delta\mathbf{Y}_{n+u}=&\,\bar{\mathbf{A}}_{n+u-1}\bar{\mathbf{A}}_{n+u-2}\cdots\bar{\mathbf{A}}_n\delta\mathbf{Y}_n\\&+\bar{\mathbf{A}}_{n+u-1}\bar{\mathbf{A}}_{n+u-2}\cdots\bar{\mathbf{A}}_{n+1}\bar{\mathbf{B}}_n\delta p_n\\&+\bar{\mathbf{A}}_{n+u-1}\bar{\mathbf{A}}_{n+u-2}\cdots\bar{\mathbf{A}}_{n+2}\bar{\mathbf{B}}_{n+1}\delta p_{n+1}\\&\;\vdots\\&+\bar{\mathbf{A}}_{n+u-1}\bar{\mathbf{B}}_{n+u-2}\delta p_{n+u-2}\\&+\bar{\mathbf{B}}_{n+u-1}\delta p_{n+u-1}.\end{aligned}$$

Choosing the values of $\delta p_n, \delta p_{n+1}, \ldots, \delta p_{n+u-1}$ such

$$(\mathbf{v}_{n+u}^{(j)})^T\delta\mathbf{Y}_{n+u}=0$$

for $j=1,2,\ldots,u$, we place the deviation $\delta\mathbf{Y}_{n+u}$ entirel the stable subspace $\mathbf{E}_s(\overline{\mathbf{Y}}_{n+u})$. From Eq. (26), with the ai Eq. (25), we obtain the u equations

$$\begin{aligned}&(\mathbf{v}_n^{(j)})^T\delta\mathbf{Y}_n\prod_{k=0}^{u-1}c_{n+k}^{(j)}\\&\quad+\sum_{i=1}^{u-1}\left((\mathbf{v}_{n+i}^{(j)})^T\bar{\mathbf{B}}_{n+i-1}\delta p_{n+i-1}\prod_{k=i}^{u-1}c_{n+k}^{(j)}\right)\\&\quad+(\mathbf{v}_{n+u}^{(j)})^T\bar{\mathbf{B}}_{n+u-1}\delta p_{n+u-1}=0,\end{aligned}$$

where $j=1,2,\ldots,u$. We solve these linear equations to tain the control law governing the parameter perturbat p_n needed at time n to be

$$p_n=\bar{p}+\frac{H}{W},$$

where $W=\mathrm{Det}(\mathbf{W})$ with $w_{ij}=(\mathbf{v}_{n+j}^{(i)})^T\bar{\mathbf{B}}_{n+j-1}\prod_{k=j}^{u-1}c_{n+k}^{(i)}$ a $H=\mathrm{Det}(\mathbf{H})$ with $h_{ij}=-(\mathbf{v}_u^{(i)})^T\delta\mathbf{Y}_n\prod_{k=0}^{u-1}c_{n+k}^{(i)}$ for $j=1$ a $h_{ij}=w_{ij}$ for $j\neq 1$. Again, in order to compensate for the fect of noise in experimental applications, we recalculate each time n the value of p_n, even though by solving the equations in Eq. (27) simultaneously we can at once obt parameter perturbations for the future u steps.

For the special case where the period-N orbit has c unstable direction ($u=1$), the control law takes the sim form

$$p_n=\bar{p}-\left(\frac{c_n^{(1)}(\mathbf{v}_n^{(1)})^T}{((\mathbf{v}_{n+1}^{(1)})^T\bar{\mathbf{B}}_n)}\right)\delta\mathbf{Y}_n.$$

Evidently, this equation and Eq. (20) are identical $N=1$.

We remark that in the above we express the control la in terms of the unstable directions of the periodic orbit. Tl approach offers several advantages over expressing cont laws using stable directions. First, in the expanded pha space, one tends to have fewer unstable directions than stat ones that include the null space. Second, since the estimat matrix elements of $\mathbf{A}$ and $\mathbf{B}$'s carry inevitable errors, few calculations reduce the chance of severe error propagatio into the control law that, in turn, affect the control perf mance. Third, it is an empirical fact that information abc unstable directions tends to be more reliably estimated frc experimental time series.

III. NUMERICAL RESULTS

A. Formation of time series

In experimental problems, we expect to encounter tv classes of continuous-time systems, autonomous and perioc cally driven. We discuss how to form discrete time series both cases so that the control laws developed in Sec. II f discrete maps are directly applicable.

First, consider an autonomous system defined as

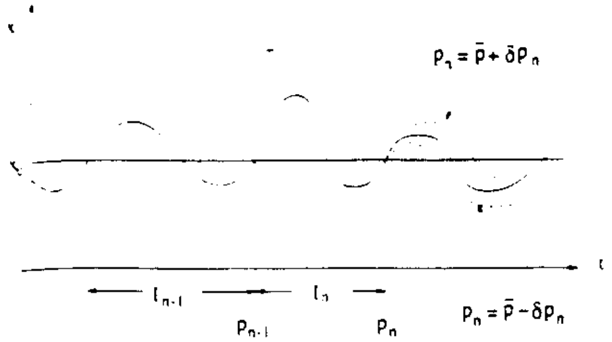

FIG. 1. Schematic illustrating the formation of interspike intervals from a continuous-time series and the effect of control on the intervals.

$$d\mathbf{Z}/dt = \mathbf{G}(\mathbf{Z},p),$$

where $\mathbf{Z} \in R^{k+1}$. Let $x = h(\mathbf{Z})$ denote a scalar observable function. Consider the plot of x versus t. We form the discrete-time series by measuring the intervals I_n between the $(n-1)$th and nth upward (or downward) crossings of some predetermined threshold $x = x_c$ (see Fig. 1). We argue that these variables I_n, which we call interspike intervals, sample the dynamics of some Poincaré map in the original $\mathbf{Z}$ phase space. Specifically, at each crossing in the x versus t plot, the condition $x = h(\mathbf{Z}) = x_c$ is met. This condition defines a k-dimensional Poincaré surface of section in the original $\mathbf{Z}$ space. Thus I_n is also the time between the $(n-1)$th and the nth crossings of the section. Suppose we parametrize this section by a k-dimensional vector $\mathbf{Q}$. Then, the successive crossings of the plane from a given direction by a chaotic trajectory give rise to a Poincaré map

$$\mathbf{Q}_{n+1} = \mathbf{P}(\mathbf{Q}_n, p). \tag{30}$$

Realizing that the interval I_n is uniquely determined by $\mathbf{Q}_{n-1}$, namely,

$$I_n = \Phi(\mathbf{Q}_{n-1}), \tag{31}$$

we complete the analogy between Eqs. (30) and (1) and the analogy between Eqs. (31) and (2).

Traditionally, one measures the continuous-time series x versus t using equally spaced sampling intervals. In the reconstructed phase space one obtains the Poincaré map by examining the crossings of some plane by the reconstructed trajectory. Due to the discreteness of the trajectory one introduces inevitable errors in the resulting Poincaré map through interpolation. In contrast, our way of forming the discrete time series using interspike intervals avoids this problem by monitoring the analog signal and thus detecting the threshold crossing precisely. Furthermore, the reconstructed interspike intervals already obey a Poincaré map. In Fig. 1 we also illustrate the effect of parametric perturbations on the interspike intervals.

Next, we consider a periodically forced system

$$d\mathbf{Z}/dt = \mathbf{G}(\mathbf{Z},t,p),$$

where $\mathbf{Z} \in R^k$ and $\mathbf{G}(\mathbf{Z},t+T,p) = \mathbf{G}(\mathbf{Z},t,p)$. Let $x = h(\mathbf{Z})$ be the scalar observable function. Since by introducing t as an additional variable one can convert a nonautononmous system to an autononmous one, the interspike intervals formation method also applies here. Another more traditional method of forming a discrete-time series $\{x_n\}$ is by measuring x at times $t_n = nT + T_0$ (stroboscopic sampling). From the theorems of [12], the dynamics reconstructed from $\{x_n\}$ in a suitable delay coordinates space represents the dynamics of the Poincaré map $\mathbf{Z}_{n+1} = \mathbf{P}(\mathbf{Z}_n)$ in the original phase space, which, in turn, is equivalent to the continuous-time dynamics described by the differential equations. Below we give two examples of controlling continuous-time chaotic systems using the methods above.

B. Control example 1

Consider the following five-dimensional system of two coupled driven Duffing oscillators:

$$\begin{aligned} \ddot{x}_1 + \gamma\dot{x}_1 + \alpha(x_1^3 - x_1) + \beta_1(x_1 - x_2) &= p_1 \sin(\omega t), \\ \ddot{x}_2 + \gamma\dot{x}_2 + \alpha(x_2^3 - x_2) + \beta_2(x_2 - x_1) &= p \sin(\omega t). \end{aligned} \tag{32}$$

For $\gamma = 0.632$, $\alpha = 4.0$, $\beta_1 = 0.1$, $\beta_2 = 0.05$, $\omega = 2.1235$, $p_1 = 1.011$, and $p = \bar{p} = p_1$, Eq. (32) exhibits a chaotic attractor of dimension $D = 3.3$. The scalar observable here is $x = x_1 + x_2$ and we sample the attractor every cycle of the external forcing. The attractor reconstructed using the time series $\{x_n\}$ in an $(m=4)$-dimensional delay coordinates space has a dimension $D = 2.3$. Figure 2(a) shows the attractor projected down to a two-dimensional space. The high-dimensional character of this attractor is apparent.

The reconstructed attractor contains a fixed point $(N=1)$ at $\mathbf{z}(\bar{p}) = (0.54, 0.54, 0.54, 0.54)^T$ with two unstable directions $(u=2)$. This fixed point corresponds to the synchronized period-1 motion of the coupled oscillators. Our objective is to stabilize this motion. From numerically generated time series we estimate a_i and b_i used in the $\mathbf{A}$ matrix and the $\mathbf{B}$ vectors to be approximately $a^{(1)} = -3.05$, $a^{(2)} = -2.23$, $a^{(3)} = 0.0$, $a^{(4)} = 0.016$ and $b^{(1)} = -0.90$, $b^{(2)} = -0.089$, $b^{(3)} = 0.78$, $b^{(4)} = -0.056$. The two unstable eigenvalues are $\lambda_1 = -1.85$ and $\lambda_2 = -1.20$. Applying the control law in Eq. (17), we stabilize the fixed point as shown in Fig. 2(b), which displays the behavior of the system before and after the control is turned on.

C. Control example 2

Consider the four-dimensional autonomous chemical reaction model [13]

$$\begin{aligned} \dot{x} &= pw/(1 + w^{10}) - 0.1x, \\ \dot{y} &= 0.1x - 0.2yz, \\ \dot{z} &= 0.2z(y - w), \\ \dot{w} &= 0.2zw - 0.1w. \end{aligned} \tag{33}$$

For $p = \bar{p} = 2.5$ this system exhibits a chaotic attractor of dimension $D = 2.2$. Assume that the observed scalar variable is x itself. By measuring the times between successive upward crossings of some threshold x_c by the x versus t function we form the interspike interval time series $\{I_n\}$. Reconstructing

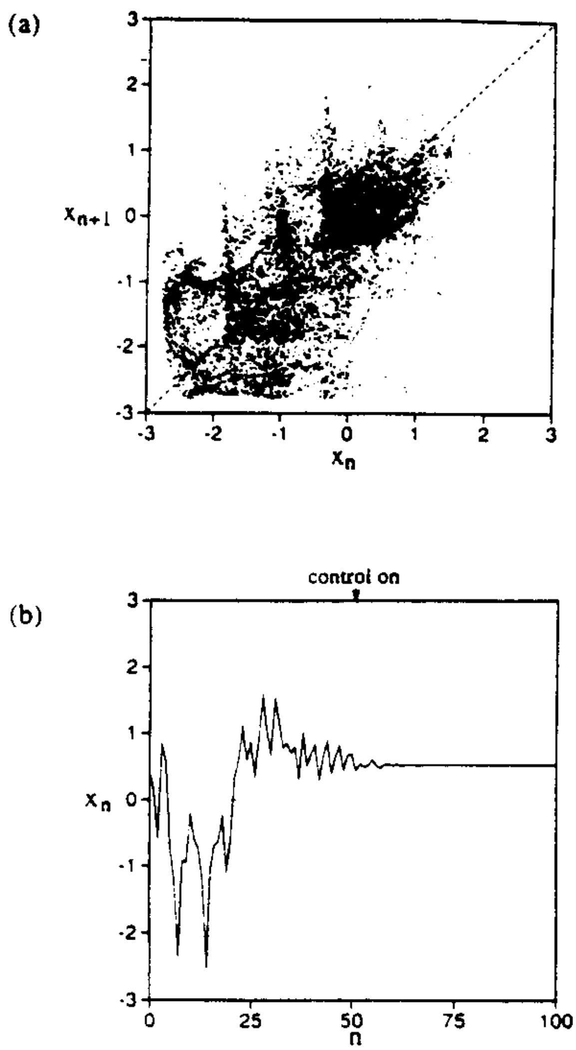

FIG. 2. (a) Two-dimensional ($m=2$) reconstructed image of the attractor from the coupled Duffing equations, Eq. (32). High-dimensional nature of the dynamics is apparent. (b) The result of applying an $m=4$ implementation of our control method. Here discrete stroboscopic samples are connected with straight lines.

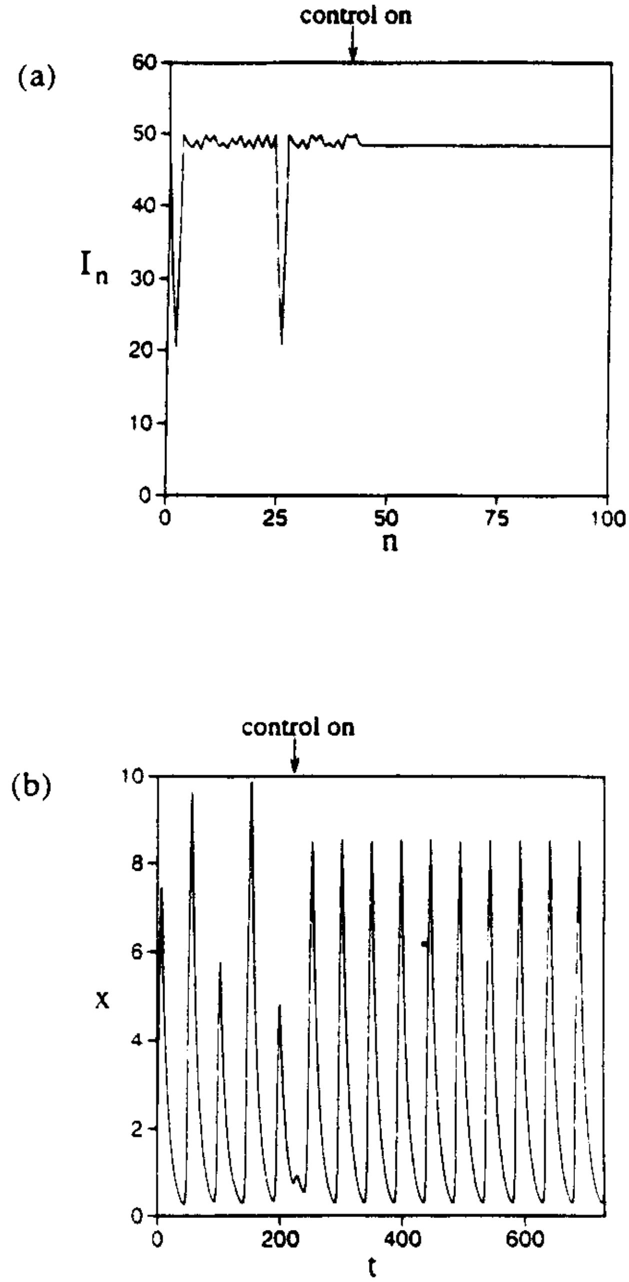

FIG. 3. Results of controlling the unstable period-1 orbit in th chemical reaction model Eq. (33) using an $m=3$ implementation o the control. (a) The interspike intervals and (b) the correspondin continuous-time series.

this discrete time series in an ($m=3$)-dimensional delay coordinate space we obtain an attractor of dimension 1.2. In this attractor there is a fixed point ($N=1$) at $\mathbf{z}_n=(48.40,48.40,48.40)^T$ and a period-2 orbit ($N=2$) cycling between $\bar{\mathbf{z}}_1(\bar{p})=(47.74,50.13,47.74)^T$ and $\bar{\mathbf{z}}_2(\bar{p})=(50.13,47.74,50.13)^T$. Both orbits are found to have one unstable direction ($u=1$).

First, consider the control of the fixed point. Set $x_c=1$. From the numerically generated time series we obtain $a^{(1)}=-1.33$, $a^{(2)}=0.41$, $a^{(3)}=-0.008$ and $b^{(1)}=-1.25$, $b^{(2)}=-3.20$, $b^{(3)}=1.95$. The unstable eigenvalue is calculated to be $\lambda_1=-1.59$. The result of applying Eq. (20) is shown in Fig. 3, where the system behavior before and after the control is turned on is displayed. Figure 3(a) is the interspike intervals and Fig. 3(b) gives the corresponding continuous time series.

Next, consider the control of the period-2 orbit. Set $x_c=3$. From the time series we estimate the elements of th $\mathbf{A}$ matrix and the $\mathbf{B}$ vectors at $\mathbf{z}_1(\bar{p})$ to be $a^{(1)}=-1.56$ $a^{(2)}=0.042$, $a^{(3)}=6.0\times10^{-5}$, and $b^{(1)}=1.81$, $b^{(2}$ $=-3.32$, $b^{(3)}=1.61$ and at $\mathbf{z}_2(\bar{p})$ to be $a^{(1)}=2.15$ $a^{(2)}=0.15$, $a^{(3)}=2.9\times10^{-3}$ and $b^{(1)}=-2.79$, $b^{(2)}=5.85$ $b^{(3)}=0.17$. The control law in Eq. (29) is completely deter mined by these values. In Fig. 4 we show the result of con trol by displaying the interspike intervals (a) and the corre sponding continuous time series (b) for before and after th control is activated.

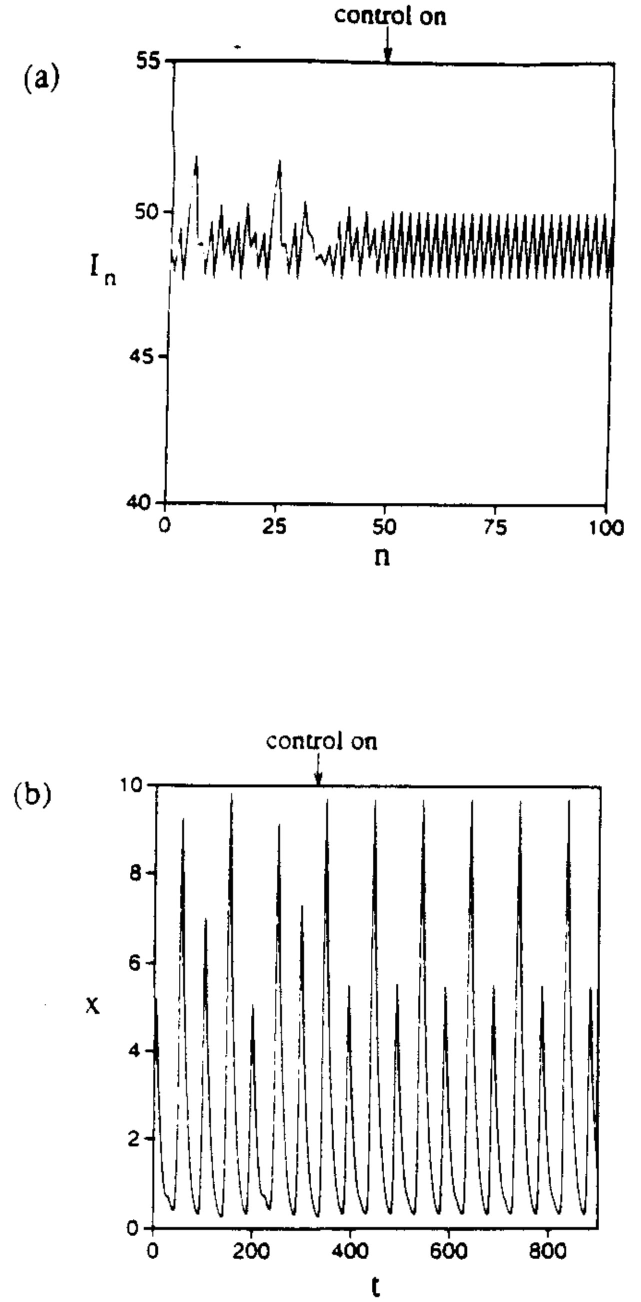

FIG. 4. Results of controlling the unstable period-2 orbit in the chemical reaction model Eq. (33) using an $m=3$ implementation of the control. (a) The interspike intervals and (b) the corresponding continuous-time series.

IV. EXPERIMENTAL RESULTS

A. Setup

Our experimental system consists of a magnetoelastic metal ribbon clamped at its lower end. The ribbon changes its Young's modulus by more than a factor of 10 in response to an external magnetic field and buckles under gravity as a result. This highly nonlinear system is placed vertically within three mutually orthogonal pairs of Helmholtz coils. The two horizontal pairs of the Helmholtz coils are used for counteracting the Earth's magnetic field while the vertical pair is used to supply an approximately uniform field along the ribbon's length. Inside the Helmholtz coils a photonic

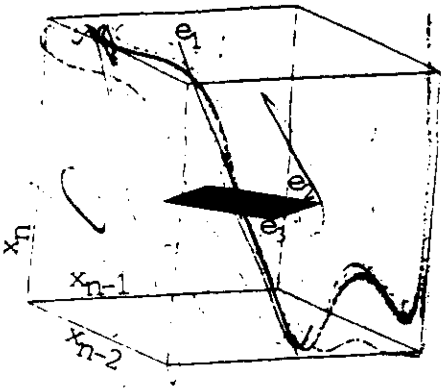

FIG. 5. Time series from the magnetoelastic ribbon reconstructed in a three-dimensional ($m=3$) delay coordinate space. The local dynamics near the fixed point is described by one unstable ($\mathbf{e}_1$) and two stable directions ($\mathbf{e}_2$ and $\mathbf{e}_3$).

sensor is used to measure the ribbon's position at a given point. This sensor is mounted a short distance above the base of the ribbon. To obtain chaos, we drive the ribbon with a time-varing magnetic field in the form $H(t)=H_{dc}+H_{ac}\sin(2\pi f t)$, which is applied along the vertical direction. For $f=1.03$ Hz, $H_{ac}=0.961$ Oe, and $H_{dc}=\bar{H}_{dc}=-1.350$ Oe the ribbon exhibits chaotic oscillations. We choose $p=H_{dc}$ as the control parameter.

Denote the position of the ribbon measured by the photonic sensor every driving period as x_n. From visual inspections of the reconstructed attractor in the $m=2$ space and from some simple estimates it is apparent that the dynamical behavior near the fixed point, which we wish to stabilize, cannot be effectively characterized by one stable direction and one unstable direction. High-dimensional embedding spaces are needed to unfold the local dynamics in this case. This observation is further confirmed by our inability to bring about the desired control using the original Ott-Grebogi-Yorke (OGY) method [2] (see below) as well as using the $m=2$ implementation of our control method, which incorporates the effect of delay coordinates and is equivalent to the Dressler and Nitsche's method [6].

Next we reconstruct the time series in an ($m=3$)-dimensional space as shown in Fig. 5. On the chaotic attractor we identify an unstable periodic orbit of period-1 by looking for saddle points lying on the diagonal. From the experimental data this fixed point is determined to be $\bar{\mathbf{z}}(\bar{p})=(6.35, 6.35, 6.35)^T$. To stabilize the system around this unstable fixed point, we choose $p=H_{dc}$ as the control parameter. When the system state point falls in the vicinity of the unstable fixed point, a small time-dependent change was made to this parameter such that the next iterate would fall onto the stable plane defined by the two stable eigenvectors. The perturbation size is calculated according to Eq. (20). To determine the matrix elements $a^{(1)}$, $a^{(2)}$, and $a^{(3)}$ for $\mathbf{A}$ in Eq. (10) we consider a close return event by choosing a point in the close vicinity of the fixed point and finding its preimage and two future iterates. The reason for using the preimage is to better represent the stable directions and the reason for using two future iterates instead of just one is to pick up the negative sign often associated with the unstable eigenvalue. To guard against the detection of a false nearest neighbor in a three-dimensional embedding space we also monitor the delay coordinate map in the $m=4$ and $m=5$ space. From the true nearest-neighbor points we do a least-squares fit to determine $a^{(1)}$, $a^{(2)}$, and $a^{(3)}$ to a high accuracy. Using 20 close return events we find $a^{(1)}=-1.033\,68$, $a^{(2)}=1.7890$, and $a^{(3)}=0.0935$, respectively. From the matrix the unstable eigenvalue was calculated to be $\lambda_1=-1.9338$. The values of $b^{(1)}$, $b^{(2)}$, and $b^{(3)}$ are calculated from the experimental data when a perturbation p_n is applied at time n immediately after a point in the map comes into the vicinity of the unstable fixed point. The perturbation lasts for the full duration of the drive period. When the future section data are measured at time $n+1$, $n+2$, and $n+3$, we calculate the coefficients $b^{(1)}$, $b^{(2)}$, and $b^{(3)}$ according to

$$b^{(1)}=\frac{\delta x_{n+1}-a^{(1)}\delta x_n-a^{(2)}\delta x_{n-1}-a^{(3)}\delta x_{n-2}}{\delta p_n},$$

$$b^{(2)}=\frac{\delta x_{n+2}-a^{(1)}\delta x_{n+1}-a^{(2)}\delta x_n-a^{(3)}\delta x_{n-1}}{\delta p_n},$$

$$b^{(3)}=\frac{\delta x_{n+3}-a^{(1)}\delta x_{n+2}-a^{(2)}\delta x_{n+1}-a^{(3)}\delta x_n}{\delta p_n}.$$

In the experiment we use a constant $\delta p_n=0.038$ Oe every time for perturbation. For a typical run in this experiment the values of $b^{(1)}$, $b^{(2)}$, and $b^{(3)}$ are determined to be 0.001 23 V/Oe, $-0.000\,118$ V/Oe, and $-0.000\,414$ V/Oe, respectively.

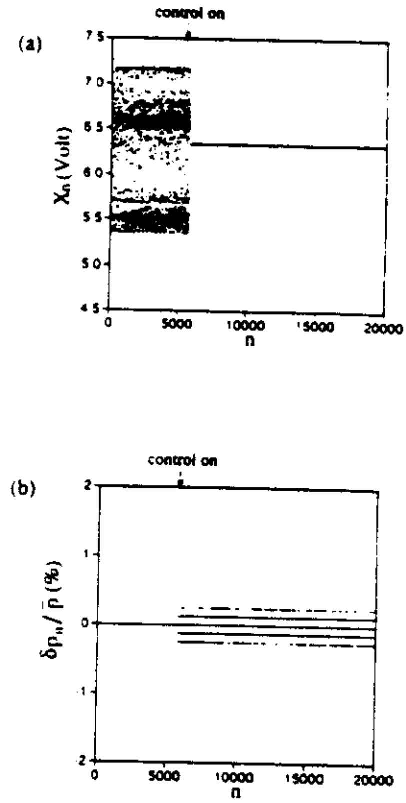

FIG. 6. Results of stabilizing the unstable period-1 orbit using an $m=3$ implementation of our control method. (a) Time series and (b) parameter perturbations. We note that the magnitude of δp_n is about 0.4% of the nominal value of $\bar{p}$, where $p=H_{dc}$ is the dc field.

B. Results

Using the $m=3$ implementation of our control method with the estimated $a^{(i)}$'s and $b^{(i)}$'s as stated above, we have successfully controlled the chaotic oscillations of the ribbon for almost 200 000 driving cycles (about 54 h) without any loss of control. Figure 6(a) shows a portion of the experimental time series before and after the application of control. The control can be maintained indefinitely. Figure 6(b) shows the perturbations applied to stabilize the period-1 orbit. Notice that the size of the perturbations is very small, typically between ± 0.0054 Oe, or about 0.4% of the nominal dc field $\bar{p}=\bar{H}_{dc}$. Figure 7(a) shows the contrast between the original OGY control [2] and our high-dimensional control with $m=3$ on the same attractor. After 830 iterates the OGY control is turned on and is unable to hold the periodic orbit even though there are numerous attempts on the close returns. The perturbed orbits would come in along the stable direction, but once the orbit reaches the unstable fixed point it starts to depart from the vicinity of the fixed point. In contrast, when our high-dimensional control is activated the system is captured into the period-1 motion rapidly. We note that the $m=2$ implementation of our method, which has the delay coordinates effect taken into account, also failed to achieve proper control. This leads us to believe that for this attractor one needs a higher-dimensional embedding space to unfold the dynamics and implement control.

We have also studied another parameter setting where the local dynamics near the fixed point can be effectively described by one stable and one unstable direction. We are able to control the period-1 orbit in this case with the original OGY method [2]. However, the interesting point is that, by applying the $m=3$ implementation of our method to the same orbit, we are able to achieve control with smaller parameter perturbations compared to the OGY case. This indicates that in some situations, although the low-dimensional control is effective, a higher-dimensional implementation may prove to be more efficient. Details of this result are planned to be presented in a future paper where we consider all the practical aspects of our control technique.

In applications, an important question is the impact of noise on the control performance. The unperturbed ribbon system has about 5% intrinsic noise. Our method is unaffected by this amount of noise. To test the method further, we have also added parametric noise to the system and found that we are able to maintain control even in the presence of about 10% of additional parametric noise, demonstrating the method's robustness. We thus believe that the technique presented in the paper is viable in practical problems where chaos control in high-dimensions is desired. Again we wish to present more detailed results on the issue of noise in a future paper.

V. CONCLUSION

Since Ott, Grebogi, and Yorke published their seminal paper on the control of chaos [2], a great deal of experimental research in nonlinear dynamics has been dedicated to the exploration of various aspects of the OGY algorithm in a

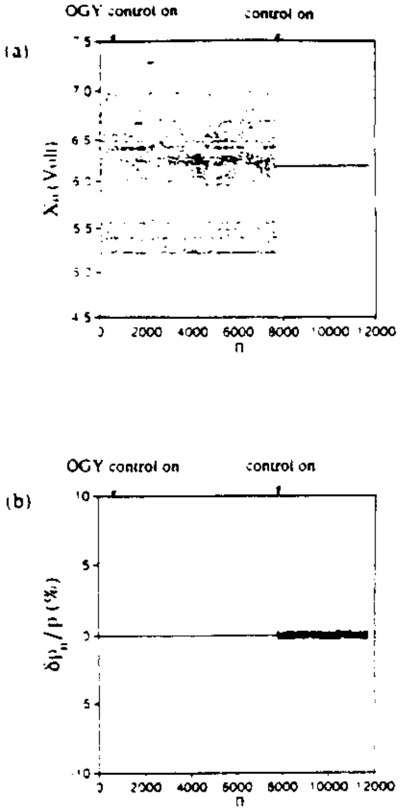

FIG. 7. Comparison of the OGY control and the $m=3$ implementation of our control method. (a) Time series and (b) parameter perturbations.

variety of systems. However, the success of the original OGY theory is limited by the fact that it applies only to systems where the dynamics near the periodic orbit is adequately described by one stable and one unstable direction. In the past few years a number of high-dimensional algorithms have been proposed to address this problem [7–9]. Due to the difficulties in obtaining the coefficients needed for control and sensitivity to noise, these methods are found to be difficult to implement experimentally.

Our main contribution in this paper is the development of a high-dimensional chaos control method that is effective and easy to implement in experiments. Based on the use of time series and delay coordinates, the method requires only small perturbations of a single control parameter to stabilize a periodic orbit in an arbitrary dimensional delay coordinate embedding space with an arbitrary number of unstable directions. In addition, by considering map-based systems our method offers the advantage that the coefficients needed for experimental implementation are easily and reliably estimated from time series data. In this regard, simple methods are proposed to extract such map-based time series from continuous-time systems. The effectiveness of the control method is demonstrated when applied to two examples of ordinary differential equations and to a physical experiment of a magnetoelastic ribbon driven by a sinusoidally varying magnetic field. Robust control is achieved in all cases. Furthermore, we mention that the method is not sensitive to noise and works well even in the presence of substantial noise.

ACKNOWLEDGMENTS

M.D. gratefully acknowledges support from the Office of Naval Research. W.L.D. is supported by the ONR Young Investigator Program. M.L.S. gratefully acknowledges support from the NSWC Independent Research Program and from the Office of Naval Research (Division of Physics and Chemistry).

APPENDIX

1. The null space of $\bar{\mathbf{A}}^{m-1}$

Using matrix blocks we rewrite $\bar{\mathbf{A}}$ defined in Eq. (13) as

$$\bar{\mathbf{A}}=\begin{pmatrix} \mathbf{A} & \mathbf{B} \\ \mathbf{Z}_0 & \mathbf{S} \end{pmatrix},$$

where $\mathbf{B}$ is an $m\times(m-1)$ matrix with $\mathbf{B}^{(i)}$ its column vectors, $\mathbf{Z}_0$ is an $(m-1)\times m$ zero matrix, and

$$\mathbf{S}=\begin{pmatrix} 0 & 1 & 0 & \cdots & 0 \\ 0 & 0 & 1 & \cdots & 0 \\ \vdots & \vdots & \vdots & \vdots & \vdots \\ 0 & 0 & 0 & \cdots & 1 \\ 0 & 0 & 0 & 0 & 0 \end{pmatrix}_{(m-1)\times(m-1)}.$$

It is easy to verify that $\mathbf{S}^{m-1}$ is a matrix of zeros. This means that the eigenvalue problem $\bar{\mathbf{A}}^{m-1}\mathbf{k}=\mathbf{0}$ has m equations for $2m-1$ unknowns from which one can find $m-1$ independent basis vectors to span the null vector $\mathbf{k}$. In other words, the null space of $\bar{\mathbf{A}}^{m-1}$ is $(m-1)$ dimensional.

2. The unstable eigenvectors of $\bar{\mathbf{A}}^T$

We wish to show that $\mathbf{v}_i$ from $\bar{\mathbf{A}}^T\mathbf{v}_i=\lambda_i\mathbf{v}_i$, $i=1,2,\ldots,u$, is orthogonal to the stable subspace spanned by $\mathbf{k}_j$, $j=u+1,u=2,\ldots,2m-1$. Consider $j=u+1,u+2,\ldots,m$. Multiply Eq. (15) from both sides by $\mathbf{k}_j^T$. The left-hand side becomes $\mathbf{k}_j^T\bar{\mathbf{A}}^T\mathbf{v}_i=(\bar{\mathbf{A}}\mathbf{k}_j)^T\mathbf{v}_i=\lambda_j\mathbf{k}_j^T\mathbf{v}_i$. Equating it with the right-hand side $\lambda_i\mathbf{k}_j^T\mathbf{v}_i$ and using $\lambda_i\neq\lambda_j$ we have $\mathbf{k}_j^T\mathbf{v}_i=\mathbf{v}_i^T\mathbf{k}_j=0$. Similarly, one can show that $\mathbf{v}_i^T\mathbf{k}_j=0$, $j=m+1,m+2,\ldots,2m-1$, by considering the eigenvalue problem of $\bar{\mathbf{A}}^{m-1}$ instead of $\bar{\mathbf{A}}$. It is straightforward to see that if the deviation $\delta\mathbf{Y}_{n+u}$ lies entirely in the space of $\mathbf{k}_j$, $j=u+1,u+2,\ldots,m,m+1,m+2,\ldots,2m-1$, then its future evolution asymptotically approaches zero under repeated applications of $\bar{\mathbf{A}}$.

3. The derivation of the control law Eq. (17) from Eq. (16)

Iterating Eq. (12) u times yields

$$\delta\mathbf{Y}_{n+u}=\bar{\mathbf{A}}^u\delta\mathbf{Y}_n+\bar{\mathbf{A}}^{u-1}\bar{\mathbf{B}}\delta p_n+\bar{\mathbf{A}}^{u-2}\bar{\mathbf{B}}\delta p_{n+1}+\cdots$$
$$+\bar{\mathbf{B}}\delta p_{n+u-1}.$$

From Eq. (16) we get

$$\lambda_1^{u-1}\delta p_n+\lambda_1^{u-2}\delta p_{n-1}+\cdots+\delta p_{n-u-1}=-\left(\frac{\lambda_1^u\mathbf{v}_1^T}{(\mathbf{v}_1^T\bar{\mathbf{B}})}\right)\delta\mathbf{Y}_n,$$

$$\lambda_2^{u-1}\delta p_n+\lambda_2^{u-2}\delta p_{n-1}+\cdots+\delta p_{n-u-1}=-\left(\frac{\lambda_2^u\mathbf{v}_2^T}{(\mathbf{v}_2^T\bar{\mathbf{B}})}\right)\delta\mathbf{Y}_n,$$

$$\vdots$$

$$\lambda_u^{u-1}\delta p_n+\lambda_u^{u-2}\delta p_{n-1}+\cdots+\delta p_{n-u-1}=-\left(\frac{\lambda_u^u\mathbf{v}_u^T}{(\mathbf{v}_u^T\bar{\mathbf{B}})}\right)\delta\mathbf{Y}_n.$$

These u linear equations contain u unknowns. Using Cramer's rule we express p_n as

$$p_n=\bar{p}+\frac{C}{D},$$

where

$$C=\mathrm{Det}\begin{pmatrix} -[\lambda_1^u\mathbf{v}_1^T/(\mathbf{v}_1^T\bar{\mathbf{B}})]\delta\mathbf{Y}_n & \lambda_1^{u-2} & \lambda_1^{u-3} & \cdots & 1\\ -[\lambda_2^u\mathbf{v}_2^T/(\mathbf{v}_2^T\bar{\mathbf{B}})]\delta\mathbf{Y}_n & \lambda_2^{u-2} & \lambda_2^{u-3} & \cdots & 1\\ \vdots & \vdots & \vdots & \vdots & \vdots\\ -[\lambda_u^u\mathbf{v}_u^T/(\mathbf{v}_u^T\bar{\mathbf{B}})]\delta\mathbf{Y}_n & \lambda_u^{u-2} & \lambda_u^{u-3} & \cdots & 1\end{pmatrix}_{u\times u} \tag{A1}$$

and

$$D=\mathrm{Det}\begin{pmatrix} \lambda_1^{u-1} & \lambda_1^{u-2} & \lambda_1^{u-3} & \cdots & 1\\ \lambda_2^{u-1} & \lambda_2^{u-2} & \lambda_2^{u-3} & \cdots & 1\\ \vdots & \vdots & \vdots & \vdots & \vdots\\ \lambda_u^{u-1} & \lambda_u^{u-2} & \lambda_u^{u-3} & \cdots & 1\end{pmatrix}_{u\times u}. \tag{A2}$$

By recognizing that D in (A2) is a slight variant of the standard Vandermonde determinant [14] we find

$$D=(-1)^{(d^2-d)/2}\prod_{1\le i<j\le u}(\lambda_j-\lambda_i).$$

Expanding the determinant in Eq. (A1) about the first column, the resulting cofactors are again variants of the Vandermonde matrix. This leads us to

$$C=\sum_{k=1}^{u}(-1)^{k+(d^2-3d+2)/2}[\lambda_k^u\mathbf{v}_k^T/(\mathbf{v}_k^T\bar{\mathbf{B}})]\delta\mathbf{Y}_n \times\prod_{1\le i<j\le u, i\ne k, j\ne k}(\lambda_j-\lambda_i).$$

After some algebra we obtain Eq. (17).

[1] E. Ott, *Chaos in Dynamical Systems* (Cambridge University Press, Cambridge, 1993).

[2] E. Ott, C. Grebogi, and J.A. Yorke, Phys. Rev. Lett. **64**, 1996 (1990).

[3] W.L. Ditto, S.N. Rauseo, and M.L. Spano, Phys. Rev. Lett. **65**, 3211 (1990); E.R. Hunt, *ibid.* **67**, 1953 (1991); R. Roy, T.W. Murphy, T.D. Maier, Z. Gills, and E.R. Hunt, *ibid* **68**, 1259 (1992); A. Garfinkel, M.L. Spano, W.L. Ditto, and J.N. Weiss, Science **257**, 1230 (1992); V. Petrov, V. Caspar, J. Masere, and K. Showalter, Nature (London) **361**, 240 (1993); S.J. Schiff, K. Jerger, D.H. Duong, T. Chang, M.L. Spano, and W.L. Ditto, *ibid.* **370**, 615 (1994); J.E.S. Socolar, D.W. Sukow, and D.J. Gauthier, Phys. Rev. E **50**, 3245 (2994); P. Parmananda, M.A. Rhode, G.A. Johnson, R.W. Rollins, H.D. Dewald, and A.J. Markworth, *ibid.* **49**, 5007 (1994).

[4] E.A. Jackson and A. Hubler, Physica D **44**, 407 (1990); B. Peng, V. Petrov, and K. Showalter, J. Phys. Chem. **95**, 4957 (1991); T. Tel, J. Phys. A **24**, L1359 (1991); K. Pyragas, Phys. Lett. A **170**, 421 (1992); Y.-C. Lai, M. Ding, and C. Grebogi, Phys. Rev. E **47**, 86 (1993); M.A. Matias and J. Guemez, Phys. Rev. Lett. **72**, 1455 (1994); M. Ding, E. Ott, and C. Grebogi, Physica D **74**, 386 (1994); D. Vassiliadis, *ibid.* **71**, 319 (1994); D.J. Christini and J.J. Collins, Phys. Rev. E (to be published).

[5] For reviews, see T.A. Shinbrot, C. Grebogi, E. Ott, and J.A. Yorke, Nature (London) **363**, 411 (1993); W.L. Ditto and L. Pecora, Sci. Am. **269** (8), 78 (1993); G. Chen and X. Dong, Int. J. Bif. Chaos **3**, 1363 (1993); E.R. Hunt and G. Johnson, IEEE Spectrum **30** (11), 32 (1993); R. Roy, Z. Gills, and K.S. Thornburg, Opt. Photon. News **5** (5), 8 (1994); E. Ott and M.L. Spano, Phys. Today **48** (5) 34 (1995).

[6] U. Dressler and G. Nitsche, Phys. Rev. Lett. **68**, 1 (1992); G. Nitsche and U. Dressler, Physica D **58**, 153 (1992).

[7] P. So and E. Ott, Phys. Rev. E **51**, 2955 (1995).

[8] V. Petrov, E. Mihaliuk, S.K. Scott, and K. Showalter, Phys. Rev. E **51**, 3988 (1995).

[9] For a sample of works dealing with chaos control in high dimensions, see F.J. Romeiras, C. Grebogi, E. Ott, and W.P. Dayawansa, Physica D **58**, 165 (1992); D. Auerbach, C. Grebogi, E. Ott, and J.A. Yorke, Phys. Rev. Lett. **69**, 3479 (1992); J.A. Sepulchre and A. Babloyantz, Phys. Rev. E **48**, 945 (1993); G. Hu and K. He, Phys. Rev. Lett. **71**, 3794 (1993); C. Reyl, L. Flepp, R. Badii, and E. Brun, Phys. Rev. E 47, 267 (1993); P. Colet, R. Roy, and K. Wiesenfeld, *ibid.* **50**, 3453 (1994); G. Hu and Z. Qu, Phys. Rev. Lett. **72**, 68 (1994); I.B Schwartz and I. Triandaf, Phys. Rev. E **50**, 2548 (1994); A Namajunas, K. Pyragas, and A. Tamasevicius, Phys. Lett. A **204**, 255 (1995).

[10] Edward Ott (private communication).

[11] J.-P. Eckmann and D. Ruelle, Rev. Mod. Phys. **57**, 617 (1985)

[12] F. Takens, in *Dynamical Systems and Turbulence*, edited by D Rand and L.S. Young (Springer-Verlag, Berlin, 1981), p. 366 T. Sauer, J.A. Yorke, and M. Casdagli, J. Stat. Phys. **65**, 57 (1991).

[13] G. Baier and S. Sahle, J. Chem. Phys. **100**, 8907 (1994).

[14] R. Bellman, *Introduction to Matrix Analysis* (McGraw-Hill New York, 1970).

Removal, suppression, and control of chaos by nonlinear design

John F Lindner and William L Ditto

Applied Chaos Laboratory, School of Physics, Georgia Institute of Technology, Atlanta GA 30332

Techniques to remove, suppress, and control the chaotic behavior of nonlinear systems are reviewed. Analysis of a forced damped nonlinear oscillator provides a brief overview of the relevant nonlinear dynamics of dissipative systems. Various techniques for suppression and control of chaos are then outlined, compared and contrasted. A unified mathematical notation facilitates the comparison. The successes of each strategy in numerical simulations and physical experiments are carefully noted. Their strengths and weaknesses are analyzed, and they are evaluated according to whether they employ feedback, are goal-oriented, are model-based, merely remove chaos–or truly exploit it. An elementary derivation of the important OGY control equation is supplied. Critical references provide an entry into the literature. It is argued that nonlinearity can be a real-world advantage, and it is hoped that this review will serve as summary of, and invitation to, the nascent field of nonlinear design.

1. INTRODUCTION

1.1 What good is chaos?

There lies a behavior between rigid regularity and pure chance. Its name is chaos. Our scientific paradigms encompass at one extreme the precise clock-like motion of periodic systems and at the other extreme the vagaries of random dice throwing chance but have curiously failed to account for commonly observed behavior between these two extremes. When we see irregularity we chauvinistically cling to randomness and disorder for explanations. Why should this be so? Why is it that when we encounter irregularity the whole vast machinery of probability and statistics is belligerently applied? Rather recently, however, the scientific community has begun to realize that the tools of chaos theory may be more appropriately applied than probabilistic techniques to the study of irregular systems. To understand why this is true one must start with a working knowledge of how chaotic systems behave.

Everybody has experience with the monotonous periodic behavior of the common clock. The incessant ticking is the very embodiment of periodicity and serves as the prime example of one end of the dynamical spectrum of behavior known as periodic "regular" behavior. Indeed its detection or production is often the holy grail of scientists, engineers, historians, doctors and other scholars. Its aliases include "normal sinus rhythm," "historical cycles," "normal modes," "frequency components," and "natural cycle of things." It seems odd that we identify perfection with relentless periodicity when all around us irregularity rules. What seems even odder is that we see irregularity as the purest happenstance or pure periodicity contaminated by dreaded random "noise." Just as the wave-particle duality has overwhelmed our notions of natural order in the quantum realm, we are finding that, at the opposite end of dynamics, purely random behavior does not totally encompass irregularity. In retrospect it was tremendous hubris to assume that our rigid notion of randomness should be the only organizational principle underlying irregularity.

Sustained irregularity has always upset our notions of how the world should behave, yet it seems to be the very embodiment of biological systems. One description of chaos, namely sustained irregular behavior, while descriptive, is too vague to embody the richness of chaotic systems. A defining feature of chaotic systems is sensitivity to initial conditions. This is vividly demonstrated by starting two identical systems in "nearly" identical states. If they are chaotic their final states can be quite different. This makes long term prediction unattainable.

Fleeting glimpses of order in disorder are quite common. We have all seen short stretches of periodic behavior in otherwise irregular systems. A tantalizing example lies in the stock market where many hope to reap windfall fortunes from analyzing short term order in the volatile market. Such short term order is a profound, even defining, feature of chaotic systems. The flesh of chaotic systems adheres to a skeleton of an infinite number of unstable periodic behaviors that seemingly come and go with no apparent pattern-or at least no apparent pattern until one looks carefully. Armed with an understanding of unstable periodic motions chaotic systems take on a much more understandable and subsequently controllable appearance.

Transmitted by Associate Editor M Gad-el-Hak

ASME Reprint No AMR179 $16

Table 1. Dictionary of Notation

$\mathbf{x}=\begin{bmatrix} x^1 \\ x^2 \end{bmatrix}$	vector as a column matrix
$\mathbf{x}^T=[x^1 \;\; x^2]$	vector as a row matrix
$\mathbf{M}=\begin{bmatrix} M_{11} & M_{12} \\ M_{21} & M_{22} \end{bmatrix}$	linear transformation matrix
$\mathbf{u}_i$	*i*th unit vector
x^i	*i*th component
$\mathbf{x}=\mathbf{x}(t)$	flow at time t
$\mathbf{x}_n$	map at iterate n
$\dot{\mathbf{x}}=\frac{d\mathbf{x}}{dt}$	time differentiation

1.2 Scope of this review

The purpose of this article is to provide an overview of various methods by which chaotic dynamics can be removed, suppressed, manipulated, or exploited. We will focus primarily on nonlinear control strategies for low-dimensional dissipative systems. Only near the end of the review will we consider higher-dimensional systems, and we will mention the important area of turbulent hydrodynamic flows only in passing.

We ourselves are intimately involved in the development of model-independent feedback techniques, but we recognize the practical importance of model-based nonfeedback strategies, and will consider both methodologies. However, we would like to stress a fundamental distinction among the various approaches: while some techniques merely suppress or remove chaotic behavior (for example, by invoking large parameter changes to drastically modify the dynamical attractor), others actually *exploit* chaotic behavior (for example, by employing minute perturbations to target periodic motions embedded in the attractor and subsequently using the "ergodicity" of the motion to switch among them). We believe that the latter approaches offer the more exciting engineering opportunities. Indeed, today we are learning how to manipulate chaos in brains and hearts, with the goal of easing arrhythmias and taming seizures. In the future, mechanical engineers may design and build structures and devices whose chaotic states are reservoirs of accessible periodic motions, which idle in chaotic rather than periodic motion to reduce metal fatigue, which respond to gentle controls with dramatic changes in function. Chaos will be engineered *in* rather than designed *out*.

1.3 Other resources

Complementary to this review, we recommend the following surveys of chaos control. Ditto and Pecora (1993) provide a general and gentle introduction, while Ditto, Spano, and Lindner (1995) offer a more technical but less broad account. Rajasekar and Lakshmanan (1993) directly compare the efficacy of several techniques in numerical experiments on a BVP oscillator. Shinbrot *et al* (1993) fashion an excellent review of the OGY technique. Keefe (1993) contrasts the OGY and Hübler techniques on a hydrodynamic model. Gad-el-Hak (1989) supplies a comprehensive reference on flow control, while Blazejczyk *et al* (1993) focus specifically on controlling chaos in mechanical systems. Chen and Dong (1993) offer an alternate general review, while Spano and Ott (1995) furnish a more recent perspective.

2. REVIEW OF NONLINEAR DYNAMICS

We first briefly review the concepts and vocabulary important to dissipative nonlinear dynamics. We illustrate them by focusing on the canonical "Duffing" oscillator. Table 1 introduces our notation.

2.1 Forced damped nonlinear oscillator

It is only a slight exaggeration to say that the forced damped nonlinear oscillator is the "hydrogen atom" of dissipative nonlinear dynamics. Duffing (1918) first studied an oscillator with a cubic stiffness term to model the nonlinear restoring force found in many mechanical systems. It has since become one of the most used and useful paradigms for nonlinear oscillations. Thompson and Stewart (1986) provide a good discussion of the Duffing oscillator. For a unit mass, the equation of motion of the forced and damped Duffing oscillator is

$$\ddot{x}+\gamma\dot{x}+kx+k'x^3=A\cos\omega t. \tag{1}$$

By introducing the velocity $v=\dot{x}$ and the phase $\varphi=\omega t$, we can write this second-order nonautonomous differential equation as a system of three autonomous first-order differential equations,

$$\left.\begin{aligned} \dot{x}&=v \\ \dot{v}&=-\gamma v-kx-k'x^3-A\cos\varphi \\ \dot{\varphi}&=\omega \end{aligned}\right\} \tag{2}$$

This system has the form

$$\dot{\mathbf{x}}=\mathbf{F}(\mathbf{x}), \tag{3}$$

where

$$\mathbf{x}=\begin{bmatrix} x \\ v \\ \varphi \end{bmatrix}. \tag{4}$$

2.2 Flows and sections in phase space

We can reduce the nonintersecting three-dimensional phase space flow that results from integrating Eq (3) to a two-dimensional map

$$\mathbf{x}_{n+1}=\mathbf{F}_{\mathbf{M}}(\mathbf{x}_n) \tag{5}$$

by intercepting the flow with a plane, or *Poincaré section*. (Strobing the motion once per forcing period achieves the same reduction.) This is illustrated in Fig 1. Notice that the phase is naturally represented as an angle.

Alternately, if we have access to only a single dynamical variable (as is often the case in experimental situations), we can reconstruct a topologically equivalent phase space flow and section by using *time delay coordinates*. Given the scalar variable of position $x(t)$, we can choose an embedding dimension d and a time delay τ and form the vector flow

$$\tilde{\mathbf{x}}(t) = \begin{bmatrix} x(t) \\ x(t-\tau) \\ x(t-2\tau) \\ \vdots \\ x(t-d\tau) \end{bmatrix} \tag{6}$$

Takens (1981) showed that, for sufficiently large embedding dimension and time delay, there exists a smooth and invertible mapping between the actual flow $\mathbf{x}(t)$ and the reconstructed flow $\tilde{\mathbf{x}}(t)$. Compare Fig 1 and Fig 2.

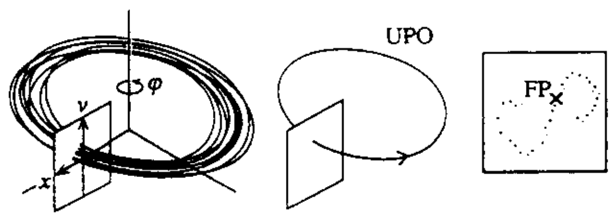

Fig 1. Flow and section illustrating an Unstable Periodic Orbit and its unstable fixed point.

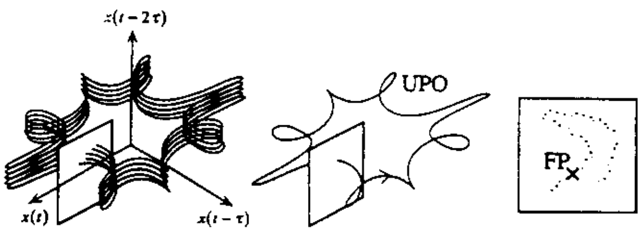

Fig 2. Strange attractor reconstructed from a delay coordinate embedding.

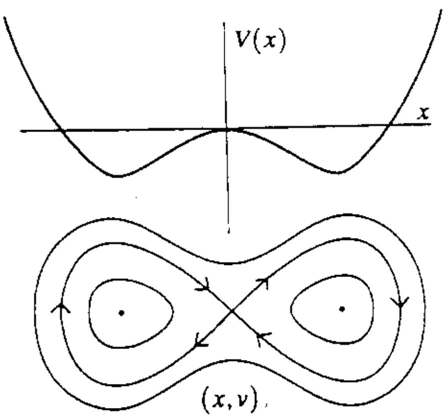

Fig 3. Potential well and phase space flow for an unforced undamped nonlinear oscillator.

2.3 Saddles, tangles, and UPOs

The Duffing attractor can be simple or complicated, depending upon the parameter regime. Fig 3 shows the potential well and phase space flow for the special unforced undamped case. Note the two stable and one unstable equilibrium points. Now imagine slowly turning on the forcing and the damping. Fig 4 schematically shows the phase space sections. In Fig 4a, note the two stable "spiral" fixed points and the one center unstable "saddle" fixed point with its stable and unstable sets, or *manifolds*. (The stable and unstable manifolds attract or repel successive iterates of the map; they are shown dotted as a reminder that they represent the map not the flow.) In Fig 4b, the forcing has increased until the stable and unstable manifolds of the saddle touch. Increasing the forcing further causes a transverse intersection, the consequences of which are visually isolated in Figs 4c-e. Because the point of intersection is simultaneously on the stable and unstable manifolds of the saddle, we can iterate it backwards and forwards to demonstrate that this single intersection requires infinitely many more intersections. Furthermore, the local expanding and contracting of the center saddle stretch and fold the manifolds as indicated. Accompanying the infinitely many intersections are infinitely many unstable periodic points. Each unstable periodic point in the section corresponds to an unstable periodic orbit, hereafter abbreviated UPO, in the phase space flow. Thus, at sufficiently low forcing the attractor is simple and the motion ordered, but at sufficiently high forcing the attractor is complicated and the motion is disordered–but with an infinite reservoir of unstable ordered motions nearby.

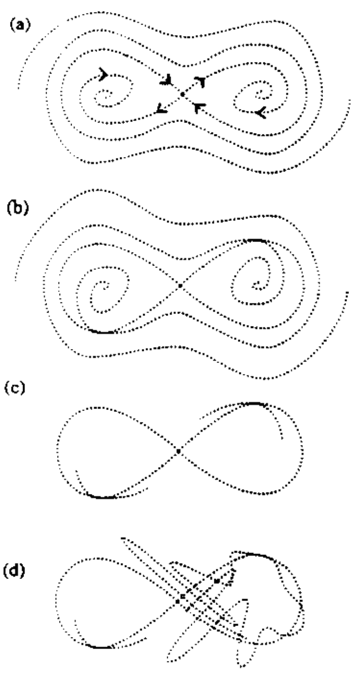

Fig 4. Phase space sections for a damped forced nonlinear oscillator. Damping and forcing combine to chaotically tangle the stable and unstable manifolds, thereby creating infinitely many unstable periodic points.

2.4 Strange chaotic attractors: Quantifying chaos

We typically characterize the nonsimple attractors exhibited by the Duffing oscillator by fractal dimensions and Lyapunov exponents.

Fractal dimensions characterize the *scaling* of the attractor. For example, if $N(R)$ is the number of boxes of size R needed to cover the attractor, and if $N(R)$ increases like

$$N(R) \sim kR^{-D}, \tag{7}$$

as R decreases, then the exponent D is the attractor's *box-counting* or *capacity* dimension. For a line $D = 1$ and for an area $D = 2$. This number, which may be fractional, is related to the number of active degrees of freedom characterizing the long-term behavior of the system.

Lyapunov exponents characterize the divergence of nearby trajectories in phase space. Specifically, if d_n is the distance between nearby trajectories in the phase space, and if d_n increases like

$$d_n \sim d_0 e^{\lambda n} = d_0 \Lambda^n. \tag{8}$$

then λ is a Lyapunov exponent and $\Lambda = e^{\lambda}$ is a Lyapunov multiplier. A system's largest Lyapunov exponent is a measure of its sensitivity to initial conditions.

A noninteger dimension indicates *strangeness*. A positive Lyapunov exponent indicates *chaos*. The traits of strangeness and chaos are typically linked. However, this need not always be the case. In particular, Ditto *et al* (1990b) recently reported the first experimental observation of a *strange nonchaotic* attractor.

3. INVENTORY OF CHAOS CONTROL TECHNIQUES

Here, in the core of the review, we describe, compare, and contrast many different suppression and control techniques. In each case, we consider a phase space flow, which for simplicity we take to be of the form

$$\dot{\mathbf{x}} = \mathbf{F}(\mathbf{x}, p), \tag{9}$$

where the vector $\mathbf{x}$ denotes the variables and the scalar p denotes an accessible parameter. Wresting order from a chaotic flow requires the transformation of one (uncontrolled) dynamics into another (desired) dynamics. Strategies may involve simply designing (or redesigning) the system, changing the operating conditions (and hence moving the system around in parameter space), or employing various kinds of feedback. Some strategies are model-based, others are model-independent; some are goal-oriented, others are not; some eliminate chaos, while others utilize it.

3.1 Entrainment to goal dynamics

If an accurate model of the system is available, we can entrain the phase space flow into a goal dynamics. For example, if we take the phase space control $\mathbf{C}(t)$ to be additive

$$\dot{\mathbf{x}} = \mathbf{F}(\mathbf{x}, p) + \mathbf{C}(t), \tag{10a}$$

with a governing system

$$\mathbf{C}(t) = \dot{\mathbf{x}}_g - \mathbf{F}(\mathbf{x}, p) \tag{10b}$$

then clearly $\mathbf{x}(t) = \mathbf{x}_g(t)$ is a solution. More generally, Lüscher and Hübler (1989) suggested entraining the phase space flow $\mathbf{x}(t)$ into a goal dynamics $\mathbf{x}_g(t)$ by adding a controlling term such that

$$\lim_{t\to\infty} |\mathbf{x}(t) - \mathbf{x}_g(t)| = 0. \tag{11}$$

Of course, the challenge is to find such a solution that has a nonzero attracting set, or *basin of entrainment*, and is stable. Jackson and Hübler (1990) studied these issues by numerically entraining orbits of the logistics map to periodic sets. They found that both the measure (size) and connectivity of the basin of entrainment depended on the mapping in a complex way.

3.2 Parametric control dynamics

We can apply an error signal to control a perturbed parameter. Huberman and Lumer (1990) suggested coupling the flow

$$\dot{\mathbf{x}} = \mathbf{F}(\mathbf{x}, p(t)) \tag{12a}$$

to a parameter dynamics governed by the error signal,

$$\dot{p} = -\varepsilon\left(x_g^i - x^i\right), \tag{12b}$$

where x^i is the ith variable and ε is the *stiffness* of the control. The error signal encourages the parameter of the system to readjust so as to reduce the error to zero. It *adaptively* controls the system. Note that the error signal is proportional to the difference between an actual and goal *variable*; alternately, the error could be taken to be proportional to the difference between an actual and goal *parameter*.

Sinha, Ramaswamy, and Rao (1990) extended and generalized this strategy in a number of ways. Their numerical experiments suggested that parametric control is robust with respect to noise and is indifferent to the exact form of the control function. Their recovery times were consistently found to be inversely related to the stiffness of the control.

3.3 Perturbations

Periodic or stochastic (random) perturbations applied to either the variables or the parameters of a nonlinear system may remove or suppress chaotic behavior. This strategy is often easy to apply but is not goal-oriented; the final state is untargeted and unpredictable.

3.3.1 Periodic

3.3.1.1 Periodic perturbations of a variable. We can suppress chaos by weak periodic external forcing. In this scheme, the phase space flow is modified by periodically perturbing (modulating) one of the components,

$$\dot{\mathbf{x}} = \mathbf{F}(\mathbf{x}, p) + \mathbf{u}_i A \cos wt, \tag{13}$$

where $\mathbf{u}_i$ is a unit vector in the ith direction. This is a simple and often easy way to adjust a system. However, the adjustments may need to be large, and the final state is unpredictable.

Braiman and Goldhirsch (1991) used this technique to tame the chaos of a periodically driven damped pendulum in a numerical experiment, as measured by a decrease in the leading Lyapunov exponent. They emphasized that a chaotic system's defining sensitivity is to weak time-dependent perturbations as well as to initial conditions.

3.3.1.2 Periodic perturbations of a parameter. We can remove or suppress chaos by resonant parametric perturbations. It is well known that an inverted pendulum can be stabilized by vertically oscillating its base. Imagine, then, modifying the phase space flow by periodically perturbing one of its parameters,

$$\dot{\mathbf{x}} = \mathbf{F}(\mathbf{x}, p + \delta p \cos w). \tag{14}$$

Lima and Pettini (1990) first proposed this technique and succeeded in removing chaos in a numerical experiment involving the Duffing oscillator. They found that parametric perturbations could convert chaotic dynamics to regular dynamics provided the perturbation amplitude was not too small (~1% of the unperturbed parameter) and provided the perturbation frequency was in resonance with the forcing frequency of the oscillator.

Fronzoni, Giocondo, and Pettini (1991) used periodic parametric perturbations to suppress chaos in a physical experiment that can be modeled as a Duffing oscillator. Their apparatus was a physical realization of the Duffing differential equation. One end of an elastic steel beam was clamped while the other end was free to move in the double-well potential created by two magnets. When they shook the apparatus electromagnetically, they observed sustained chaotic motion of the beam. They then modulated the magnetic fields, and hence the shape of the potential, by varying the current through copper coils wrapped around the magnets. Small modulations at particular resonant frequencies were successful in regularizing the motion

Azevedo and Rezende (1991) succeeded in suppressing chaos in a microwave-pumped spin-wave-instability experiment. Their apparatus consisted of a small polished ferromagnetic sphere at the center of a microwave cavity placed between the poles of a biasing magnet. For certain parameters, the amplitude of the reflected microwave radiation developed chaotic oscillations due to nonlinear interactions between spin-wave modes. However, a small modulation of the biasing magnetic field, induced by current flowing in a small copper loop inserted into the cavity, was able to suppress this chaos. They measured the reduction in chaos by the decrease in the (information) dimension of the chaotic attractor reconstructed from the time series using delay coordinates, and by the change in the power spectra of the oscillations.

3.3.2 Stochastic Perturbations Of Variables

We can suppress chaos by the simple device of adding external noise,

$$\dot{\mathbf{x}} = \mathbf{F}(\mathbf{x}, p) + \mathbf{N}(t), \tag{15}$$

where $\mathbf{N}(t)$ is a stochastic process.

Rajasekar and Lakshmanan (1993) numerically integrated the Bonhoeffer-Van der Pol oscillator in a chaotic regime, adding Gaussian random numbers every time step. For sufficiently large spread (standard deviation) of this simulated noise, the maximal Lyapunov exponent became negative and the system lost its sensitive dependence on initial conditions. Interestingly, although the added noise appeared to smear out the attractor, its (correlation) dimension remained nonintegral; it became a strange nonchaotic attractor.

3.4 Stabilizing UPOs

Techniques that use feedback to stabilize one of the many unstable periodic orbits, or UPOs, embedded in a chaotic attractor truly exploit chaos, rather than merely removing or suppressing it. They turn chaos into an advantage.

3.4.1 Switching parametric feedback

Given a target flow, we can regularize the motion by making small adjustments to a parameter according to whether a variable is too large or too small. Let

$$\dot{\mathbf{x}} = \mathbf{F}(\mathbf{x}, p + \delta p(t)), \tag{16a}$$

with the controller

$$dp(t) = \varepsilon \operatorname{sgn}\left(x^i(t) - x_g^i(t)\right), \tag{16b}$$

where ε is the stiffness of the control signal.

Singer, Wang, and Bau (1991) used such a discontinuous (on-off, switching) feedback controller to stabilize nonstable stationary flows in a physical experiment and its numerical model. Their system consisted of a convection loop under thermal and gravity gradients, which they modeled by the Lorenz equations. Their apparatus consisted of a water pipe bent into a torus in the vertical plane. They warmed the lower half of the pipe with a resistance heater, cooled the upper half with a coolant jacket, and monitored the vertical and horizontal temperature differences. The convection loop was capable of no motion (at low heating rates), steady clockwise or counter-clockwise flow (at higher rates), or chaotic flow (at still higher rates). The chaotic flow was "laminarized" by incrementing or decrementing the heating rate by a preset amount, depending upon whether or not the vertical temperature difference was above or below an average value. The control was robust with respect to small amplitude disturbances. However, Chen and Bau (1993) commented that switching-type functions can result in control "chattering" and in practice should be replaced with smoother functions.

3.4.2 Intermittent feedback control of UPOs

In a seminal contribution to the control of chaos, Ott, Grebogi, and Yorke (1990), often abbreviated as OGY, realized for the first time that chaos itself, if controlled, could be useful and desirable. A chaotic system's extreme sensitivity to initial conditions and to parameter changes makes long-term prediction impractical, but also makes fine-tuned weak control possible. Small carefully chosen perturbations of an accessible parameter can stabilize one of many UPOs embedded in a strange attractor. The UPOs themselves can be found by searching a Poincaré section for close returns. Furthermore, the chaotic attractor can be used as a path to flexibly steer the dynamics from one controlled periodic orbit to another.

The *local* computational models required to accomplish control can be obtained entirely from an experimental time series without any *a priori* analytic *global* model (at least for low-dimensional systems). This and the freedom to switch among various UPOs make the OGY technique model-independent and goal-oriented.

3.4.2.1 Overview of the OGY control strategy. Following OGY, we first reduce the phase space flow

$$\dot{\mathbf{x}} = \mathbf{F}(\mathbf{x},p), \mathbf{x} \in R^N, \tag{17}$$

to a map on a Poincaré section

$$\mathbf{x}_{n+1} = \mathbf{F}_M(\mathbf{x}_n,p), \mathbf{x}_n \in R^{N-1} \tag{18}$$

A periodic point of the map represents a UPO of the flow. For simplicity, we consider a fixed point (period-1),

$$\mathbf{x}_f = \mathbf{F}(\mathbf{x}_f, p_0), \tag{19}$$

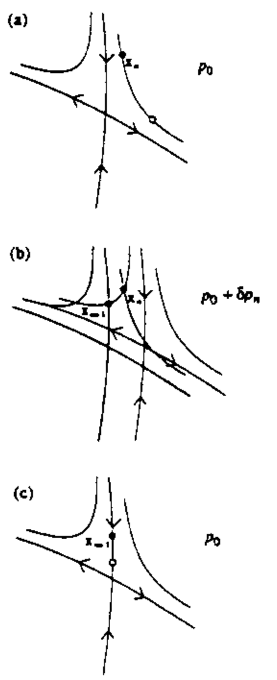

Fig 5. Nearby iterate (a) will miss fixed point, but perturbation shifts the fixed point and its manifolds (b) so that next iterate falls on stable manifold (c).

where p_0 denotes a nominal parameter value. In terms of the relative displacement $\delta\mathbf{x}_n \equiv \mathbf{x}_n - \mathbf{x}_f$ and the relative parameter perturbation $\delta p_n \equiv p_n - p_0$, we linearize the map nearby the fixed point as

$$\delta\mathbf{x}_{n+1} - \mathbf{M}\delta\mathbf{x}_n + \mathbf{s}\delta p_n, \tag{20}$$

where the shift vector $\mathbf{s} = \partial\mathbf{F}/\partial p$ and the map matrix of partial derivatives $\mathbf{M} = \partial\mathbf{F}/\partial\mathbf{x}$ are each evaluated at the fixed point. We assume that the relative perturbation is proportional to the relative distance from the fixed point and try a linear control law,

$$\delta p_n \sim -\mathbf{K}^T\delta\mathbf{x}_n, \tag{21}$$

where $\mathbf{K}$ is the proportionality vector. Thus, near the fixed point the linearized map becomes (by combining Eq (20) and Eq (22))

$$\delta\mathbf{x}_{n+1} \sim \mathbf{C}\delta\mathbf{x}_n, \tag{22}$$

where the control matrix

$$\mathbf{C} \equiv \mathbf{M} - \mathbf{s}\mathbf{K}^T. \tag{23}$$

This is a typical control problem. If we choose the proportionality vector $\mathbf{K}$ such that the moduli of the eigenvalues of the control matrix $\mathbf{C}$ are all less than unity, then iterates of the map will contract toward the fixed point,

$$\lim_{n\to\infty} \delta\mathbf{x}_n = 0, \tag{24}$$

and the UPO will be stabilized. Ogata (1990) provides a good reference on control engineering.

In practice, we find the map $\mathbf{M}$ and shift $\mathbf{s}$ by doing a linear fit to close returns in the section. We turn the perturbations on only when the iterates "ergodically" wander near the fixed point. (It is typical in chaotic systems for iterates to wander close to any chosen point.) Thus, the system is trapped precisely when the required perturbations are small,

$$\left|\mathbf{K}^T\delta\mathbf{x}_n\right| < \delta p_{\max}. \tag{25}$$

Various other control strategies based on Eq (23) are possible. An excellent review of the OGY strategy is the one by Shinbrot, Ott, Grebogi, and Yorke (1993).

3.4.2.2 Elementary derivation of the OGY control formula. Here we present a simple and pedagogical derivation of the original OGY control formula. Stabilizing a UPO is akin to balancing a marble on a horse's saddle: the saddle must be jiggled back and forth in the direction of the horse's ribs (rather than in the direction of its backbone). Figs 5 and 6 present the derivation as a proof without words.

We assume that the section is two-dimensional and that the fixed point is a "saddle" with one stable and one unstable manifold. Fig 5 illustrates the strategy. We summarize it as

$$\mathbf{x}_{n+1} = \mathbf{F}_M(\mathbf{x}_n, p_0 + \delta p_n), \tag{26a}$$

where the perturbation is

$$\delta p_n = \begin{cases} -k\delta x_n^{\perp}, \delta p_n \le \delta p_{max} \\ 0, \quad \delta p_n > \delta p_{max} \end{cases}. \tag{26b}$$

Motion of the map iterates in the vicinity of the fixed point is governed by the stable $|\lambda_s| < 1$ and unstable $|\lambda_u| > 1$ eigenvalues along the stable and unstable eigenvectors of the linearized map matrix **M**. Fig 6 projects the iterates onto the direction perpendicular to the stable direction. We demand that the *next* iterate fall on the stable (attracting) manifold, so that its distance perpendicular to the stable manifold vanishes:

$$\delta x_{n+1}^{\perp} = 0. \tag{27}$$

To accomplish this we must shift the fixed point by (refer to Fig 6)

$$s^{\perp}\delta p_n = -\lambda_u \delta x_n'^{\perp}, \tag{28}$$

where

$$\delta x_n'^{\perp} = \delta x_n^{\perp} - s^{\perp}\delta p_n. \tag{29}$$

Thus, by combining Eq (28) and Eq (29), the necessary perturbation is

$$\delta p_n = \frac{\lambda_u}{\lambda_u - 1}\frac{\delta x_n^{\perp}}{s^{\perp}}. \tag{30}$$

Note that we require $\lambda_u \neq 1$ and $s^{\perp} \neq 0$. In terms of the more general formalism above, Eq (30) is a special case of Eq (21) where the proportionality vector **K** has been chosen so that the eigenvalues of the control matrix **C** vanish in the direction perpendicular to the stable direction and are the same as the eigenvalues of the map matrix **M** in the stable direction.

OGY verified this control strategy in numerical experiments involving the two-dimensional Hénon map. They found that the length of the chaotic transient (or time-to-control) decreased as the maximum allowed parameter perturbation increased. Furthermore, they showed that control in the presence of noise and local modeling errors necessitated larger perturbations, and sometimes chaotic outbursts would occur as the orbit escaped in spite of the control.

Note that control of higher-period orbits requires merely a simple extension to the OGY strategy. This is because a period-n orbit of a map is a fixed point (period-1) of a new map which is composited of n of the original maps. For example, if x_1 is a period-2 point of a map f,

$$\left.\begin{aligned} x_2 &= f(x_1) \\ x_1 &= f(x_2) \end{aligned}\right\}, \tag{31a}$$

then x_1 is also a period-1 (fixed) point of the composite map f_2, where

$$x_1 = f(x_2) = f(f(x_1)) \equiv f_2(x_1). \tag{31b}$$

Ditto, Rauseo, and Spano (1990a) quickly implemented the OGY strategy in a physical experiment by controlling a chaotic system around UPOs of period-1 and period-2, and by switching between them at will. Their apparatus consisted of a vertical magnetoelastic ribbon clamped at its base. The stiffness of the ribbon was a very nonlinear function of an applied magnetic field. Small changes in the magnetic field could soften the ribbon so that it would buckle under gravity. A sinusoidal field alternately stiffened it and softened it so that, at high enough frequencies (~1Hz), chaotic motion ensued. A light sensor measured the position of the ribbon once per forcing period. Analysis of the resulting "stroboscopic" time series allowed identification of low-order UPOs and their local dynamics (shift vector and map matrix) in the section. Applications of OGY perturbations, Eq (30), to a DC magnetic field easily controlled the UPOs. Furthermore, they found that control was insensitive to errors in modeling the local dynamics.

More recently, Starret and Tagg (1995) used two variations of the OGY method to control the chaotic oscillations of a simple and well-known mechanical system: a parametrically driven pendulum. Their apparatus consisted of a brass pendulum mounted on an aluminum frame that oscillated vertically in response to a motor driven crank. Using eddy-current damping as the control parameter, they were easily able to stabilize the motion about several UPOs, both rotational (end-over-end) and librational (back-and-forth). They achieved control even when the phase space section was spread out, making a representation as a one-dimensional map infeasible (see Section 3.4.3.2). Furthermore, control was effective using either of two feedback rules: proportional adjustments of damping for fixed time intervals or fixed levels of damping for proportional time intervals. The latter variation was particularly simple, as it required only an on-off actuator.

3.4.3.1 OGY with delay coordinates. Dressler and Nitsche (1992) realized that the original OGY control formula of Eq

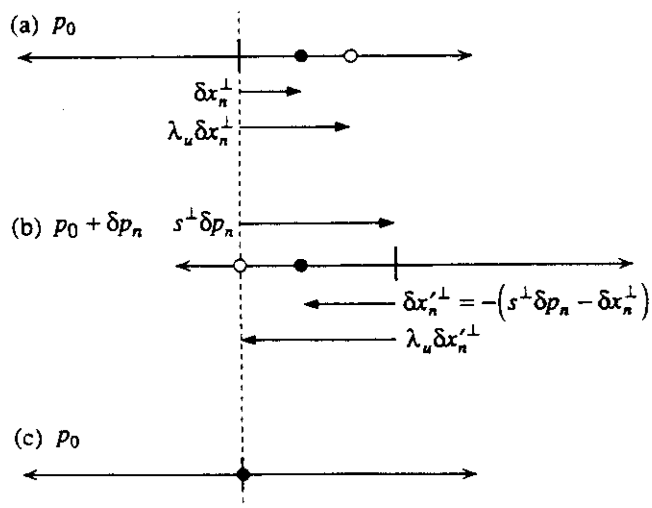

Fig 6. Previous figure collapsed onto the direction perpendicular to the stable manifold. Projected point, represented by the black dot, would iterate away from fixed point in (a), except perturbation applied in (b) causes it to move onto fixed point in (c).

30 must be modified if the attractor is reconstructed from delay coordinates. In this case, because the coordinates of the delay vector are obtained at different times when different parameters apply, the section map depends on the current parameter *and* on (at least) the previous parameter:

$$\mathbf{x}_{n+1} = \mathrm{F}_{\mathrm{M}}\left(\mathbf{x}_n p_n, p_{n+1}\right). \tag{32}$$

Further, to avoid the possible instability of a growing perturbation, Dressler and Nitsche modified the OGY control criterion by requiring that the next perturbation be zero *and* the next but one iterate be stabilized:

$$\left.\begin{aligned}\delta p_{n+1} &= 0\\ \delta x_{n+2}^{\perp} &= 0\end{aligned}\right\}. \tag{33}$$

(Contrast Eq (33) with Eq (27)) As a result, the current perturbation depended recursively on the previous perturbation,

$$\delta p_n = c_1 \delta x_n^{\perp} + c_2 \delta p_{n-1}, \tag{34}$$

where the constants c_1 and c_2 enfold information about the local dynamics. They tested this modified control equation in numerical experiments on the Duffing attractor, reconstructed from a time series by a three-dimensional delay coordinate embedding, and found it to be superior to the unmodified control in that it succeeded in cases where the original failed.

Subsequently, Romeiras, Grebogi, Ott, and Dayawansa (1992) defined a new embedding vector,

$$\bar{\mathbf{x}}_{n+1} = \begin{bmatrix}\mathbf{x}_{n+1}\\ p_n\end{bmatrix}, \tag{35}$$

and introduced generalized matrices to retain the OGY framework. Romeiras *et al* also extended OGY in several other directions. They exploited control theory to provide a more general choice of feedback matrix. They adddressed the problems of implementation in higher dimensions and the stabilization of periodic points with more than one unstable eigenvalues. In particular, they illustrated OGY control in a numerical experiment on a model of the kicked double rotor, whose equations of motion reduced to a four-dimensional dissipative map.

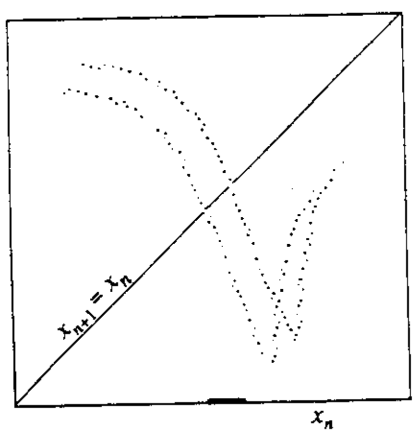

Fig 7. Chaotic attractor of a highly dissipative system can be characterized by a one-dimensional return map.

3.4.3.2 OGY and highly dissipative systems: OPF. In a highly dissipative system, the contraction in the phase space is so large that the attractor is squeezed down to low dimensions. In cases were the contraction is such that the attractor can be well described by a one-dimensional map in a two-dimensional delay coordinate embedding (or "time-one return map"), then the OGY technique simplifies to a geometrical algorithm involving Occasional Proportional Feedback (OPF). The map becomes one-dimensional

$$x_{n+1} = F_M\left(x_n, p\right), \tag{36a}$$

and the control becomes

$$\delta p_n = \frac{\delta x_n}{s}, \tag{36b}$$

where $s = dx/dp$. Notice that the feedback is simply proportional to the distance to the periodic point. See Fig 7. The OPF technique has proven to be especially useful in controlling high-frequency chaos in diodes and lasers.

Inspired by the pioneering magnetoelastic ribbon experiment of Ditto *et al*, Hunt (1991) developed the OPF into an analog technique to control chaos in an electrical circuit consisting of a rectifying diode in series with an inductor (and resistor), which were sinusoidally driven. Hunt sampled the peak current at the driving frequency and, if it was in a given window, modulated the drive voltage with a signal proportional to the current offset. He manually adjusted the current window's size and center in seeking stable orbits. This technique successfully controlled high-period orbits (up to period-36!) on millisecond and faster (53 kHz ~1/0.05 ms) time scales. Note, however, that these were generic reductions from chaotic to periodic; there was no systematic way to stabilize a particular orbit.

Roy, Murphy, Maier, Gills, and Hunt (1992) utilized the OPF analog variation of OGY to control optical chaos on microsecond time scales. The apparatus was a multimode laser with an intracavity period-doubling crystal. A specific orientation of the crystal would render the laser intensity output chaotic. The source of the chaos was the nonlinear global coupling of longitudinal modes of the system. In the absence of any periodic forcing, the intensity of the laser was sampled at natural period of relaxation of the laser cavity. Using the OPF technique, Roy *et al* converted the chaotic output of the laser to a periodic output (at ~100 kHz).

Working independently, Peng, Petrov, and Showalter (1991) devised and demonstrated OPF in numerical experiments by controlling an open three-variable isothermal self-catalyzing chemical reaction Then Petrov *et al* (1993) utilized OPF to control the chaotic regime of a famous oscillatory chemical system, the Belousov-Zhabotinsky reaction, in which cerium, acidified by sulfuric acid, catalyzes the oxidation and bromination of malonic acid. The flow rate of the reactants into and out of a continuously stirred tank determined whether the system exhibited steady, periodic, or chaotic behavior. The attractor was reconstructed from smoothed values of the potential of a bromide electrode. Feedback was applied to the system by varying the flow rates of cerium and bromate (but holding constant the flow rate of malonic acid). Oscillatory behavior of the chemical reaction could be converted back and forth among period-1, period-2, and chaos simply by adjusting the proportional feedback.

3.4.3.3 OGY and recursion in highly dissipative systems: RPF. OPF can fail if the attractor changes when a control parameter is altered. Rollins, Parmananda, and Sherard (1993) applied the insights of Dressler and Nitsche to the OPF technique to forge a Recursive Proportional Feedback (RPF) technique to overcome this problem. In this scheme, the return map becomes

$$x_{n+1} = F_M(x_n, p_n, p_{n+1}). \tag{37a}$$

and the control is

$$\delta p_n = k_1 \delta x_n + k_2 \delta p_{n-1}, \tag{37b}$$

where the constants k_1 and k_2 enfold the local dynamics. Like the OPF, the RPF is useful in highly dissipative systems where dynamics exhibits a nearly one-dimensional return map, but it can succeed where the OPF will fail, as Rollins *et al* demonstrated in numerical simulations of a three-dimensional electrochemical model and a two-dimensional bacterial model.

Subsequently, Parmananda, Sherard, Rollins, and Dewald (1993) provided experimental verification of the RPF algorithm. The apparatus was an electrochemical cell with a (rotating and dissolving) copper anode and a platinum cathode in a sodium acetate-acetic acid buffer. Successive current minima between the anode and the cathode provided the time series. The potential between the anode and a reference electrode provided the control parameter. RPF was used to stabilize the chaotic dissolution of the anode as a period-1 orbit, corresponding to large amplitude oscillations only.

3.4.3.4 OGY and no accessible parameters: PPF. If a chaotic system admits no accessible system parameter, it may be possible to affect control by altering a system variable instead. Suppose we can move the variables along a specific direction $\mathbf{u}_i$, then if the map is

$$\mathbf{x}_{n+1} = \mathbf{F}_M(\mathbf{x}_n), \tag{38}$$

we define a new map by

$$\mathbf{x}_{n+1} = \mathbf{F'}_M(\mathbf{x}_n, p) \equiv \mathbf{F}_M(\mathbf{x}_n + p\mathbf{u}_i), \tag{39}$$

and proceed with the OGY strategy.

Garfinkel, Spano, Ditto, and Weiss (1992) invented this method of chaos control, called Proportional Perturbation Feedback (PPF), of necessity, when first controlling cardiac chaos. In this experiment, they induced a section of a rabbit's heart to beat chaotically by the injecting the drug ouabain (pronounced "wah-bane"). No adjustable parameter could be modified quickly enough to implement OGY control. Instead, they used electrical stimuli to ***shorten*** (but not lengthen) interbeat intervals. They calculated the necessary advance in the next beat to place the state point directly onto the stable manifold of the fixed point. Thus, rather than move the saddle, they instead moved the system state point in the opposite direction. While they were unable, in these early experiments, to achieve a "normal" period-1 heartbeat, they did replace the chaotic beating with a period-3 beat. (The period-3 was an artifact of the control).

Figure 8 illustrates PPF control. Figure 8a is a return plot of I_n *vs* I_{n-1} typically constructed from (heart beat) interbeat interval data. Note the presence of an unstable fixed point along the 45-degree line. Figure 8b demonstrates how to pull the interval down onto the stable direction and consequently onto the unstable fixed point. The intervals between beats

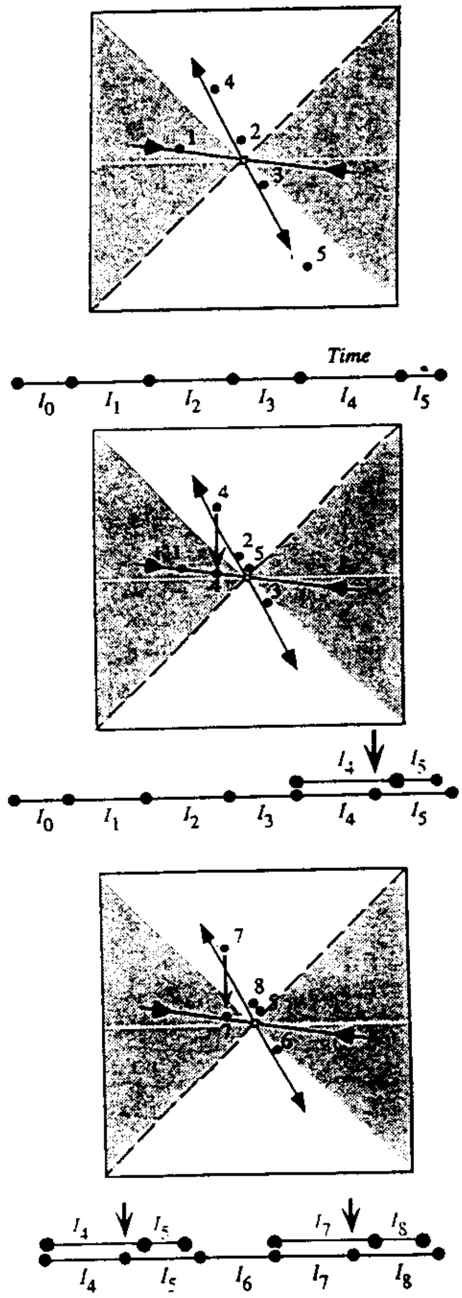

Fig 8. PPF control as applied to chaos in the heart and brain.

and the control stimuli are shown below the return map. (The gray points are without control). Figure 8c depicts the subsequent behavior of the system under control Note that the stimuli (arrows) are applied only intermittently.

Building upon their success using PPF to control cardiac chaos, Schiff *et al* (1994) succeeded in demonstrating chaos, and its control and *anti-control*, in the brain. This collaboration studied *in vitro* brain slice preparations. Return plots of interburst intervals, recorded with microelectrodes, exhibited the stable and unstable manifolds of unstable fixed points. Minute electrical impulses modified the timing of the intervals so as to place the state point either on stable manifolds (for control) or near unstable manifolds (for anti-control). Anti-control converted rhythmic bursting to aperiodic bursting, with a minimum of interventions. Such ability might one day be useful in breaking up epileptic seizures.

3.4.3.5 OGY and complex eigenvalues: MED. The original OGY formula Eq (30) is inappropriate when complex eigenvalues or multiple unstable eigenvalues occur. Reyl, Flepp, Badii, and Brun (1993) introduced a Minimal Expected Deviation (MED) variation of OGY to circumvent these problems. Instead of demanding that the next iterate fall on the stable manifold of the target fixed point, they required merely that the next iterate come as close as possible. They minimized

$$\|\delta \mathbf{x}_{n+1}\| = \|\mathbf{M}\delta \mathbf{x}_n + s\delta p_n\|, \tag{40}$$

to obtain the new control law

$$s\delta p_n = -(s/s)^T \mathbf{M}\delta \mathbf{x}_n, \tag{41}$$

(see Figure 9) or

$$\delta p_n = -\frac{s^T \mathbf{M}\delta \mathbf{x}_n}{s^2} \tag{42}$$

Note how the map matrix appears in this expression rather than the unstable eigenvalue .

Reyl *et al* used the MED technique to successfully control a chaotic system whose attractor needed to be embedded in a six-dimensional space. Their apparatus was an NMR laser with a sinusoidally modulated quality factor. In their experiments, the MED technique proved more reliable than the original OGY technique.

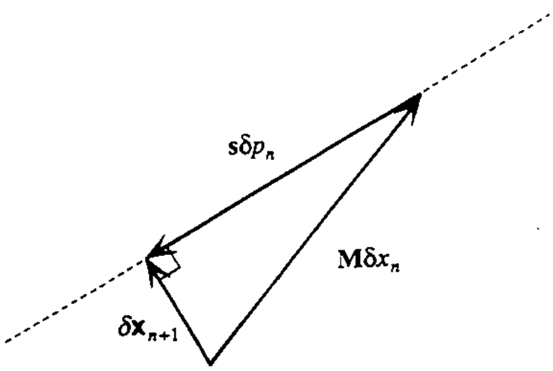

Fig 9. Control law for the MED technique

3.4.4 Continuous feedback control of UPOs

Continuous as well as intermmitent perturbations can stabilize a desired UPO without altering it. The OGY strategy is based on maps from sections, and hence its calculated small and rare perturbations are applied intermittently, allowing occasional bursts of lost control. In addition, the OGY method can stabilize only those UPOs whose expanding directions are sufficiently small; specifically, the time between perturbations must be small compared to the reciprocal of the maximal Lyapunov exponent. Pyragas (1992) introduced the strategy of continuous control to overcome these limitations.

3.4.4.1 Continuous external feedback. We can use negative feedback to modify a variable of the flow based upon the motion of an external oscillator. Let

$$\dot{\mathbf{x}} = \mathbf{F}(\mathbf{x}, p) + p\mathbf{u}_i C(t), \tag{43a}$$

where the control signal is sensitive to the ith variable

$$C(t) = \varepsilon\left(x_g^i(t) - x^i(t)\right), \tag{43b}$$

and where the external oscillator goal $\mathbf{x}_g(t) = \mathbf{x}_g(t+T)$ is periodic, and the stiffness $\varepsilon > 0$ is positive. The critical feature of this control is that it does not change the flow if $\mathbf{x}(t) = \mathbf{x}_g(t)$ is a UPO extracted from the chaotic attractor. Furthermore, when stabilization obtains $\mathbf{x}(t) \sim \mathbf{x}_g(t)$ and the control perturbation becomes very small. Because the control is continuous, it is also permanent, and no chaotic bursts result. The control can be initiated at any time, even when the flow is far from the UPO. However, excessively large perturbations can drive some systems to alternative solutions.

Qu, Hu, and Ma (1993) numerically investigated controlling chaos by continuous feedback in the Lorenz and Duffing models. They modified the above feedback rule to include a diagonal perturbation stiffness (weight) matrix :

$$C(t) = \mathbf{E}\left(\mathbf{x}_g(t) - \mathbf{x}(t)\right). \tag{43c}$$

These numerical experiments suggested that higher-dimensional systems may be controlled by feeding back a single variable, but not always; in some cases it was found necessary to feedback several variables.

3.4.4.2 Continuous delayed feedback. We can simplify the above strategy by replacing the external periodic oscillator by a delayed output signal from the system itself. Let

$$\dot{\mathbf{x}} = \mathbf{F}(\mathbf{x}, p) + \mathbf{u}_i C(t) \tag{44a}$$

where the control signal is now

$$C(t) = \varepsilon\left(x^i(t-\tau) - x^i(t)\right), \tag{44b}$$

where τ is the delay time. Notice that if $\tau = T$ control does not change the flow so long as $\mathbf{x}(t) = \mathbf{x}_g(t)$. Again, the hope is that appropriate choice of stiffness can stabilize the UPO.

Pyragas (1992) introduced such a strategy and used it to stabilize the Rössler system and the Duffing oscillator in numerical experiments. Unfortunately, for the Rössler system, the delayed perturbations were sometimes able to stabilize multiple orbits, not just the desired orbit, depending upon the initial conditions. The strategy's advantage is that, in a physical experiment, no computer or external perturbation would be needed to perform the control.

Subsequently, Pyragas and (1993) did succeed in using continuous delayed feedback to control a physical system, namely an analog electrical circuit using a simple delay line. The experiment required no computer analysis of the system and was robust to noise.

3.4.4.3 Continuous synchronizing feedback. Pyragas (1993) combined the above ideas of controlling chaos with the idea of *synchronizing* chaos, suggested by work of Pecora and Carroll (1990), to synchronize the current behavior of a system with its past behavior. Here the continuous feedback perturbation is proportional to the difference between the current and past output signals of one of the system variables. In this way, he was able to control aperiodic orbits in numerical experiments on the Duffing, Lorenz, and Rössler systems.

4. IMPROVEMENTS TO CONTROL

We briefly discuss supplementary techniques to improve the ease and utility of using small, intermittent perturbative feedback to control chaotic dynamics. Two types of problems can arise. First, before "capturing" a phase space trajectory with an OGY-like strategy, we must wait until it happens to "ergodically" wander nearby a fixed point in the section. This may take a long time. Second, system parameters may vary with time, thereby altering the local and global structure of the underlying dynamical attractor. This nonstationarity is common in biological applications where, for example, the sample may be dying. The techniques of targeting and tracking have been developed to overcome these difficulties.

4.1 Targeting

The exponential sensitivity of chaotic systems to tiny perturbations (the "butterfly effect") can be used to rapidly direct orbits from an arbitrary initial state to a desired state. Different trajectories arising from small changes in parameters or initial conditions may be patched together to come arbitrarily close to a desired target.

Shinbrot *et al* (1990) first introduced this strategy and verified it in a numerical experiment involving the Hénon map. In a typical case, an initial condition that would need more than 6000 iterations of the map to reach a tiny target area, was directed there in only 12 iterations. Furthermore, they showed that targeting was effective if the noise and modeling errors were sufficiently small.

Kostelich *et al* (1993) demonstrated that targeting could be done in higher dimensions. They numerically studied the kicked double rotor, which they reduced to a four-dimensional mapping whose attractor had a (Lyapunov) dimension of 2.8. In a typical case, an initial condition that would need more than 10^{11} iterations of the map to reach a tiny target area, was directed there in only 35 iterations. This efficiency was possible because Kostelich *et al* first spent about 10^6 iterations building a "tree of paths" leading to the target

However, to date targeting has been achieved experimentally in only one system. Shinbrot, Ditto, *et al* (1992) successfully targeted states in the magnetoelastic ribbon, the attractor of which was low-dimensional.

4.2 Tracking

Several groups have experimentally demonstrated that UPOs can continue to be controlled while system parameters are continuously varied, even through bifurcations. Heretofore unobtainable phase space regions can be reached with this method. In addition, tracking may be critical to chaos control applications in the heart and brain, biological systems which are typically nonstationary.

Carroll *et al* (1992) tracked a UPO of a Duffing-like electrical circuit as they slowly drove the system through a bifurcation. Gills *et al* (1992) extended the range over which OPF stabilized a multimode laser by an order of magnitude by tracking an unstable steady state as the pump excitation was slowly varied. This boosted the power output 15-fold. Recently, In, Ditto, and Spano (1995) achieved tracking in a mechanical system, the magnetolastic ribbon, using the full OGY technique.

5. AT THE FRONTIER

Here we summarize two important areas of active and future exploration, the control of higher-dimensional chaos and the control of spatiotemporal chaos. The areas are related because spatiotemporal chaotic systems typically have many degrees of freedom and their dynamics often lie on very high-dimensional attractors. We will focus on efforts to extend the techniques in our inventory (Section 3) that work well for low-dimensional, spatially isolated systems, to higher-dimensional, spatially coupled systems.

The related and technologically very important subject of the control of turbulent fluild flow is beyond the scope of this review. However, Gad-el-Hak (1993) provides an exciting futuristic introduction to the interactive control of turbulent boundary layers. Shermer (1992) extends the nonfeedback model-based control of Hübler (Section 3.1) to suppressing vortex shedding. Keefe (1993) compares and contrasts the Hübler and OGY techniques in a hydrodynamic model.

5.1 Higher-Dimensional Chaos

The dynamics of many systems is not confined to a lower-dimensional attractor but roams over many dimensions. Control of such systems is more difficult due to their complicated nature. For example, OGY control may not be feasible due to the large amount of information (shift vector, map matrix) that must be extracted from the data.

Auerbach, Grebogi, Ott, and Yorke (1992) extended the OGY scheme in an attempt to overcome this problem. This still model-independent extension requires knowledge only of a single time series. It has succeeded in controlling higher-dimensional chaos in a numerical experiment involving the kicked double rotor. However, unless the contracting directions are very strong, significant information must still be extracted from the time series, and this technique has still not succeeded in controlling a physical system.

Ultimately, higher-dimensional targeting and multivariant control (simultaneously varing more than one parameter) may be essential to successfully adapting OGY control strategies to higher dimensional chaos. Certainly, any successful practical control strategy will be judged on its effectiveness on higher-dimensional systems.

5.2 Spatiotemporal Chaos

When is a spatially extended system chaotic? If the system evolves in time, it is chaotic if its high-dimensional dynamics is governed by a phase space attractor with a positive Lyapunov exponent. But if the system itself is chaotic, must its evolving *spatial* patterns be disordered? If so, how do we quantify this disorder? Can we consistently calculate spatial Lyapunov exponents by singling out one space dimension as a time dimension? How do we test for spatial chaos in a *static* system? These issues of spatiotemporal or "space-time" chaos are currently under active investigation. Here we report on several groups who have studied the behavior of spatially coupled systems whose elements in isolation exhibit low-dimensional chaos.

Sepulchre and Babloyantz (1993) extended the OGY control technique to stabilize the chaotic oscillations of a 9 × 9 network of coupled oscillators in a numerical experiment. At nonzero coupling the dimensionality of the network was determined not to be low, suggesting a very large number of unstable degrees of freedom. Several unstable periodic motions of the network were found and subsequently stabilized by small periodic microkicks to every oscillator. (As in the PPF technique, the perturbations were applied to the variables, not to the parameters.)

Is distributed control necessary to control a network of oscillators? Is a subnetwork of controlling nodes sufficient? Four numerical experiments and one recent physical experiment suggest that global control of certain convectively unstable media may be achieved locally. Gang and Kaifen (1993) successfully employed negative feedback to control an anisotropic one-dimensional open system described by a partial differential equation. One technique was to inject a monochromatic wave (feedback in k-space). A second technique was to pin the system at one place in space (feedback in x-space). In each case, the local control propagated throughout the entire system.

Similarly, Auerbach (1994) succeeded in controlling a chain of asymmetrically coupled quadratic maps. In this case, controllers were distributed periodically in space, each perturbing a local parameter based on local measurements. The local control was convected downstream.

Aranson, Levine, and Tsimring (1994) proposed a technique for controlling certain isotropic convectively unstable media. These media include unstable defects which can break up and nucleate more defects. (Certain models of cardiac tissue are examples.) Control was obtained by stabilizing one such defect which then swept all chaotic fluctuations away.

Recently, Johnson, Löcher, and Hunt (1995) stabilized wave patterns in a convectively unstable medium, in both a physical and a numerical experiment. Their apparatus consisted of 32 coupled diode resonator circuits driven by a 70 kHz sinusoidal source. A single controller at the first diode resonator was able to stabilize the 32-element array. Johnson *et al* verified their results in a numerical experiment involving the control of coupled logistics maps.

Thus, to date local control begets global control only in special media.

6. CONCLUSION

Because nonlinear systems can exhibit chaos, they admit possibilities and opportunities that simple systems do not. Nonlinear systems and chaotic networks can be thought of as infinite reservoirs of unstable periodic motions. Nonlinear design can exploit these possibilities. It is likely that practical chaos control will utilize some or all of the techniques reviewed here. We are excited about the future of chaos control, and hope to encourage nonlinear thinking and nonlinear design.

7. ACKNOWLEDGEMENT

The authors thank the referees, whose careful reading of the MS significantly improved this review. Linder thanks The College of Wooster for making possible his sabbatical at Georgia Tech. Ditto is grateful for financial support from the Office of Naval Research.

REFERENCES

Aranson I, Levine H, and Tsimring L (1994), Controlling spatiotemporal chaos, *Phys Rev Letter* **72** 2561-2564.

Auerbach D (1994), Controlling extended systems of chaotic elements, *Phys Rev Lett.* **72** 1184-1187.

Auerbach D, Grebogi C, Ott E, and Yorke JA (1992), Controlling chaos in higher dimensional systems, *Phys Rev Lett* **69** 4379-3482.

Azevedo A and Rezende SM (1991), Controlling chaos in spin-wave instabilities, *Phys Rev Lett* **66** 1342–1345 .

Blazejczyk B, Kapitaniak T, Wojewoda J, and Brindley J (1993), Controlling chaos in mechanical systems, *AMR* **46** (7) 385-391.

Braiman Y and Goldhirsch I (1991), Taming chaotic dynamics with weak periodic perturbations, *Phys Rev Lett* **66** 2545-2548.

Carroll TL, Triandaf I, Schwartz I, and Pecora L (1992), Tracking unstable orbits in an experiment, *Phys Rev A* **46** 6189–6192.

Chen G and Dong X (1993), From chaos to order - Perspectives and methodologies in controlling chaotic nonlinear dynamical systems, *Int J Bif & Chaos* **3**(6) 1363-1409.

Chen YH and Bau HH (1993), Comment and reply on "Controlling a chaotic system", *Phys Rev Lett* **69** 3128-3129.

Ditto WL and Pecora LM (1993), Mastering chaos, *Sci Am* **269**(2) 78-84.

Ditto WL, Spano ML, and Lindner JF (1995), Techniques for the control of chaos, (to appear in *Physica D*).

Ditto WL, Rauseo SN, and Spano ML (1990a), Experimental control of chaos, *Phys Rev Lett* **65** 3211-3214.

Ditto WL, Spano ML, Savage HT, Rauseo SN, Heagy J, and Ott E (1990b), Experimental observation of a strange nonchaotic attractor, *Phys Rev Lett* **65** 533-536.

Duffing G (1918), *Erzwungene Schwingungen bei Veränderlicher Eigenfrequenz*, F Vieweg u Sohn, Braunschweig.

Fronzoni L, Giocondo M, and Pettini M (1991), Experimental evidence of suppression of chaos by resonant parametric perturbations, *Phys Rev A* **43** 6483-6487.

Gad-el-Hak M (1989), Flow control, *Appl Mech Reviews* **42**(10) 261-293.

Gad-el-Hak M (1994), Interactive control of turbulent boundary layers: a futuristic overview, *AIAA J* **32**(9) 1753-1765.

Gang H and Kaifen H (1993), Controlling chaos in systems described by partial differential equations, *Phys Rev Lett* **71** 3794-3797.

Garfinkel A, Spano ML, Ditto WL, and Weiss JN (1992), Controlling cardiac chaos, *Science* **257** 1230-1235.

Gills Z, Iwata C, Roy R, Schwartz IB, and Triandaf I (1992), Tracking unstable steady states: extending the stability regime of a multimode laser system, *Phys Rev Lett* **69** 3169-3172.

Huberman BA and Lumer E (1990), Dynamics of adaptive systems, *IEEE Trans on Circuits and Syst* **37** 547-550 .

Hunt ER (1991), Stabilizing high-period orbits in a chaotic system: The diode resonator, *Phys Rev Letter* **67** 1953-1955 .

In V, Ditto WL, and Spano ML (1995), Adaptive control and tracking of chaos in a magnetoelastic ribbon, *Phys Rev E* **51** R1-R4.

Jackson EA and Hübler A (1990), Periodic entrainment of chaotic logistic map dynamics, *Physica D* **44** 407-420.

Johnson GA, Löcher M, and Hunt ER (1995), Stabilized spatiotemporal waves in a convectively unstable open flow system: Coupled diode resonators, *Phys Rev E* **51** R1625-R1628.

Keefe LR (1993), Two nonlinear control schemes contrasted on a hydrodynamiclike model, *Phys Fluids A* **5** 931-947.

Kostelich EJ, Grebogi C, Ott E, and Yorke JA (1993), Higher dimensional targeting, *Phys Rev E* **47** 305-310.

Lüscher E and Hübler A (1989), Resonant stimulation of complex systems, *Helv Phys Acta* **6**, 544-551.

Lima R and Pettini M (1990), Suppression of chaos by resonant parametric perturbations, *Phys Rev A* **41** 726-733.

Nitsche G and Dressler U (1992), Controlling chaotic dynamical systems using time delay coordinates, *Physica D* **58** 153-164.

Ogata K (1990), *Control Engineering*, Prentice Hall, Englewood Cliffs, NJ.

Ott E, Grebogi C, and Yorke JA (1990), Controlling chaos, *Phys Rev Lett* **64** 1196-1199.

Parmananda P, Sherard P, Rollins RW, and Dewald HD (1993), Control of chaos in an electrochemical cell, *Phys Rev E* **47** R3003-R3006.

Pecora LM and Carroll TL (1990), Synchronization in chaotic systems, *Phys Rev Lett* **64** 821-824.

Peng B, Petrov V, and Showalter K (1991), Controlling chemical chaos, *J Phys Chem* **95** 4957-4959.

Petrov V, Gaspar V, Masere J, and Showalter K (1993), Controlling chaos in the Belousov-Zhabotinsky reaction, *Nature* **361** 240-243.

Pyragas K (1992), Continuous control of chaos by self-controlling feedback, *Phys Letter A* **170** 421-428.

Pyragas K,(1993), Predictable chaos in slightly perturbed unpredictable chaotic systems, *Phys Lett A* **181** 203-210.

Pyragas K and Tamasevicius A (1993), Experimental control of chaos by delayed self-controlling feedback, *Phys Lett A* **180** 99-102.

Qu Z, Hu G, and Ma B (1993), Controlling chaos via continuous feedback, *Phys Lett A* **178** 265-270.

Rajasekar S and Lakshmanan M (1993), Algorithmms for controlling chaotic motion: Application for the BVP oscillator, *Physica D* **67** 282-300.

Reyl C, Flepp L, Badii R, and Brun E (1993), Control of NMR-laser chaos in high-dimensional embedding space, *Phys Rev E* **47** 267-272.

Rollins RW, Parmananda P, and Sherard P (1993), Controlling chaos in highly dissipative systems: A Simple recursive algorithm, *Phys Rev E* **47** R780-R783.

Romeiras FJ, Grebogi C, Ott E, and Dayawansa WP (1992), Controlling chaotic dynamical systems, *Physica D* **58** 165-192.

Roy R, Murphy Jr TW, Maier TD, Gills Z, and Hunt ER (1992), Dynamical control of a chaotic laser: Experimental stabilization of a globally coupled system, *Phys Rev Lett* **68** 1259-1262.

Schiff SJ, Jerger K, Duong DH, Chang T, Spano ML, and Ditto WL (1994), Controlling chaos in the brain, *Nature* **370** 615-620.

Sepulchre JA and Babloyantz A (1993), Controlling chaos in a network of oscillators, *Phys Rev E* **48** 945-950.

Shermer R (1992), Control of vortex shedding in a two-dimensional flow past a plate, *Phys Rev A* **46** 7614-7617.

Shinbrot T, Ditto W, Grebogi C, Ott E, Spano M, and Yorke JA (1992), Using the sensitive dependence of chaos (the "Butterfly Effect") to direct trajectories in an experimental chaotic system, *Phys Rev Lett* **68** 2863-2866.

Shinbrot T, Grebogi C, Ott E, and Yorke JA (1993), Using small perturbations to control chaos, *Nature* **363** 411-417.

Shinbrot T, Ott E, Grebogi C, and Yorke JA (1990), Using chaos to direct trajectories to targets, *Phys Rev Lett* **65** 3215-3218.

Singer J, Wang YZ, and Bau HH (1991), Controlling a chaotic system, *Phys Rev Lett* **66** 1123-1125.

Sinha S, Ramaswamy R, and Rao JS (1990), Adaptive control in nonlinear dynamics, *Physica D* **43** 118-128.

Spano ML and Ott E (1995), Controlling chaos, *Physics Today* **48**(6) 34-40.

Starret J and Tagg R (1995), Control of a chaotic parametrically driven pendulum, *Phys Rev Lett* **74** 1974-1977.

Takens F (1981), in *Dynamical Systems and Turbulence*, Rand D and Young LS (eds), Springer, Berlin.

Thompson JMT and Stewart HB (1986), *Nonlinear Dynamics and Chaos*, John Wiley & Sons, Chichester.

__John F Lindner__ received his BS (summa cum laude) in Physics from the University of Vermont in 1982 and his PhD in Physics from the California Institute of Technology in 1988. He has since taught and conducted research at The College of Wooster in Wooster, Ohio. Currently, he is an Associate Professor of Physics at Wooster and an Adjunct Associate Professor of Physics at the Georgia Insititute of Technology in Atlanta. He specializes in computational physics and his research interests in nonlinear dynamics include control of chaos, spatiotemporal chaos, and stochastic resonance.

__William L Ditto__ was born in Anchorage Alaska in 1959. He graduated from the University of California at Los Angeles with a BS in Physics in 1980. In 1988 he received his PhD in Theoretical Physics (Field Theory) from Clemson University.

Ditto subsequently worked for the department of the Navy in Washington DC where he demonstrated the first experimental control of chaos. As a consequence, his work has twice been featured on the cover of Science News, and has been reported in numerous articles in Science, Nature, Scientific American *and* Time *magazine. Ditto's work has led to practical applications of chaos research. He has licensed control of chaos technology to the health care industry with the goal of developing smart heart defibrillators to reduce fatalities in heart attack victims.*

He is also working on control of chaos strategies for the possible control of epilepsy. Ditto recently established the Applied Chaos Laboratory in the School of Physics at the Georgia Institute of Technology, has organized numerous conferences on the applications of chaos and has written many articles on chaos.

PHYSICAL REVIEW E

STATISTICAL PHYSICS, PLASMAS, FLUIDS, AND RELATED INTERDISCIPLINARY TOPICS

THIRD SERIES, VOLUME 51, NUMBER 4 PART A — APRIL 1995

RAPID COMMUNICATIONS

The Rapid Communications section is intended for the accelerated publication of important new results. Since manuscripts submitted to this section are given priority treatment both in the editorial office and in production, authors should explain in their submittal letter why the work justifies this special handling. A Rapid Communication should be no longer than 4 printed pages and must be accompanied by an abstract. Page proofs are sent to authors.

Adaptive control and tracking of chaos in a magnetoelastic ribbon

Visarath In and William L. Ditto
Applied Chaos Laboratory, School of Physics, Georgia Institute of Technology, Atlanta, Georgia 30332

Mark L. Spano
Naval Surface Warfare Center, Silver Spring, Maryland 20903
(Received 30 August 1994)

We have implemented the tracking of unstable orbits using the full control method of Ott, Grebogi, and Yorke (OGY). (Previous implementations have used only limiting cases of the OGY method.) The implementation is achieved in a mechanical system, the magnetoelastic ribbon. In addition, a method is demonstrated whereby the OGY control parameter may be optimized using only experimental data.

PACS number(s): 05.45.+b, 75.80.+q

The control of chaotic systems has generated tremendous interest in the scientific community. Since the pioneering work of Ott, Grebogi, and Yorke [1] demonstrated that chaotic systems could be readily controlled (OGY method), an enormous amount of work has demonstrated that the control of chaos provides a powerful tool for anyone attempting to manipulate chaotic systems (for a review see Refs. [2,3]). Recently adaptive control techniques known as *tracking* have been devised to extend the reach of control of chaos techniques to account for a problem encountered by applied scientists and engineers known as drift or nonstationarity. Schwartz and Triandaf [4] devised an extension to the OGY method which adaptively tracks and maintains control of unstable periodic orbits through large parameter changes. Recent experiments have dramatically demonstrated successful tracking in circuits [5], lasers [6], and, in a remarkable experiment by Petrov and collaborators, in the Belousov-Zhabotinksy (BZ) chemical reaction [7]. The tracking procedure as implemented in electronic circuits by Carroll *et al.* [5] and in multimode lasers by Gills *et al.* [6] is based upon the occasional proportional feedback method (OPF) of chaos control, a limiting case of the OGY method [6]. The implementation of tracking in the BZ reaction [7] is founded on a one-dimensional map-based chaos control algorithm which is a one-dimensional simplification of the OGY algorithm particularly well suited for use in a low-dimensional, highly dissipative chaotic system in combination with Petrov's stability analysis routine.

The main contributions of this paper are the following: (1) experimental demonstration of tracking based on the classic OGY chaos control algorithm; (2) experimental demonstration of tracking in a mechanical system; and (3) an adaptive and very general method of optimizing OGY control that requires very little additional computation and work.

The experimental system consisted of a gravitationally buckled, amorphous magnetoelastic ribbon driven parametrically by a sinusoidally varying magnetic field [8]. The ribbon is clamped at its lower end and its position is measured at a point a short distance above the clamp. The Young's modulus of the ribbon can be varied by more than a factor of 10 by the application of an external magnetic field. We apply an ac magnetic field of amplitude H_{ac} and frequency f added to a dc field of amplitude H_{dc}, such that $H_{applied}(t)=H_{dc}+H_{ac}\sin(2\pi ft)$. In this experiment we choose $f=1.18$ Hz, $H_{ac}=1.05$ Oe and typically H_{dc} is between -1.02 and -1.80 Oe. To implement the OGY control algorithm, we measure the position ξ_j of a point on the ribbon once every driving period. We then construct a delay coordinate embedding by plotting the current position ξ_j vs ξ_{j-d}, where d is the delay.

[1] E. Ott, C. Grebogi, and J. A. Yorke, Phys. Rev. Lett. **64**, 1196 (1990).
[2] T. A. Shinbrot, C. Grebogi, E. Ott, and J. A. Yorke, Nature **363**, 411 (1993).
[3] W. L. Ditto and L. M. Pecora, Sci. Am. **269**, 78 (1993).
[4] I. B. Schwarz and I. Triandaf, Phys. Rev. A **46**, 7439 (1992).
[5] T. L. Carroll, I. Triandaf, I. Schwartz, and L. Pecora, Phys. Rev. A **46**, 6189 (1992).
[6] Z. Gills, C. Iwata, R. Roy, I. B. Schwartz, and I. Triandaf, Phys. Rev. Lett. **69**, 3169 (1992).
[7] V. Petrov, M. J. Crowley, and K. Showalter, Phys. Rev. Lett. **72**, 2955 (1994).
[8] W. L. Ditto, S. Rauseo, R. Cawley, C. Grebogi, G. H. Hsu, E. Kostelich, E. Ott, H. T. Savage, R. Segnan, M. L. Spano, and J. A. Yorke, Phys. Rev. Lett. **63**, 923 (1989).
[9] W. L. Ditto, S. N. Rauseo, and M. L. Spano, Phys. Rev. Lett. **65**, 3211 (1990).
[10] M. L. Spano, W. L. Ditto, and S. N. Rauseo, J. Intell. Mater. Syst. Struct. **2**, 482 (1991).
[11] A. Garfinkel, M. L. Spano, W. L. Ditto, and J. Weiss, Science **257**, 1230 (1992).
[12] S. J. Schiff, K. Jerger, D. H. Duong, T. Chang, M. L. Spano, and W. L. Ditto, Nature **370**, 615 (1994).

Evidence for Determinism in Ventricular Fibrillation

Francis X. Witkowski,[1] Katherine M. Kavanagh,[1] Patricia A. Penkoske,[1] Robert Plonsey,[2] Mark L. Spano,[3]
William L. Ditto,[4] and Daniel T. Kaplan[5]

[1] *University of Alberta, Edmonton, Alberta, Canada T6G 2R7*
[2] *Department of Biomedical Engineering, Duke University, Durham, North Carolina, 27708-0281*
[3] *Naval Surface Warfare Center, Silver Spring, Maryland 20903*
[4] *School of Physics, Georgia Institute of Technology, Atlanta, Georgia, 30332-0430*
[5] *Department of Physiology, McGill University, Montreal, Quebec, Canada H3G 2Y6*

(Received 9 September 1994; revised manuscript received 16 November 1994)

Using a recently formulated technique for *in vivo* cardiac transmembrane current estimation, we examined ventricular fibrillation for evidence of deterministic linear and nonlinear structure. Both unstable fixed point analysis and a newly formulated measure of nonlinear determinism indicated that ventricular fibrillation *in vivo* exhibits deterministic dynamics similar to those previously used in chaos control.

PACS numbers: 87.22.–q, 05.45.+b, 87.45.Bp

Ventricular fibrillation (VF) is a frenzied and irregular heart rhythm disturbance that renders the heart incapable of sustaining life [1]. VF is always fatal within minutes unless externally terminated by the passage of a large electrical current through the heart muscle. The use of "chaos control" techniques to stabilize small patches of heart tissue has been reported [2], and recent theoretical work suggests that similar strategies may be applicable to spatially extended systems such as ventricular fibrillation (VF) in the whole heart [3].

In prior analysis of experimental data VF has often been treated as a random and irregular process. This approach precludes the development of feedback control strategies that would use small stimuli to terminate VF. For this reason, it is important to uncover any deterministic dynamics that underlie VF. Here we report that by using a new technique for measuring cardiac transmembrane current (I_m) *in vivo* [4,5], and by applying recently developed methods for the identification of deterministic structure in time series [6], we have found evidence for deterministic dynamics in VF. The same sort of dynamics has been successfully exploited in the control of physical and biological chaotic systems [2,7–14]. The presence of observably deterministic dynamics from excitable cardiac tissue has been controversial [15–20].

Our experimental preparations consisted of open-chest anesthetized dogs, whose hearts were studied *in vivo* after VF was electrically induced [5]. I_m was measured from ventricular epicardium without cell disruption. Using this experimental technique, we have recently been able to reliably differentiate propagated electrical activation from passive electrotonic alterations [5]. This effectively identifies local electrophysiological events for subsequent analysis. The ratio of the areas derived from

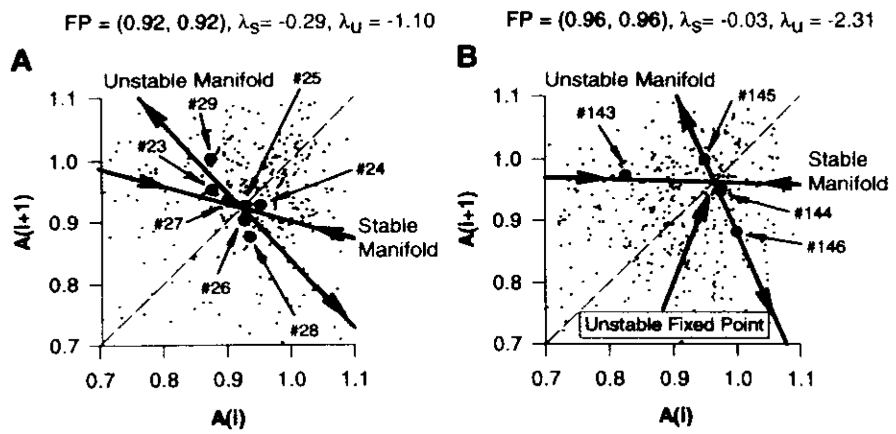

FIG. 1. (a) Return plot of the time series generated by the ratio of negative to positive area $A(i)$ under the transmembrane current for a typical 1 min interval of *in vivo* ventricular fibrillation illustrating the local structure of the chaotic attractor. The range of data displayed was narrowed to more clearly demonstrate the points contributing to the local structure. Note the flip saddle structural appearance for points 23 through 29. Coordinates for the calculated unstable fixed point (FP), stable eigenvalue (λ_s), and unstable eigenvalue (λ_u) for this visitation of the unstable fixed point are provided above the plot. Diagonal dashed line is the line of identity $[A(i+1) = A(i)]$. (b) Another saddle structure [points 143–146] generated by a second representative VF time series with abbreviations as in (a).

 0031-9007/95/75(6)/1230(4)$06.00

the inwardly and outwardly directed I_m, $A(i)$, as well as the deflection-to-deflection interval $D(i)$, was computed for each nonelectrotonic deflection [i.e., $A(i) > 0$] during VF, where $i = 1, 2, \ldots,$ indexes the deflection number. The 30 episodes of VF analyzed provided 17 125 deflections for analysis.

Initial examination for evidence of determinism in these time series involved return plots of $A(i + 1)$ versus $A(i)$ and of similarly plotted interval data during the course of VF (see Fig. 1). The shape of the cloud of points in such a two-dimensional plot does not reveal any simple dependence of $A(i + 1)$ on $A(i)$. However, the sequence of points does suggest the existence of a deterministic mechanism involving an unstable fixed point [2,7–10]. A fixed point may occur only when $A(i + 1) = A(i)$.

A type of unstable fixed point often encountered in chaotic systems is a "saddle." There is a fixed point at the center of the saddle, and stable and unstable manifolds that intersect at the fixed point. In a two-dimensional plot of this kind, the slopes of the stable and unstable manifolds at the fixed point are numerically equal to the eigenvalues of their respective manifolds at the fixed point. If the state of the system, as represented by a point in the $[A(i), A(i + 1)]$ plane, is quite close to the stable manifold but not close to the fixed point, subsequent iterates will first move closer toward the fixed point along the stable manifold and then move away along the unstable manifold as indicated in the sequences shown in Fig. 1. In analyzing experimental data, where the directions or even the existence of the manifolds are not known *a priori*, we invert the above logic and use the presence of such a sequence of points as the initial evidence for the existence of a fixed point and related stable and unstable manifolds.

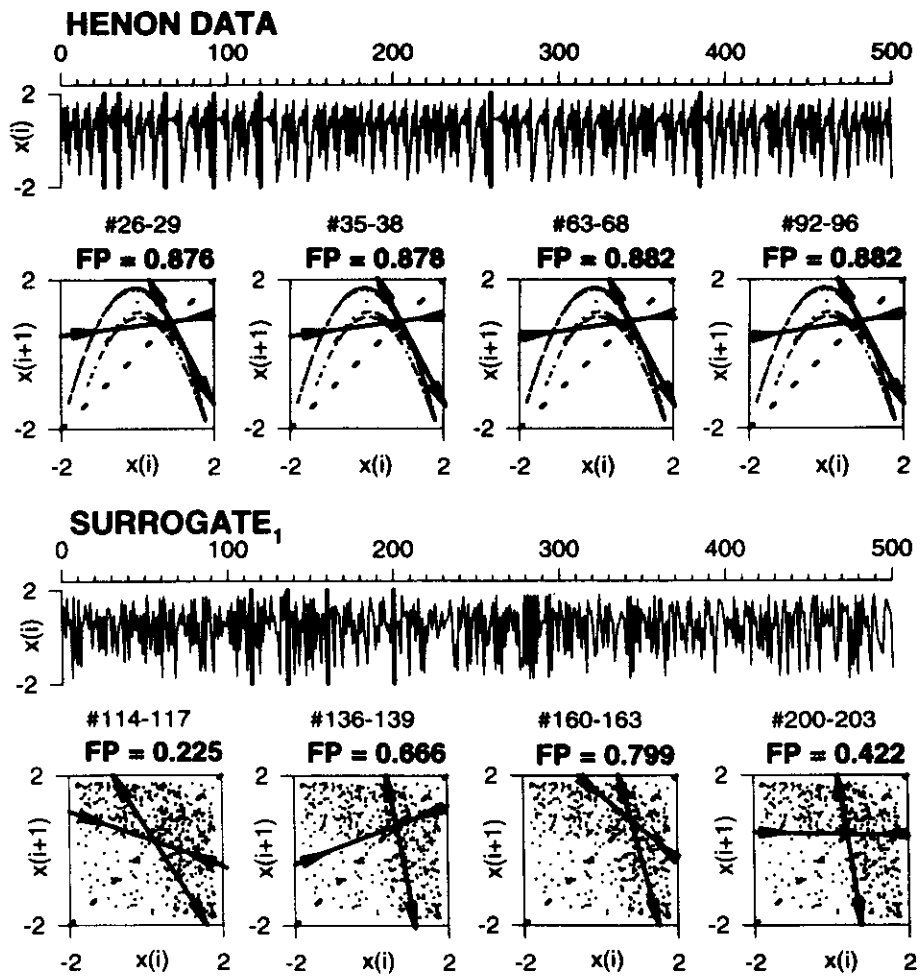

FIG. 2. Time series for the Henon map, $\{x(i + 1) = 1.4 + 0.3y(i) - x(i)^2, y(i + 1) = x(i)\}$, with seven visitations to the fixed point automatically detected by scanning the time series (vertical lines). Return plots for the first four visitations presented below with their respective stable and unstable manifolds. For the Henon map, the unstable fixed point is known to be characterized by fixed point = 0.884, $\lambda_u = -1.924$. From scanning the time series FP = 0.882 ± 0.0002 and $\lambda_u = -1.973 \pm 0.007$. The second time series, labeled Surrogate$_1$, is an example of one of the 10 surrogates formed from the Henon time series. When this surrogate time series is scanned, four putative fixed points are obtained, which demonstrate a marked variation in both fixed point location and architecture. Statistical significance between this Henon time series and the mean of 10 surrogates was found to have a sigma value >50. When varying amounts of white noise were added to the Henon data, the ability to discern a difference between it and its surrogates deteriorated; at 20% added noise the sigmal value = 3.6, and at 25% added noise it was less than 3.

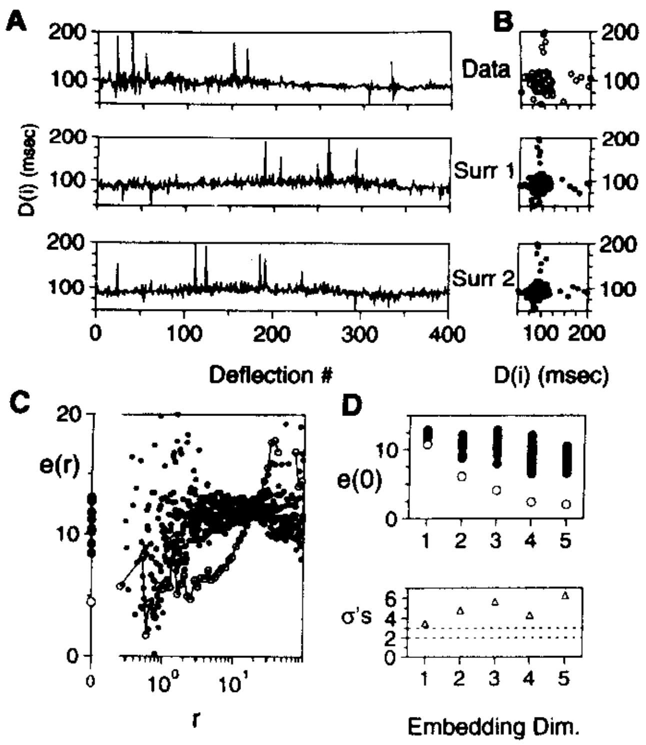

FIG. 4. (a) Interdeflection interval $D(i)$ time series (top frame), and two surrogate data time series with the same histogram and autocorrelation function. (b) The return plot $D(i+1)$ versus $D(i)$ for the time series in (a). (c) e versus r (calculated as previously described [6]) for the $D(i)$ time series (open circles) and 10 surrogate data sets. The considerable spread of the surrogates for small r is due to the short length of the time series. The projection to $e(r = 0)$ is shown on the left-hand axis. An imbedding dimension of 3 is used here. (d) $e(r = 0)$ versus embedding dimension for the $D(i)$ time series (open circles) and the surrogates. The bottom frame shows the deviation of $e(r = 0)$ of the $D(i)$ time series from the mean of $e(r = 0)$ of the surrogates, in terms of the standard deviation of the surrogates. A deviation of >3 standard deviations at embedding dimension 3 was the criterion used for statistical significance.

analyzed the $A(i)$ and $D(i)$ time series using two other nonlinear statistics: mean log prediction error and correlation dimension [21]. Similar overall results were obtained. The increased proportion of positive results when compared to the unstable fixed point analysis most likely reflects the improved noise immunity of the technique. As an example, the evidence for nonlinear determinism was readily detected in the Henon data with additive noise levels of up to 50%, but significance by the unstable fixed point technique could only be demonstrated up to 20% added noise.

The two complementary approaches described above, one of which tests for local determinism and the other for global determinism, clearly indicate that there are strong deterministic components to VF. The deterministic components are similar to those identified in other chaotic systems in which control was possible [2,7–10]. A major point of this study is that VF is perhaps not best understood in terms of the low-dimension versus high-dimension paradigm that has dominated nonlinear dynamics data analysis for the past decade. Instead, we present evidence that VF contains episodes of simple dynamics interwoven with a background of much more complicated dynamics. Although the work here suggests that the dynamics of VF might be amenable to chaotic control techniques, the practical implementation of such control is still highly speculative and will present significant challenges.

We thank K. Jones and S. Stephens for expert technical assistance. The authors gratefully acknowledge support from MRC grants (F. X. W., P. A. P., K. M. K., D. T. K.), Alberta Heritage Foundation for Medical Research grants (F. X. W., K. M. K.), an NIH grant (R. P.), an Office of Naval Research Investigator Award (W. L. D.), and the Physics Division of the Office of Naval Research (M. L. S. and W. L. D.).

[1] M. S. Eisenberg, A. Hallstrom, and L. Bergner, N. Engl. J. Med. **306**, 1340 (1982).
[2] A. Garfinkel, M. L. Spano, W. L. Ditto, and J. N. Weiss, Science **257**, 1230 (1992).
[3] I. Aranson, H. Levine, and L. Tsimring, Phys. Rev. Lett. **72**, 2561 (1994).
[4] F. X. Witkowski, K. M. Kavanagh, P. A. Penkoske, and R. Plonsey, Circ. Res. **72**, 424 (1993).
[5] F. X. Witkowski, R. Plonsey, P. A. Penkoske, and K. M. Kavanagh, Circ. Res. **74**, 507 (1994).
[6] D. T. Kaplan, Physica (Amsterdam) **73D**, 38 (1994).
[7] E. Ott, C. Grebogi, and J. A. Yorke, Phys. Rev. Lett. **64**, 1196 (1990).
[8] W. L. Ditto, S. N. Rauseo, and M. L. Spano, Phys. Rev. Lett. **65**, 3211 (1990).
[9] W. L. Ditto and L. M. Pecora, Sci. Am. **269**, No. 2, 78 (1993).
[10] T. Shinbrot, C. Grebogi, E. Ott, and J. A. Yorke, Nature (London) **363**, 411 (1993).
[11] R. Roy, T. W. Murphy, Jr., T. D. Maier, Z. Gills, and E. R. Hunt, Phys. Rev. Lett. **68**, 1259 (1992).
[12] E. R. Hunt, Phys. Rev. Lett. **67**, 1953 (1991).
[13] V. Petrov, V. Gaspar, J. Masere, and K. Showalter, Nature (London) **361**, 240 (1993).
[14] S. J. Schiff, K. Jerger, D. H. Duong, T. Chang, M. L. Spano, and W. L. Ditto, Nature (London) **370**, 615 (1994).
[15] M. R. Guevara, L. Glass, and A. Schrier, Science **214**, 1350 (1981).
[16] A. L. Goldberger, V. Bhargava, B. J. West, and A. J. Mandell, Physica (Amsterdam) **19D**, 282 (1986).
[17] D. R. Chialvo, R. S. Gilmour, Jr., and J. Jalife, Nature (London) **343**, 653 (1990).
[18] D. T. Kaplan and R. J. Cohen, Circ. Res. **67**, 886 (1990).
[19] F. X. Witkowski and P. A. Penkoske, in *Mathematical Approaches to Cardiac Arrhythmias*, edited by J. Jalife (New York Academy of Sciences, New York, 1990), p. 219.
[20] P. V. Bayly *et al.*, J. Cardiovasc. Electrophys. **4**, 533 (1993).
[21] J. Theiler, S. Eubank, A. Longtin, B. Galdrikian, and J. D. Farmer, Physica (Amsterdam) **58D**, 77 (1992).

CONTROLLING CHAOS

The extreme sensitivity and complex behavior that characterize chaotic systems prohibit long-range prediction of their behavior but paradoxically allow one to control them with tiny perturbations.

Edward Ott and Mark Spano

A violent order is disorder; and
A great disorder is an order. These
Two things are one.
—Wallace Stevens, *Connoisseur of Chaos* (1942)

Scientists in many fields are recognizing that the systems they study often exhibit a type of time evolution known as chaos. Its hallmark is wild, unpredictable behavior, a state often perplexing and unwelcome to those who encounter it. Indeed this highly structured and deterministic phenomenon was in the past frequently mistaken for noise and viewed as something to be avoided in most applications. Recently researchers have realized that chaos can actually be advantageous in many situations and that when it is unavoidably present, it can often be controlled to obtain desired results. In this article, we present some of the basic ideas behind the feedback control of chaos, review a few illustrative experimental results and assess the status and future promise of the field.[1]

Dynamical systems

A dynamical system is one whose evolution is deterministic in the sense that its future motion is determined by its current state and past history. The system may be as simple as a swinging pendulum or as complicated as a turbulent fluid.

Figure 1 shows a simple mechanical system set up at the Naval Surface Warfare Center by William Ditto, now at the Georgia Institute of Technology, and his coworkers. The system consists of a magnetoelastic metal ribbon clamped at its lower end. The Young's modulus of the ribbon can be decreased by more than an order of magnitude by applying a magnetic field parallel to the ribbon, thereby causing it to buckle.[2] This highly nonlinear system is placed in a vertical magnetic field of the form $H(t) = H_{dc} + H_{ac}\cos(2\pi ft)$, where f is on the order of 1 hertz. The position of one point on the ribbon is monitored by an optical sensor located at a spot near the ribbon's base. With appropriate choices of the dc and ac field amplitudes, the temporal motion of this simple system is observed to be chaotic. Here time is a continuous variable t. In other dynamical systems time can be a discrete integer-valued variable n. A continuous-time dynamical system like the ribbon can be represented by ordinary differential equations.

An example of a discrete-time dynamical system is a d-dimensional map,

$$\mathbf{y}_{n+1} = \mathbf{G}(\mathbf{y}_n) \tag{1}$$

where $\mathbf{y}$ is d-dimensional. Given an initial condition $\mathbf{y}_0$ at time $n = 0$, the system state at time $n = 1$ is $\mathbf{y}_1 = \mathbf{G}(\mathbf{y}_0)$; at time $n = 2$, it is $\mathbf{y}_2 = \mathbf{G}(\mathbf{y}_1)$; and so on.

Physicists are used to dealing with continuous-time systems. Newton's equations of motion, Maxwell's equations and Schrödinger's equation are all formulated in continuous time. However, continuous-time dynamical systems can often profitably be reduced to discrete-time systems.

For example, assume that we sample the state of the periodically driven magnetoelastic ribbon (figure 1) once every drive period—at the times $t = T, 2T, 3T, \ldots, nT$, where $T=1/f$. Then $\mathbf{y}_n$ denotes the system state at time nT. Because the system is deterministic, the state at time $(n + 1)T$ is uniquely determined by the state at time nT. That is, an equation of the form of equation 1 holds. It turns out to be quite easy to do this sampling for driven experimental systems by strobing the experimental data acquisition at the drive frequency.

In experiments it is sometimes difficult to measure the full state vector of the system. As an extreme example, assume that one can measure only a single scalar function of the system state. In this case, it has been shown that a delay coordinate embedding provides a useful representation of the system state.[3] For example, for a discrete-time system, if the observed scalar is w_n, then the delay coordinate vector $\mathbf{W}_n$ replaces the vector $\mathbf{y}_n$ from equation 1, where

$$\mathbf{W}_n=[w_n, w_{n-1}, w_{n-2}, \ldots, w_{n-(q-1)}] \tag{2}$$

The number of delays q should be large enough to reproduce the dynamics of the system. Essentially the information contained in a measurement of all of a system's variables at a single time is reconstructed from measurements of a single variable at q different times.

A common feature of (non-Hamiltonian) dynamical systems is the presence of "attractors." If typical initial conditions located in some region of phase space (or a

EDWARD OTT is a professor of physics and of electrical engineering and a member of the Institute for Plasma Research and the Institute for Systems Research at the University of Maryland, College Park. MARK SPANO is a senior research physicist at the Naval Surface Warfare Center, in Silver Spring, Maryland, and a visiting scholar at the Applied Chaos Laboratory of the Georgia Institute of Technology, in Atlanta.

MAGNETOELASTIC RIBBON that undergoes chaotic motion. The 10-cm-long metallic glass ribbon changes its Young's modulus by more than an order of magnitude in response to an applied magnetic field. The related change in its stiffness causes it to buckle under the force of gravity. An optical sensor measures its position at a single point near its base once each drive period. **FIGURE 1**

delay coordinate embedding) approach a set of values asymptotically with time, we call that set the attractor. A chaotic attractor is a geometric object that is neither pointlike nor space filling. Chaotic attractors typically have fractal (noninteger) dimensions and so are often called strange attractors. Figure 2b shows a chaotic attractor (gray) from the magnetoelastic ribbon experiment pictured in figure 1. All initial conditions eventually evolve into motion confined to this set of points.

Once on the attractor, the system state bounces around it ergodically. That is, the state eventually comes arbitrarily close to any point on the attracting set. Even when the actual state space dimension, (the dimensionality of $\mathbf{y}$ in equation 1) is large (or, as in the case of a spatially continuous system like the ribbon, infinite), the fractal dimension of the strange attractor is often fairly low (between 1 and 2 for the ribbon attractor in figure 2b). For the most part, chaos control techniques have been formulated and implemented for low-dimensional strange attractors (attractor dimensions less than four or five), and we will limit our discussion to this situation.

Sensitivity and orbit complexity

The two most common ways of characterizing chaos are exponential sensitivity and orbit complexity. These are not independent properties, but rather two sides of the same chaos coin. Either may be viewed as a way of defining chaos.

Exponential sensitivity refers to the fact that if we consider two chaotic orbits initially displaced only slightly from each other, then the displacement between the two orbits grows exponentially with time. What might have been a very tiny separation between the orbits eventually becomes a large displacement (on the order of the attractor size). Thus small errors eventually defeat any attempt to predict the exact longtime evolution of a chaotic system.

Orbit complexity means that many different kinds of motion are possible on a chaotic attractor. One manifestation of this is that chaotic attractors typically have embedded within them an infinity of unstable periodic orbits. By a periodic orbit we mean an orbit that repeats itself after some characteristic time. The colored regions in figure 2b mark the location of periodic orbits on the attractor. In particular, an initial condition $\mathbf{y}_0$ in the center of the green dots maps to a $\mathbf{y}_1$ located at the same point, $\mathbf{y}_1 = \mathbf{y}_0$, which maps to a $\mathbf{y}_2$ also at the same point, $\mathbf{y}_2 = \mathbf{y}_0$; this point is a period-one orbit. An initial condition in the center of one of the red regions maps to the center of the other red region and then back to the original red region; the orbit cycles repeatedly between the two red regions, which makes it a period-two orbit. The four blue regions in figure 2b show the location of a period-four orbit.

The periodic orbits embedded in a chaotic attractor are all unstable in that if one displaces the system state slightly from a periodic orbit, this displacement grows exponentially in time. Thus periodic orbits are typically presence of chaos can be an advantage. Any one of a number of different orbits can be stabilized, and one can select the orbit that gives the best system performance. Thus we have the flexibility of easily switching the system behavior by controlling a different periodic orbit. On the other hand, if the attractor is not chaotic but is, say, periodic, then small perturbations typically can change the orbit only slightly. We are stuck with whatever system performance the stable periodic orbit gives, and we have no option for substantial improvement, short of making large alterations in the system.

To be concrete, one might wish to build chaos into a system for the same reason that the newer "fly-by-wire" fighter planes are designed to be unstable: The built-in instability gives the planes more maneuverability and lets them respond quickly to the pilot's commands. In a similar fashion, building chaos into a system might provide it with more flexibility than would otherwise be possible.

Methods for controlling chaos

There are various methods by which one may control a chaotic system. One such method is based on the fact that the points on the attractor do not bounce around randomly, but instead approach and depart from the vicinity of unstable periodic orbits in a highly structured fashion. In a region near each periodic orbit, the system state point tends to move toward the periodic orbit from certain positions (stable manifolds) and to move away from the periodic orbit from other positions (unstable manifolds). The exponentially increasing speed with which the state point moves in each direction is governed by the stable and unstable eigenvalues, respectively.

For simplicity, consider a two-dimensional map that has one stable direction (implying an eigenvalue with magnitude less than unity) and one unstable direction (with eigenvalue greater than unity). This situation is analogous to a ball rolling under the influence of gravity on a saddle-shaped surface. Chaos control reduces to finding a way to move this saddle so that the ball remains balanced on the saddle's (unstable) equilibrium point.

The procedure goes as follows (see figure 3): When a point begins to move away from the desired periodic orbit (the saddle's equilibrium point) along the unstable manifold, we shift the saddle slightly (by perturbing some system parameter) so that the point now lies on the stable manifold. The natural motion of the system will now tend to move it toward the unstable periodic point rather than away from it. In a perfect world we could turn off the perturbation when the system arrives at the desired periodic orbit. But small errors in our control calculations and the noise inherent in any experimental system will tend to knock the system off this desired orbit again, so we will repeat the previous step as needed to keep the system under control.

An important point to remember is that this procedure does not require a model of the system. All that is needed is to determine experimentally the local geometry around the chosen unstable periodic point: the position of the saddle, the stable and unstable directions, the steepness of these directions (that is, the stable and unstable eigenvalues) and, finally, the shift in the position of the saddle with a small change in some system parameter. As has

CHAOS CONTROL VS. CHAOS MAINTENANCE

illiam Ditto of the Georgia Institute of Technology, Steven Schiff of Children's Hospital in Washington, DC, and I recently conducted experiments on the hippocampus of the temporal lobe of the rat brain.[16] When bathed in artificial cerebrospinal fluid containing high levels of potassium, the brain exhibited spontaneous bursts of synchronized neuronal activity in a portion of the hippocampus designated CA3. These bursts can trigger seizure-like discharges in a nearby region, CA1. As in the heart experiments, we measured and plotted the interburst intervals as an embedding. Employing the same techniques as in the heart experiment, control was achieved. (See figure below.)

The relevance of these experiments to such brain-seizure disorders as epilepsy is not clear. It may be that controlling these bursts to make them more periodic may actually increase the seizure activity. As an alternative, we implemented a new technique for the maintenance of chaos in this system. Sometimes dubbed "anti-control," this technique is actually a form of control that keeps the system away from low-period orbits. The figure shows a crude application for the neural system. Much improved versions have been studied computationally by Weiming Yang and his coworkers at Florida Atlantic University and the University of Maryland and implemented experimentally by Visarath In and his coworkers at Georgia Tech.[17]

MARK SPANO

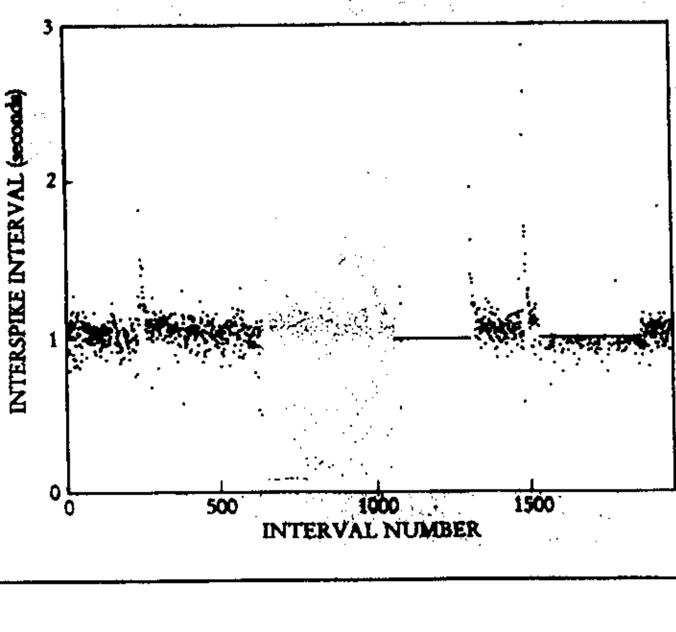

DATA FROM A RAT BRAIN hippocampus during exposure to high levels of potassium. The data in red indicate chaotic interludes; green and blue indicate double-pulse control and single-pulse control, respectively. Also shown (in pink) is a related method known variously as "anti-control" or the "maintenance of chaos."

DIODE RESONATOR DATA. The system consists of two coupled diode resonators, each a series combination of an inductor and a p–n junction diode. It is driven sinusoidally at 50–100 kHz. **a:** Poincaré section formed by sampling the currents through the two branches each drive cycle. **b:** Stabilized period-62 orbit. Only half of the attractor is shown. (Courtesy of Earle Hunt, Ohio University.) **FIGURE 4**

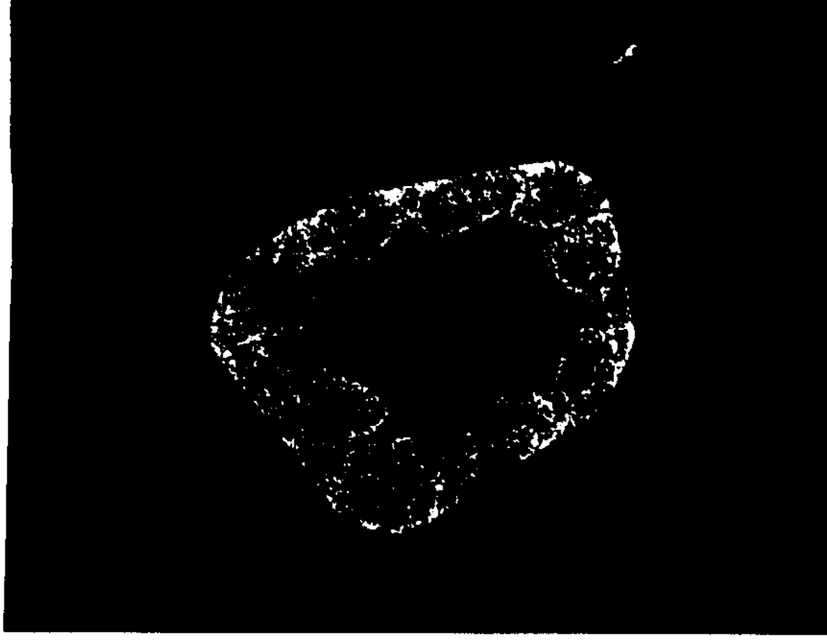

a

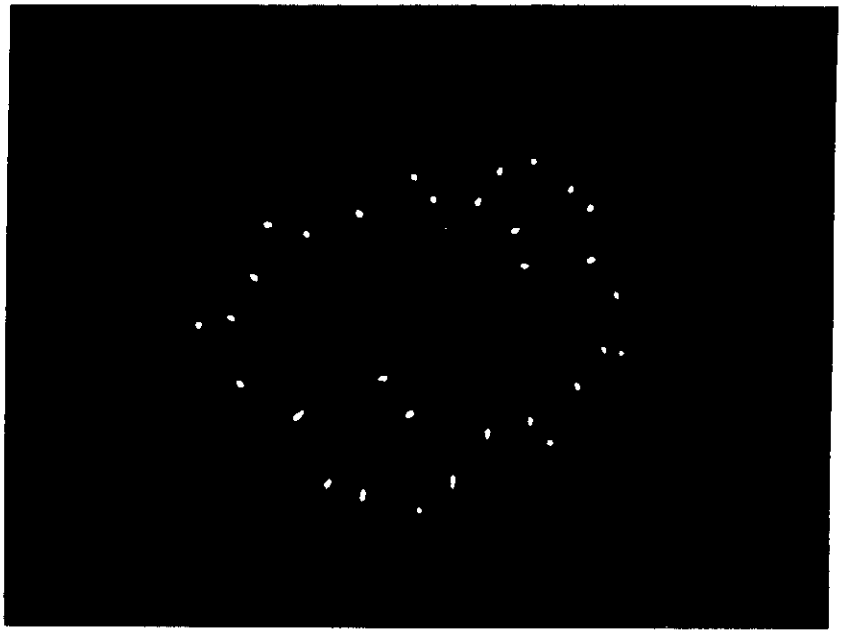

b

approach, based on the work of Ute Dressler and Gregor Nitsche of the Daimler-Benz Research Institute in Germany,[4] uses a recursive method to make available a wider choice of system parameters for control.

Heart tissue. An experiment on an *in vitro* rabbit heart septum used the drug ouabain to induce arrhythmias in the autonomous beating of the heart tissue.[8] A discrete-time embedding was constructed using the intervals between heartbeats as the system variable of interest. For this induced arrhythmia, the presence of deterministic chaos was confirmed by the observation of repeated approaches of the system state to a period-one orbit, with each approach along the same stable direction and with corresponding departures along the same unstable direction. In this case, however, it was not possible to find a system parameter that would move the system state point onto the stable manifold. But it *was* possible to intervene directly in the system by injecting a premature heartbeat at an interval timed to place the system state point onto the stable manifold. The dynamics of the system then naturally tended to carry it toward the (unstable) period-one motion. However, because it was possible only to shorten the interbeat interval and not to lengthen it, the control achieved was, at best, period three. Further control experiments are studying an artificially perfused canine heart undergoing ventricular fibrillation.[9]

New directions

The arena of chaos control is growing at an accelerating pace. Here we present some new directions; one of the more exciting and controversial results appears in the box on page 37.

Communications. In work by Scott Hayes and his coworkers at the Army Research Laboratory, a chaotically behaving oscillator is manipulated by a small control so that the oscillator output can carry information. As an example, they controlled a signal from an oscillator whose free-running state is a sequence of positive and negative peaks. Taking these peaks to represent the binary digits 1 and 0, respectively, they used the controlled signal to encode information.[10] The same idea should be applicable to other kinds of signal sources, such as a chaotic laser.

Tracking. One situation often encountered in experiments is that the system undergoes some slow change with time (sometimes called "drift"), either intentionally or unintentionally. Once chaos control has been established, an important concern is whether it will be possible to maintain control despite this drift. Recent methods developed by Ira Schwartz and his coworkers at the Naval Research Laboratory accommodate such slow changes by tracking the location of the controlled unstable orbit as well as its stability properties.[11]

This tracking technique has been used by Tom Carroll and his coworkers (also of the Naval Research Lab) in an electronic circuit, by Zelda Gills and her coworkers at Georgia Tech in a multimode laser system, by Valery Petrov and his coworkers at West Virginia University in the B–Z reaction and by Visarath In and his coworkers at Georgia Tech in the magnetoelastic ribbon.[12]

Targeting. As we saw in the ribbon experiment, it might take an unacceptably long time for the ergodically wandering, uncontrolled system to come close enough to the desired orbit to be captured by a small control. Given an initial condition A and a small target region B, how can we apply small controlling perturbations in such a

nature

INTERNATIONAL WEEKLY JOURNAL OF SCIENCE

Volume 378 No. 6556 30 November 1995 $10.00

Taming chaos

CLIP clamped on MHC class II

How we remember images

A cool brown dwarf

DNA sequencing
PRODUCT REVIEW

Taming spatiotemporal chaos with disorder

Y. Braiman*†, John F. Lindner*‡ & William L. Ditto*

* Applied Chaos Laboratory, School of Physics, Georgia Institute of Technology, Atlanta, Georgia 30332, USA
‡ The College of Wooster, Wooster, Ohio 44691, USA

DISORDER and noise in physical systems usually tend to destroy spatial and temporal regularity, but recent research into nonlinear systems provides intriguing counter-examples. In the phenomenon of stochastic resonance[1], for example, the presence of noise improves the ability of some nonlinear systems to transfer information reliably. Noise can also remove chaos in a model oscillator[2], and facilitate synchronization in an extended array of bistable elements[3]. Here we explore the use of disorder as a means to control spatiotemporal chaos[4-8] in coupled arrays of forced, damped, nonlinear oscillators. Chaotic behaviour in spatially extended systems, especially in biology and physiology[9,10], might be amenable to control, as occurs in low-dimensional temporally chaotic systems[11,12]. In our numerical experiments, one- and two-dimensional arrays of identical oscillators behave chaotically, but the introduction of slight, uncorrelated differences between the oscillators induces ordered motion characterized by complex but regular spatiotemporal patterns.

If our oscillators are identical, then our arrays are chaotic. (Nearby trajectories in the phase space of the array diverge exponentially, as measured by a positive Lyapunov exponent). Making the oscillators non-identical by introducing disorder into a parameter that characterizes their behaviour, removes the chaos and freezes-in complex spatiotemporal patterns by frequency-locking the motion to harmonics and subharmonics of the forcing. (Frequency-locking is distinct from phase-locking: the former tames chaos whereas the latter need not, as a synchronized array may be chaotic.) This phenomenon appears robust with respect to both the parameter range and the size and realization of the disorder. In fact, when we numerically calculate the leading Lyapunov exponent of the array as a function of the size of the disorder, we find large regions in parameter space where disorder leads to complete frequency-synchronization of the array. Moreover, we have observed this effect in multiple systems.

To demonstrate the phenomenon clearly, we first suggest an intentionally simple example. We consider a one-dimensional array (or chain) of forced, damped, nonlinear pendula governed by the equation

$$ml_n^2\ddot{\theta}_n + \gamma\dot{\theta}_n = -mgl_n \sin\theta_n + \tau' + \tau\sin\omega t$$
$$+ \kappa(\theta_{n+1} - \theta_n) + \kappa(\theta_{n-1} - \theta_n)$$

where $n = 1, 2, \ldots, N$, and where the ends are free ($\theta_0 = \theta_1$ and $\theta_N = \theta_{N+1}$). For simplicity, we take the acceleration due to gravity $g = 1.0$ and the mass of the pendulum bob $m = 1.0$. Other parameters are damping $\gamma = 0.75$, length $l_n = 1.0$, d.c. torque $\tau' = 0.7155$, a.c. torque $\tau = 0.4$, angular frequency $\omega = 0.25$, coupling $\kappa = 0.5$. We numerically integrate the equations of motion using a fourth-order Runge Kutta technique with a time step $dt = T/2{,}500$, where $T = 2\pi/\omega$.

Each isolated (uncoupled) pendulum operates in a region of parameter space consisting of a region of chaotic orbits separating regions of qualitatively distinct periodic orbits. The default length $l = 1.0$ results in chaotic motion, characterized by a posi-

† Present address: School of Physics, Emory University, Atlanta, Georgia 30322, USA.

tive Lyapunov exponent. Shortening the pendulum results in an overturning motion, a 'rotation', wherein the applied a.c. and d.c. torques combine to rotate the pendulum 360° over the top. Lengthening the pendulum results in a non-overturning motion, a 'libration', wherein the applied torques are insufficient to fully overcome the pendulum's increased rotational inertia.

Figure 1 depicts the continuous spatiotemporal evolution of arrays of $N=128$ pendula. Time increases from left to right. The colours code the angular velocities of the pendula; red indicates negative velocities and blue positive velocities; the saturation of the colours decreases to zero (white) as the angular speed decreases to zero. Thus narrow bands of red and blue lines represent sudden rapid motion of the arrays. Figure 1*a* depicts an example of the evolution of a homogeneous array. The predominance of blue over red is a consequence of the d.c. term in the torque. The evolution not only appears disordered but is in fact chaotic: the system is characterized by a positive leading Lyapunov exponent. The subsequent panels depict what happens when the array is disordered by uniformly varying the lengths of the pendula.

Figure 1*b* depicts one example of introducing a uniform and symmetric disorder of ±20% so that the pendula lengths are uniformly distributed in the interval [0.8, 1.2]. After a short transient (not shown), a relatively simple but non-trivial pattern, periodic in space and time, emerges. This pattern repeats every two forcing periods, as indicated by the horizontal black bar. Figure 1*c* depicts a second example of ±20% disorder. Operating on a different random realization of lengths, and beginning with a different set of random initial conditions, the array self-organizes a more complex spatiotemporal pattern, one that repeats every 20 forcing periods. Finally, Fig. 1*d* depicts an example of introducing a uniform and symmetric disorder of ±10% so that the pendula lengths are uniformly distributed in the interval [0.9, 1.1]. This trial resulted in an especially complex pattern. Although the bottom edge of the array repeats every forcing period, other segments repeat every three, four, six and twelve forcing periods, so that the entire array repeats every 24 periods. Through repeated trials we can thus obtain a rich variety of periodic spatiotemporal patterns.

If we disorder the pendula asymmetrically, by either shortening all of them or lengthening all of them, then either rotation or libration dominates the motion. If the lengths are decreased, a fraction of the pendula rotate easily and these quickly entrain the others until the entire array is rotating end-over-end in unison. If the lengths are increased, a fraction of the pendula only librate and these quickly inhibit the others from rotating.

We have obtained similar results in higher dimensions. Figure 2 illustrates a two-dimensional example of a square array of 128 × 128 pendula. Here each pendulum is coupled to its four nearest neighbours. We represent the angular velocities of the square array once for each forcing period. Introducing ±20% spread in the pendula lengths converts the chaotic motion of the homogeneous array (forcing periods 17-24) into the complex periodic motion of the inhomogeneous array (forcing periods 91-98). Large areas of the array repeat after two forcing periods, whereas some small regions repeat after three or four forcing periods.

We have observed similar phenomena in other extended systems. For example, in numerical experiments (Y.B., J.F.L. and W.L.D., manuscript in preparation), we have used nonuniform realizations of disorder to convert the chaotic motion of a homogeneous array of forced damped Duffing oscillators, described by $\ddot{x}_n + \gamma\dot{x}_n = kx - k'x^3 + A\sin\omega t + \kappa(x_{n+1} - x_n) + \kappa(x_{n-1} - x_n)$, into the periodic motion of the corresponding inhomogeneous array. In one example the oscillators of the homogeneous but chaotic array freely explore both wells of the Duffing double-well potential. However, introducing the appropriate inhomogeneity localizes all the oscillators in a single well, thereby regularizing the motion.

We should like to distinguish two elementary mechanisms by which disorder may stabilize a chaotic system. One mechanism requires small but non-zero disorder, whereas the other may involve arbitrarily large disorder. We have observed both these mechanisms at work in the pendulum array and Duffing array in different parameter regimes. (In fact we believe that both mechanisms are involved in the formation of the patterns in Figs 1 and 2). The first mechanism can be best understood by considering the topology of a system's dynamical attractors. An extended system occupies a large many-dimensional parameter space, including all the parameters of the individual components of the system. If the system is dissipative, every neighbourhood in parameter space is typically associated with very many dynamical attractors. Disordering the system by changing its parameters moves it in parameter space and consequently transforms its attractors. Often even a small amount of disorder can shift the dynamics from a chaotic attractor to a nearby periodic attractor. (This topological feature of attractors is often exploited in the control of chaos.) The disorder needed to stabilize a chaotic array depends on both the distance and the direction in parameter space to the nearest periodic attractor. These are controlled by the magnitude and the distribution of the disorder. In our pendulum array, two simple but qualitatively distinct periodic motions, namely synchronized libration and synchronized rotation (both following the external a.c. drive), exist nearby in parameter space and can be reached by lengthening or shortening all the pendula. Many complex nonchaotic motions (attractors), like the ones depicted in Fig. 1 also exist nearby in parameter space and these can be reached by shortening some pendula and lengthening others. For this mechanism to work, it is not essential to remove some or all of the pendula from their chaotic regimes. Indeed, we have succeeded in stabilizing

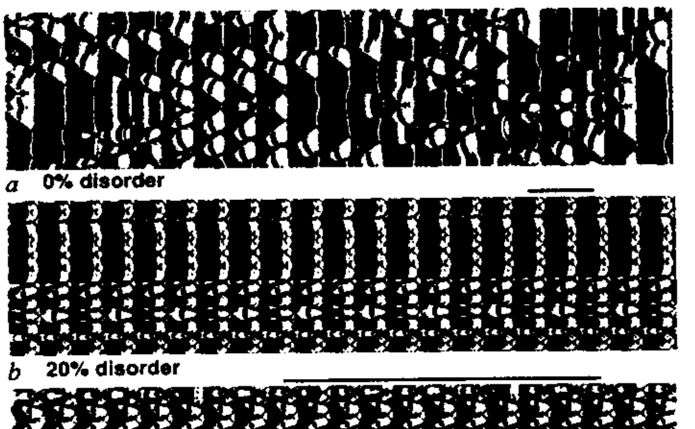

FIG. 1 Spatiotemporal evolution of chains of $N=128$ coupled pendula. Time increases continuously from left to right. The colours code angular velocities; blue indicates positive velocity and red negative velocities. Horizontal black bars indicate the length (*a*, *b*) or half length (*c*, *d*) of periodic spatiotemporal patterns. Parameters are: $\gamma=0.75$, $\tau'=0.7155$, $\tau=0.4$, $\omega=0.25$, $T=25.13$, $\kappa=0.5$.

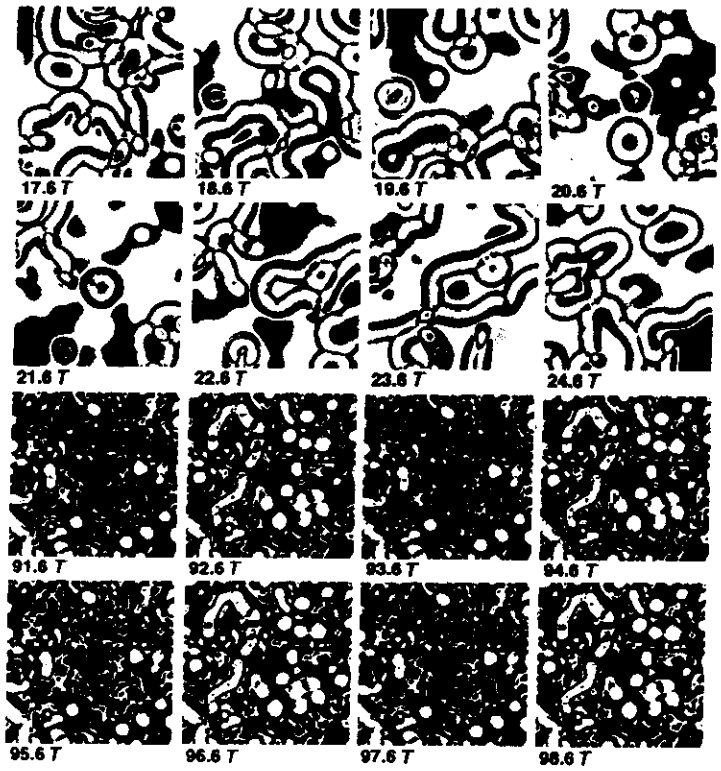

FIG. 2 Spatiotemporal evolution of a grid of $N = 128 \times 128$ coupled pendula. The time evolution is 'strobed' once each forcing period T. Disordering the grid converts chaotic motion (top) into periodic motion (bottom). The colours and parameters are the same as in Fig. 1.

an array while keeping all the pendula in their chaotic regimes. We obtained this result by creating a simple example of nine different pendula each of which is chaotic when uncoupled but all of which form a periodic array when coupled.

The second simple mechanism by which disorder may stabilize a chaotic array can involve arbitrarily large perturbations. Disorder can be used to remove some of the oscillators of an array from their chaotic band, thereby creating distinctly different populations of oscillators. The periodic population can lock the remaining chaotic population to the external a.c. drive, thereby creating periodic solutions to the equations of motion. (To demonstrate the possibility that coupling stable and unstable maps can yield a stable solution one can analyse the simple linear map $x_n^{t+1} = \mu_n x_n^t + \kappa(x_{n+1}^t - x_n^t) + \kappa(x_{n-1}^t - x_n^t)$. The uncoupled maps $\mu_n = 0$ have fixed points $x_n = 0$ that are stable if $\mu_n < 1$ and unstable if $\mu_n > 1$. The coupled maps have a stable fixed point $\mu_n = 0$ even when some $\mu_n > 1$.) This second mechanism does not restrict the size of the disorder. Indeed, we found an example, in a different pendulum array, in which 75% uniform disorder optimizes spatiotemporal order by minimizing the leading Lyapunov exponent.

Disorder can tame chaos and foster periodic patterns. We hope that this work will stimulate further study into the regularizing and pattern-forming potential of disorder in extended systems. This phenomenon is possible in situations where arrays of nonlinear elements have a natural or unavoidable spread of features. Our results suggest that the role of disorder in spatially extended systems may be less of a randomizing influence than an intrinsic mechanism of pattern formation, self organization and control. □

Received 22 June; accepted 25 October 1995.

1. Wiesenfeld, K. & Moss, F. *Nature* **373**, 33–36 (1995).
2. Lindner, J. F., Meadows, B. K., Ditto, W. L., Inchiosa, M. E. & Bulsara, A. R. *Phys. Rev. Lett.* **75**, 3–6 (1995).
3. Rajasekar, S. & Lakshmanan, M. *Physica* D**67**, 282–300 (1993).
4. Sepulchre, J. A. & Babloyantz, A. *Phys. Rev.* E**48**, 945–950 (1993).
5. Gang, H. & Kaifen, H. *Phys. Rev. Lett.* **71**, 3794–3797 (1993).
6. Auerbach, D. *Phys. Rev. Lett.* **72**, 1184–1187 (1994).
7. Aranson, I., Levine, H. & Tsimring, L. *Phys. Rev. Lett.* **72**, 2561–2564 (1994).
8. Johnson, G. A., Löcher, M. & Hunt, E. R. *Phys. Rev.* E**51**, R1625–R1628 (1995).
9. Garfinkel, A., Spano, M. L., Ditto, W. L. & Weiss, J. N. *Science* **257**, 1230–1235 (1992).
10. Schiff, S. J., Jerger, K., Duong, D. H., Chang, T., Spano, M. L. & Ditto, W. L. *Nature* **370**, 615–620 (1994).
11. Shinbrot, T. A., Grebogi, C., Ott, E. & Yorke, J. A. *Nature* **363**, 411–417 (1993).
12. Ditto, W. L. & Pecora, L. M. *Scient. Am.* **269** (2), 78–84 (1993).

ACKNOWLEDGEMENTS. We thank K. Wiesenfeld for helpful discussions. J.F.L. thanks The College of Wooster for making possible his sabbatical at Georgia Tech.

Controlling chaos in the brain

Steven J. Schiff, Kristin Jerger, Duc H. Duong, Taeun Chang,
Mark L. Spano & William L. Ditto

Reprinted from Nature, Vol. 370, August 25, 1994 'ssue

Controlling chaos in the brain

Steven J. Schiff*, Kristin Jerger*, Duc H. Duong*, Taeun Chang*, Mark L. Spano† & William L. Ditto‡

* Department of Neurosurgery, Children's National Medical Center and The George Washington University School of Medicine, Washington DC 20010, USA
† Naval Surface Warfare Center, White Oak Laboratory, Silver Spring, Maryland 20903, USA
‡ School of Physics, Georgia Institute of Technology, Atlanta, Georgia 30332, USA

In a spontaneously bursting neuronal network *in vitro*, chaos can be demonstrated by the presence of unstable fixed-point behaviour. Chaos control techniques can increase the periodicity of such neuronal population bursting behaviour. Periodic pacing is also effective in entraining such systems, although in a qualitatively different fashion. Using a strategy of anticontrol such systems can be made less periodic. These techniques may be applicable to *in vivo* epileptic foci.

FOLLOWING the recent theoretical prediction that chaotic physical systems might be controllable with small perturbations[1,2], there has been rapid and successful application of this technique to mechanical systems[3], electrical circuits[4], lasers[5] and chemical reactions[6,7]. Following the demonstration of the control of chaos in arrhythmic cardiac tissue[8], there are no longer any technical barriers to applying these techniques to neural tissue.

One of the hallmarks of the human epileptic brain during periods of time in between seizures is the presence of brief bursts of focal neuronal activity known as interictal spikes. Often such spikes emanate from the same region of brain from which the seizures are generated but the relationship between the spike patterns and seizure onsets remains unclear[9,10]. Several types of *in vitro* brain slice preparations, usually after exposure to convulsant drugs that reduce neuronal inhibition, exhibit population burst-firing activity that in many ways seems analogous to the interictal spike[11]. One of these preparations is the high potassium concentration ($[K^+]$) model, where slices from the hippocampus of the temporal lobe of the rat brain (a frequent site of epileptogenesis in the human) are exposed to artificial cerebrospinal fluid containing 6.5–10 mM $[K^+]$[12]. After exposure to high $[K^+]$, spontaneous bursts of synchronized neuronal activity originate in a region known as the third part of the cornu ammonis or CA3 (ref. 13). Impulses from the CA3 bursts are propagated through a recurrent collateral fibre tract (the Schaffer collateral fibres) from CA3 to CA1, where electrographic seizure-like discharges can frequently be observed[14]. A detailed computer model of the high $[K^+]$ burst discharges in CA3 successfully replicates many of the experimental findings[15] (reviewed in ref. 16). Although it is difficult to identify determinism in long time series of such bursting activity using nonlinear prediction techniques, some evidence of determinism was recently identified[17,18]. We sought to determine whether such neuronal bursting activity was amenable to control.

There have been substantial efforts to influence neuronal activity with electric fields and currents. Regarding the *in vitro* hippocampal slice, brief direct current (d.c.) currents from nonpolarizable electrodes in the perfusion bath can influence the evoked excitability of pyramidal cells in normal $[K^+]$ when the electric fields are suitably oriented[19]. Apparently similar effects can be achieved with brief currents from monopolar polarizable microelectrodes placed directly into the tissue[20,21]. To our knowledge the use of electrical stimulation to entrain spontaneous burst discharges from CA3 in high $[K^+]$ has not been attempted, whether indirectly with electric fields or with direct stimulation of the nerve cells themselves. Direct stimulation can be accomplished for CA3 neurons by stimulating the Mossy fibre neurons that synapse on the CA3 pyramidal cells (orthodromic stimulation) or by stimulating branches of the CA3 pyramidal cell axons (Schaffer collateral fibres) and allowing the action potentials to propagate into the pyramidal cells in a retrograde fashion (antidromic stimulation).

With the observation that it was feasible to entrain burst discharges from CA3 with both orthodromic and antidromic stimulation (K.J. and S.J.S., manuscript in preparation), we were in a position to ask the following questions: (1) is there evidence for deterministic chaotic behaviour in this preparation; and (2) could such activity be controlled?

If one observes the timing of events from a chaotic physical system, those events are aperiodic. The timing of events evolves from one unstable periodicity to another. Furthermore the approach to these unstable periodicities shows recurring patterns

a

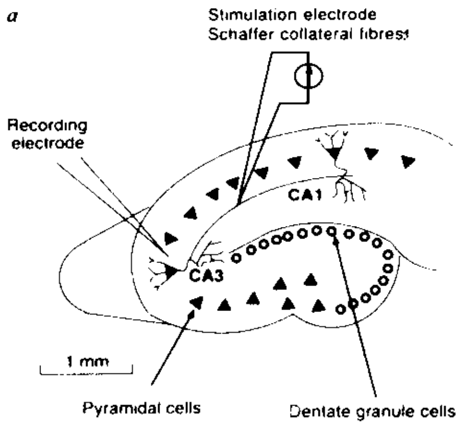

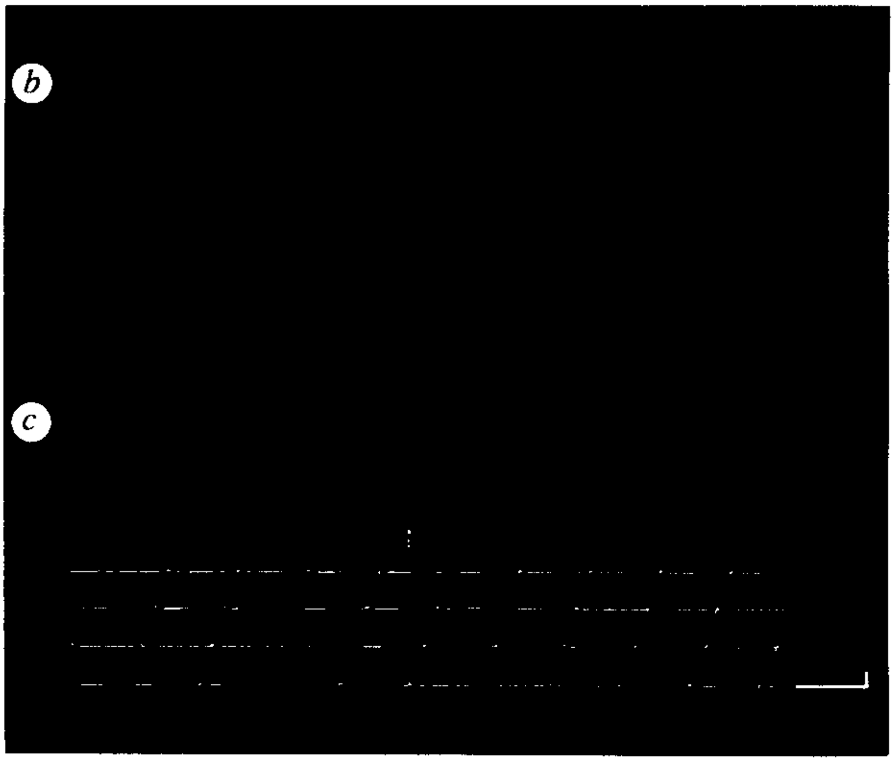

FIG. 1 *a*, Schematic diagram of the transverse hippocampal slice, and arrangement of recording electrodes. Female Sprague–Dawley rats weighing 125–150 g were anaesthetized with diethyl-ether and decapitated. Transverse slices 400 μm thick were prepared from the hippocampus with a tissue chopper and placed in an interface-type perfusion chamber at 32–35 °C. Slices were perfused with artificial cerebrospinal fluid (ACSF) flowing at 2 ml min^{-1} and composed of 155 mM Na^+, 136 mM Cl^-, 3.5 mM K^+, 1.2 mM Ca^{2+}, 1.2 mM Mg^{2+}, 1.25 mM PO_4^{2-}, 24 mM HCO_3^-, 1.2 mM SO_4^{2-}, and 10 mM dextrose. After 90 min of incubation, slices were tested for viability by recording a greater than 2 mV unitary population spike in the stratum pyramidale of CA1, in response to stimulation of Schaffer collateral fibres in the stratum radiatum with 100 μs constant current 50–150 μA square-wave pulses delivered at 0.1 Hz through tungsten microelectrodes. Recordings were made with 2–4-MΩ glass needle electrodes filled with 150 mM NaCl. With confirmation of viability, the perfusate was switched to ACSF containing 8.5 mM $[K^+]$ and 141 mM $[Cl^-]$. After 15–20 min of high $[K^+]$ perfusion, spontaneous burst firing could be recorded from CA3a or CA3b. Recordings were digitized across 12 bits at 5 kHz with a Digidata 1200 analogue to digital converter (Axon Instruments), and stored on a personal computer using Axotape 2.0 (Axon Instruments). CA3 interburst intervals were measured with Datapac II (Run Technologies). For control purposes, a separate computer system, digitizing across 16 bits at 1 kHz, identified spontaneous bursts from CA3 using a threshold and peak amplitude detection strategy. This computer triggered a stimulator (Model S8800, Grass Corp.) linked to a photoelectric stimulus isolation unit (Model SIU7, Grass Corp.), to deliver 100-μs constant current square-wave pulses to the Schaffer collateral fibres through a tungsten microelectrode. At times, double pulses consisting of pairs of 100-μs pulses with 150-μs interpulse intervals were used. *b*, Shown are 100 s of recording from an extracellular electrode within CA3 following exposure to 8.5 mM $[K^+]$. The upper four traces in red show the burst discharges occurring at irregular intervals. The lower four traces in blue show the effect of turning on chaos control. When control of chaos pulses are delivered to the Schaffer collateral fibres, large stimulation artefacts are seen at the onset of a burst. Note that each control pulse evokes a synchronized discharge in CA3. As control becomes more stable, the bursts become increasingly periodic, as seen most clearly on the bottom trace. Note that the control pulses are delivered only intermittently. The plot of the full series of these intervals before and during control is seen in the first half of the plot in Fig. 3. *c*, Shown are 100 s of recording from the same experiment before (red) and after (yellow) the initiation of periodic pacing. Note that periodic pulses immediately entrain the population bursts in the fifth tracing (10/10 pulses), but by the sixth tracing, there is occasional escape behaviour evident when the population bursts just before the delivered pulse (seen in 3/10 bursts in tracing 6, 2/11 in tracing 7, and 2/10 in tracing 8). The plot of the full series of these intervals before and during periodic pacing is seen in the second half of the plot in Fig. 3. The calibration mark indicates 5 mV ordinate and 1 s abscissa.

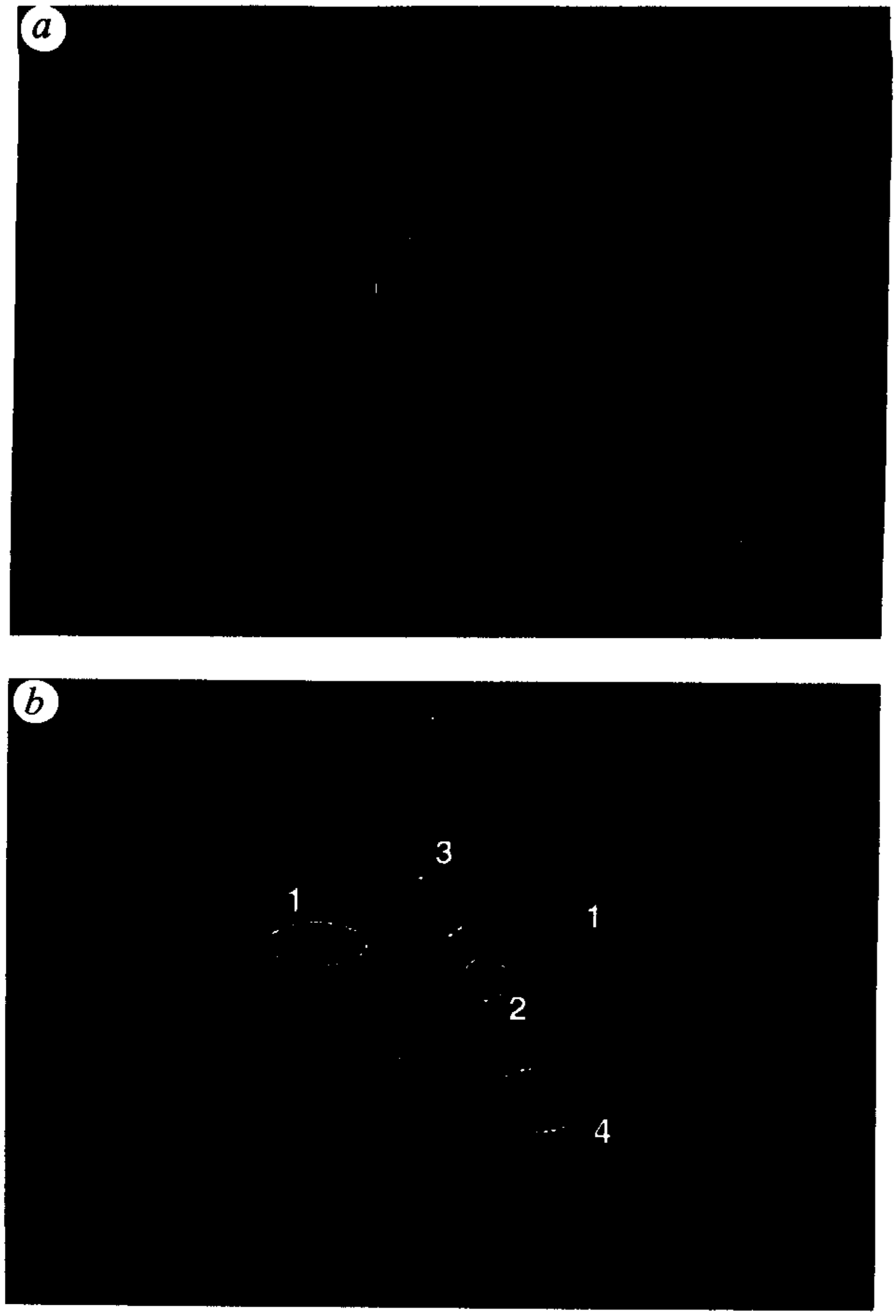

FIG. 2 *a*, Return plots of interburst intervals I_n versus the previous interval I_{n-1} without control. Seven sequential points are colour coded and numbered 1–7. Note that as the trajectory crosses the line of identity along a particular direction from 1 to 2, the next points take a peculiar sequence that starts close to the line of identity at point 3, and then alternates on either side of the line of identity and progressively diverges from it along a nearly straight line for points 3–7. The points coloured in green (1, 2), define a stable direction or manifold, whereas the points in red (3–7) define an unstable manifold. The intersection of these manifolds with the line of identity defines the unstable fixed point. Note that, as for other physical and biological systems[3,8], the saddle observed in these preparations is a flip saddle; that is, while the distances of successive state points from the fixed point increase in an exponential fashion along the unstable manifold, the state points alternate on opposite sides of the line of identity. *b*, Return plot showing multiple colour-coded trajectories that did not follow each other in time. The starting point for each sequence, numbered 1 in each, began at burst numbers 87 (blue), 210 (red) and 317 (green), out of a total series of 320 bursts. The stable manifold is shown with arrows pointing towards the unstable fixed point, and the unstable manifold has arrows drawn in the direction away from the unstable fixed point. Note that each sequence starts at a point roughly the same distance from the unstable fixed point in a region close to the stable manifold. Each trajectory follows roughly the same path, and after closely approaching the unstable fixed point for the points labelled 2 (red, green and blue), there evolves for each trajectory a sequence of exponentially diverging jumps (on alternating sides of the line of identity along the unstable manifold). Although the trajectories are clustered along the unstable manifold for four bursts, the fifth bursts are widely scattered (not shown). This is the manifestation of the sensitivity to initial conditions typical of chaotic systems. These plots show clear evidence for nonrandom structure in these trajectories, and their patterns bear the hallmarks of deterministic chaos.

which can be quantitatively understood by examining the relationship between the timing of sequential events. This can be visualized using a plot which is a type of a return map. Such a map plots the present interval between events, I_n, versus the jth previous interval, I_{n-j}. Periodicities (of period j) are revealed on such a plot as intersections with the line of identity, $I_n = I_{n-j}$. In a chaotic system these intersections are known as unstable fixed points. These unstable fixed points are deterministically approached from a direction called the stable direction or manifold and exponentially diverge from these points along the unstable direction or manifold. This type of local geometry has the shape of a saddle. Chaos control[1,3,8] consists of the identification and characterization of these saddles, followed by a control intervention which exploits the local geometry of the saddle to increase the periodic behaviour of the system.

We demonstrate here three separate approaches to control: periodic pacing, an implementation of chaos control theory, and the inverse of chaos control which we term anticontrol.

Brain slice preparation

Hippocampal slices were prepared using standard techniques[18]. Glass micropipette electrodes in CA1 and CA3 were used to record neuronal activity, and a computer calculated and delivered appropriately timed control pulses. The anatomy of the transverse hippocampal slice and arrangement of electrodes are illustrated in Fig. 1*a*, and details of the experimental preparation are summarized in the figure legend.

Chaos identification and control

A key feature of chaotic systems is that they contain an infinite number of unstable periodic fixed points[22]. That these spontaneously active neuronal networks are chaotic was supported by evidence of unstable fixed points in the return maps with the characteristics shown in Fig. 2*a*, *b*. These candidate unstable fixed points met four criteria. First, the sequence of points approaches the unstable fixed-point candidate along a stable direction and diverges from it along an unstable direction.

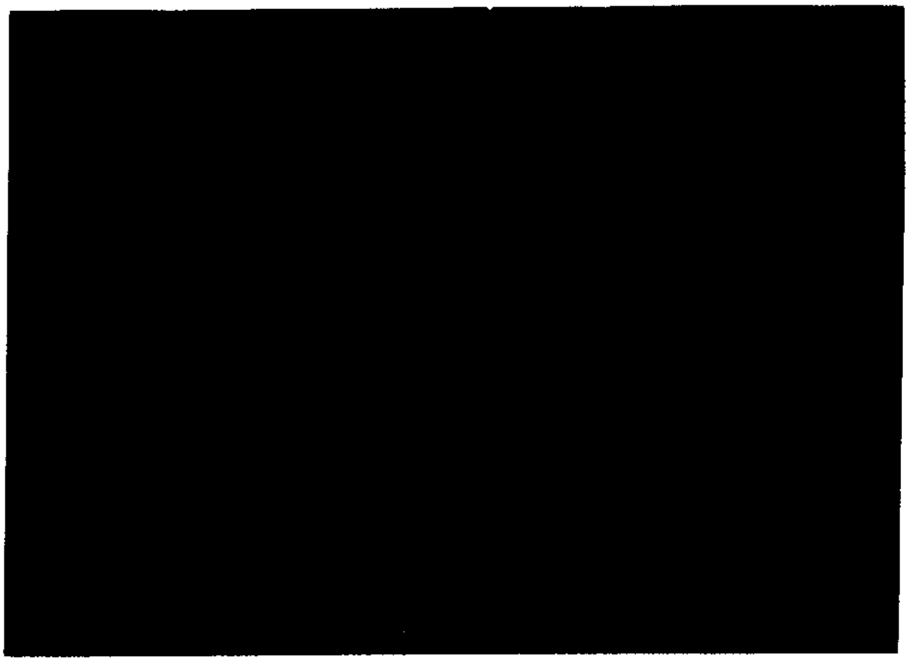

FIG. 3 Plot showing chaotic (red) interburst intervals I_n before and after single-pulse chaos control (blue) and single-pulse periodic pacing (yellow). Burst number is indicated by n. Note the qualitative differences in the control achieved with each method. Raw data from the onsets of chaos control and periodic pacing are shown in Fig. 1*b, c*.

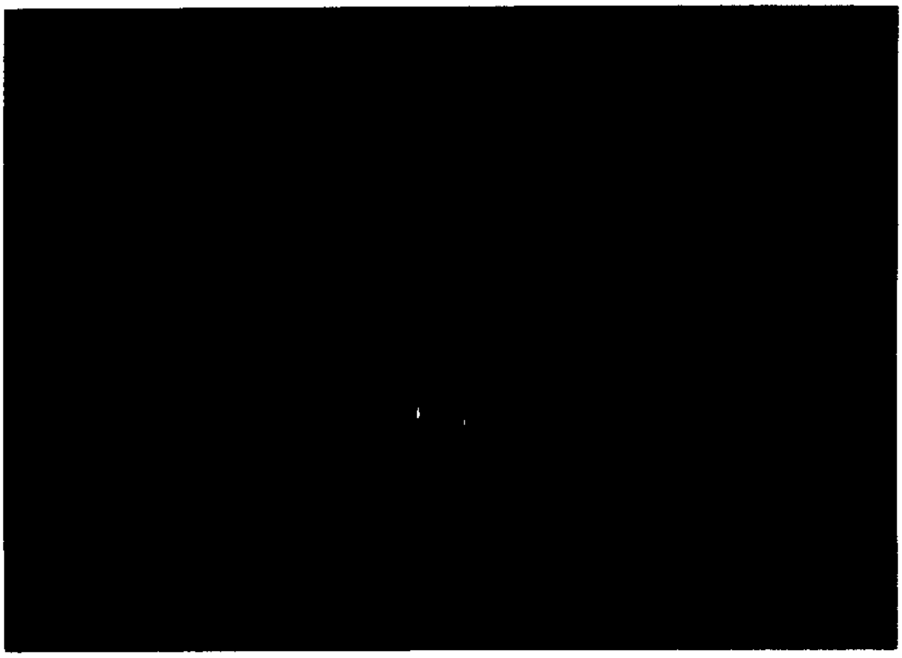

FIG. 4 Comparison of anticontrol (pink), double-pulse chaos control (green) and single-pulse control (blue). Note how anticontrol reduces the periodicity of the preparation. Also note that double-pulse control is more effective than single-pulse control, as was generally the case (see Table 1).

Second, the departing trajectory must be locally linear. Third, multiple approaches to the same candidate along the same stable direction with the corresponding departures along the same unstable direction must be detected. Last, the distances of the departing points from the candidate fixed point must increase exponentially, thereby demonstrating the sensitivity to initial conditions that is the defining feature of chaos. Although short single approaches to candidate unstable fixed points can be occasionally observed in random data, multiple approaches fitting these stringent criteria will not be seen.

In the implementation of these criteria, we excluded higher period behaviour (period 2, period 3, and so on), insisted that the geometry about the fixed point candidates be a flip saddle, and set criteria for the minimum acceptable linearity of the unstable manifold. We also set criteria for limits on the rates of approach and divergence of the trajectories. Because on these return plots it is easily shown that the eigenvalues (local rates of expansion and contraction along the respective manifolds) are simply the slopes of the respective manifolds, it is important to note that we found that the stable manifolds had negative slopes with magnitudes less than 1 and that the unstable manifolds had negative slopes with magnitudes greater than 1, further supporting the presence of chaos in these data (see Fig. 2).

Our chaos control technique begins with a learning phase consisting of the identification of unstable fixed points and the performance of local linear least-square fits to obtain the stable and unstable directions along with the rates of approach and divergence along them. The control phase consisted of waiting until the system executed a close approach to the unstable fixed point (within a small radius ε) along the stable direction, followed by an intervention that modified the timing of the predicted next interval in order to place it back onto the stable manifold. In this way we use the saddle structure inherent in the chaotic dynamics to bring the system back to the desired unstable fixed point with minimal intervention.

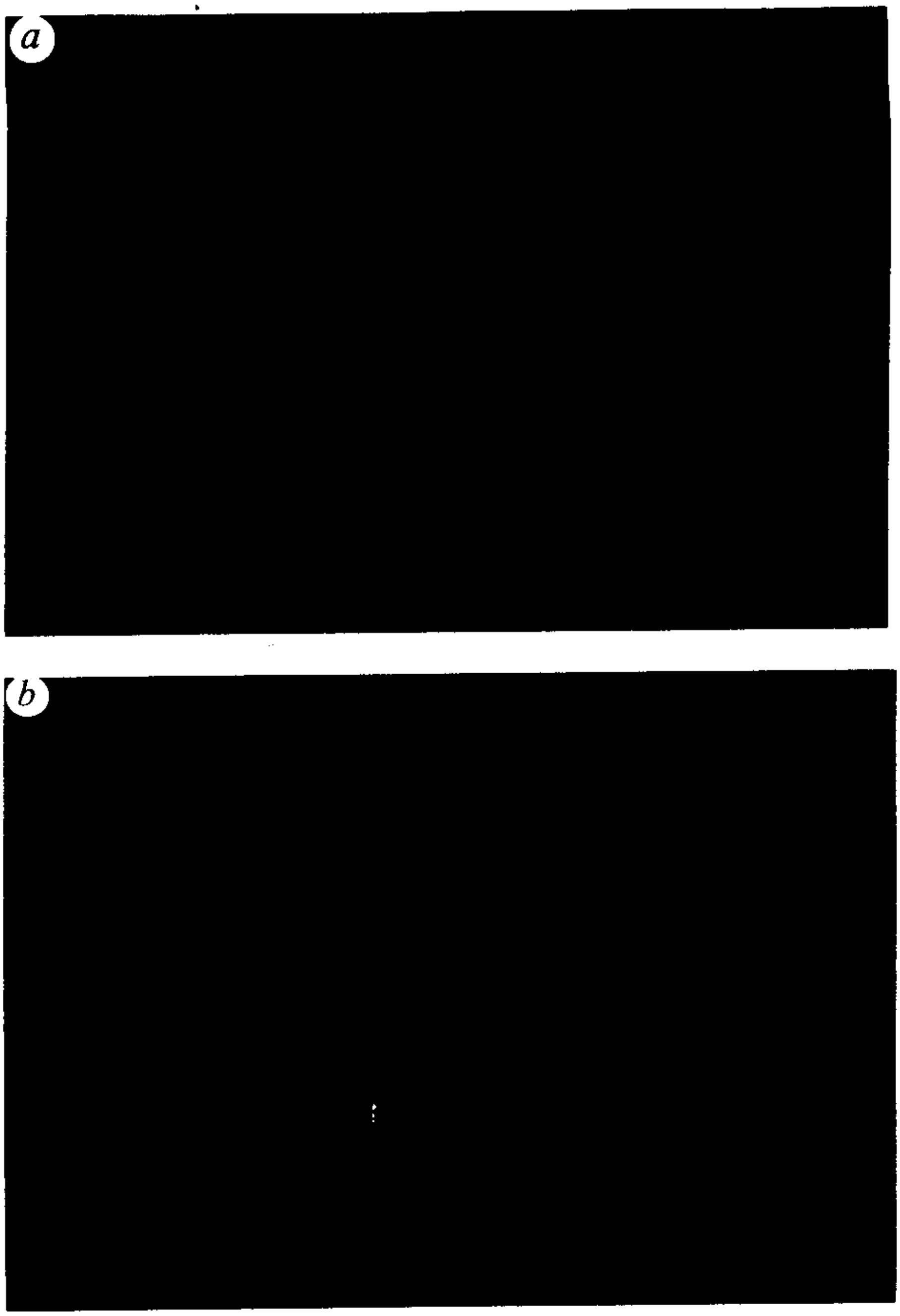

FIG. 5 Comparison of double-pulse chaos control (green) with double-pulse periodic pacing (orange) in an exceptional experiment where double-pulse chaos control was not very tight, and where double pulse periodic pacing was a better control method. Note the frequent escapes and recaptures of control with the chaos control method. This example helps illustrate how the chaos control method differed from overdrive periodic pacing. *b*, Experimental run where a wide range of control behaviours were observed. There are 5 sequential attempts to identify unstable fixed points and learn the manifold structure. Each control run is coded in blue. The first control run demonstrates what we classify as good control in Table 1. After relearning, the second attempt at control was also good, but at a higher fixed point (where the period of the underlying periodic orbit of the fixed point is larger). The third trial, despite learning nearly the identical fixed point as the previous trial, chose different manifolds and the control was not as good. We call such control runs, where intervals I_n larger than the fixed point are selectively eliminated partial control; note that this is a manifestation of the manifold selection and not just a function of the mean frequency of stimulation. This point is further clarified in the fourth and fifth control runs. The fourth control run selected a larger fixed point than the previous runs but control was a failure. The fifth and final control run of this sequence, despite selection of the highest fixed point of this series, achieved partial control with more adequate manifold and fixed-point selection.

In the following experiments, for periodic pacing, we used the same pulse interval as our calculated unstable fixed point. For anticontrol, we chose an interval that placed the next point on a line that was completely off the manifolds. We somewhat arbitrarily chose a direction that was the mirror image of the unstable manifold about the line of identity. This anticontrol technique proved effective in diverting the state of the system away from the stable direction and therefore from the unstable fixed point.

Experimental results

We did 91 experimental trials on 22 hippocampal slices from 9 rats. These trials consisted of combinations of chaos control, periodic pacing and anticontrol using both single and double stimulation pulses (Table 1). Double pulses were used at times to increase the effectiveness of stimulation.

Figure 1*b* shows an example of the synchronized burst discharges recorded extracellularly in CA3. The upper four traces show the burst discharges occurring at irregular intervals before control. On the fifth tracing chaos control pulses are delivered to the Schaffer collateral fibres, seen as large artefacts at the onset of a burst. Note that each control pulse can evoke a synchronized discharge in CA3, but control pulses are only given intermittently. As control becomes more stable, as seen most clearly on the bottom trace, the spontaneous bursts become increasingly periodic. We examined the relationship between burst intensity (duration, integrated amplitude and root mean

TABLE 1 Summary of experiments

	Chaos control		Periodic pacing		Anticontrol	
	Single	Double	Single	Double	Single	Double
Good	10	4	6	2	4	1
Partial	15	2	5	0	—	—
Bad	21	0	6	0	16	0
Total	46	6	17	2	20	1

square deviation) and interburst interval but found no correlations. The plot of the full series of these intervals before and during control is seen in the first half of the plot in Fig. 3.

Figure 1*c* shows 100 s of recording from the same experimental run before and after the initiation of periodic pacing. Note that now pulses immediately entrain the population bursts in the fifth tracing, but by the sixth tracing there is occasional escape behaviour evident when the population burst-fires just before the delivered pulses. The plot of the full series of these intervals before and during periodic pacing is seen in the second half of the plot in Fig. 3.

Figure 3 illustrates burst intervals before, during and after both single-pulse chaos control and single-pulse periodic pacing. Note that there is a qualitative difference in the control achieved with each method, as was seen from the traces of raw data shown in Fig. 1*b*, *c*.

Figure 4 compares the effects of anticontrol, double-pulse chaos control and single-pulse chaos control for another experiment. Here, the effect of anticontrol in reducing the periodicity of the preparation is clearly seen. We also demonstrated an increase in the effectiveness of double over single pulsing for this experiment.

Figure 5*a* illustrates an experiment where double-pulse chaos control and periodic pacing were compared, but the degree of control with chaos control was not as good as with periodic pacing. This experiment was exceptional, because most of the double-pulse experiments achieved very tight control (see Fig. 4, and summary in Table 1). Note that even with the increased stimulation of double pulsing, chaos control was not simply overdrive pacing, in that there were frequent escapes and recaptures of control consistent with the interactive control hypothesis.

Figure 5*b* illustrates the full gamut of results obtained with single-pulse chaos control. The first control trial demonstrated good control. Note that during this control sequence, the quality of the control improved. We then allowed the algorithm to relearn the fixed point and it chose one with a longer interval, again with good control. Whether this is a manifestation of the non-stationary nature of the system, or truly reflects the presence of multiple unstable period 1 fixed points is unclear. Relearning a third time, the algorithm selected different manifolds without substantially changing the value of the fixed point, but the control is not as good. This third control run exhibited what we call partial control in the results shown in Table 1; in partial control, manifold selection was not optimal, and time intervals longer than those of the chosen fixed-point interval appear eliminated. Relearning a fourth time, a fixed point is chosen at a longer interval than the previous three attempts. This was a control failure. Nevertheless, relearning a fifth time with an even longer fixed-point interval gave partial control. This sequence demonstrates that the quality of control is not simply a function of the frequency chosen, the control is critically dependent on the quality of the fixed points and manifolds selected.

Discussion

This is the second attempt at achieving control of a chaotic biological system[8] with a derivative method of Ott, Grebogi and Yorke[1]. The observation of small-scale structure and the identification of stable and unstable manifolds near unstable fixed points for many of these burst-firing slices demonstrated the presence of deterministic chaos in this simple neuronal system. For this preparation, complicated control theory is not required just to achieve relatively fast periodic behaviour. Above certain frequencies, periodic pacing was effective in entraining the spontaneous burst discharges in CA3. However, the quality of control with periodic pacing was not equivalent with the chaos control method; furthermore, the chaos control method has the advantage over overdrive periodic pacing in terms of its ability to identify and track fixed points over time. In addition, the control of chaos strategy offers the ability to break up fixed-point behaviour with anticontrol. The anticontrol method used here uses a minimal number of stimuli needed to prevent periodic behaviour.

Although it was easy to observe the unstable manifolds from this preparation, it was difficult to place accurately the stable manifold. This is because the system has many degrees of freedom (that is, is high dimensional), and the expectation of fully disentangling its dynamics with a two-dimensional embedding is simplistic. In addition, increasing amounts of noise in a system will increase the frequency of escapes from control and eventually render control impossible[1]. Despite these difficulties, good or partial control could frequently be achieved with our implementation of chaos control. The application of new theoretical techniques recently developed for the control of high dimensional systems[23] could improve the reliability of control for such neuronal preparations.

We experimented with several variants of stimulation delivery. In addition to single pulses, double pulses were used and were often more effective in achieving higher quality control. We also explored limiting the delivery of control pulses by prohibiting consecutive control pulses without an intervening spontaneous burst. This latter method was less effective than permitting consecutive pulsing.

Because this neuronal preparation shares similar characteristics with epileptic interictal spike foci, we believe these methods may be applied to such foci. Although it is impossible to predict what effect increasing the periodicity of epileptic foci will have, the opposite effect of breaking up fixed-point periodic behaviour with anticontrol could be a more useful intervention. □

Received 11 May; accepted 5 July 1994.

1. Ott, E., Grebogi, C. & Yorke, J. A. *Phys. Rev. Lett.* **64,** 1196–1199 (1990).
2. Shinbrot, T., Grebogi, C., Ott, E. & Yorke, J. A. *Nature* **363,** 411–417 (1993).
3. Ditto, W. L., Rauseo, S. N. & Spano, M. L. *Phys. Rev. Lett.* **65,** 3211–3214 (1990).
4. Hunt, E. R. *Phys. Rev. Lett.* **67,** 1953–1955 (1991).
5. Roy, R., Murphy, T. W., Maier, T. D. & Gills, Z. *Phys. Rev. Lett.* **68,** 1259–1262 (1992).
6. Petrov, V., Gaspar, V., Masere, J. & Showalter, K. *Nature* **361,** 240–243 (1993).
7. Rollins, R. W., Parmananda, P. & Sherard, P. *Phys. Rev.* E**47,** R780 (1993).
8. Garfinkel, A., Spano, M., Ditto, W. L. & Weiss, J. *Science* **257,** 1230–1235 (1992).
9. Gotman, J. *Can. J. neurol. Sci.* **18,** 573–576 (1991).
10. Katz, A., Marks, D. A., McCarthy, G. & Spencer, S. S. *Electroenceph. clin. Neurophysiol.* **79,** 153–156 (1991).
11. Pedley, T. A. & Traub, R. D. in *Current Practice of Clinical Electroencephalography* 2nd edn (eds Daly, D. D. & Pedley, T. A.) 107–137 (Raven, New York, 1990).
12. Rutecki, P. A., Lebeda, F. J. & Johnston, D. *J. Neurophysiol.* **54,** 1363–1374 (1985).
13. Korn, S. J., Giacchino, J. L., Chamberlin, N. L. & Dingledine, R. *J. Neurophysiol.* **57,** 325–341 (1987).
14. Traynelis, S. F. & Dingledine, R. *J. Neurophysiol.* **59,** 259–276 (1988).
15. Traub, R. D. & Dingledine, R. *J. Neurophysiol.* **64,** 1009–1018 (1990).
16. Traub, R. D. & Miles, R. *Neuronal Networks of the Hippocampus* (Cambridge Univ. Press, Cambridge, 1991).
17. Chang, T., Schiff, S. J., Sauer, T., Gossard, J.-P. & Burke, R. E. *Biophys. J.* **67,** 671–683 (1994).
18. Schiff, S. J., Jerger, K., Chang, T., Sauer, T. & Aitken, P. G. *Biophys. J.* **67,** 684–691 (1994).
19. Jefferys, J. G. R. *J. Physiol.* **319,** 143–152 (1981).
20. Durand, D. *Brain Res.* **382,** 139–144 (1986).
21. Kayyali, H. & Durand, D. *Expl Neurol.* **113,** 249–254 (1991).
22. Ott, E. *Chaos in Dynamical Systems* (Cambridge Univ. Press, Cambridge, 1993).
23. Auerbach, D., Grebogi, C., Ott, E. & Yorke, J. A. *Phys. Rev. Lett.* **69,** 3479–3482 (1992).

ACKNOWLEDGEMENTS. We thank P. G. Aitken for his invaluable teaching and advice and S. Mahan for research assistance. We gratefully acknowledge support from an NIMH grant (S.J.S.), the Children's Research Institute (S.J.S. and T.C.), an Office of Naval Research Young Investigator Award (W.L.D.), the Naval Surface Warfare Center's Independent Research Program (M.L.S.) and the Physics Division of the Office of Naval Research (M.L.S. and W.L.D.) The contribution of software from Manugistics Inc. is greatly appreciated.